

Propionate metabolism in yeast and plants



Inaugural-Dissertation

zur Erlangung des Doktorgrades
der Mathematisch-Naturwissenschaftlichen Fakultät der Heinrich Heine
Universität Düsseldorf

vorgelegt von

Jan Wiese
aus Soest

Düsseldorf, März 2014

aus dem Institut für Biochemie der Pflanzen
der Heinrich-Heine-Universität Düsseldorf

Gedruckt mit der Genehmigung der
Mathematisch-Naturwissenschaftlichen Fakultät der
Heinrich-Heine-Universität Düsseldorf

Referent: Prof. Dr. Andreas P. M. Weber

Korreferent: PD Dr. Nicole Linka

Tag der mündlichen Prüfung: 2. Juni 2014

Erklärung

Ich versichere an Eides Statt, dass ich die vorliegende Dissertation eigenständig und ohne unerlaubte Hilfe unter Beachtung der „Grundsätze zur Sicherung guter wissenschaftlicher Praxis“ an der Heinrich-Heine-Universität Düsseldorf angefertigt habe. Die Dissertation habe ich in der dieser oder in ähnlicher Form noch bei keiner anderen Institution eingereicht. Ich habe bisher keine erfolglosen Promotionsversuche unternommen.

Düsseldorf, den 28.03.2014

Jan Wiese

Contents

I. Preface	2
II.1 Summary	3
II.2 Zusammenfassung	4
III. Introduction	10
IV. Manuscripts	19
IV.1 Manuscript 1: Stress-inducible yeast MPV17 protein 1 coordinates TCA cycle intermediate availability and is implicated in propionate metabolism...19	
IV.2 Manuscript 2: Participation of Arabidopsis PMP22 in the metabolism of fatty and branched-chain amino acids renders it crucial to peroxisome function and plant performance in abiotic stress conditions.....65	
IV.3 Manuscript 3: The implication of peroxisomal metabolite transport in propionic and isobutyric acid metabolism is important for amino acid respiration.....134	
V. Concluding remarks and outlook	167
VI. Published Manuscripts	172
VI.1 Manuscript 4: Agrobacterium-mediated <i>Arabidopsis thaliana</i> transformation: an overview of T-DNA binary vectors, floral dip and screening for homozygous lines.....172	
VI.2 Manuscript 5: An engineered plant peroxisome and its application in biotechnology.....183	
VII. Acknowledgements	194

I. Preface

This thesis is divided into independent sections, written as manuscripts. *Manuscript 1* and *Manuscript 2* focus on the physiological role of MPV17/PMP22 (Peroxisomal Membrane Protein of 22 kDa) domain proteins by analysis of loss-of-function mutants. *Manuscript 1* presents work about *Saccharomyces cerevisiae* Stress-inducible Yeast MPV17 protein1 (Sym1p) and its implication in tricarboxylic acid (TCA) cycle intermediate availability and involvement in propionate metabolism. *Manuscript 2* provides a detailed investigation of *in vitro* features and *in vivo* roles of *Arabidopsis thaliana* peroxisomal membrane protein of 22 kDa (PMP22). *Manuscript 3* highlights the role of peroxisomal transport proteins in amino acid metabolism. The manuscripts are submission-ready versions and the discussions include an outlook of possible directions for future research.

Unit V concludes Manuscripts 1-3. Unit VI contains previous publications. *Manuscript 4* deals with the impact of plant peroxisomes on biotechnological applications and was published as Kessel-Vigelius et al., 2013, Plant Sci 210, 232-240. *Manuscript 5* describes the *Agrobacterium*-mediated *Arabidopsis thaliana* transformation (Bernhardt et al., 2012, J Endocytobiosis Cell Res 22, 19-28).

II.1 Summary

The subcellular compartmentation of eukaryotic cells led to the evolution of varied translocation mechanism for solutes across organelle membranes to enable substrate and energy homeostasis (Lunn, 2007). This thesis contributes to knowledge of metabolite transfer across mitochondrial and peroxisomal membranes. The molecular function of MPV17/PMP22-type family proteins, such as the mouse peroxisomal membrane protein 2 (Pxm2) or the Stress-inducible Yeast MPV17 protein 1 (Sym1p) was previously unknown. Preliminary research pointed to a function as metabolite channels (Rokka et al., 2009; Reinhold et al., 2012). In humans MPV17 loss causes lethal diseases, therefore the yeast mutant of the functional orthologue, *sym1Δ*, was established to gain insight in *MPV17* function (Trott and Morano, 2004; Spinazzola et al., 2006; Dallabona et al., 2010).

Our studies revealed Sym1p to coordinate availability of TCA cycle intermediates at restrictive growth conditions (*Manuscript 1*). At the same conditions metabolites originating from mitochondrial pyruvate (Ljungdahl and Daignan-Fornier, 2012) showed elevated levels. Feeding of TCA and glyoxylate cycle intermediates enabled wild-type growth at 37°C. *Saccharomyces cerevisiae* depended on 2-methylcitrate-cycle activity to use propionate and methylmalonate as sole carbon source at 37°C. Sym1p was required for growth on propionate and methylmalonate. Genetic analyses confirmed that *SYM1* is implicated in the 2-methylcitrate cycle and that the 2-methylcitrate cycle is needed for methylmalonate degradation. We identified a gene, which encodes a peroxisomal MPV17/PMP22 protein in yeast, which we termed *SYM2* due to structural and regulatory similarities. Similar to Sym1p, Sym2p was needed to support growth on ethanol at 37°C. On the basis of our results we discuss possible transport mechanisms of Sym1p and Sym2p.

The physiological role of the plant peroxisomal protein of 22 kDa (PMP22; Tugal et al., 1999; Murphy et al., 2003) was addressed by analysis of T-DNA and miRNA mutants (*Manuscript 2*). In *pmp22* we detected compromised growth of seedling hypocotyls. PMP22 was needed for activity fatty acid β -oxidation and glyoxylate cycle. Without functional PMP22 the conversion of storage oil into respiratory substrates and gluconeogenic Carbon units was impaired. This was particularly obvious during extended darkness and natural senescence through damage of

Photosystem II. *pmp22* mutants manifested a defect in reproductive fitness, because total seed yield as well as protein and amino acid content of seeds were reduced. Growth of *pmp22* mutants was sensitive to the presence of branched chain amino acids (BCAA) and associated catabolites (isobutyrate, propionate and acrylate). The CoA esters isobutyryl-CoA and propionyl-CoA are released in the mitochondrion by degradation from valine and isoleucine. Heterologous expression of mitochondria-targeted PMP22 suppressed the growth phenotype of the *sym1Δ* yeast mutant defective in a metabolite channel. We concluded, that also PMP22 forms a metabolite channel. Phenotypic similarities to a peroxisomal mutant in valine catabolism led to the discussion that PMP22 catalyzes the export of 3-hydroxypropionate, the end product of peroxisomal BCAA conversion.

In humans defects in metabolic conversion of propionyl-CoA have been associated with severe diseases (Desviat et al., 2004). In plants these molecules are released in the process of BCAA degradation. BCAA degradation is important in stressed plants, because the reactions involve reduction of the mitochondrial ubiquinone pool and thus sustain mitochondrial respiration and energy metabolism (Araujo et al., 2010).

This work shows the involvement of peroxisomal β -oxidation in the metabolism of mitochondrial-generated propionyl-CoA and isobutyryl-CoA in *Arabidopsis thaliana* (*Manuscript 3*). We describe the yet uncharacterized relation between β -oxidation and amino acid metabolism. On the basis of our experimental evidence we developed a model in which the peroxisomal ABC transporter 1 (PXA1; Zolman et al., 2001; De Marcos Lousa et al., 2013) is implicated in the import of the C₃ and C₄ monocarboxylic acid CoA esters and acts in synergy with peroxisomal adenine nucleotide carrier (PNC; Arai et al., 2008; Linka et al., 2008) in the detoxification of BCAA catabolites. Loss-of PXA1 and PNC, but also peroxisomal NAD/CoA carrier (PXN; Agrimi et al., 2012; Bernhardt et al., 2012) function resulted in sensitivity to extended darkness, premature senescence and reduced reproductive fitness due to impaired fatty acid degradation and altered amino acid metabolism.

References

- Agrimi, G., Russo, A., Pierri, C.L., and Palmieri, F.** (2012). The peroxisomal NAD⁺ carrier of *Arabidopsis thaliana* transports coenzyme A and its derivatives. *J Bioenerg Biomembr* **44**: 333–340.
- Arai, Y., Hayashi, M., and Nishimura, M.** (2008). Proteomic identification and characterization of a novel peroxisomal adenine nucleotide transporter supplying ATP for fatty acid beta-oxidation in soybean and *Arabidopsis*. *The Plant Cell* **20**: 3227–3240.
- Araujo, W.L., Ishizaki, K., Nunes-Nesi, A., Larson, T.R., Tohge, T., Krahnert, I., Witt, S., Obata, T., Schauer, N., Graham, I.A., Leaver, C.J., and Fernie, A.R.** (2010). Identification of the 2-Hydroxyglutarate and Isovaleryl-CoA Dehydrogenases as Alternative Electron Donors Linking Lysine Catabolism to the Electron Transport Chain of *Arabidopsis* Mitochondria. *The Plant Cell* **22**: 1549–1563.
- Bernhardt, K., Wilkinson, S., Weber, A.P.M., and Linka, N.** (2012). A peroxisomal carrier delivers NAD⁺ and contributes to optimal fatty acid degradation during storage oil mobilization. *The Plant Journal* **69**: 1–13.
- Dallabona, C., Marsano, R.M., Arzuffi, P., Ghezzi, D., Mancini, P., Zeviani, M., Ferrero, I., and Donnini, C.** (2010). Sym1, the yeast ortholog of the MPV17 human disease protein, is a stress-induced bioenergetic and morphogenetic mitochondrial modulator. *Human Molecular Genetics* **19**: 1098–1107.
- De Marcos Lousa, C., Van Roermund, C.W.T., Postis, V.L.G., Dietrich, D., Kerr, I.D., Wanders, R.J.A., Baldwin, S.A., Baker, A., and Theodoulou, F.L.** (2013). Intrinsic acyl-CoA thioesterase activity of a peroxisomal ATP binding cassette transporter is required for transport and metabolism of fatty acids. *Proceedings of the National Academy of Sciences* **110**: 1279–1284.
- Desviat, L.R., Pérez, B., Pérez-Cerdá, C., Rodríguez-Pombo, P., Clavero, S., and Ugarte, M.** (2004). Propionic acidemia: mutation update and functional and structural effects of the variant alleles. *Molecular Genetics and Metabolism* **83**: 28–37.
- Linka, N., Theodoulou, F.L., Haslam, R.P., Linka, M., Napier, J.A., Neuhaus, H.E., and Weber, A.P.M.** (2008). Peroxisomal ATP import is essential for seedling development in *Arabidopsis thaliana*. *The Plant Cell* **20**: 3241–3257.
- Ljungdahl, P.O. and Daignan-Fornier, B.** (2012). Regulation of Amino Acid, Nucleotide, and Phosphate Metabolism in *Saccharomyces cerevisiae*. *Genetics* **190**: 885–929.
- Lunn, J.E.** (2007). Compartmentation in plant metabolism. *J. Exp. Bot.* **58**: 35–47.
- Murphy, M.A., Phillipson, B.A., Baker, A., and Mullen, R.T.** (2003). Characterization of the targeting signal of the *Arabidopsis* 22-kD integral peroxisomal membrane protein. *Plant Physiology* **133**: 813–828.
- Reinhold, R., Krüger, V., Meinecke, M., Schulz, C., Schmidt, B., Grunau, S.D., Guiard, B., Wiedemann, N., van der Laan, M., Wagner, R., Rehling, P., and Dudek, J.** (2012). The channel-forming Sym1 protein is transported by the TIM23 complex in a presequence-independent manner. *Molecular and Cellular Biology* **32**: 5009–5021.
- Rokka, A., Antonenkov, V.D., Soininen, R., Immonen, H.L., Pirilä, P.L., Bergmann, U., Sormunen, R.T., Weckström, M., Benz, R., and Hiltunen, J.K.** (2009). Pxmp2 Is a Channel-Forming Protein in Mammalian Peroxisomal Membrane. *PLoS ONE* **4**: e5090.
- Spinazzola, A. et al.** (2006). MPV17 encodes an inner mitochondrial membrane protein and is mutated in infantile hepatic mitochondrial DNA depletion. *Nat. Genet.* **38**: 570–575.
- Trott, A. and Morano, K.A.** (2004). SYM1 is the stress-induced *Saccharomyces cerevisiae* ortholog of the mammalian kidney disease gene Mpv17 and is required for ethanol metabolism and tolerance during heat shock. *Eukaryotic Cell* **3**: 620–631.
- Tugal, H.B., Pool, M., and Baker, A.** (1999). *Arabidopsis* 22-kilodalton peroxisomal membrane protein. Nucleotide sequence analysis and biochemical characterization. *Plant Physiology* **120**: 309–320.
- Zolman, B.K., Silva, I.D., and Bartel, B.** (2001). The *Arabidopsis* pxa1 mutant is defective in an ATP-binding cassette transporter-like protein required for peroxisomal fatty acid beta-oxidation. *Plant Physiology* **127**: 1266–1278.

II.2 Zusammenfassung

Die subzelluläre Kompartimentierung der eukaryotischen Zelle führte zur Evolution verschiedener Metabolitranslokationssysteme in den Membranen von Organellen, um die Substrat- und Energiehomöostase zu ermöglichen (Lunn, 2007). Diese Dissertation trägt zum Wissen über Metabolitransfer über die peroxisomale und mitochondriale Membran bei. Die molekulare Funktion von Membranproteinen der MPV17/PMP22-Familie, wie z.B. des peroxisomalen Membranproteins 2 (Pmp2) der Maus und des Stress-induzierbaren Hefe MPV17 Proteins 1 (Sym1p) war bisher unbekannt. Frühere Studien deuteten darauf hin, dass diese Membranproteine Metabolitkanäle bilden (Rokka et al., 2009; Reinhold et al., 2012). Im Menschen führt der Verlust von MPV17 zu tödlichen Krankheiten, weshalb die Hefemutante des funktionellen Orthologs *sym1Δ* etabliert wurde, um die Funktion von MPV17 zu entschlüsseln (Trott and Morano, 2004; Spinazzola et al., 2006; Dallabona et al., 2010).

Diese Arbeit zeigt, dass Sym1p in Ethanol-Medium bei 37°C für die Verfügbarkeit von Zitrat-Zyklus-Intermediaten notwendig ist (*Manuskript 1*). Gleichzeitig führte diese Bedingung in *sym1Δ* zu erhöhter Konzentration von Aminosäuren und Carboxylaten, die mitochondrial ausgehend von Pyruvat synthetisiert werden (Ljungdahl and Daignan-Fornier, 2012). Die Zuführung von Zitrat- oder Glyoxylat-Zyklus-Intermediaten ermöglichte das wild-typische Wachstum von *sym1Δ* bei 37°C. Zudem konnten wir nachweisen, dass Hefen mithilfe des 2-methylzitrat-Zyklus bei 37°C Propionat als einzige Kohlenstoffquelle nutzen können. Die Aktivität von Sym1p war notwendig, um Propionat und Methylmalonat als Kohlenstoffquelle nutzen zu können. Genetische Analysen zeigten, dass *SYM1* im Zusammenhang mit dem Methylzitrat-Zyklus steht und dass der Methylzitrat-Zyklus wichtig für den Abbau von Methylmalonat ist. Wir identifizierten in *S. cerevisiae* ein peroxisomales MPV17/PMP22 Protein, das wir aufgrund struktureller und regulatorischer Ähnlichkeiten Sym2p nannten. Ähnlich wie Sym1p zeigte sich auch Sym2p als notwendig für das Wachstum bei erhöhter Temperatur und hoher Konzentration von Ethanol. Die Ergebnisse erlaubten die Diskussion möglicher Transportmodi von Sym1p und Sym2p.

Die physiologische Bedeutung des pflanzlichen peroxisomalen Membranproteins von 22 kDa (PMP22; Tugal et al., 1999; Murphy et al., 2003) zeigte sich in der Analyse

von T-DNA und RNAi Mutanten (*Manuskript 2*). In *pmp22* Mutanten war das Wachstum des Hypokotyls von Keimlingen beeinträchtigt. PMP22 war notwendig für die Aktivität der β -Oxidation von Fettsäuren und des Glyoxylat-Zyklus. Ohne PMP22 konnte die Umwandlung von Speicherfett in respiratorische Substrate und glukoneogenetische Kohlenstoffeinheiten nicht erfolgen. Vor allem während verlängerter Dunkelheit und in natürlicher Seneszenz führte die Reduzierung von PMP22 zur Beschädigung des Photosystems II. Zudem manifestierte sich in *pmp22* Mutanten ein Defekt in der reproduktiven Fitness, denn *pmp22* Mutanten produzierten weniger Saatgut und *pmp22* Samen enthielten weniger Protein und Aminosäuren. Das Wachstum von *pmp22* Linien zeigte sich sensitiv gegenüber der Präsenz verzweigtkettiger Aminosäuren, Isobutyrat und Propionat. Letztere werden mitochondrial beim Abbau verzweigtkettiger Aminosäuren freigesetzt. Die heterologe Expression von modifiziertem PMP22 in *sym1 Δ* , das durch die Fusion mit einem mitochondrialen *targeting* Peptid, in die mitochondriale Membran inseriert wurde, führte zur Aufhebung des *sym1 Δ* Wachstumsphänotyps. Dies erlaubte die Schlussfolgerung, dass PMP22 einen Metabolit-Kanal bildet. Phänotypische Übereinstimmungen mit einer Mutante im Valin-Katabolismus legte die Vermutung nahe, dass PMP22 den Export von 3-Hydroxypropionat, dem Endprodukt des peroxisomalen Propionat-Abbaus, katalysiert.

Defekte im Propionyl-CoA-Abbau sind beim Menschen mit schwerwiegenden Krankheiten assoziiert (Desviat et al., 2004). Auch in Pflanzen werden diese Moleküle beim Abbau verzweigtkettiger Aminosäuren freigesetzt. Der Abbau ist in gestressten Pflanzen wichtig, da die Reaktionen zur Reduktion des mitochondrialen *Ubiquinon-pools* führen und somit die mitochondriale Atmung und den Energiestoffwechsel aufrechterhalten (Araujo et al., 2010).

Diese Arbeit behandelt die Beteiligung peroxisomaler β -oxidation am Metabolismus der mitochondrial anfallenden Zwischenprodukte Propionyl-CoA sowie Isobutyryl-CoA in *Arabidopsis thaliana* (*Manuskript 3*). Dabei wird die bisher uncharakterisierte Rolle peroxisomaler β -Oxidation im Aminosäurestoffwechsel erläutert. Die Ergebnisse führten zur Entwicklung eines Modells, in dem der peroxisomale ABC-Transporter-1 (PXA1; Zolman et al., 2001; De Marcos Lousa et al., 2013) Propionyl-CoA und Isobutyryl-CoA in die Peroxisomen importiert und der peroxisomale Adenin-

Nukleotid-Transporter (PNC; Arai et al., 2008; Linka et al., 2008) benötigt wird, um C₃ und C₄ Monocarboxylate zu degradieren. PXA1, PNC und der peroxisomale NAD/CoA Translokator (PXN; Agrimi et al., 2012; Bernhardt et al., 2012) sind wichtig im Energiestoffwechsel der verlängerten Nacht. Der Verlust dieser Aktivitäten führte zu frühzeitiger Seneszenz und verringerter reproduktiver *Fitness*.

Referenzen

- Agrimi, G., Russo, A., Pierri, C.L., and Palmieri, F.** (2012). The peroxisomal NAD⁺ carrier of *Arabidopsis thaliana* transports coenzyme A and its derivatives. *J Bioenerg Biomembr* **44**: 333–340.
- Arai, Y., Hayashi, M., and Nishimura, M.** (2008). Proteomic identification and characterization of a novel peroxisomal adenine nucleotide transporter supplying ATP for fatty acid beta-oxidation in soybean and *Arabidopsis*. *The Plant Cell* **20**: 3227–3240.
- Araujo, W.L., Ishizaki, K., Nunes-Nesi, A., Larson, T.R., Tohge, T., Krahnert, I., Witt, S., Obata, T., Schauer, N., Graham, I.A., Leaver, C.J., and Fernie, A.R.** (2010). Identification of the 2-Hydroxyglutarate and Isovaleryl-CoA Dehydrogenases as Alternative Electron Donors Linking Lysine Catabolism to the Electron Transport Chain of *Arabidopsis* Mitochondria. *The Plant Cell* **22**: 1549–1563.
- Bernhardt, K., Wilkinson, S., Weber, A.P.M., and Linka, N.** (2012). A peroxisomal carrier delivers NAD⁺ and contributes to optimal fatty acid degradation during storage oil mobilization. *The Plant Journal* **69**: 1–13.
- Dallabona, C., Marsano, R.M., Arzuffi, P., Ghezzi, D., Mancini, P., Zeviani, M., Ferrero, I., and Donnini, C.** (2010). Sym1, the yeast ortholog of the MPV17 human disease protein, is a stress-induced bioenergetic and morphogenetic mitochondrial modulator. *Human Molecular Genetics* **19**: 1098–1107.
- De Marcos Lousa, C., Van Roermund, C.W.T., Postis, V.L.G., Dietrich, D., Kerr, I.D., Wanders, R.J.A., Baldwin, S.A., Baker, A., and Theodoulou, F.L.** (2013). Intrinsic acyl-CoA thioesterase activity of a peroxisomal ATP binding cassette transporter is required for transport and metabolism of fatty acids. *Proceedings of the National Academy of Sciences* **110**: 1279–1284.
- Desviat, L.R., Pérez, B., Pérez-Cerdá, C., Rodríguez-Pombo, P., Clavero, S., and Ugarte, M.** (2004). Propionic acidemia: mutation update and functional and structural effects of the variant alleles. *Molecular Genetics and Metabolism* **83**: 28–37.
- Linka, N., Theodoulou, F.L., Haslam, R.P., Linka, M., Napier, J.A., Neuhaus, H.E., and Weber, A.P.M.** (2008). Peroxisomal ATP import is essential for seedling development in *Arabidopsis thaliana*. *The Plant Cell* **20**: 3241–3257.
- Ljungdahl, P.O. and Daignan-Fornier, B.** (2012). Regulation of Amino Acid, Nucleotide, and Phosphate Metabolism in *Saccharomyces cerevisiae*. *Genetics* **190**: 885–929.
- Lunn, J.E.** (2007). Compartmentation in plant metabolism. *J. Exp. Bot.* **58**: 35–47.
- Murphy, M.A., Phillipson, B.A., Baker, A., and Mullen, R.T.** (2003). Characterization of the targeting signal of the *Arabidopsis* 22-kD integral peroxisomal membrane protein. *Plant Physiology* **133**: 813–828.
- Reinhold, R., Krüger, V., Meinecke, M., Schulz, C., Schmidt, B., Grunau, S.D., Guiard, B., Wiedemann, N., van der Laan, M., Wagner, R., Rehling, P., and Dudek, J.** (2012). The channel-forming Sym1 protein is transported by the TIM23 complex in a presequence-independent manner. *Molecular and Cellular Biology* **32**: 5009–5021.
- Rokka, A., Antonenkov, V.D., Soininen, R., Immonen, H.L., Pirilä, P.L., Bergmann, U., Sormunen, R.T., Weckström, M., Benz, R., and Hiltunen, J.K.** (2009). Pxmp2 Is a Channel-Forming Protein in Mammalian Peroxisomal Membrane. *PLoS ONE* **4**: e5090.
- Spinazzola, A. et al.** (2006). MPV17 encodes an inner mitochondrial membrane protein and is mutated in infantile hepatic mitochondrial DNA depletion. *Nat. Genet.* **38**: 570–575.
- Trott, A. and Morano, K.A.** (2004). SYM1 is the stress-induced *Saccharomyces cerevisiae* ortholog of the mammalian kidney disease gene Mpv17 and is required for ethanol metabolism and tolerance during heat shock. *Eukaryotic Cell* **3**: 620–631.
- Tugal, H.B., Pool, M., and Baker, A.** (1999). *Arabidopsis* 22-kilodalton peroxisomal membrane protein. Nucleotide sequence analysis and biochemical characterization. *Plant Physiology* **120**: 309–320.
- Zolman, B.K., Silva, I.D., and Bartel, B.** (2001). The *Arabidopsis* pxa1 mutant is defective in an ATP-binding cassette transporter-like protein required for peroxisomal fatty acid beta-oxidation. *Plant Physiology* **127**: 1266–1278.

III. Introduction

Propionic or propanoic acid ($\text{CH}_3\text{-CH}_2\text{-COO}^-$) is a weak monocarboxylic acid and an intermediate or end product of carbon metabolic pathways in pro- and eukaryotes (Schneider et al., 2011).

Propionic acid metabolism in procaryotes

Propionibacteria are named for their ability to synthesize propionate (Delwiche, 1948). Dairy propionibacteria ferment lactate to form acetate, propionate and CO_2 , which contribute to the flavor of cheese and are responsible for the “holes” in Emmental cheese (Poonam et al., 2012). On human skin propionibacteria are facultative parasites and influence skin odor due to decomposition of sweat components to odiferous short-chain fatty acids (Elsner, 2006).

Propionyl-CoA carboxylation in the 3-hydroxypropionate cycle has been described as CO_2 fixation pathway in the photosynthetic bacterium *Chloroflexus aurantiacus* (Strauss and Fuchs, 1993). Propionate associated pathways are subject to metabolic engineering in microorganisms, because intermediates are valuable for biofuel or biodegradable bioplastic (polyhydroxyalkanoate) production (Lindenkamp et al., 2012; Keller et al., 2013).

Propionic acid inhibits microbial growth at 0.1-1% (w/v) and is largely used in the preservation of perishable beverage, dairy and bakery products (Suhr and Nielsen, 2004). Nevertheless many bacteria are able to grow on propionate as sole carbon source and connect the metabolic conversion to malonate and tricarboxylic acid pathways (Suvorova et al., 2012), mechanism also employed by eukaryotes (Desviat et al., 2004).

Propionic acid metabolism in eukaryotes

In eukaryotes propionate will be converted to propionyl-CoA, which is a cell growth inhibitor, as it interferes with the activity of enzymes central to mitochondrial energy metabolism (Brock and Buckel, 2004; Schwab et al., 2006). Eukaryotic cells have evolved several metabolic routes for detoxification, which will be outlined below.

Saccharomyces cerevisiae converts propionate to pyruvate (Pronk et al., 1994). The process starts with a coenzyme A (CoA) transferase to produce propionyl-CoA from

propionate. Propionyl-CoA and oxaloacetate condense to 2-methylcitrate. 2-methylcitrate synthesis occurs either in the mitochondrion via the specific 2-methylcitrate synthase Cit3p or in the peroxisome by the rather unspecific citrate synthase isoform Cit2p (Graybill et al., 2007). 2-methylcitrate is converted to 2-methylisocitrate and subsequently cleaved to succinate and pyruvate by 2-methylisocitrate lyase activity. In *S. cerevisiae* this enzyme (Icl2p) is located in the mitochondrion (Heinisch et al., 1996; Luttk et al., 2000; Huh et al., 2003). Succinate is converted to oxaloacetate in the tricarboxylic acid (TCA) cycle to reenter the cycle. Pyruvate is converted to acetyl-CoA to enter the TCA cycle or is aminated to Alanine (Pronk et al., 1994). In *S. cerevisiae* propionate is speculated to be released by decarboxylation of 2-oxobutanoate during threonine degradation in the mitochondrion (Luttk et al., 2000).

In *Homo sapiens* propionyl-CoA cytotoxicity is manifested in propionic aciduria. This autosomal recessive disorder is highly lethal and relates to defects in propionate degradation (Fenton and Gravel, 2001; Schwab et al., 2006). Propionyl-CoA carboxylase activity prevents propionyl-CoA accumulation by conversion to methyl-malonyl-CoA, which is subsequently transformed to succinyl-CoA. Succinyl-CoA enters the TCA-cycle. The involved enzymes localize to the mitochondrion (Friedberg et al., 1956). Biochemically, propionic aciduria is characterized by accumulation of methyl-malonic acid and, due to activation of alternative pathways of propionate oxidation, by accumulation of propionate, 3-hydroxypropionate and 2-methylcitrate (Fenton and Gravel, 2001). In humans, the degradation of branched chain amino acids (BCAA), methionine, threonine, cholesterol and odd-chain fatty acids gives rise to the propionyl-CoA (Schwab et al., 2006; Morath et al., 2007).

In plants propionyl-CoA is derived from the breakdown of chlorophyll, odd-chain fatty acids, valine and isoleucine (Lucas et al., 2007). Propionic acid is the second most abundant organic acid in soil (Conrad and Klose, 1999), therefore roots are constantly exposed to propionate and exogenous propionate naturally influences plant metabolism in the root. Peroxisomal β -oxidation is required for propionyl-CoA degradation in *Arabidopsis thaliana*. Plants oxidize propionyl-CoA to 3-hydroxypropionate via acrylyl-CoA. Probably, 3-hydroxypropionate is further converted to acetyl-CoA in the mitochondrion (Lucas et al., 2007). Growth of loss-of-

function mutants of peroxisomal acyl-CoA oxidases and 3-hydroxyisobutyryl-CoA hydrolase were shown to be propionate sensitive (Zolman, 2001; Zolman et al., 2008; Khan et al., 2011).

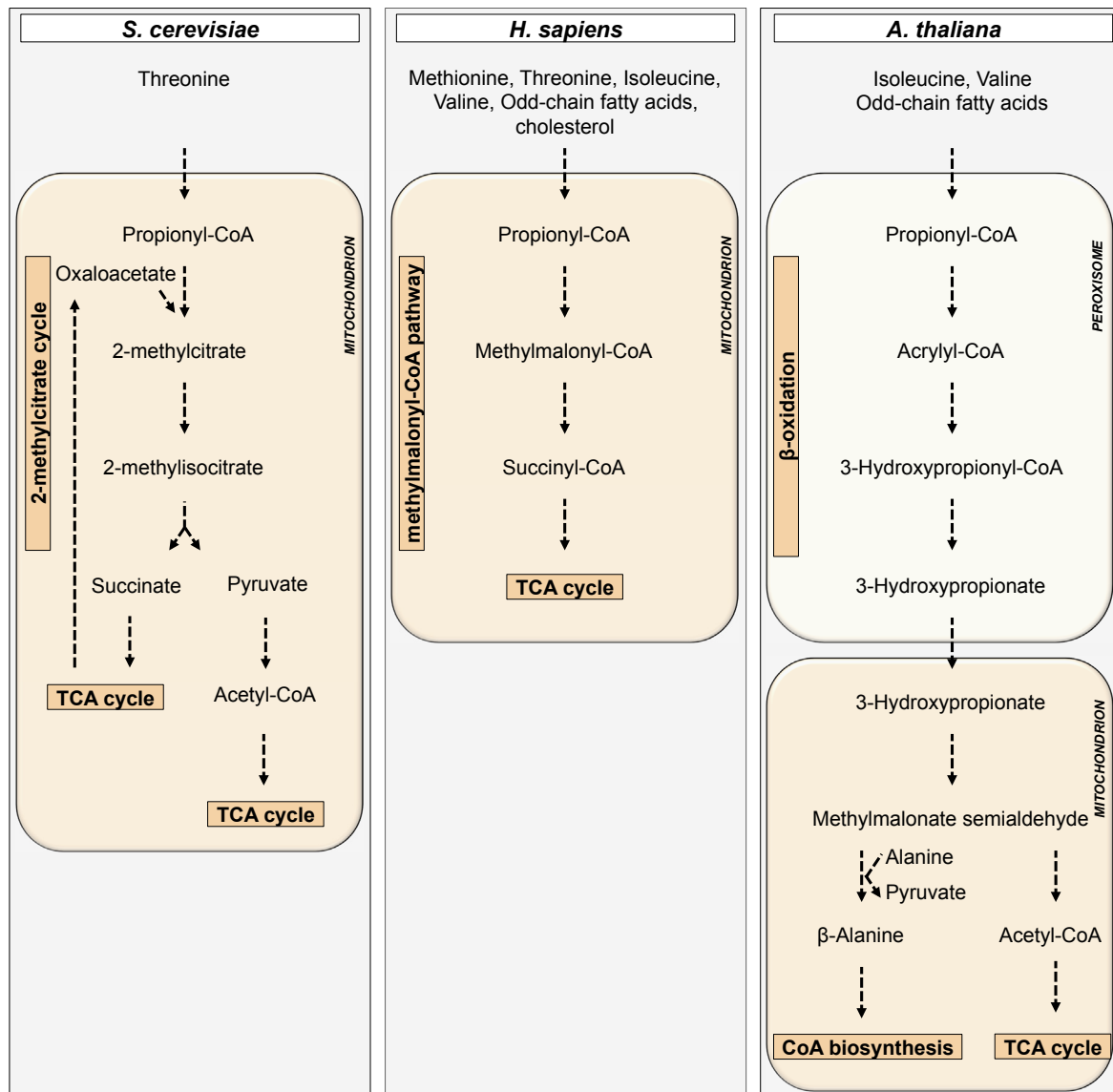


FIGURE 1. Overview of propionate metabolism in *S. cerevisiae*, *H. sapiens* and *A. thaliana*. *Saccharomyces cerevisiae* converts propionate to pyruvate by implication of the 2-methylcitrate cycle. *Homo sapiens* metabolism employs the methylmalonyl-CoA pathway: carboxylation of propionyl-CoA leads to formation of methylmalonyl-CoA, which enters the TCA cycle after conversion to Succinyl-CoA. In *S. cerevisiae* and *H. sapiens* propionate degradation occurs in mitochondria. In *A. thaliana* propionyl-CoA degradation depends on peroxisomal β -oxidation to generate 3-hydroxypropionate, which is exported to mitochondria to be converted to β -alanine or acetyl-CoA.

Propionate conversion involves mitochondria

In yeast, humans and plants mitochondria are needed for propionate degradation. These organelles of 0.1-0.5 μ M are surrounded by two lipid-bilayers. Mitochondria are known as the powerhouse of the cells and central to cellular energy metabolism

by oxidative phosphorylation of ADP to ATP (Mackenzie and McIntosh, 1999; Logan, 2006). The TCA cycle, located in the mitochondrial matrix, supplies the respiratory electron chain with reducing power to pump electrons into the inner membrane space. This generates an electrogenic gradient across the inner mitochondrial membrane, which drives ATP synthesis.

In plants, peroxisomes are needed for propionate degradation

Peroxisomes are ubiquitous and essential plant organelles surrounded by a single lipid bilayer with a diameter of 0.5 - 3 μm . In plants, they harbor major pathways of the central carbon metabolism. Most prominent roles of peroxisomes are storage oil mobilization during early seedling establishment and detoxification of phosphoglycolate in the photorespiratory C_2 cycle of photosynthetic leaves (Hu et al., 2012). Peroxisomal pathways are tightly associated to mitochondrial, cytosolic and plastidic metabolism. Therefore, transport processes of both substrates and cofactors across the peroxisomal membrane is needed for peroxisome function (Visser et al., 2007; Rottensteiner and Theodoulou, 2006; Linka and Esser, 2012; Linka and Theodoulou, 2013).

Plant peroxisomal membranes need to be permeable to propionate

In plants propionate metabolism comprises mitochondria and peroxisomes. This necessitates transport of intermediates across organellar membranes. Membrane proteins catalyze the transport of molecules across membranes in order to metabolically connect cellular compartments (Linka and Weber, 2010). To date, three peroxisomal metabolite transporters have been described in *Arabidopsis thaliana*: the two peroxisomal nucleotide carrier (PNC1 and PNC2; Arai et al., 2008; Linka et al., 2008), the fatty-acid ABC-Transporter (PXA1; Hayashi et al., 1998; Zolman et al., 2001; Footitt et al., 2002) and the peroxisomal NAD/CoA carrier (PXN; Agrimi et al., 2012; Bernhardt et al., 2012). Compared to other subcellular membranes such as the plastid inner envelope, the inner mitochondrial membrane and the plasma membrane the plant peroxisomal membrane remains as one of the least characterized (Linka and Theodoulou, 2013). The identification of peroxisomal membrane proteins (PMPs) is highly challenging (Reumann, 2011). Mitochondrial and plastidial (membrane) proteins typically feature an N-terminal targeting signal (Balsera et al., 2009). Peroxisomal membrane targeting differs from that of matrix proteins (Theodoulou et

al., 2013). For matrix proteins the import process is well described, as the posttranslational sorting of soluble proteins from the cytosol depends on either a C-terminal tripeptide (Consensus: [small]-[basic]-[aliphatic]) or an N-terminal nonapeptide (Consensus: R[L/I/Q]X₅HL; Hu et al., 2012). Proteomics and bioinformatics combined with *in vivo* subcellular studies led to the identification of a postulated majority of peroxisomal matrix proteins (Reumann et al., 2004). Peroxisomal membrane protein import is not well understood. Depending on the insertion mechanism two distinct membrane peroxisomal targeting signals (mPTSs) have been postulated: either positively charged amino residues close to a transmembrane domain or the latter in combination with a nearby or coinciding untypical ER targeting signal. This sequence is not stringent enough to allow identification of PMPs in an *in silico* approach. Reports either describe a posttranslational import of proteins from the cytosol via PEX19, or co-translational ER import into a peroxisomal ER subdomain from which membranes are transported into pre-existing peroxisomes or form new peroxisomes (Mullen and Trelease, 2006; Hu et al., 2012). For the identification of new PMPs experimental proteomics is highly challenging due to low quantities of membranes for the described isolation procedures. In recent attempts several peroxisome biogenesis proteins were identified along with PMP22, PXN and PNC2 (Eubel et al., 2008; Reumann et al., 2009).

MPV17/PMP22 proteins are present in membranes of yeast, animals and plants

Recently, MPV17/PMP22 proteins were implicated with transmembrane transport (Rokka et al., 2009; Reinhold, 2012). Local protein alignment analysis revealed that a absence of prokaryotic homologues, but presence in virtually all eukaryotes (the excavate phylum is supposed to be an exception; Wiese J., unpublished). *S. cerevisiae*, *H. sapiens* and *A. thaliana* display MPV17/PMP22 isoforms in peroxisomes (Tugal et al., 1999; Brosius, 2001; Rokka et al., 2009); Manuscript 1&2 of this thesis) and mitochondria (Trott and Morano, 2004; Spinazzola et al., 2006; Krick et al., 2008; Klodmann et al., 2011) and plants also have these proteins in membranes of the plastid (Ferro et al., 2003; Froehlich et al., 2003; Zybailov et al., 2008). Stress-inducible Yeast Mpv17 protein 1 (Sym1p) localizes to the mitochondrial inner membrane and is involved in an ethanol metabolic process. It was also established that Sym1p and mouse peroxisomal PXMP2 form channels in artificial

lipid bilayers (Rokka et al., 2009; Reinhold, 2012) and are involved in transmembrane transport of short carboxylic acid. The pores were described to allow free diffusion of compounds with molecular masses up to 300 Da (Antonenkov and Hiltunen, 2012).

Aim of this thesis

The goals of this thesis were to generate insight of the metabolite translocation mechanisms and the translocators' effect on sustaining metabolic networks, with a focus on propionate and peroxisomes. Therefore, we describe aspects of the propionyl-CoA metabolism in yeast and plants with a focus on intracellular metabolite transport across mitochondrial and peroxisomal membranes. The roles of *Saccharomyces cerevisiae* Sym1p, *Arabidopsis thaliana* PMP22 and the plant peroxisomal cofactor transport proteins PNC, PXA1 and PXN in propionyl-CoA metabolism were addressed.

Previously it was thought that yeasts are unable to grow on propionate as sole carbon source (Graybill et al., 2007). We could show that yeasts are able to grow on propionate as sole carbon source at elevated temperature, but not at 30°C (*Manuscript 1*). We further addressed whether Sym1p is functionally connected to the 2-methylcitrate cycle and the dependencies between the 2-methylcitrate cycle and methylmalonate conversions. We analyzed intracellular metabolites of *sym1Δ* and showed that the protein is required for TCA intermediate availability. Furthermore we identified the paralogous Sym2p as peroxisomal MPV17/PMP22 protein and discussed its putative function.

As heterologous expression of *Arabidopsis* PMP22 targeted to *sym1Δ* mitochondria led to suppression of the *sym1Δ* growth phenotype (*Manuscript 2*). Therefore, we studied the role of PMP22 in the export of peroxisomal β -oxidation products. To this end we established *Arabidopsis thaliana* RNAi mutants with reduced content of PMP22 and analyzed the physiology of these plants.

Furthermore, our research pointed to a role of PXA1 in import of propionate into plant peroxisomes and we investigated the role of the co-factor transporter PNC and PXN in the metabolism of propionate (*Manuscript 3*).

References

- Agrimi, G., Russo, A., Pierri, C.L., and Palmieri, F.** (2012). The peroxisomal NAD⁺ carrier of *Arabidopsis thaliana* transports coenzyme A and its derivatives. *J Bioenerg Biomembr* **44**: 333–340.
- Antonenkov, V.D. and Hiltunen, J.K.** (2012). *Biochimica et Biophysica Acta. BBA - Molecular Basis of Disease*: 1–13.
- Arai, Y., Hayashi, M., and Nishimura, M.** (2008). Proteomic identification and characterization of a novel peroxisomal adenine nucleotide transporter supplying ATP for fatty acid beta-oxidation in soybean and *Arabidopsis*. *The Plant Cell* **20**: 3227–3240.
- Balsera, M., Soll, J., and Bölter, B.** (2009). Protein import machineries in endosymbiotic organelles. *Cell. Mol. Life Sci.* **66**: 1903–1923.
- Bernhardt, K., Wilkinson, S., Weber, A.P.M., and Linka, N.** (2012). A peroxisomal carrier delivers NAD⁺ and contributes to optimal fatty acid degradation during storage oil mobilization. *The Plant Journal* **69**: 1–13.
- Brock, M. and Buckel, W.** (2004). On the mechanism of action of the antifungal agent propionate. *Eur J Biochem* **271**: 3227–3241.
- Brosius, U.** (2001). Two Different Targeting Signals Direct Human Peroxisomal Membrane Protein 22 to Peroxisomes. *Journal of Biological Chemistry* **277**: 774–784.
- Conrad, R. and Klose, M.** (1999). Anaerobic conversion of carbon dioxide to methane, acetate and propionate on washed rice roots. *FEMS Microbiol. Ecol.* **30**: 147–155.
- Delwiche, E.A.** (1948). Mechanism of Propionic Acid Formation by *Propionibacterium pentosaceum*. *Journal of Bacteriology* **56**: 811–820.
- Desviat, L.R., Pérez, B., Pérez-Cerdá, C., Rodríguez-Pombo, P., Clavero, S., and Ugarte, M.** (2004). Propionic acidemia: mutation update and functional and structural effects of the variant alleles. *Molecular Genetics and Metabolism* **83**: 28–37.
- Elsner, P.** (2006). Antimicrobials and the skin physiological and pathological flora. *Curr. Probl. Dermatol.* **33**: 35–41.
- Eubel, H., Meyer, E.H., Taylor, N.L., Bussell, J.D., O'Toole, N., Heazlewood, J.L., Castleden, I., Small, I.D., Smith, S.M., and Millar, A.H.** (2008). Novel Proteins, Putative Membrane Transporters, and an Integrated Metabolic Network Are Revealed by Quantitative Proteomic Analysis of *Arabidopsis* Cell Culture Peroxisomes. *Plant Physiology* **148**: 1809–1829.
- Fenton, W.A. and Gravel, R.A.** (2001). Disorders of propionate and methylmalonate metabolism. The metabolic and molecular bases of inherited disease **8**: 2165–2193.
- Ferro, M., Salvi, D., Brugière, S., Miras, S., Kowalski, S., Louwagie, M., Garin, J., Joyard, J., and Rolland, N.** (2003). Proteomics of the chloroplast envelope membranes from *Arabidopsis thaliana*. *Mol. Cell Proteomics* **2**: 325–345.
- Footitt, S., Slocombe, S.P., Larner, V., Kurup, S., Wu, Y., Larson, T., Graham, I., Baker, A., and Holdsworth, M.** (2002). Control of germination and lipid mobilization by COMATOSE, the *Arabidopsis* homologue of human ALDP. *EMBO J.* **21**: 2912–2922.
- Friedberg, F., Adler, J., and Lardy, H.A.** (1956). The carboxylation of propionic acid by liver mitochondria. *J. Biol. Chem.* **219**: 943–950.
- Froehlich, J.E., Wilkerson, C.G., Ray, W.K., McAndrew, R.S., Osteryoung, K.W., Gage, D.A., and Phinney, B.S.** (2003). Proteomic study of the *Arabidopsis thaliana* chloroplastic envelope membrane utilizing alternatives to traditional two-dimensional electrophoresis. *J. Proteome Res.* **2**: 413–425.
- Graybill, E.R., Rouhier, M.F., Kirby, C.E., and Hawes, J.W.** (2007). Functional comparison of citrate synthase isoforms from *S. cerevisiae*. *Archives of Biochemistry and Biophysics* **465**: 26–37.
- Hayashi, M., Toriyama, K., Kondo, M., and Nishimura, M.** (1998). 2,4-Dichlorophenoxybutyric acid-resistant mutants of *Arabidopsis* have defects in glyoxysomal fatty acid beta-oxidation. *The Plant Cell* **10**: 183–195.
- Heinisch, J.J., Valdés, E., Alvarez, J., and Rodicio, R.** (1996). Molecular genetics of ICL2, encoding a non-functional isocitrate lyase in *Saccharomyces cerevisiae*. *Yeast* **12**: 1285–1295.

- Hu, J., Baker, A., Bartel, B., Linka, N., Mullen, R.T., Reumann, S., and Zolman, B.K.** (2012). Plant peroxisomes: biogenesis and function. *The Plant Cell* **24**: 2279–2303.
- Huh, W.-K., Falvo, J.V., Gerke, L.C., Carroll, A.S., Howson, R.W., Weissman, J.S., and O'Shea, E.K.** (2003). Global analysis of protein localization in budding yeast. *Nature* **425**: 686–691.
- Keller, M.W., Schut, G.J., Lipscomb, G.L., Menon, A.L., Iwuchukwu, I.J., Leuko, T.T., Thorgersen, M.P., Nixon, W.J., Hawkins, A.S., Kelly, R.M., and Adams, M.W.W.** (2013). Exploiting microbial hyperthermophilicity to produce an industrial chemical, using hydrogen and carbon dioxide. *Proceedings of the National Academy of Sciences* **110**: 5840–5845.
- Khan, B.R., Adham, A.R., and Zolman, B.K.** (2011). Peroxisomal Acyl-CoA oxidase 4 activity differs between Arabidopsis accessions. *Plant Mol Biol* **78**: 45–58.
- Klodmann, J., Senkler, M., Rode, C., and Braun, H.-P.** (2011). Defining the protein complex proteome of plant mitochondria. *PLANT PHYSIOLOGY* **157**: 587–598.
- Krick, S., Shi, S., Ju, W., Faul, C., Tsai, S.-Y., and Böttinger, E.P.** (2008). Mpv17l protects against mitochondrial oxidative stress and apoptosis by activation of Omi/HtrA2 protease. *Proceedings of the National Academy of Sciences* **105**: 14106–14111.
- Lindenkamp, N., Schürmann, M., and Steinbüchel, A.** (2012). A propionate CoA-transferase of *Ralstonia eutropha* H16 with broad substrate specificity catalyzing the CoA thioester formation of carboxylic acids. *Appl Microbiol Biotechnol* **97**: 7699–7709.
- Linka, N. and Esser, C.** (2012). Transport proteins regulate the flux of metabolites and cofactors across the membrane of plant peroxisomes. *Front Plant Sci* **3**: 3.
- Linka, N. and Theodoulou, F.L.** (2013). Metabolite transporters of the plant peroxisomal membrane: known and unknown. *Subcell. Biochem.* **69**: 169–194.
- Linka, N. and Weber, A.P.M.** (2010). Intracellular metabolite transporters in plants. *Molecular Plant* **3**: 21–53.
- Linka, N., Theodoulou, F.L., Haslam, R.P., Linka, M., Napier, J.A., Neuhaus, H.E., and Weber, A.P.M.** (2008). Peroxisomal ATP import is essential for seedling development in *Arabidopsis thaliana*. *The Plant Cell* **20**: 3241–3257.
- Logan, D.C.** (2006). The mitochondrial compartment. *J. Exp. Bot.* **57**: 1225–1243.
- Lucas, K.A., Filley, J.R., Erb, J.M., Graybill, E.R., and Hawes, J.W.** (2007). Peroxisomal metabolism of propionic acid and isobutyric acid in plants. *J. Biol. Chem.* **282**: 24980–24989.
- Luttik, M.A., Kötter, P., Salomons, F.A., van der Klei, I.J., van Dijken, J.P., and Pronk, J.T.** (2000). The *Saccharomyces cerevisiae* ICL2 gene encodes a mitochondrial 2-methylisocitrate lyase involved in propionyl-coenzyme A metabolism. *Journal of Bacteriology* **182**: 7007–7013.
- Mackenzie, S. and McIntosh, L.** (1999). Higher plant mitochondria. *The Plant Cell* **11**: 571–586.
- Morath, M.A., Okun, J.G., Müller, I.B., Sauer, S.W., Hörster, F., Hoffmann, G.F., and Kölker, S.** (2007). Neurodegeneration and chronic renal failure in methylmalonic aciduria—A pathophysiological approach. *J Inherit Metab Dis* **31**: 35–43.
- Mullen, R.T. and Trelease, R.N.** (2006). The ER-peroxisome connection in plants: development of the “ER semi-autonomous peroxisome maturation and replication” model for plant peroxisome biogenesis. *Biochim. Biophys. Acta* **1763**: 1655–1668.
- Poonam, Pophaly, S.D., Tomar, S.K., De, S., and Singh, R.** (2012). Multifaceted attributes of dairy propionibacteria: a review. *World J. Microbiol. Biotechnol.* **28**: 3081–3095.
- Pronk, J.T., van der Linden-Beuman, A., Verduyn, C., Scheffers, W.A., and van Dijken, J.P.** (1994). Propionate metabolism in *Saccharomyces cerevisiae*: implications for the metabolon hypothesis. *Microbiology (Reading, Engl.)* **140 (Pt 4)**: 717–722.
- Reinhold, R., Krüger, V., Meinecke, M., Schulz, C., Schmidt, B., Grunau, S.D., Guiard, B., Wiedemann, N., van der Laan, M., Wagner, R., Rehling, P., and Dudek, J.** (2012). The channel-forming Sym1 protein is transported by the TIM23 complex in a presequence-independent manner. *Molecular and Cellular Biology* **32**: 5009–5021.
- Reumann, S.** (2011). Toward a definition of the complete proteome of plant peroxisomes: Where experimental proteomics must be complemented by bioinformatics. *Proteomics*

- 11: 1764–1779.
- Reumann, S., Ma, C., Lemke, S., and Babujee, L.** (2004). AraPeroX. A database of putative Arabidopsis proteins from plant peroxisomes. *Plant Physiology* **136**: 2587–2608.
- Reumann, S., Quan, S., Aung, K., Yang, P., Manandhar-Shrestha, K., Holbrook, D., Linka, N., Switzenberg, R., Wilkerson, C.G., Weber, A.P.M., Olsen, L.J., and Hu, J.** (2009). In-Depth Proteome Analysis of Arabidopsis Leaf Peroxisomes Combined with in Vivo Subcellular Targeting Verification Indicates Novel Metabolic and Regulatory Functions of Peroxisomes. *Plant Physiology* **150**: 125–143.
- Rokka, A., Antonenkov, V.D., Soininen, R., Immonen, H.L., Pirilä, P.L., Bergmann, U., Sormunen, R.T., Weckström, M., Benz, R., and Hiltunen, J.K.** (2009). Pxmp2 Is a Channel-Forming Protein in Mammalian Peroxisomal Membrane. *PLoS ONE* **4**: e5090.
- Rottensteiner, H. and Theodoulou, F.L.** (2006). The ins and outs of peroxisomes: co-ordination of membrane transport and peroxisomal metabolism. *Biochim. Biophys. Acta* **1763**: 1527–1540.
- Schneider, K., Asao, M., Carter, M.S., and Alber, B.E.** (2011). *Rhodobacter sphaeroides* Uses a Reductive Route via Propionyl Coenzyme A To Assimilate 3-Hydroxypropionate. *Journal of Bacteriology* **194**: 225–232.
- Schwab, M.A., Sauer, S.W., Okun, J.G., Nijtmans, L.G.J., Rodenburg, R.J.T., van den Heuvel, L.P., Dröse, S., Brandt, U., Hoffmann, G.F., Laak, Ter, H., Kölker, S., and Smeitink, J.A.M.** (2006). Secondary mitochondrial dysfunction in propionic aciduria: a pathogenic role for endogenous mitochondrial toxins. *Biochem. J.* **398**: 107–112.
- Spinazzola, A. et al.** (2006). MPV17 encodes an inner mitochondrial membrane protein and is mutated in infantile hepatic mitochondrial DNA depletion. *Nat. Genet.* **38**: 570–575.
- Strauss, G. and Fuchs, G.** (1993). Enzymes of a novel autotrophic CO₂ fixation pathway in the phototrophic bacterium *Chloroflexus aurantiacus*, the 3-hydroxypropionate cycle. *Eur J Biochem* **215**: 633–643.
- Suhr, K.I. and Nielsen, P.V.** (2004). Effect of weak acid preservatives on growth of bakery product spoilage fungi at different water activities and pH values. *Int. J. Food Microbiol.* **95**: 67–78.
- Suvorova, I.A., Ravcheev, D.A., and Gelfand, M.S.** (2012). Regulation and Evolution of Malonate and Propionate Catabolism in Proteobacteria. *Journal of Bacteriology* **194**: 3234–3240.
- Theodoulou, F.L., Bernhardt, K., Linka, N., and Baker, A.** (2013). Peroxisome membrane proteins: multiple trafficking routes and multiple functions? *Biochem. J.* **451**: 345–352.
- Trott, A. and Morano, K.A.** (2004). SYM1 is the stress-induced *Saccharomyces cerevisiae* ortholog of the mammalian kidney disease gene Mpv17 and is required for ethanol metabolism and tolerance during heat shock. *Eukaryotic Cell* **3**: 620–631.
- Tugal, H.B., Pool, M., and Baker, A.** (1999). Arabidopsis 22-kilodalton peroxisomal membrane protein. Nucleotide sequence analysis and biochemical characterization. *Plant Physiology* **120**: 309–320.
- Visser, W.F., Van Roermund, C.W.T., Ijlst, L., Waterham, H.R., and Wanders, R.J.A.** (2007). Metabolite transport across the peroxisomal membrane. *Biochem. J.* **401**: 365–375.
- Zolman, B.K.** (2001). chy1, an Arabidopsis Mutant with Impaired beta -Oxidation, Is Defective in a Peroxisomal beta -Hydroxyisobutyryl-CoA Hydrolase. *Journal of Biological Chemistry* **276**: 31037–31046.
- Zolman, B.K., Martinez, N., Millius, A., Adham, A.R., and Bartel, B.** (2008). Identification and characterization of Arabidopsis indole-3-butyric acid response mutants defective in novel peroxisomal enzymes. *Genetics* **180**: 237–251.
- Zolman, B.K., Silva, I.D., and Bartel, B.** (2001). The Arabidopsis pxa1 mutant is defective in an ATP-binding cassette transporter-like protein required for peroxisomal fatty acid beta-oxidation. *Plant Physiology* **127**: 1266–1278.
- Zybailov, B., Rutschow, H., Friso, G., Rudella, A., Emanuelsson, O., Sun, Q., and van Wijk, K.J.** (2008). Sorting signals, N-terminal modifications and abundance of the chloroplast proteome. *PLoS ONE* **3**: e1994.

IV.1 Manuscript 1

Stress-inducible yeast MPV17 protein 1 coordinates TCA cycle intermediate availability and is implicated in propionate metabolism.

Jan Wiese, Andreas P.M. Weber and Nicole Linka[¶]

Department of Plant Biochemistry, Heinrich-Heine University Düsseldorf, 40225 Düsseldorf, Germany

[¶] Corresponding author

Abstract

Mutations in the nuclear genes encoding human *Mpv17* or the functional yeast orthologue *Sym1p* result in mitochondrial DNA depletion. In humans *MPV17* loss provokes lethal diseases, therefore the yeast mutant was exploited to gain insight in *Mpv17* function.

Mitochondrial *Sym1p* has been described to be required for maintenance of respiratory function at elevated temperature. Consequently at 37°C *sym1Δ* cells were compromised to grow on non-fermentable carbon sources. Furthermore *SYM1* ablation was detrimental to glycogen accumulation, mitochondrial ultrastructure and mtDNA replication at elevated temperatures. *Sym1p* forms an ion channel in artificial lipid bilayers and the *sym1Δ* growth defects were suppressed by either supply of amino acids anaplerotic to the tricarboxylic acid (TCA) cycle or multi-copy expression of yeast endogenous mitochondrial carrier family members that transport TCA cycle intermediates across the mitochondrial inner membrane.

The biochemical role of *Sym1p* is still unclear. This study revealed *Sym1p* to coordinate availability of TCA intermediates. At restrictive growth conditions metabolites originating from mitochondrial pyruvate conversion showed elevated levels. Feeding of individual TCA or glyoxylate cycle intermediates allowed for *sym1Δ* growth to proceed at 37°C. Furthermore we showed *Sym1p* to be required for growth on propionate and methylmalonate. Deletion of *SYM1* in the background of 2-methylcitrate cycle mutants led to increased sensitivity to ethanol than in the single mutants. We show that 2-methylcitrate-cycle activity is needed for methylmalonate degradation. Finally, we report the paralogous *Sym2p* to localize to the peroxisomal membrane and revealed *sym2Δ* growth to be compromised by high levels of ethanol. We discuss possible transport mechanisms of *Sym1p* and *Sym2p*.

Introduction

Stress-inducible Yeast MPV17 protein 1 (Sym1p) is an integral mitochondrial inner membrane protein with a C-terminal MPV17/PMP22 (peroxisomal membrane protein of 22 kDa) domain (Trott and Morano, 2004; Spinazzola et al., 2006). Mutation of human *Mpv17* causes a hepatocerebral form of mitochondrial DNA depletion syndrome (MDDS) associated with heterogeneous clinical phenotypes. MDDS patients frequently die in infancy or early childhood after exhibiting hypoglycemia, organ dysfunction and neurological symptoms (Suomalainen and Isohanni, 2010). Sym1p is considered a functional orthologue of MPV17 as evidenced by genetic complementation (Trott and Morano, 2004). Yeast *sym1Δ* has been used as a model to study *Mpv17*^{-/-} related MDSS (Spinazzola et al., 2006; Dallabona et al., 2010). To date molecular functions of both MPV17 and Sym1p remain unknown.

Mitochondrial DNA is essential for oxidative phosphorylation, because it encodes components of the mitochondrial respiratory chain (Rötig and Poulton, 2009). *sym1Δ* is respiratory deficient at elevated temperature: activity of mitochondrial complex II, succinate dehydrogenase, catalyzing oxidation of succinate to fumarate in the tricarboxylic acid (TCA) cycle is lowered, which is accompanied by reduced mitochondrial electron flow (Dallabona et al., 2010). However, loss of SDH was not associated with mitochondrial DNA depletion (Smith et al., 2007). Nevertheless, *sym1Δ* growth is compromised on non-fermentable carbon sources at 37°C and on rich media glycogen accumulation was reduced (Trott and Morano, 2004; Dallabona et al., 2010). Glycogen synthesis is initiated during nutrient limitation and depends on TCA cycle intermediate export to the cytosol (Wilson et al., 2010).

In a multicopy suppressor screen of yeast endogenous genes, overexpression of mitochondrial carrier family proteins (Ymc1p or Odc1p) compensated for *SYM1* loss (Dallabona et al., 2010). *YMC1* and *ODC1* were identified to enable utilization of fatty acids as sole carbon source by importing peroxisome derived dicarboxylic acids (Trotter et al., 2005). 2-Oxodicarboxylate carrier (e.g. Odc1p) export 2-ketoadipate to the cytosol in exchange for TCA cycle intermediates such as 2-oxoglutarate and citrate (Fiermonte et al., 2001; Palmieri et al., 2001). This led to hypothesize that Sym1p is involved in metabolite transport (Dallabona et al., 2010). Recently, Sym1p was shown to form a ion channel in artificial lipid bilayers and the calculated pore size of about 1.6 nm theoretically allows transfer of small solutes (Reinhold et al.,

2012). The mouse homologue Pxmp2 was shown to enable translocation of pyruvate and 2-oxoglutarate across the peroxisomal membrane (Rokka et al., 2009).

Sym1p is needed to maintain mitochondrial ultrastructure. *sym1Δ* exhibited balloon shaped *cristae* (Dallabona et al., 2010). The disorganization of the mitochondrial inner membrane and associated protein-DNA nucleoid complexes was proposed to lead to failures in mtDNA replication and thus causes mtDNA depletion as a secondary effect (Dallabona et al., 2010). Also in mammals mitochondrial inner membrane shape loss and MDSS are hypothesized to be indirect consequences of MPV17 loss: in *Mpv17^{-/-}* mice some tissues had intact mtDNA, though MDSS symptoms were persistent (Viscomi et al., 2009).

Genes associated with the mtDNA depletion syndrome are either directly involved in maintaining mitochondrial DNA or supplying desoxynucleotides for mtDNA synthesis (Suomalainen and Isohanni, 2010). Also a mutation of the TCA cycle enzyme succinyl-CoA ligase (*Sucla2^{-/-}*) causes MDSS. Here, it is thought to arise due to loss of interaction with nucleoside diphosphate kinase, which is directly involved in mtDNA synthesis (van Hove et al., 2010). In *Sucla2^{-/-}* conversion of methylmalonyl-CoA to succinyl-CoA is restricted and consequently *Sucla2^{-/-}* patients display methylmalonic and methylcitric aciduria (Ostergaard et al., 2007). Methylmalonyl-CoA and 2-methylcitrate are intermediates of propionyl-CoA metabolism (Fenton and Gravel, 2001). In humans propionyl-CoA is released in the degradation of amino acids, odd-chain fatty acids and cholesterol (Schwab et al., 2006). Propionyl-CoA will be carboxylated to methylmalonyl-CoA, which enters the TCA cycle after isomerization to succinyl-CoA (Desviat et al., 2004). Methylmalonic acid (MMA) and methylmalonyl-CoA were shown to inhibit mitochondrial energy metabolism, by affecting mitochondrial respiration complexes and succinate transport (Saad et al., 2006; Mirandola et al., 2008; Melo et al., 2012).

In humans propionic aciduria has largely the same symptoms as methylmalonic aciduria (Deodato et al., 2006). In yeast propionate is thought to arise from oxidative decarboxylation of 2-oxobutanoate, which is produced in mitochondria during threonine degradation (Luttik et al., 2000) and an increase in propionic acid was measured when cells were exposed to ethanol (Li et al., 2012). It was speculated that propionate is shuttled across membranes as propionylcarnitine in exchange for carnitine in yeast and humans (Indiveri et al., 1998; Palmieri et al. 1999). In humans

mutations of the catabolic pathways of isoleucine, valine and threonine are associated with MMA aciduria. Propionic acid induced stress is accompanied by reduced ATP and also by higher pyruvate levels (Lourenço et al., 2011) and propionyl-CoA inhibits several CoA-dependent enzymes including pyruvate dehydrogenase (Maerker et al., 2005; Horswill et al., 2001; Deodato et al., 2006).

Work of Sumegi et al. (1990) suggested that *S. cerevisiae* followed the mammalian methylmalonyl-CoA pathway of propionate conversion. Comparison of enzyme activities in the methylmalonyl-CoA pathway and the 2-methylcitric acid cycle pointed towards propionate metabolism by the 2-methylcitric acid cycle (Figure 1; Pronk et al., 1994). Later this was confirmed revelation that Baker's yeast relies on citrate synthase 3 (Cit3p) activity to catalyze condensation of propionyl-CoA and oxaloacetate to 2-methylcitrate (Graybill et al., 2007). After isomerization to 2-methylisocitrate the mitochondrial isocitrate lyase (Icl2p) cleaves 2-methylisocitrate into pyruvate and succinate (Luttik et al., 2000).

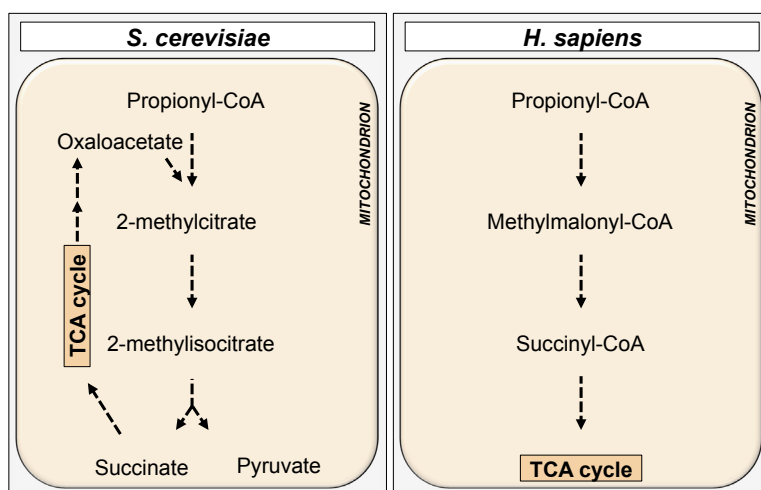


FIGURE 1. Overview of mitochondrial propionyl-CoA metabolism in *Saccharomyces cerevisiae* and *Homo sapiens*.

Here, we address if Sym1p is involved in propionyl-CoA metabolism. Propionate exposure was previously associated to an increased mtDNA mutation frequency in aerobically grown *S. cerevisiae* (Piper, 1999). Deletion of *SYM1* in the background of propionate degrading enzymes led to enhanced ethanol sensitivity. Growth restrictions in *sym1Δ* were accompanied by a lack in TCA intermediate availability. We discuss the importance and role of *SYM1* paralogue *SYM2* (*YOR292C*). We show its peroxisomal localization and an involvement in ethanol metabolism.

Results

Our studies specify roles of *SYM1* and its paralogue *YOR292c*, hereafter referred to as *SYM2* due to structural and co-regulatory parallels (Fig. S1/S2).

Sym1p is required to counteract genotoxic stress

The general stress response in *S. cerevisiae* is mainly controlled by the transcription factor Msn2/4p (Domitrovic et al., 2006), which was suggested to bind to the *SYM1* promoter region (Dallabona et al., 2010). *sym1Δ* were unable to grow on non-fermentable carbon sources at 37°C (Trott and Morano, 2004). We investigated growth of *sym1Δ* in other environmental stress conditions. To this end, *sym1Δ* performance was monitored in YPD supplemented with growth manipulating concentrations of protein denaturants, osmotically active solutes, oxidants, heavy metals and Geldanamycin, which inhibits central heat shock chaperone HSP90 (Cardenas et al., 1999; Burg et al., 2007; Szopinska et al., 2011; Rios et al., 2013). In comparison to the wild-type *sym1Δ* displayed no sensitivity to these compounds at 30°C, thus Sym1p can be excluded to determine resistance to the applied stress (Figure 2). At temperatures >36°C yeasts activate a protecting transcriptional program, which was termed the heat shock response (Morano et al., 2012). *SYM1* was first characterized due to transcriptional upregulation in heat shock (Trott and Morano, 2004). At 37°C we observed a mild reduction of growth in hyperosmotic conditions (1.2 M NaCl; 0.5 M Urea). A need of Sym1p was more obvious in response to manganese and cobalt cations. Here *sym1Δ* growth was inhibited and characterized by a higher frequency of *petite* colonies than in the wild-type control. Preliminary research linked formation of *petite* colonies to non-functional mitochondrial respiration, as a result of defective mtDNA replication (Baruffini et al., 2010). Both manganese and cobalt are genotoxic and known to damage nuclear and mitochondrial DNA (Assem et al., 2011; Simonsen et al., 2012). Thus our finding is in line with an earlier report, which associated mutated *SYM1* with abnormal mitochondrial genome maintenance (Spinazzola et al., 2006). Hence, at 37°C Sym1p contributes to cellular viability by protecting the cell from mtDNA depletion. Thus it may be inferred that the Sym1p mediated mechanism of thermotolerance is linked to mtDNA maintenance.

Transcriptome profiling of *sym1Δ* in restrictive growth conditions unraveled abnormal expression of metabolic genes rather than conventional stress regulatory genes.

Based on these previous findings altered carbohydrate flux in *sym1Δ* was assumed (Trott and Morano, 2004; visualized in Figure S3).

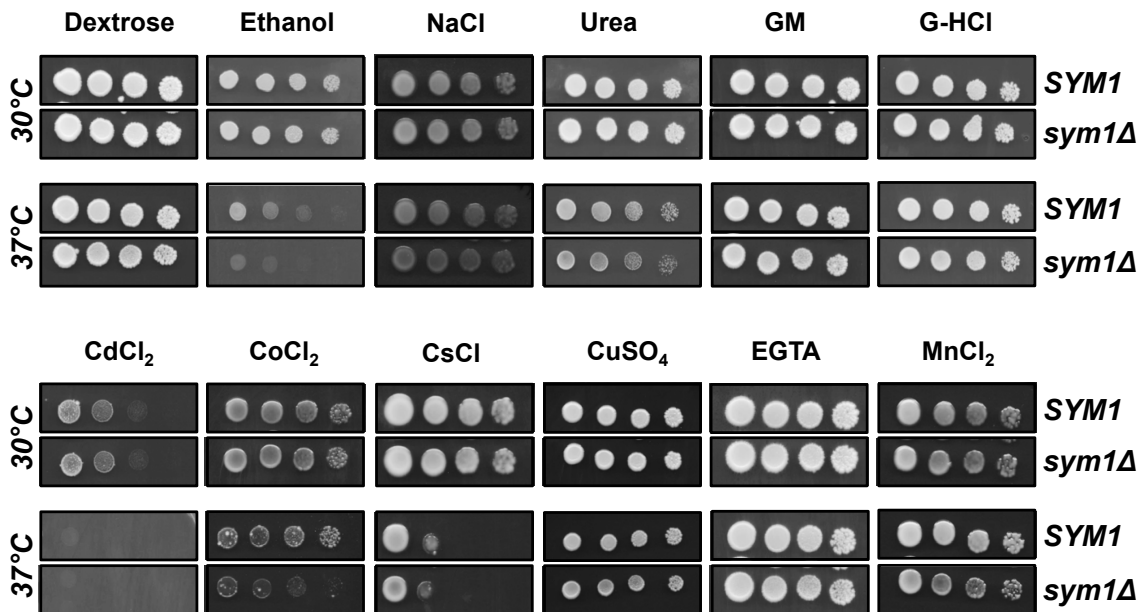


FIGURE 2. Growth of *sym1Δ* on "stress media".

In hyperosmotic, denaturing and oxidative conditions *sym1Δ* displayed wild-type growth at 30°C, but a mild sensitivity to 1.2 M NaCl, 0.5 M Urea, 5 mM Cobalt chloride (CoCl₂) and 6 mM Manganese chloride (MnCl₂). Other compounds were concentrated as following: Geldanamycin (GM) 10mM, Guanidinium-Hydrochloride (G-HCl) 5 mM, Cadmium chloride (CdCl₂) 7.5 mM, Cesium chloride (CsCl) 100 mM, Copper sulfate (CuSO₄) 12 mM, Ethylene glycol tetra-acetic acid (EGTA) 2 mM. The extent of *sym1Δ* growth restriction is exemplified by the ethanol control (YP + 2 % (v/v) ethanol). Cells grown in YPD were serially diluted and spotted. The plates were photographed after three or four (Cobalt, Cadmium) days of incubation at 30°C or 37°C.

In permissive growth Sym1p is needed to accumulate glycogen

Dallabona et al. (2010) described a defect of *sym1Δ* in gluconeogenesis on glucose medium at 37°C. Our analysis shows that *sym1Δ* cells were able to synthesize glycogen, as shown by qualitative co-staining of the glycogen contents in comparison to the glycogen-free *gsy1Δ gsy2Δ* control (Farkas et al., 1991; Figure 3A). However, unlike wild-type cells, after 72 h of growth *sym1Δ* cells ceased accumulation of glycogen and started to degrade stored glycogen reserves. The premature glycogen consumption points to an impaired energy status in *sym1Δ*.

sym1Δ glycogen depletion occurs independently of mitochondrial C₄ export

Glycogen is synthesized with implication of gluconeogenesis, which is initiated by conversion of pyruvate, malate or oxaloacetate in the cytosol (Ljungdahl and Daignan-Fornier, 2012). The mitochondrial carrier family protein UCP2 has been suggested to export C₄ compounds such as malate to the cytosol coupled

to the import of organic phosphate. In humans UCP2 prevented mitochondrial accumulation of glutamine derived C₄ metabolites (Voza et al., 2014). We constitutively expressed the highly similar *Arabidopsis thaliana* UCP2 in *sym1Δ* (29% identity to human UCP2) to test for recovery of gluconeogenic flux. UCP2 expression did not suppress *sym1Δ* phenotypes (Figure 3B). Under the premise of functional expression, the conclusion would be that Sym1p function does not reside in pure Carbon export. The multicopy suppressors Ymc1p and Odc1p counter exchange carboxylates. Odc1p may import 2-oxoglutarate in exchange for 2-oxoadipate or enable shuttling of malate/aspartate for indirect transfer of reducing equivalents (Palmieri et al., 2001) and thus support mitochondrial respiration by provision of cytosolic or peroxisomal metabolites.

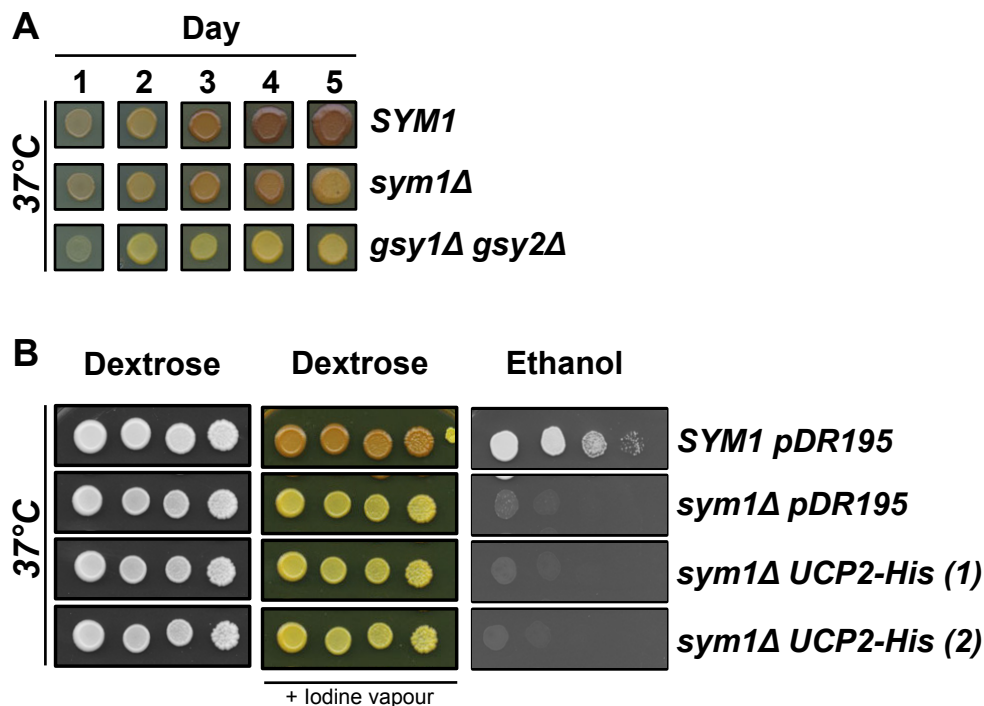


FIGURE 3. Sym1p is required to for accumulation of glycogen reserves at 37°C.

(A) Photograph of glycogen stained SYM1, *sym1Δ* and *gsy1Δ gsy2Δ* cells in a time course. *gsy1Δ gsy2Δ* cells are devoid of glycogen synthase activity and therefore unable to produce glycogen. Cells grown in YPD were serially diluted and spotted. Because no growth defects were observed at 30°C, only representative 37°C plates are shown. After the indicated time of growth cells were exposed to iodine vapor to stain glycogen (brownish color) and photographed.

(B) Expression of AtUCP2 does not suppress *sym1Δ* phenotypes. Cells transformed with the empty expression vector (pDR195) were spotted as control. The strains UCP2-His (1)/(2) were obtained from independent transformation events. After 5 days of growth cells were (exposed to iodine vapor to stain glycogen) photographed.

Sym1p coordinates TCA cycle intermediate availability

We performed metabolite profiling to address the potential cause of the glycogen depletion, but also to identify the basis of respiratory deficiency with ethanol as carbon source at 37°C. We chose to extract polar intracellular metabolites in rich

media with ethanol as sole carbon source: a condition which allows *sym1Δ* cells to grow, but with a considerably reduced rate in comparison to the wild type (Figure 4A). We extracted metabolites one, three and 18 h after shift to 37°C (Figure 4B). Rich medium (yeast extract/bacto-peptone) without ethanol was used as control. To our surprise, utilization of yeast extract and peptone as C-source led to reduced cell density of *sym1Δ* after 18 h of growth in liquid medium compared to the wild-type (Figure 4C) and the growth reduction was visible in serial dilution drop tests on YP medium (Figure 8B). This result showed *SYM1* function to be independent of ethanol.

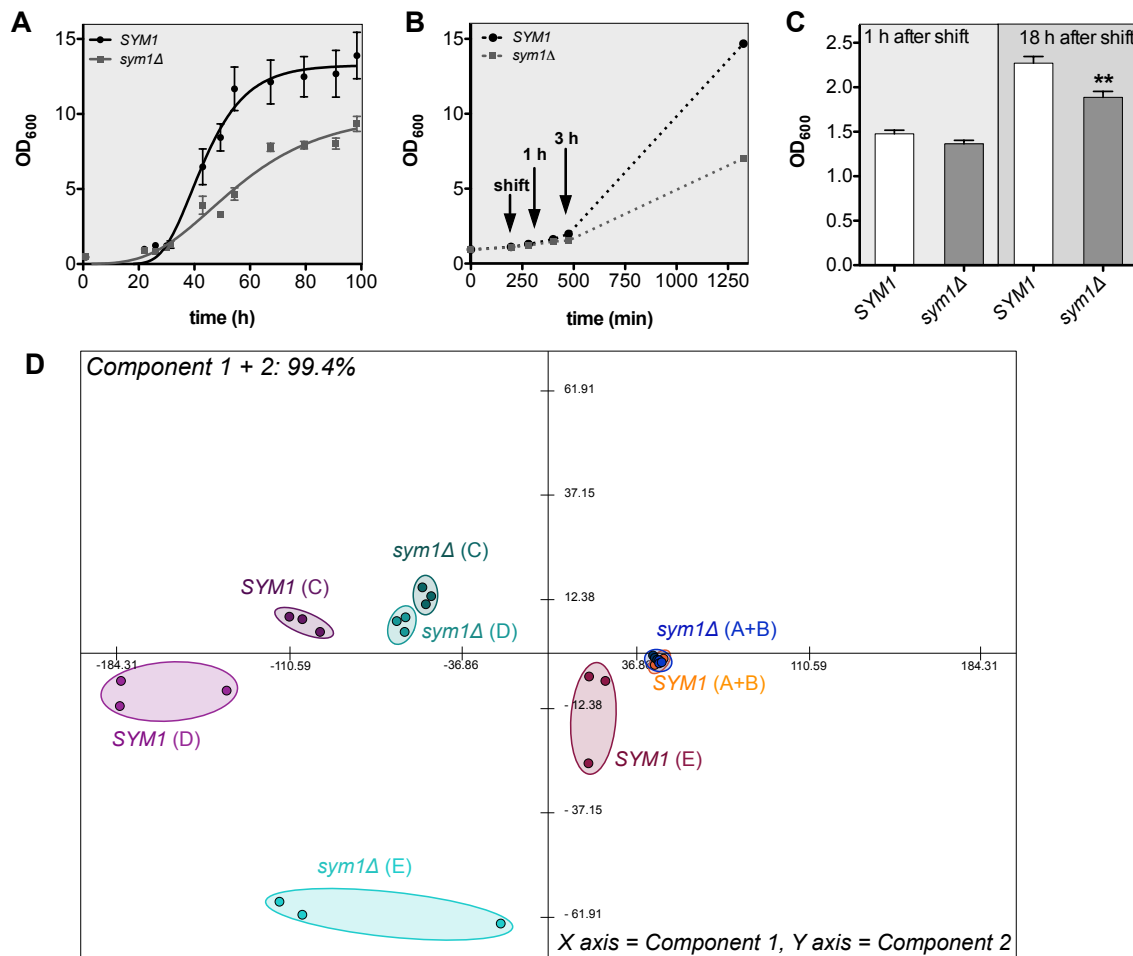


FIGURE 4. *Sym1p* requirement for wild-type growth at 37°C is reflected by a PCA analysis. **(A)** Mean OD_{600} (+SE; $n=5$) during growth of SYM1 and *sym1Δ* in YPE at 37°C. The growth curve is a non-linear regression of the data by the Gompertz growth equation (Zwietering et al., 1990). **(B)** Representative OD_{600} values for growth of SYM1 and *sym1Δ* in YPE after shift from 30°C to 37°C (*time points of harvest for metabolite extraction indicated*). **(C)** Mean OD_{600} (+SE; $n=3$) of SYM1 and *sym1Δ* cultures in YP medium after shift from 30°C to 37°C (at the time point of harvest for metabolite extraction). **(D)** 2D-PCA score plot of metabolite profiles. The plots were applied for the 24 annotated metabolites detected in YP grown cells 1 h (A) or 18 h (B) after shift to 37°C or YPE grown cells 1 h (C), 3 h (D) and 18 h (E) after shift to 37°C. PCA was conducted by the MultiExperiment Viewer (Saeed et al., 2003). Biological replicates are encircled. PCA: principal component analysis

Metabolite contents barely changed in the yeast extract/bacto-peptone control. This was confirmed by principal component analysis (PCA), which revealed *sym1Δ* and wild-type to have almost identical variations in metabolite levels (Figure 4D). None of the quantified metabolites showed a significant reduction in *sym1Δ* (Figure 5 and 6).

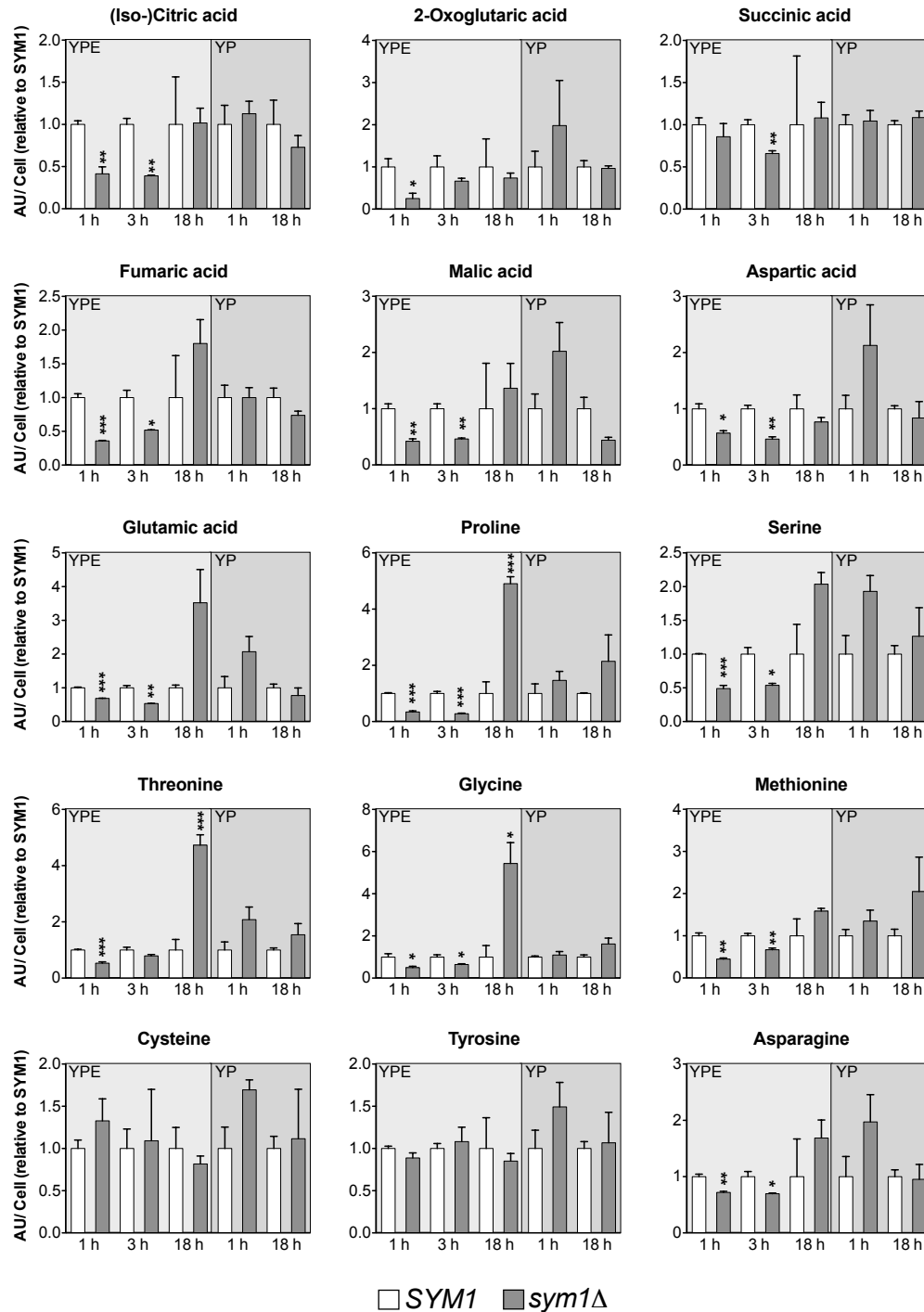


FIGURE 5. Plots of mean content (+SE; n=3) of TCA intermediates and amino acids in arbitrary units of SYM1 and *sym1Δ* cells grown in YPE and YP after shift from 30°C to 37°C. Differences between the mean of biological replicates were marked as statistically significant (t-test) with the SYM1 control by (*), (**), or (***) at respective significance levels of ($P < 0.05$), ($P < 0.01$) or ($P < 0.001$).

The growth difference in YP was reflected in significantly elevated lactate and alanine levels in *sym1Δ* 18 h after the shift to 37°C. Both, when fed the mutant as sole carbon source were poorly used to support growth (Dallabona et al., 2010; Figure 7). This indicated catabolic pathways to be compromised. Typically, alanine and lactate are converted within the mitochondrion to pyruvate to support respiratory growth.

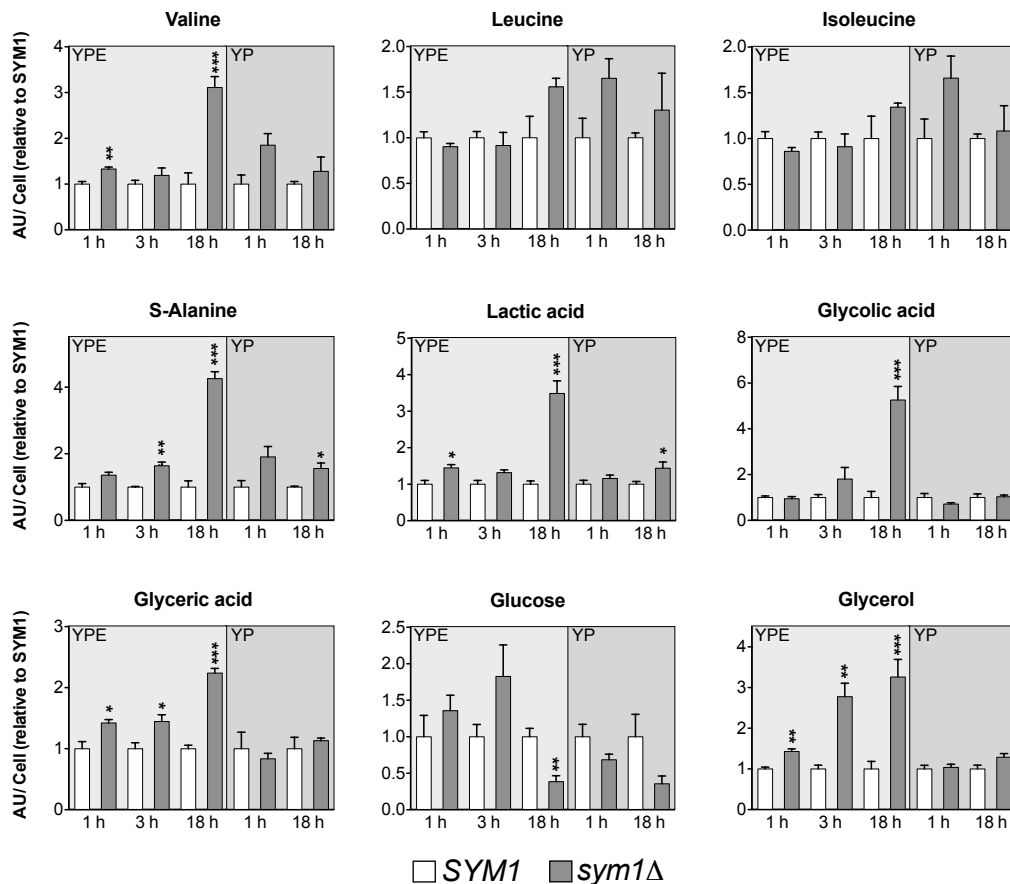


FIGURE 6. Plots of mean content (+SE; n=3) of amino acids, short chain carboxylic acid and carbohydrates in arbitrary units of SYM1 and *sym1Δ* cells grown in YPE and YP after shift from 30°C to 37°C. Differences between the mean of biological replicates were marked as statistically significant (t-test) with the SYM1 control by (*), (**) or (***) at respective significance levels of (P < 0.05), (P < 0.01) or (P < 0.001).

PCA analysis of metabolites extracted from ethanol grown cells revealed highly divergent metabolite variation pattern between the mutant and wild type (Figure 4D). The TCA intermediates malate, (iso)citrate, fumarate, succinate and 2-oxoglutarate were reduced in the early shift, but recovered to wild-type niveau after 18 h. Aspartate, glutamate and proline that can be easily interconverted to TCA cycle intermediates were depleted too (Figure 5). The analysis indicated *sym1Δ* cells to have a deregulated flux through the TCA cycle immediately after shift to 37°C. Thus, the *sym1Δ* growth compromise is likely due to a lack of TCA cycle intermediate

availability. After 18 h of growth the defect was compensated, but accompanied by increased contents of threonine, proline and glycine. C₃ molecules such as glycerate, glycolate, glycerol and lactate displayed progressively increasing levels until 18 h of growth. As in the ethanol free medium alanine featured higher levels in *sym1Δ*, but notably also in the early phase after the temperature shift (Figure 6). Valine was significantly increased 1 h and 18 h after shift. Furthermore, after 18 h of growth in YPE we detected lower levels of glucose, which is consistent with the assumption of altered gluconeogenic flux.

Sym1p exerts negligible effect on fatty acid composition

Membrane fluidity adjustment is central to ethanol and heat tolerance and is connected to fatty acid metabolism (Piper, 1995; Dinh et al., 2008). Fatty acid synthesis is linked to TCA cycle activity and depends on cellular acetyl-CoA pools (Tehlivets et al., 2007). We addressed if *sym1Δ* growth restriction is related to restrictions in fatty acid metabolism and measured contents of major membrane fatty acid constituents (Figure 6A). C16:0, C16:1, C18:0 and C18:1 were quantified after 18 h of growth in either YP or YPE at 37°C. We did not detect significant differences in the relative membrane composition of fatty acids normalized to dry weight. The successful adjustment of lipid compositions is reflected in the C18:0 desaturation in YPE. Ethanol tolerance was described to depend on increased of oleic acid (C18:1) content (You et al., 2003). *sym1Δ* desaturated C18:0 to C18:1, as indicated by increase C18:1 in ethanol medium (Figure 7A). Therefore, Sym1p mechanism of ethanol tolerance might not be connected to membrane adjustments.

We also tested growth on oleic acid as sole carbon source. Oleic acid degradation is initiated in peroxisomes and releases acetyl-CoA or succinate in the cytosol, which is imported into mitochondria for degradation via the TCA cycle. At 30°C *sym1Δ* is able to grow on oleic acid (Figure 7B). At 37°C *sym1Δ* did not display wild-type growth, which was probably due to defects in mitochondrial utilization of oleic acid degradation products.

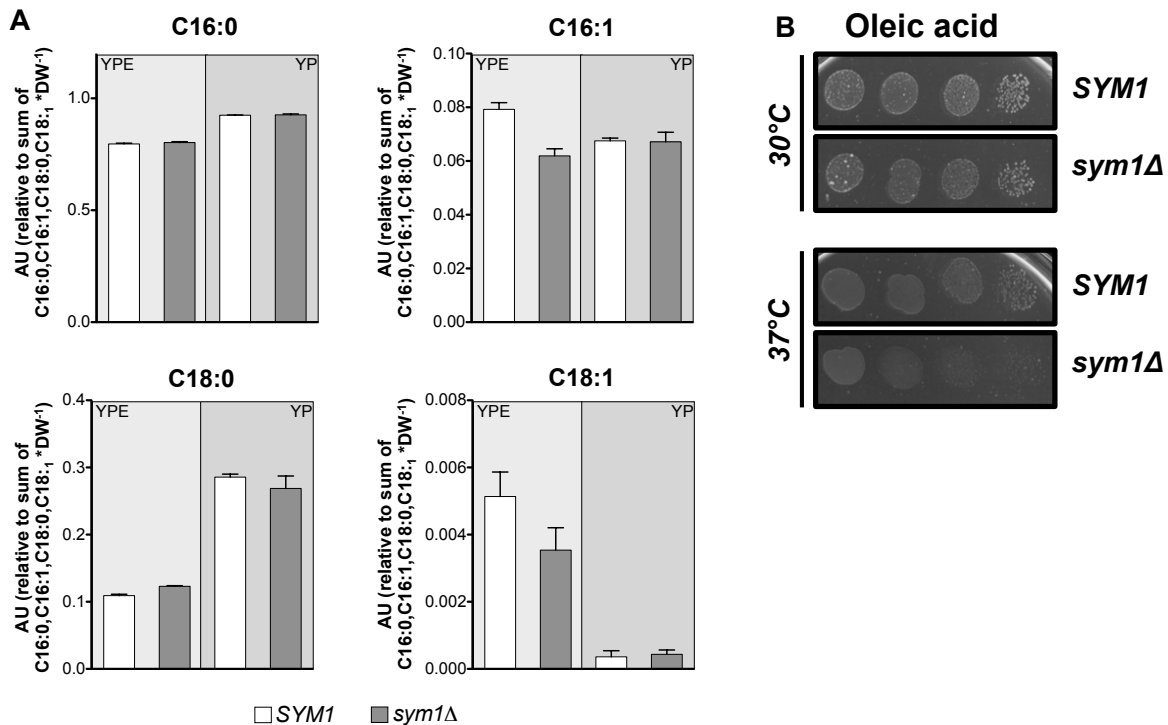


FIGURE 7. Analysis of fatty acid metabolism in *sym1Δ*.

(A) Mean of fatty acid methyl ester levels (+SE; n=4) relative to dry weight normalized contents of C16:0,16:1,18:0,18:1 in *SYM1* and *sym1Δ*. Data shown in arbitrary units.

(B) Growth of *SYM1* and *sym1Δ* on 0.1 % (w/v) oleic acid (C18:1) as sole carbon source. Cells grown in YPD were transferred to 0.3 % glucose for 24 h, serially diluted and spotted. The plates were photographed after 14 days of incubation at 30°C or 37°C.

At 37°C sym1Δ is able to grow on pyruvate, succinate, glycolate and glyoxylate

Multicopy expression of yeast endogenous TCA cycle intermediate transporting Mitochondrial Carrier Family (MCF) members *YMC1* and *ODC1* was able to suppress the growth phenotype (Dallabona et al., 2010). Thus we expected, that supply of individual TCA cycle intermediates would lead to growth improvement. Growth on TCA intermediates had different effects in comparison to the Yeast-Extract/Bacto-Peptide control (Figure 8), which had no extra C-source. Oxaloacetate diminished *sym1Δ* growth. In contrast to citrate, supply of malate led to slightly better but not wild-type growth. Provision of 5 mM concentrated pyruvate or succinate almost restored wild-type growth, whereas 100 mM pyruvate completely restored wild-type growth.

C₂ acids such as glycolic acid and glyoxylic acid also restored the growth to wild-type niveau. Feeding of amino acids did not have a positive effect. Supply of aspartate did not result in the rescue of growth at 37°C as previously published by Dallabona et al. (2010). In summary, exogenous supply of C₂-C₆ carboxylic acids at 37°C altered metabolism in a way that enabled wild-type growth.

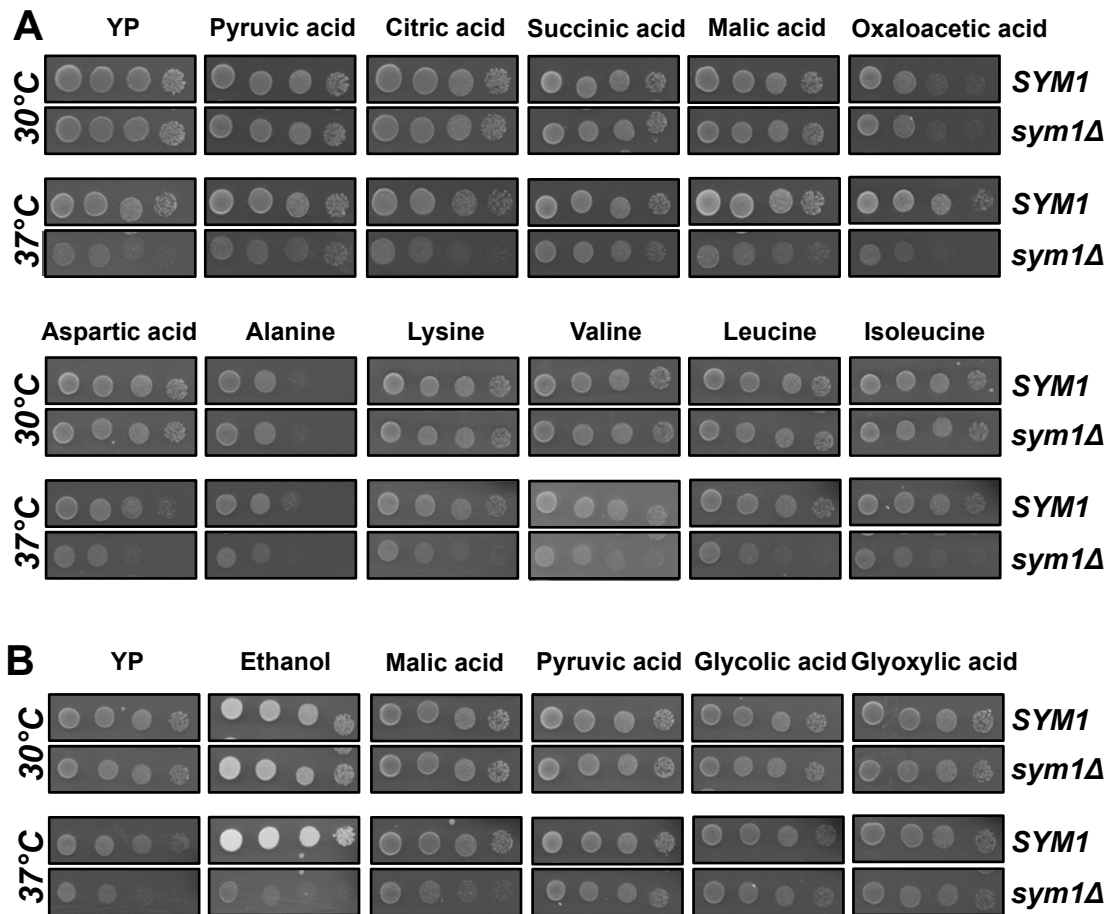


FIGURE 8. Analysis of *sym1Δ* growth on several carbon sources.

(A) Photographs of *SYM1* and *sym1Δ* in 30°C/37°C on Yeast-extract/Bacto-peptone medium supplemented with 5 mM of pyruvate, citrate, succinate, malate and oxaloacetate.

(B) Photographs of *SYM1* and *sym1Δ* in 30°C/37°C on Yeast-extract/Bacto-peptone medium supplemented with 100 mM of pyruvate, malate, glycolate and glyoxylate.

The extent of *sym1Δ* growth restriction is exemplified by the ethanol control (YP + 2% (v/v) ethanol). Cells grown in YPD were serially diluted and spotted. The plates were photographed after 4 days of incubation at 30°C or 37°C.

***sym1Δ* was unable to grow on propionate as sole carbon source**

Sym1p was suggested to form an aqueous channel (Reinhold et al., 2012) permeable to small solutes and the peroxisomal mouse homologue was shown to facilitate translocation of C₃ carboxylic acids across the peroxisomal membrane (Rokka et al., 2009). We showed that C₃ compounds such as lactate and glycerate were increased in *sym1Δ*. In yeasts the C₃ monocarboxylic acid propionate is degraded within mitochondria (Graybill et al., 2007) and has previously been described to have mutagenic effects towards mtDNA (Piper, 1999). Therefore, we tested if *SYM1* is implicated in propionic acid metabolism.

At 30°C we did not observe growth on propionate as sole Carbon-source (Figure 9). This reflects published knowledge, that at 30°C citrate synthase 2 mediated conversion of propionate to 2-methylcitrate in the peroxisome inhibits

growth (Graybill et al., 2007). Surprisingly at 37°C propionate sustained growth as sole carbon source for *SYM1*, but not *sym1Δ*. *sym1Δ* growth was completely blocked by 20 mM propionate as sole carbon source. Furthermore, growth in Yeast-extract/Bacto-peptone/propionate medium was reduced for *sym1Δ* compared to the control and led to an increased frequency of *petite* colonies in *sym1Δ*. This implies that mitochondrial metabolism is compromised and that *sym1Δ* is more sensitive to the mtDNA mutagenic effect of propionate. In the presence of glucose propionate did not exert an inhibitory effect on *sym1Δ* growth. Sym1p might allow for growth on propionate, because it relocates propionate metabolic processes to mitochondria, rather than peroxisomes and minimizes peroxisomal 2-methylcitrate synthesis.

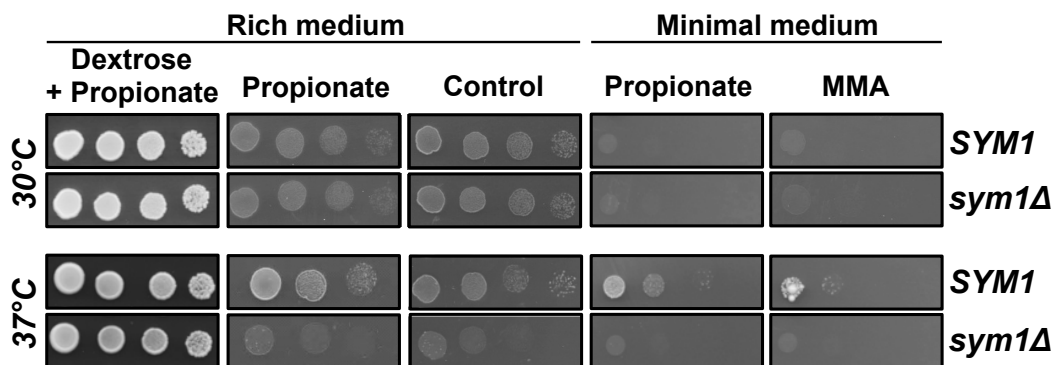


FIGURE 9. Propionic acid sustained growth assays. 20 mM propionate. Photographs of *SYM1* and *sym1Δ* grown at 30°C/37°C on medium supplemented with propionate and propionate free controls in rich (Yeast-extract/Bacto-peptone) medium or minimal (yeast-nitrogen-base including auxotrophy markers) medium supplied with 20 mM of propionate or 20 mM methylmalonic acid (MMA). Cells grown in YPD were kept 24 h at 30°C in 0.3 % glucose, serially diluted and spotted. The plates were photographed after 3 or 14 (minimal medium plates) days of incubation at 30°C or 37°C. MMA: methylmalonic acid.

SYM1 is implicated in MMA and propionate metabolic pathways, which are connected in S. cerevisiae

Theoretically altered TCA cycle activity could lead to a build up of succinyl-CoA, which might be converted to propionyl-CoA via methylmalonyl-CoA as reported for bacteria (Haller et al., 2000) and animals (Fenton and Gravel, 2001; van Grinsven et al., 2009;). There are indications for the methylmalonyl-CoA pathway to occur in yeast (Sumegi et al., 1990). Similar to propionate, wild-type growth on methylmalonate (MMA) was possible at 37°C but not at 30°C. *sym1Δ* cells were unable to grow on MMA. Comparison of enzyme activities led to hypothesize that yeasts mainly employ the 2-methylcitrate pathways for propionyl-CoA degradation (Pronk et al., 1994). Mitochondrial Cit3p has been shown to be a specific 2-methylcitrate synthase (Graybill et al., 2007). After isomerization to 2-methylisocitrate

by Aco1p or Pdh1p mitochondrial 2-methylcitrate lyase Icl2p hydrolyses 2-methylisocitrate into succinate and pyruvate (Luttik et al., 2000). *icl2Δ* displayed reduced growth on propionate as sole carbon source at 37°C (Figure 9A). This is the first *in vivo* evidence of Icl2p to be required for propionate degradation. This had previously been assumed due to transcriptional induction in propionate medium and *in vitro* activity (Luttik et al., 2000). Interestingly *icl2Δ* was also sensitive to high levels of ethanol (4 %) and unable to grow on MMA as sole Carbon source (Figure 10A). This suggested that MMA leads to formation of propionate or 2-methylcitrate and that the 2-methylcitrate pathway is essential for MMA degradation.

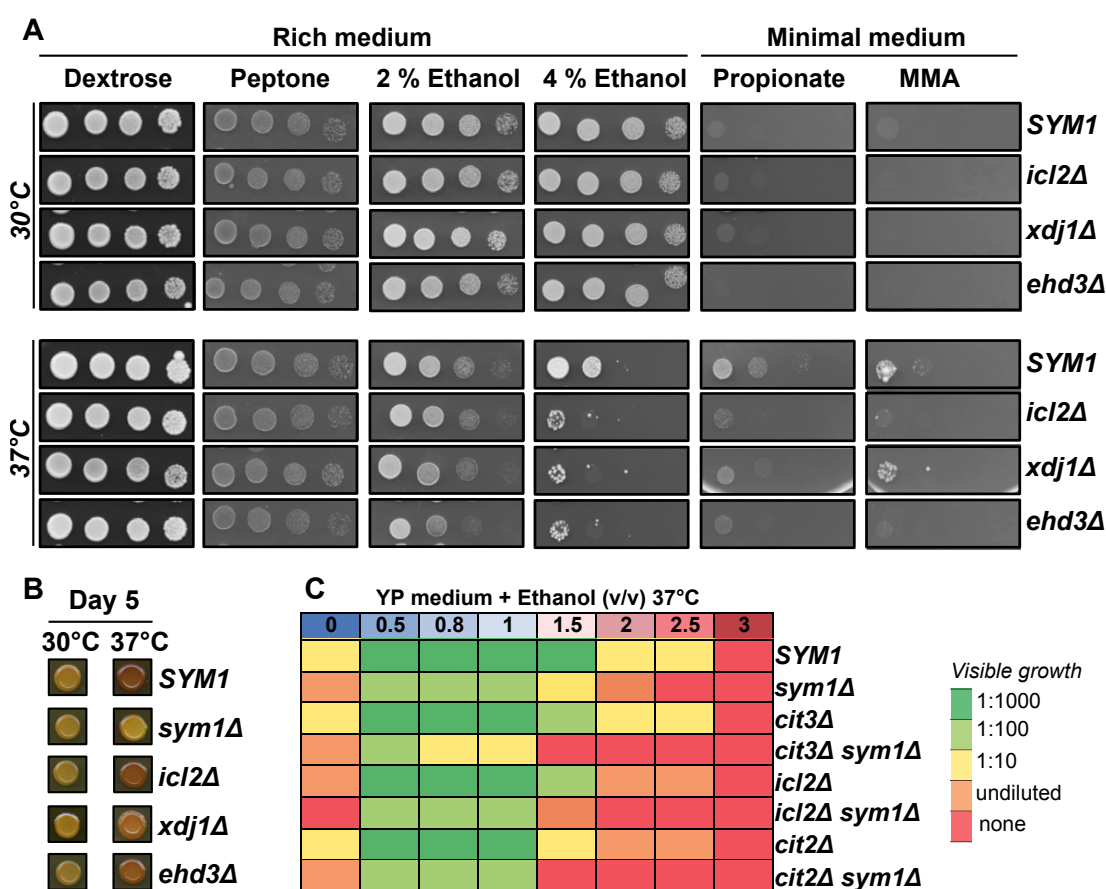


FIGURE 10. Analysis of growth of strains defective in enzymes of the 2-methylcitrate cycle and mutants with a putative defect in the methylmalonyl-CoA pathway.

(A) Photographs of *SYM1* and *icl2Δ*, *xdj1Δ* and *ehd3Δ* grown at 30°C/37°C on medium supplemented with the indicated carbon source in rich (Yeast-extract/Bacto-peptone) medium or minimal (yeast-nitrogen-base plus auxotrophy markers) medium. 20 mM of propionate and methylmalonate (MMA) were added to minimal medium. Cells grown in YPD were kept 24 h at 30°C in 0.3 % glucose, serially diluted and spotted. The plates were photographed after 3 or 14 (minimal medium plates) days of incubation at 30°C or 37°C. MMA: methylmalonic acid.

(B) Photograph of glycogen stained *SYM1* and *sym1Δ*, *icl2Δ*, *xdj1Δ* and *ehd3Δ* cells after 5 days growth in YPD. Cells were exposed to iodine vapor to stain glycogen (brownish color) and photographed.

(C) Ethanol resistance profile of *SYM1*, *sym1Δ*, *cit3Δ*, *icl2Δ*, *cit2Δ* and double mutants at 37°C. Cells were grown in YPD, serially diluted and spotted on YP plates with varying ethanol concentrations. Growth was scored after 3 days by determination of the maximal dilution that allowed for visible growth, as indicated by the color code.

In humans methylmalonic acidemia is an indicator for mitochondrial DNA depletion syndrome (MDS; Miller et al., 2011) but also associated with accumulation of propionate (Deodato et al., 2006). To test if *sym1Δ* mitochondrial DNA depletion is due to involvement in methylmalonate-CoA metabolic processes we aimed to identify candidates for methylmalonate detoxification and test if these genes are also unable to grow at *sym1Δ* restrictive growth conditions. BLAST analysis of a yeast homologue of human methylmalonyl-CoA mutase suggested Xdj1p to be the only candidate with sufficient sequence similarity. The protein had previously been shown to localize to mitochondria and assumed to facilitate import of mitochondrial proteins (Breker et al., 2014). *XDJ1* overexpression was detrimental to cells and under strong promoters even lethal (Sahi et al., 2013). The latter is a phenotype not observed for other DnaJ-like proteins. In our analyses *xdj1Δ* was sensitive to ethanol at 37°C and showed mild reduction of growth on propionate and MMA as sole carbon source (Figure 10A). The phenotype could be explained by methyl-malonyl-CoA mutase activity, but could also be an indirect effect if mitochondrial MMA degrading enzymes would be import substrates of Xdj1p.

By sequence similarity to known methylmalonyl-CoA dehydrogenases we identified yeast Ehd3p as a candidate enzyme (Table S2). In a preliminary study authors suspected Ehd3p as a peroxisomal β -oxidation gene, but could not reveal phenotypic differences of *ehd3Δ* to wild-type cells and measured negligible 3-hydroxyisobutyryl-CoA hydrolase activity of the recombinant protein (Hiltunen et al., 2003). Later the mitochondrial localization of Ehd3p was revealed by proteomics (Sickmann et al., 2003; Reinders et al., 2006). A large-scale survey identified this protein to have an increased frequency of spontaneous mitochondrial genome loss (Hess et al., 2009). Similar to *ICL2* and *CIT3* and *EHD3* is upregulated in ethanol containing media (Luttik et al., 2000; Hiltunen et al., 2003; Graybill et al., 2007). At 37°C *ehd3Δ* displayed a reduced growth on ethanol and was unable to grow on propionate and MMA as sole carbon source.

The fact that *ICL2* was required for optimal growth on ethanol at 37°C indicates the importance of propionate catabolism at *sym1Δ* restrictive growth conditions. Interestingly corresponding to *sym1Δ*, *ehd3Δ* and *xdjΔ* had mildly reduced glycogen contents after 5 days growth on YPD in a qualitative staining (Figure 10B). Loss of *SYM1* in the background of *icl2Δ*, *cit3Δ* and *cit2Δ* resulted in increased sensitivity to ethanol (Figure 10C). This indicated *Sym1p* to operate in propionate metabolism.

Furthermore the connection to the peroxisome emphasized *SYM1* to be needed for respiration of glyoxylate cycle derived carbon units.

Sym2p localizes to the peroxisome and sym2Δ growth is ethanol sensitive

We were interested in the function of Sym1p's paralogous protein Sym2p, which shares 31 % identical amino acids and an overall similarity of 49 % (Figure S1). Several repetitive sequences and sequence motives are shared in the *SYM1* and *SYM2* promoters (Carlson et al., 2007) and the genes seem to be co-regulated (Figure S2A). Both promoters feature predicted binding by oleate response associated transcription factor Adr1p, but also they seem both to be expressed in amino acid starvation conditions as they share binding by Gcn4p (Hinnebusch and Natarajan, 2002; Figure S2C). Therefore, we hypothesize *the SYM2* gene product to have a function similar to *SYM1*.

In a high throughput study Sym2p was suggested to localize to the vacuole (Huh et al., 2003). In our analysis Sym2-YFP colocalized with the CFP-PTS1 peroxisome marker (Figure 11A). The vacuolar localization was already questioned due to the presence of an oleate responsive element (Visser et al., 2007). We grew *sym2Δ* on oleic acid plates at 30°C and 37°C and observed wild-type growth, which suggested that *SYM2* was dispensable for oleic acid utilization.

Unlike *SYM1*, the *SYM2* promoter displays STRE elements, which were found in stress-sensitive genes (Estruch, 2000; Causton et al., 2001). We detected a growth defect for *sym2Δ* on 4 % ethanol, but not 2 % ethanol. Glycogen amounts were comparable to the wild-type over time in YPD-dependent growth at 37°C. Metabolite profiling revealed a significant increase of alanine and branched-chain amino acids levels after 18 h growth in YP medium at 37°C (Figure 12). TCA cycle or glyoxylate cycle intermediates were not significantly changed.

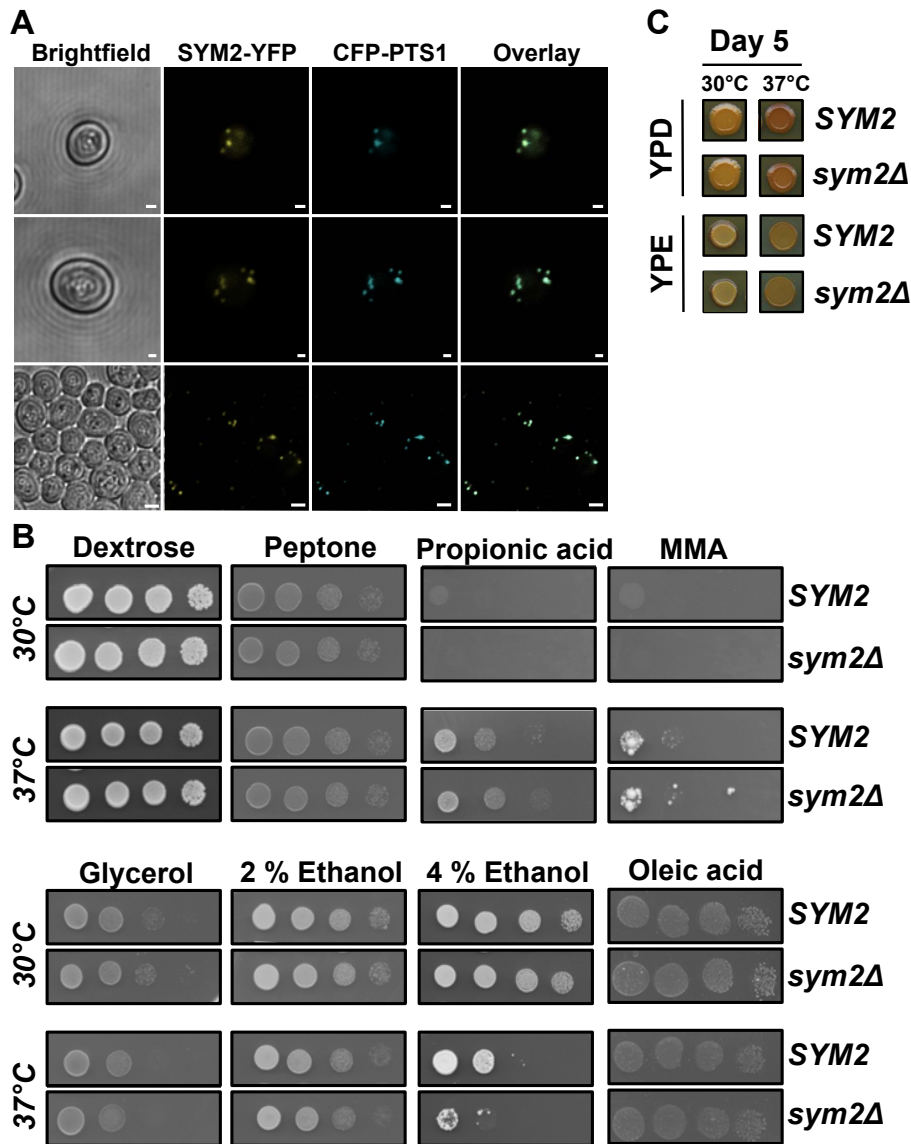


FIGURE 11. Localization of *SYM2* gene product and analysis of *sym2Δ* growth.

(A) *SYM2*-YFP co-localizes to the CFP-PTS1 peroxisome marker. BY4742 cells carrying pAG426GPD *Sym2*-GFP and pNL6 CFP-PTS1 grown in SC-URA plates containing 2 % ethanol/glycerol as carbon source. Images were taken by confocal fluorescence microscopy of overnight cultures immobilized in 3 % (w/v) agarose. Scale bar: upper rows: 1 μ M, lowest row 2 μ M.

(B) Photographs of *SYM2* and *sym2Δ* grown at 30°C/37°C on medium supplemented with the indicated carbon source in rich (Yeast-extract/Bacto-peptone) medium or minimal (yeast-nitrogen-base + auxotrophy markers) medium. 20 mM of propionate, methylmalonate (MMA) or 0.1 % (v/v) oleic acid were added to minimal medium. Cells grown in YPD were kept 24 h at 30°C in 0.3 % glucose, serially diluted and spotted. The plates were photographed after three or 14 (oleic acid, propionate, MMA, 4 % ethanol) days of incubation at 30°C or 37°C. MMA: methylmalonic.

(C) Photograph of glycogen stained *SYM2*, *sym2Δ* after five days of growth on YPD plates. Cells grown in YPD were serially diluted and spotted. After the indicated time of growth cells were exposed to iodine vapor to stain glycogen (brownish color) and photographed.

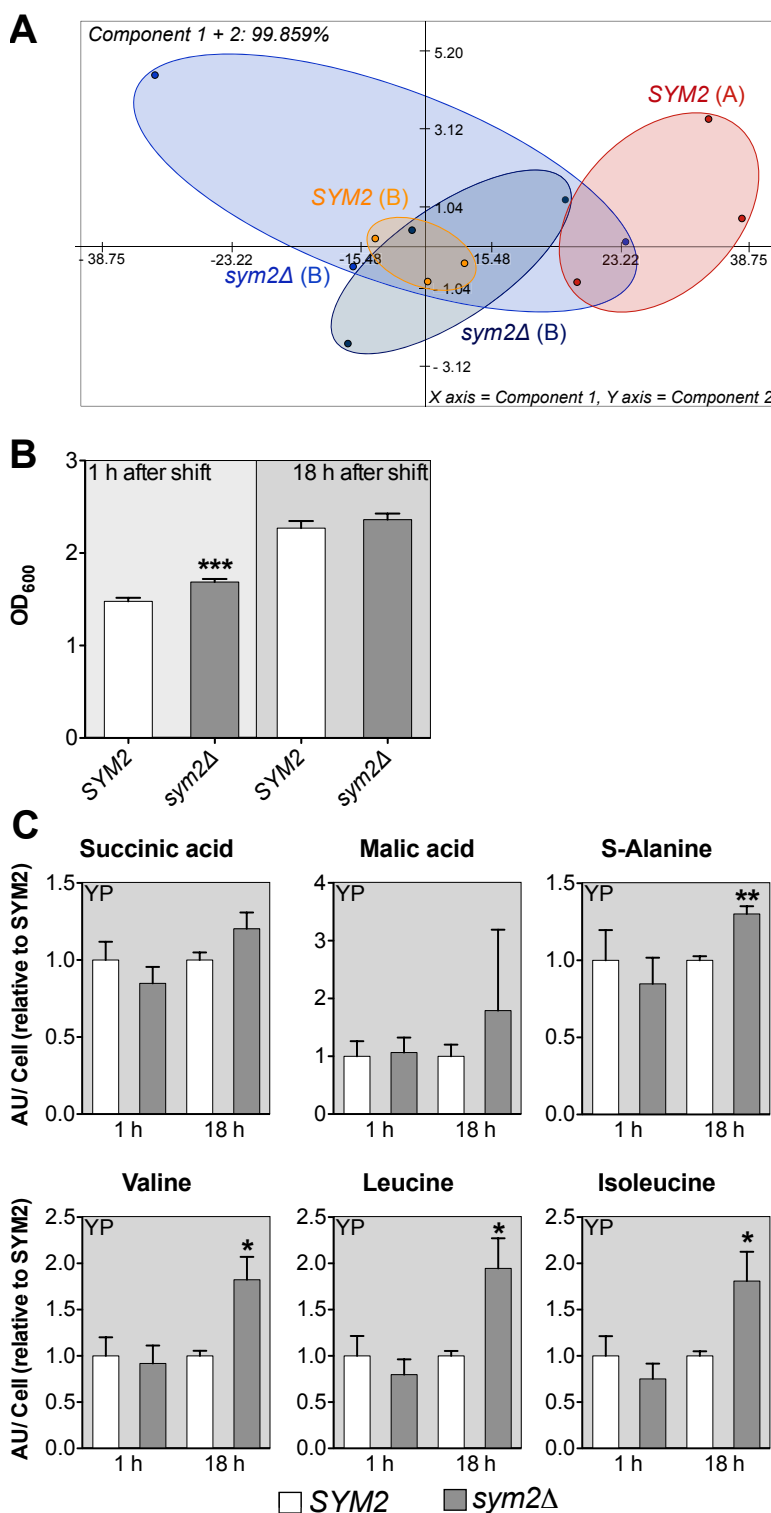


FIGURE 12. Analysis of *sym2Δ* growth and metabolites in Yeast extract/Bacto-peptone medium at 37°C.

(A) 2D-PCA score plot of metabolite profiles. The plots were applied for the 24 annotated metabolites detected in YP grown cells 1 h (A) or 18 h (B) after shift to 37°C or YPE grown cells 1 h (C), 3 h (D) and 18 h (E) after shift to 37°C. PCA was conducted by the MultiExperiment Viewer (Saeed et al., 2003). Biological replicates are encircled. PCA: principal component analysis

(B) Mean OD₆₀₀ (+SE; n=3) of SYM2 and *sym2Δ* cultures in YP medium after shift from 30°C to 37°C (at the time point of harvest for metabolite extraction).

(C) Plots of mean content (+SE; n=3) of succinic acid, malic acid, alanine, valine, leucine and isoleucine short chain carboxylic acid and carbohydrates in arbitrary units of SYM2 and *sym2Δ* cells grown in YPE and YP after shift from 30°C to 37°C. Differences between the mean of biological replicates were marked as statistically significant (t-test) with the SYM1 control by (*), (**) or (***) at respective significance levels of (P < 0.05), (P < 0.01) or (P < 0.001).

Discussion

This report describes growth of *sym1Δ* and *sym2Δ* to be compromised by high levels of ethanol at elevated temperature and establishes a link to TCA cycle intermediate availability in *sym1Δ* growth restriction. *sym1Δ* growth was supported by mitochondrial and peroxisomal substrates. Furthermore, we revealed that mtDNA depletion might be connected to an implication in propionate/methylmalonate (MMA) metabolic pathways.

Sym1p and Sym2p are required for ethanol resistance

Ethanol predominantly harms the integrity of cellular membranes by altering fluidity and permeability, which could potentially result in dissipation of transmembrane electrochemical gradients (Stanley et al., 2010). Heat and ethanol influence protein conformations, which is detrimental to catalytic activities. The cells counteract these detrimental effects by activation of a gene expression program and alteration of carbon flux that allows for growth to proceed. *SYM1* was previously identified as a component in ethanol and thermotolerance (Trott and Morano, 2004; Bravim et al., 2013). Here we also present *SYM2* as member of stress tolerance genes.

Sym1p is involved in metabolite transport

Sym1p has been demonstrated to form an aqueous pore in artificial lipid bilayers (Reinhold et al., 2012). In line with this finding, the homologous mammalian Pxmp2 protein has been postulated to render the peroxisomal membrane permeable to C₂-C₆ carboxylic acids (Rokka et al., 2009). Our data demonstrates limited TCA cycle activity due to shortage of intermediates. A possible explanation would be a failure in Carbon partitioning between mitochondria and the cytosol as suggested by *ODC1/YMC1* mediated suppression of the growth defect. These mitochondrial carrier family proteins play anaplerotic roles to the TCA cycle by counter exchanging carboxylic acids. *UCP2* expression did not suppress the *sym1Δ* growth phenotype. Sym1p cargo and mechanism of ethanol tolerance remain unknown. Hypothetically Sym1p could act in detoxification of a toxic molecule such as propionate by translocation to the site of degradation, export of anabolites to the cytosol, import of a molecule into mitochondria that they fail to synthesize, or a combination of the options.

Transcriptomic and metabolic profiling indicate malfunctioning TCA cycle and a buildup of mitochondrial pyruvate in sym1Δ

In repressive growth conditions *sym1Δ* is characterized by the inhibition of specific enzymes (Dallabona et al., 2010) and low availability of TCA substrates: pools of 2-oxoglutarate, (iso-)citrate, succinate, fumarate and malate, as well as TCA cycle anaplerotic amino acids such as aspartate, glutamate and proline, were depleted. It may be inferred from transcriptomic profiling that not only succinate dehydrogenase but also the preceding enzyme succinyl-CoA synthetase (Lsc1/2p) displays reduced activity. An increased transcription of *ACH1* was observed (Trott and Morano, 2004). The *ACH1* gene product could potentially circumvent succinyl-CoA synthetase activity, by transferring the CoA moiety from succinyl-CoA to acetate and release succinate and acetyl-CoA (Fleck and Brock, 2009).

In *sym1Δ* the plasma-membrane branched-chain amino acid permease encoding *BAP2* gene was transcriptionally induced (Trott and Morano, 2004), which was previously shown to occur at low intracellular amino acid concentrations (Grauslund et al., 1995) and reflects our findings of reduced amino acids levels at one and three hours after shift to 37°C. Increased amino acid import could also explain why certain amino acids were highly increased in *sym1Δ* after 18 h of growth in YPE.

Loss of *SYM1* led to low intracellular concentrations of malate and citrate directly after shift to 37°C in YPE. In the TCA cycle oxaloacetate is the intermediate between malate and citrate. Oxaloacetate might therefore also be low. *sym1Δ* cells were shown to upregulate *PYC2* (Trott and Morano, 2004), which could lead to increased pyruvate carboxylation to yield oxaloacetate, an initial substrate of the gluconeogenic pathway (Haarasilta and Oura, 1975). Both isoenzymes of pyruvate carboxylase are exclusively cytosolic and with ethanol as sole carbon source pyruvate carboxylation requires export of pyruvate from the mitochondria (Pronk et al., 1996).

Genes involved in the synthesis of trehalose and glycogen were upregulated in *sym1Δ*. *S. cerevisiae* produces the energy reserve glycogen and the molecular chaperone trehalose during nutrient starvation and stress conditions (Singer and Lindquist, 1998). Glycogen biosynthetic enzyme encoding genes are induced in the stationary phase of growth (Wilson et al., 2010). The premature glycogen consumption in *sym1Δ* indicates a change in intracellular energy status, as apparent from reduced glucose content. To conclude *sym1Δ* transcriptomic and metabolic

analyses reflect malfunctioning respiratory metabolism and gluconeogenesis, whereas the cause remains to be unraveled.

Alanine and valine were more abundant in *sym1Δ* than in the wild type. Specifically these two amino acids were also shown to exhibit a higher abundance in propionate-adapted cells (Lourenço et al., 2011). Both are synthesized from pyruvate (Ljungdahl and Daignan-Fornier, 2012). Pyruvate was suggested to increase in propionate adapted cells (Lourenço et al., 2011). Leucine and isoleucine, which are also synthesized from pyruvate (Zelenaya-Troitskaya et al., 1995), displayed wild-type levels in the mutant and did not follow the general trend of amino acid depletion immediately after shift to 37°C. The accumulation could be explained by the lack of TCA activity and use of alternative pathways for pyruvate conversion. Otherwise, cytosolic gluconeogenesis could serve to metabolize pyruvate, but lowered ATP/ADP ratio and actual glycogen content (Figure 3) render this option unlikely to occur. But maybe the predominant mitochondrial pyruvate utilization indicates a failure in export of pyruvate to the cytosol. Pyruvate could also be converted to lactate within mitochondria and lactate was also higher concentrated *sym1Δ*. Hyperlactemia was frequently reported for patients with MPV17 mutations (Parini et al., 2009). To conclude, at 37°C Sym1p coordinates carbon flux.

Altered carbon flow in TCA cycle succinyl-CoA synthase mutants causes mtDNA depletion and methylmalonic aciduria

Patients with mutations in the human Sym1p functional orthologue MPV17 suffer from mtDNA depletion syndrome (MDSS). Genes causing mtDNA depletion generally regulate intra-mitochondrial nucleotide pools and of all MDSS causing genes only *Mpv17* function remains unknown (Spinazzola et al., 2006; Suomalainen and Isohanni, 2010). We showed that *SYM1* enhances tolerance to genotoxins such as cobalt and manganese and confirm an implication of Sym1p in mtDNA maintenance.

In humans mutation of the TCA cycle enzyme succinyl-CoA synthetase leads to MDSS due to essential interaction with nucleoside diphosphate kinase to regulate mitochondrial nucleotide supply (Kowluru et al., 2002; Ostergaard, 2008). Succinyl-CoA synthetase mutation results in accumulation of methylmalonyl-CoA and MMA. MMA accumulates because substrate imbalance restricts its conversion to succinyl-CoA via methylmalonyl-CoA (Carrozzo et al., 2007; Ostergaard et al., 2007). MMA impedes mitochondrial oxidative metabolism by inhibition of respiratory complexes,

2-oxoglutarate dehydrogenase and succinyl-CoA synthetase, but also by lower availability of respiratory substrates (Morath et al., 2008; Melo et al., 2012). MMA was shown to inhibit succinate and glutamate-supported oxygen consumption in isolated mitochondria, which was not observed after nonselective permeabilization of the mitochondrial membrane by alamethicin (Mirandola et al., 2008). This would argue MMA to be an inhibitor of succinate transport. Dietary supply of succinate improved symptoms of *Mpv17^{-/-}* patients (Kaji et al., 2009). We showed that *sym1Δ* accomplished almost wild-type growth on YP supplemented with succinate at 37°C. Methylmalonic acid was not detected by GC-MS in wild type and *sym1Δ* extracts from YPE (37°C) grown cells, but *sym1Δ* was unable to use MMA as sole carbon source.

We searched for known enzymes in MMA metabolism to gain more insight in MMA metabolism of *S. cerevisiae*. Analogous to human metabolism, methylmalonyl-CoA may arise in the yeast by isomerization of succinyl-CoA to methylmalonate catalyzed by methylmalonyl-CoA mutase. Local alignment search suggested Xdj1p to catalyze this step. Interestingly, overexpression of this protein was lethal, which has not been observed for highly similar DnaJ-like proteins (Sahi et al., 2012) and would be consistent with the assumption of an inhibitory effect by increased release of methylmalonyl-CoA. The mutant defective in the putative methylmalonyl-CoA decarboxylase Ehd3p has been found to have a higher frequency of mtDNA mutation (Hess et al., 2009), which could be a secondary effect of MMA accumulation (Kölker and Okun, 2005). Notably, *xdj1Δ* and *ehd3Δ* mutants could not grow on propionate/MMA and were sensitive to ethanol at 37°C. Future research should address enzyme activities of Xdj1p and Ehd3p to determine the implication in MMA degradation. Interestingly also *icl2Δ* failed to grow on methylmalonic acid as sole carbon source, which indicates that the 2-methylcitrate pathway is needed for MMA detoxification and implies MMA to be a source of propionyl-CoA. The exchange of MMA/2-Oxoglutarate has been proposed for mammalian mitochondria based on defective glutamate respiration in the presence of MMA (Melo et al., 2012). This transport could potentially also be achieved by Ymc1, Odc1 or Sym1p.

Sym1p is involved propionyl-CoA metabolism

Weak organic acid stress exerted by propionate has been shown to inhibit amino acid uptake systems. The plasma membrane ABC-Transporter Pdr12p is needed for

propionate tolerance, because it acts as an efflux pump and prevents intracellular accumulation of propionate (Holyoak et al., 1999).

In humans propionic aciduria displays principally the same symptoms as methylmalonic aciduria (Desviat et al., 2004; Morath et al., 2008) and defects in the catabolic pathways of isoleucine, valine and threonine are not only associated with MMA aciduria but also lead to accumulation of propionate. In Baker's yeast propionyl-CoA is an intermediate from oxidative decarboxylation of 2-oxobutanoate, which is produced by mitochondrial *Ilv1p* in threonine degradation, which occurs for example in the biosynthesis of branched-chain amino acids (Luttik et al., 2000). The function of the 2-methylcitrate pathway was previously unclear, because it was thought that cells were unable to use propionate as sole carbon source. At 37°C the inhibitory potential of propionate disappeared for wild-type cells (Figure 9/10). It was assumed that at 30°C *Cit2p* activity renders growth sensitive to propionate, because the toxic 2-methylcitrate, cannot be exported out of the peroxisome for degradation (Graybill et al., 2007). *CIT2* is a gene required for thermotolerance and also expressed at 37°C, which allows for the conclusion that at 37°C either 2-methylcitrate synthase activity was reduced or the peroxisomal membrane was permeable to 2-methylcitrate.

Propionate degrading enzymes, such as *Icl2p* and *Pdh1p*, were shown to be induced by propionate, ethanol and threonine (Luttik et al., 2000). In yeast cells intracellular propionate concentrations positively correlated with extracellular ethanol concentration: in 2.5 % ethanol propionate increased by a factor of 1.6 compared to the ethanol-free control and in 10 % Ethanol it is 6 times higher (Li et al., 2012). Notably mitochondria seem to be the sole site of propionate production and degradation. *sym1Δ* is compromised in growth with propionate as carbon source.

Propionate exposure was previously described to be accompanied by a reduced intracellular ATP/ADP ratio (Lourenço et al., 2011). On the one hand *sym1Δ* inability to grow on propionate could reflect a general respiration deficiency, but on the other hand *Sym1p* could be involved in propionate transport. *Sym1p* could be needed to import propionate into mitochondria and export pyruvate to the cytosol, which would explain higher levels of pyruvate connected molecules and failure of glycogen accumulation. Loss of propionate import would render the yeast unable to use it for respiration.

Another mechanism of *Sym1p* transport could reside in pyruvate export versus

pathway is employed to support growth on propionate as indicated by earlier *in vitro* characterizations (Luttik et al., 2000; Graybill et al., 2007). Interestingly the mutants were also sensitive to elevated temperature and presence of ethanol, which again point to a high probability that these conditions provoke endogenous production of propionate. The fact that the double mutants *cit3Δ sym1Δ* and *icl2Δ sym1Δ* were more sensitive to ethanol than either of the single mutants indicates an implication of *SYM1* in propionate degradation. Mutant with a putative defect in methylmalonyl-CoA metabolism (*ehd3Δ* and *xdj1Δ*) also showed this phenotype and furthermore establish a connection between propionate and MMA metabolism.

SYM2 encodes a peroxisomal MPV17/PMP22 protein

Other eukaryotes (mammals and plants) were described to have peroxisomal MPV17/PMP22 proteins (Tugal et al., 1999; Rokka et al., 2009), while it was thought that baker's yeast does not have a peroxisomal isoform. Initially mammalian Mpv17 was reported to localize to peroxisomes (Zwacka et al., 1994). Our analysis of Sym1p localization *in planta* showed that the protein localizes to the peroxisomal membrane, when the N-terminus was masked by YFP (Figure S4), even though it was previously shown that Sym1p is targeted to mitochondria independently of an N-terminal targeting signal (Reinhold et al., 2012). The *SYM2* gene product was suggested to localize to the vacuole (Huh et al., 2003). Here, we report on Sym2p to localize to the peroxisomal membrane. As expected due to stress responsive elements in *SYM2* upstream non-coding region, *sym2Δ* growth is sensitive to ethanol. Respiratory growth on ethanol is supported by peroxisomal glyoxylate cycle activity to generate acetyl-CoA, malate and citrate.

Intra- and extraperoxisomal localization of glyoxylate cycle enzymes requires the shuttling of acetyl-carnitine, citrate and glyoxylate across the peroxisomal membrane (van Roermund et al., 1999; Kunze and Hartig, 2013). The genes encoding the corresponding transport proteins have not yet been identified. Antonenkov et al., (2009) reported on pore-forming activities in yeast peroxisomal membranes, that would allow for passage of glyoxylate cycle intermediates.

Structural homology to Sym1p leads to the assumption that also Sym2p forms a channel. In the peroxisomal membrane this Sym2p could allow translocation of glyoxylate cycle intermediates, which is likely due to the presence of an oleate responsive element (Visser et al., 2007). *sym2Δ* was able to use oleic acid as sole carbon source and growth was indistinguishable from the wild type (Figure 11).

Potentially, acetyl-carnitine export from the peroxisome was sufficient to support growth (van Roermund et al., 1999) and co-export of carboxylic acids is not necessary. Sym2p activity might become important, if acetyl-carnitine transport is compromised, which raises the question whether oleic acid or acetate growth is possible in the background of *cat2Δ*, which is defective in peroxisomal carnitine transfer (van Roermund et al., 1999). In 4 % ethanol peroxisomal acetyl-CoA conversion could be important for cellular growth and reduction of glyoxylate cycle intermediate transport could explain the observed reduction in growth. An effect on cellular metabolism by *SYM2* at 37°C was unraveled by an increase in alanine and branched-chain amino acid levels, when cells grew in yeast extract/bacto-peptone medium.

Mechanism of sym1Δ rescue by feeding of C₂-C₆ carboxylic acids could involve action of the glyoxylate cycle

The fact that *sym1Δ cit2Δ* is more sensitive to ethanol than either one of the single mutants, evidences that *SYM1* establishes a link between peroxisomal and mitochondrial metabolism. This was the basis for the identification of *YMC1* and *ODC1* (Trotter et al., 2005). *sym1Δ* was described to be unable to grow on non-fermentable carbon sources (Dallabona et al., 2010). Cit2p produced carbon units promote growth of *sym1Δ* as reflected by amelioration of growth by exogenous supply of glyoxylate cycle intermediates succinate, malate and isocitrate (Figure 8). Furthermore, high levels of glyoxylate, but also glycolate were shown to support growth of *sym1Δ* at 37°C. These can support peroxisomal metabolism to yield isocitrate and succinate. High levels of glyoxylate have been shown to occur in growth in the presence of glucose (Rintala et al., 2007). An involvement of *SYM1* in succinate import would explain beneficial effects of the peroxisomal glyoxylate cycle and higher cytosolic succinate levels would make mitochondrial succinate import more efficient.

Conclusion

We discussed several transport functions of Sym1p and Sym2p based on our observations. Future research will need to determine, which function can be attributed to Sym1p and Sym2p. They might be general diffusion pores for a set of carboxylic acids. Especially the implications in propionate ad MMA conversion could be addressed by monitoring flux of labeled substrates and respiratory capacities.

Material and Methods

Chemicals were purchased from Sigma-Aldrich. Reagents and enzymes for recombinant DNA techniques were obtained from Clontech, Invitrogen, New England Biolabs and Promega.

Yeast strains and media

Yeast strains used in this study were BY4741 derivatives (listed in Table M1). The double mutants *cit2Δ sym1Δ*, *cit3Δ sym1Δ* and *icl2Δ sym1Δ* were obtained by disrupting the SYM1 gene in the single mutants by replacing SYM1 ORF with HygR. The HygR was amplified for the deletion cassette from pAG24 obtained from Euroscarf with Primers listed in Table M2. Cells were cultured in yeast nitrogen base (YNB) medium [0.67 % YNB without amino acids (BD Biosciences)] supplemented with appropriate amino acids and bases for auxotrophy. YP medium contained 1 % Bacto-yeast extract and 2 % Bacto-peptone. Media were solidified with 20 g/L agar. YPD/YPE contained 2 % glucose/ethanol. Minimal medium for oleic acid growth assays were composed of 0.67 % (w/v) yeast nitrogen base, 0.1 % (w/v) Yeast extract, 2 % (w/v) Bacto-agar, 0.5 % (w/v) Na₂HPO₄ (pH 6.0), 0.1 % (v/v) oleic acid and 0.4 % Tween-80. Other minimal media were composed of 0.67 % (w/v) YNB, 0.1% (w/v) His, Leu, Met, Lys and Ura, 15 mM methylmalonate or 20 mM propionate. Cells were spotted on minimal plates after 24 h nutrient deprivation in 0.67 (w/v) Yeast Nitrogen Base with 0.3 % (w/v) glucose at 30°C. Plate additives were adjusted to pH 7.0.

Cloning procedures and plasmids vectors

Restriction-enzyme digestions, *Escherichia coli* transformation and plasmid extractions were performed using standard methods (Russell and Sambrook, 2001). *S. cerevisiae* genes were PCR amplified using BY4741 genomic DNA as template with the appropriate forward and reverse primers as listed in Table M2. SYM1 was fused to YFP for in planta localization studies by insertion of the CDS in pUBN-YFP (Grefen et al., 2010). SYM2 was cloned pAG426-GPD (Alberti et al., 2007; obtained from Addgene) for C-terminal YFP fusion. Arabidopsis UCP2 was amplified from *A. thaliana* leaf cDNA and inserted into *HindIII/BamHI* opened pDR195 (Rentsch et al., 1995). Cells were transformed with the expression constructs using the lithium chloride method (Schiestl and Gietz, 1989). Transformants were selected on

synthetic complete minimal medium lacking uracil (SC-Ura), or uracil and leucine (SC-Leu-Ura).

Determination of glycogen content

Glycogen content was qualitatively determined by incubation of cells to iodine vapor. 5 mL potassium iodide beads were placed beneath inverted plates. Glycogen accumulating strains stained brown, whereas cells that do not remain yellow.

Fluorescence microscopy

Yeast transformants expressing SYM2-YFP and CFP-PTS1 (Linka et al., 2008) were grown overnight at 30°C in SC-Leu-Ura with 1 % ethanol and 1 % glycerol and pipetted on a 3 % agarose gel on glass slides for microscopy. Fluorescence microscopy was done with a Zeiss confocal Laser Scan microscope LSM780. Transient expression for localization studies of YFP-SYM1 in *Nicotiana tabacum* was done as described in Breuers et al. (2012). Three days after co-infiltration with a peroxisome CFP marker (Linka et al., 2008) epidermal cells were analyzed with a Laser scanning microscope Olympus Fluoview1000.

Fatty acid profiling

Fatty acids from lyophilized cells were analysed by gas chromatography - electron impact - time of flight - mass spectrometry (GC-EI-TOF-MS), following conversion to methyl esters after (Browse et al., 1986). The fatty acid 17:0 was used as an internal standard to enable quantification.

Metabolite analysis

For metabolite analysis cells were grown overnight in YPD, diluted to an OD₆₀₀ of 1 and grown for 3 hours in YP/YPE at 30°C. Then cells were shifted to 37°C. Preparation of samples for metabolic analysis was performed similar as described in Dunn and Winder (2011). Briefly, 10 mL of culture were transferred into -80°C quenching solution (60:40 Methanol: Water, 0.85 (w/v) ammoniumhydrogen carbonate (pH 5.5), pelleted at 2,500 g at -15°C, washed with 0.85 % (w/v) NaCl and centrifuged at 2,500 g at 4°C. The pellet was resuspended in 650 µL 80 % (v/v) methanol, 50 µM Ribitol and subsequently 600 µL chloroform was added. Cells were disrupted by freeze thaw cycling on dry ice. The supernatant was then diluted with 350 µL 50 µM ribitol and the upper fraction after centrifugation was used for analysis.

50 μL of the supernatant was dried and used for further analysis by gas chromatography/electron-impact/time-of-flight mass spectrometry, as previously described (Lee and Fiehn, 2008). Metabolite content was expressed relative to the ribitol standard. All samples were analyzed with three independent biological replicates. After confirmation of equal cell size of SYM1 and *sym1* Δ , we calibrated OD_{600} to cells/mL by a non-linear fit with the Gompertz equation (Zwietering et al., 1990; $R=0.97$) as indicated in Figure M1. At the harvest point we measured the OD_{600} and then calculated cells/mL by the equation $\text{Cells}(\text{OD}_{600})=4.572 \times 10^8 \cdot e^{\ln(7.316 \times 10^6 / 4.571 \times 10^8) \cdot e^{-0.1659 \cdot \text{OD}_{600}}}$ for normalization.

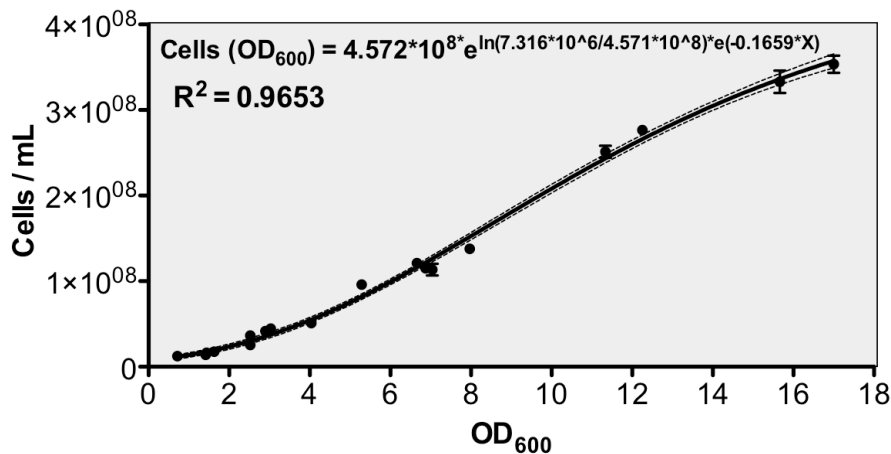


FIGURE M1. Plot of Gompertz fit (Zwietering et al., 1990) of *S. cerevisiae* cells/mL calculated from cell counts for different OD_{600} values.

Bioinformatic and statistical analysis

PCA score plots were generated with the Multiple Experiment Viewer (Saeed et al., 2003). Statistical analysis was performed with GraphPad Prism 5.0. Quantitative analysis results are presented as means +SE from repeated experiments as indicated in the figure legends. Pairwise Student's t test was used to analyze statistical significance.

Supplemented data

Fig. S1 Multiple sequence alignment of *Saccharomyces cerevisiae* Sym1p (mitochondrial), Sym2p (peroxisomal), *Homo sapiens* MPV17 (mitochondrial), *Mus musculus* Pxmp2 (peroxisomal) and *Arabidopsis thaliana* PMP22 (peroxisomal).

Fig. S2 Co-regulation and promoter analysis of *Saccharomyces cerevisiae*

SYM1/2

- Fig. S3** Model of the transcriptionally upregulated genes in *sym1Δ* cells in response to ethanol at 37°C
- Fig. S4** Confocal microscopic images of YFP-Sym1p localization taken from epidermis cells of four-week-old tobacco leaves co-expressing the peroxisomal marker CFP-PTS1
- Tab. S1** BLAST identification of a methylmalonyl-CoA mutase in *S. cerevisiae*
- Tab. S2** BLAST identification of a methylmalonyl-CoA decarboxylase in *S. cerevisiae*
- Tab. M1** *Escherichia coli*, *Saccharomyces cerevisiae* and *Agrobacterium tumefaciens* strains used in this study
- Tab. M2** Oligonucleotides used in this study

Acknowledgements

Wayne Wilson kindly provided the *gsy1Δ gsy2Δ* strain (WW100). Elisabeth Klemp and Katrin Weber helped with GC-MS analysis. Martin Schroers helped with fatty acid extraction. David Gagneul cloned the UCP2 expression construct.

Author contributions

Jan Wiese performed all experiments and wrote the manuscript. Andreas P.M. Weber and Nicole Linka provided lab space, equipment and helpful discussions.

References

- Alberti, S., Gitler, A.D., and Lindquist, S.** (2007). A suite of Gateway cloning vectors for high-throughput genetic analysis in *Saccharomyces cerevisiae*. *Yeast* **24**: 913–919.
- Antonenkov, V.D., Mindthoff, S., Grunau, S., Erdmann, R., and Hiltunen, J.K.** (2009). An involvement of yeast peroxisomal channels in transmembrane transfer of glyoxylate cycle intermediates. *Int. J. Biochem. Cell Biol.* **41**: 2546–2554.
- Assem, F.L., Holmes, P., and Levy, L.S.** (2011). The mutagenicity and carcinogenicity of inorganic manganese compounds: a synthesis of the evidence. *J Toxicol Environ Health B Crit Rev* **14**: 537–570.
- Baruffini, E., Ferrero, I., and Foury, F.** (2010). In vivo analysis of mtDNA replication defects in yeast. *Methods* **51**: 426–436.
- Baskaran, S., Chikwana, V.M., Contreras, C.J., Davis, K.D., Wilson, W.A., DePaoli-Roach, A.A., Roach, P.J., and Hurley, T.D.** (2011). Multiple glycogen-binding sites in eukaryotic glycogen synthase are required for high catalytic efficiency toward glycogen. *J. Biol. Chem.* **286**: 33999–34006.
- Bravim, F., Lippman, S.I., da Silva, L.F., Souza, D.T., Fernandes, A.A.R., Masuda, C.A., Broach, J.R., and Fernandes, P.M.B.** (2013). High hydrostatic pressure activates gene expression that leads to ethanol production enhancement in a *Saccharomyces cerevisiae* distillery strain. *Appl. Microbiol. Biotechnol.* **97**: 2093–2107.
- Breker, M., Gymrek, M., Moldavski, O., and Schuldiner, M.** (2014). LoQAtE--Localization and Quantitation ATlas of the yeast proteome. A new tool for multiparametric dissection of single-protein behavior in response to biological perturbations in yeast. *Nucleic Acids Res.* **42**: D726–30.
- Breuers, F.K.H., Bräutigam, A., Geimer, S., Welzel, U.Y., Stefano, G., Renna, L., Brandizzi, F., and Weber, A.P.M.** (2012). Dynamic Remodeling of the Plastid Envelope Membranes - A Tool for Chloroplast Envelope in vivo Localizations. *Front Plant Sci* **3**: 7.
- Browse, J., McCourt, P.J., and Somerville, C.R.** (1986). Fatty acid composition of leaf lipids determined after combined digestion and fatty acid methyl ester formation from fresh tissue. *Anal. Biochem.* **152**: 141–145.
- Burg, M.B., Ferraris, J.D., and Dmitrieva, N.I.** (2007). Cellular response to hyperosmotic stresses. *Physiol. Rev.* **87**: 1441–1474.
- Cardenas, M.E., Cruz, M.C., Del Poeta, M., Chung, N., Perfect, J.R., and Heitman, J.** (1999). Antifungal activities of antineoplastic agents: *Saccharomyces cerevisiae* as a model system to study drug action. *Clin. Microbiol. Rev.* **12**: 583–611.
- Carlson, J.M., Chakravarty, A., DeZiel, C.E., and Gross, R.H.** (2007). SCOPE: a web server for practical de novo motif discovery. *Nucleic Acids Res.* **35**: W259–64.
- Carrozzo, R. et al.** (2007). SUCLA2 mutations are associated with mild methylmalonic aciduria, Leigh-like encephalomyopathy, dystonia and deafness. *Brain* **130**: 862–874.
- Causton, H.C., Ren, B., Koh, S.S., Harbison, C.T., Kanin, E., Jennings, E.G., Lee, T.I., True, H.L., Lander, E.S., and Young, R.A.** (2001). Remodeling of yeast genome expression in response to environmental changes. *Mol. Biol. Cell* **12**: 323–337.
- Dallabona, C., Marsano, R.M., Arzuffi, P., Ghezzi, D., Mancini, P., Zeviani, M., Ferrero, I., and Donnini, C.** (2010). Sym1, the yeast ortholog of the MPV17 human disease protein, is a stress-induced bioenergetic and morphogenetic mitochondrial modulator. *Hum. Mol. Genet.* **19**: 1098–1107.
- Deodato, F., Boenzi, S., Santorelli, F.M., and Dionisi-Vici, C.** (2006). Methylmalonic and propionic aciduria. *Am J Med Genet C Semin Med Genet* **142C**: 104–112.
- Desviat, L.R., Perez, B., Perez-Cerda, C., Rodriguez-Pombo, P., Clavero, S., and Ugarte, M.** (2004). Propionic acidemia: mutation update and functional and structural effects of the variant alleles. *Mol. Genet. Metab.* **83**: 28–37.
- Dinh, T.N., Nagahisa, K., Hirasawa, T., Furusawa, C., and Shimizu, H.** (2008). Adaptation of *Saccharomyces cerevisiae* cells to high ethanol concentration and changes in fatty acid composition of membrane and cell size. *PLoS ONE* **3**: e2623.
- Do Y Lee and Fiehn, O.** (2008). High quality metabolomic data for *Chlamydomonas reinhardtii*. *Plant Methods* **4**: 7.

- Domitrovic, T., Fernandes, C.M., Boy-Marcotte, E., and Kurtenbach, E.** (2006). High hydrostatic pressure activates gene expression through Msn2/4 stress transcription factors which are involved in the acquired tolerance by mild pressure precondition in *Saccharomyces cerevisiae*. *FEBS Lett.* **580**: 6033–6038.
- Dunn, W.B. and Winder, C.L.** (2011). Sample preparation related to the intracellular metabolome of yeast methods for quenching, extraction, and metabolite quantitation. *Meth. Enzymol.* **500**: 277–297.
- Estruch, F.** (2000). Stress-controlled transcription factors, stress-induced genes and stress tolerance in budding yeast. *FEMS Microbiol. Rev.* **24**: 469–486.
- Farkas, I., Hardy, T.A., Goebel, M.G., and Roach, P.J.** (1991). Two glycogen synthase isoforms in *Saccharomyces cerevisiae* are coded by distinct genes that are differentially controlled. *J. Biol. Chem.* **266**: 15602–15607.
- Fenton, W.A. and Gravel, R.A.** (2001). Disorders of propionate and methylmalonate metabolism. *The metabolic and molecular bases of inherited disease* **8**:2165-2193.
- Fiermonte, G., Dolce, V., Palmieri, L., Ventura, M., Runswick, M.J., Palmieri, F., and Walker, J.E.** (2001). Identification of the human mitochondrial oxodicarboxylate carrier. Bacterial expression, reconstitution, functional characterization, tissue distribution, and chromosomal location. *J. Biol. Chem.* **276**: 8225–8230.
- Fleck, C.B. and Brock, M.** (2009). Re-characterisation of *Saccharomyces cerevisiae* Ach1p: fungal CoA-transferases are involved in acetic acid detoxification. *Fungal Genet. Biol.* **46**: 473–485.
- Grauslund, M., Didion, T., Kielland-Brandt, M.C., and Andersen, H.A.** (1995). BAP2, a gene encoding a permease for branched-chain amino acids in *Saccharomyces cerevisiae*. *Biochim. Biophys. Acta* **1269**: 275–280.
- Graybill, E.R., Rouhier, M.F., Kirby, C.E., and Hawes, J.W.** (2007). Functional comparison of citrate synthase isoforms from *S. cerevisiae*. *Arch. Biochem. Biophys.* **465**: 26–37.
- Grefen, C., Donald, N., Hashimoto, K., Kudla, J., Schumacher, K., and Blatt, M.R.** (2010). A ubiquitin-10 promoter-based vector set for fluorescent protein tagging facilitates temporal stability and native protein distribution in transient and stable expression studies. *Plant J.* **64**: 355–365.
- Grunau, S., Mindthoff, S., Rottensteiner, H., Sormunen, R.T., Hiltunen, J.K., Erdmann, R., and Antonenkov, V.D.** (2009). Channel-forming activities of peroxisomal membrane proteins from the yeast *Saccharomyces cerevisiae*. *FEBS J.* **276**: 1698–1708.
- Haarasilta, S. and Oura, E.** (1975). On the activity and regulation of anaplerotic and gluconeogenic enzymes during the growth process of baker's yeast. The biphasic growth. *Eur. J. Biochem.* **52**: 1–7.
- Haller T., Buckel T., Rétey J., Gerlt J.A.** (2000). Discovering new enzymes and metabolic pathways: conversion of succinate to propionate by *Escherichia coli*. *Biochemistry* **39**: 4622–4629.
- Hess, D.C. et al.** (2009). Computationally driven, quantitative experiments discover genes required for mitochondrial biogenesis. *PLoS Genet.* **5**: e1000407.
- Hibbs, M.A., Hess, D.C., Myers, C.L., Huttenhower, C., Li, K., and Troyanskaya, O.G.** (2007). Exploring the functional landscape of gene expression: directed search of large microarray compendia. *Bioinformatics* **23**: 2692–2699.
- Hiltunen, J.K., Mursula, A.M., Rottensteiner, H., Wierenga, R.K., Kastaniotis, A.J., and Gurvitz, A.** (2003). The biochemistry of peroxisomal beta-oxidation in the yeast *Saccharomyces cerevisiae*. *FEMS Microbiol. Rev.* **27**: 35–64.
- Hinnebusch, A.G. and Natarajan, K.** (2002). Gcn4p, a master regulator of gene expression, is controlled at multiple levels by diverse signals of starvation and stress. *Eukaryotic Cell* **1**: 22–32.
- Holyoak, C.D., Bracey, D., Piper, P.W., Kuchler, K., and Coote, P.J.** (1999). The *Saccharomyces cerevisiae* weak-acid-inducible ABC transporter Pdr12 transports fluorescein and preservative anions from the cytosol by an energy-dependent mechanism. *J. Bacteriol.* **181**: 4644–4652.
- Horswill, A.R., Dudding, A.R., and Escalante-Semerena, J.C.** (2001). Studies of Propionate Toxicity in *Salmonella enterica* Identify 2-Methylcitrate as a Potent Inhibitor of

- Cell Growth. *J. Biol. Chem.* **276**: 19094–19101.
- Huh, W.-K., Falvo, J.V., Gerke, L.C., Carroll, A.S., Howson, R.W., Weissman, J.S., and O'Shea, E.K.** (2003). Global analysis of protein localization in budding yeast. *Nature* **425**: 686–691.
- Indiveri, C., Iacobazzi, V., Giangregorio, N., and Palmieri, F.** (1998). Bacterial overexpression, purification, and reconstitution of the carnitine/acylcarnitine carrier from rat liver mitochondria. *Biochem. Biophys. Res. Commun.* **249**: 589–594.
- Kaji, S. et al.** (2009). Fluctuating liver functions in siblings with MPV17 mutations and possible improvement associated with dietary and pharmaceutical treatments targeting respiratory chain complex II. *Mol. Genet. Metab.* **97**: 292–296.
- Kowluru, A., Tannous, M., and Chen, H.-Q.** (2002). Localization and characterization of the mitochondrial isoform of the nucleoside diphosphate kinase in the pancreatic beta cell: evidence for its complexation with mitochondrial succinyl-CoA synthetase. *Arch. Biochem. Biophys.* **398**: 160–169.
- Kölker, S. and Okun, J.G.** (2005). Methylmalonic acid—an endogenous toxin? *Cell. Mol. Life Sci.* **62**: 621–624.
- Kunze, M. and Hartig, A.** (2013). Permeability of the peroxisomal membrane: lessons from the glyoxylate cycle. *Front Physiol* **4**: 204.
- Li, H., Ma, M.-L., Luo, S., Zhang, R.-M., Han, P., and Hu, W.** (2012). Metabolic responses to ethanol in *Saccharomyces cerevisiae* using a gas chromatography tandem mass spectrometry-based metabolomics approach. *Int. J. Biochem. Cell Biol.* **44**: 1087–1096.
- Linka, N., Theodoulou, F.L., Haslam, R.P., Linka, M., Napier, J.A., Neuhaus, H.E., and Weber, A.P.M.** (2008). Peroxisomal ATP import is essential for seedling development in *Arabidopsis thaliana*. *Plant Cell* **20**: 3241–3257.
- Ljungdahl, P.O. and Daignan-Fornier, B.** (2012). Regulation of amino acid, nucleotide, and phosphate metabolism in *Saccharomyces cerevisiae*. *Genetics* **190**: 885–929.
- Lourenço, A.B., Ascenso, J.R., and Sá-Correia, I.** (2011). Metabolic insights into the yeast response to propionic acid based on high resolution ¹H NMR spectroscopy. *Metabolomics* **7**: 457–468.
- Luttik, M., Kötter, P., and Salomons, F.A.** (2000). The *Saccharomyces cerevisiae* ICL2 gene encodes a mitochondrial 2-methylisocitrate lyase involved in propionyl-coenzyme A metabolism. *Journal of ...*
- Maerker, C., Rohde, M., Brakhage, A.A., and Brock, M.** (2005). Methylcitrate synthase from *Aspergillus fumigatus*. Propionyl-CoA affects polyketide synthesis, growth and morphology of conidia. *FEBS J.* **272**: 3615–3630.
- Melo, D.R., Miranda, S.R., Assunção, N.A., and Castilho, R.F.** (2012). Methylmalonate impairs mitochondrial respiration supported by NADH-linked substrates: involvement of mitochondrial glutamate metabolism. *J. Neurosci. Res.* **90**: 1190–1199.
- Miller, C., Wang, L., Ostergaard, E., Dan, P., & Saada, A.** (2011). The interplay between *SUCLA2*, *SUCLG2*, and mitochondrial DNA depletion. *Biochimica et Biophysica Acta-Molecular Basis of Disease*, **1812**(5): 625–629.
- Mirandola, S.R., Melo, D.R., Schuck, P.F., Ferreira, G.C., Wajner, M., and Castilho, R.F.** (2008). Methylmalonate inhibits succinate-supported oxygen consumption by interfering with mitochondrial succinate uptake. *J. Inherit. Metab. Dis.* **31**: 44–54.
- Morano, K.A., Grant, C.M., and Moye-Rowley, W.S.** (2012). The response to heat shock and oxidative stress in *Saccharomyces cerevisiae*. *Genetics* **190**: 1157–1195.
- Morath, M.A., Okun, J.G., Müller, I.B., Sauer, S.W., Hörster, F., Hoffmann, G.F., and Kölker, S.** (2008). Neurodegeneration and chronic renal failure in methylmalonic aciduria—a pathophysiological approach. *J. Inherit. Metab. Dis.* **31**: 35–43.
- Ostergaard, E.** (2008). Disorders caused by deficiency of succinate-CoA ligase. *J. Inherit. Metab. Dis.* **31**: 226–229.
- Ostergaard, E., Hansen, F.J., Sorensen, N., Duno, M., Vissing, J., Larsen, P.L., Faeroe, O., Thorgrimsson, S., Wibrand, F., Christensen, E., and Schwartz, M.** (2007). Mitochondrial encephalomyopathy with elevated methylmalonic acid is caused by *SUCLA2* mutations. *Brain* **130**: 853–861.
- Palmieri, L., Lasorsa, F.M., Iacobazzi, V., Runswick, M.J., Palmieri, F., and Walker, J.E.**

- (1999). Identification of the mitochondrial carnitine carrier in *Saccharomyces cerevisiae*. *FEBS Lett.* **462**: 472–476.
- Palmieri, L., Agrimi, G., Runswick, M.J., Fearnley, I.M., Palmieri, F., and Walker, J.E.** (2001). Identification in *Saccharomyces cerevisiae* of Two Isoforms of a Novel Mitochondrial Transporter for 2-Oxoadipate and 2-Oxoglutarate. *J. Biol. Chem.* **276**: 1916–1922.
- Parini, R. et al.** (2009). Glucose metabolism and diet-based prevention of liver dysfunction in MPV17 mutant patients. *J. Hepatol.* **50**: 215–221.
- Piper, P.W.** (1995). The heat shock and ethanol stress responses of yeast exhibit extensive similarity and functional overlap. *FEMS Microbiol. Lett.* **134**: 121–127.
- Piper, P.W.** (1999). Yeast superoxide dismutase mutants reveal a pro-oxidant action of weak organic acid food preservatives. *Free Radic. Biol. Med.* **27**: 1219–1227.
- Pronk, J.T., van der Linden-Beuman, A., Verduyn, C., Scheffers, W.A., and van Dijken, J.P.** (1994). Propionate metabolism in *Saccharomyces cerevisiae*: implications for the metabolon hypothesis. *Microbiology (Reading, Engl.)* **140 (Pt 4)**: 717–722.
- Pronk, J.T., Yde Steensma, H., and van Dijken, J.P.** (1996). Pyruvate metabolism in *Saccharomyces cerevisiae*. *Yeast* **12**: 1607–1633.
- Reinders, J., Zahedi, R.P., Pfanner, N., Meisinger, C., and Sickmann, A.** (2006). Toward the complete yeast mitochondrial proteome: multidimensional separation techniques for mitochondrial proteomics. *J. Proteome Res.* **5**: 1543–1554.
- Reinhold, R., Krüger, V., Meinecke, M., Schulz, C., Schmidt, B., Grunau, S.D., Guiard, B., Wiedemann, N., van der Laan, M., Wagner, R., Rehling, P., and Dudek, J.** (2012). The channel-forming Sym1 protein is transported by the TIM23 complex in a presequence-independent manner. *Mol. Cell. Biol.* **32**: 5009–5021.
- Rentsch, D., Laloi, M., Rouhara, I., Schmelzer, E., Delrot, S., and Frommer, W.B.** (1995). NTR1 encodes a high affinity oligopeptide transporter in *Arabidopsis*. *FEBS Lett.* **370**: 264–268.
- Rintala, E., Pitkänen, J.-P., Vehkomäki, M.-L., Penttilä, M., and Ruohonen, L.** (2007). The ORF YNL274c (GOR1) codes for glyoxylate reductase in *Saccharomyces cerevisiae*. *Yeast* **24**: 129–136.
- Ríos, G., Cabedo, M., Rull, B., Yenush, L., Serrano, R., and Mulet, J.M.** (2013). Role of the yeast multidrug transporter Qdr2 in cation homeostasis and the oxidative stress response. *FEMS Yeast Res.* **13**: 97–106.
- Rokka, A., Antonenkov, V.D., Soininen, R., Immonen, H.L., Pirilä, P.L., Bergmann, U., Sormunen, R.T., Weckström, M., Benz, R., and Hiltunen, J.K.** (2009). Pxm2 is a channel-forming protein in Mammalian peroxisomal membrane. *PLoS ONE* **4**: e5090.
- Rötig, A. and Poulton, J.** (2009). Genetic causes of mitochondrial DNA depletion in humans. *Biochim. Biophys. Acta* **1792**: 1103–1108.
- Russell, D.W. and Sambrook, J.** (2001). *Molecular cloning. A laboratory manual.*
- Saad, L.O., Mirandola, S.R., and Maciel, E.N.** (2006). Lactate dehydrogenase activity is inhibited by methylmalonate in vitro. *Neurochem. Res.*
- Saeed, A.I. et al.** (2003). TM4: a free, open-source system for microarray data management and analysis. *BioTechniques* **34**: 374–378.
- Sahi, C., Kominek, J., Ziegelhoffer, T., Yu, H.Y., Baranowski, M., Marszalek, J., and Craig, E.A.** (2013). Sequential duplications of an ancient member of the DnaJ-family expanded the functional chaperone network in the eukaryotic cytosol. *Mol. Biol. Evol.* **30**: 985–998.
- Schiestl, R.H. and Gietz, R.D.** (1989). High efficiency transformation of intact yeast cells using single stranded nucleic acids as a carrier. *Curr. Genet.* **16**: 339–346.
- Schwab, M.A., Sauer, S.W., Okun, J.G., Nijtmans, L.G.J., Rodenburg, R.J.T., van den Heuvel, L.P., Dröse, S., Brandt, U., Hoffmann, G.F., Laak, Ter, H., Kölker, S., and Smeitink, J.A.M.** (2006). Secondary mitochondrial dysfunction in propionic aciduria: a pathogenic role for endogenous mitochondrial toxins. *Biochem. J.* **398**: 107–112.
- Sickmann, A. et al.** (2003). The proteome of *Saccharomyces cerevisiae* mitochondria. *Proc. Natl. Acad. Sci. U.S.A.* **100**: 13207–13212.
- Simonsen, L.O., Harbak, H., and Bennekou, P.** (2012). Cobalt metabolism and toxicology--

- a brief update. *Sci. Total Environ.* **432**: 210–215.
- Singer, M.A. and Lindquist, S.** (1998). Thermotolerance in *Saccharomyces cerevisiae*: the Yin and Yang of trehalose. *Trends Biotechnol.* **16**: 460–468.
- Smith, E.H., Janknecht, R., and Maher, L.J.** (2007). Succinate inhibition of alpha-ketoglutarate-dependent enzymes in a yeast model of paraganglioma. *Hum. Mol. Genet.* **16**: 3136–3148.
- Spinazzola, A. et al.** (2006). MPV17 encodes an inner mitochondrial membrane protein and is mutated in infantile hepatic mitochondrial DNA depletion. *Nat. Genet.* **38**: 570–575.
- Stanley, D., Bandara, A., Fraser, S., Chambers, P.J., and Stanley, G.A.** (2010). The ethanol stress response and ethanol tolerance of *Saccharomyces cerevisiae*. *J. Appl. Microbiol.* **109**: 13–24.
- Sumegi, B., Sherry, A.D., and Malloy, C.R.** (1990). Channeling of TCA cycle intermediates in cultured *Saccharomyces cerevisiae*. *Biochemistry* **29**: 9106–9110.
- Suomalainen, A. and Isohanni, P.** (2010). Mitochondrial DNA depletion syndromes--many genes, common mechanisms. *Neuromuscul. Disord.* **20**: 429–437.
- Szopinska, A., Degand, H., Hochstenbach, J.-F., Nader, J., and Morsomme, P.** (2011). Rapid response of the yeast plasma membrane proteome to salt stress. *Mol. Cell Proteomics* **10**: M111.009589–M111.009589.
- Tehlivets, O., Scheuringer, K., and Kohlwein, S.D.** (2007). Fatty acid synthesis and elongation in yeast. *Biochim. Biophys. Acta* **1771**: 255–270.
- Trott, A. and Morano, K.A.** (2004). SYM1 is the stress-induced *Saccharomyces cerevisiae* ortholog of the mammalian kidney disease gene Mpv17 and is required for ethanol metabolism and tolerance during heat shock. *Eukaryotic Cell* **3**: 620–631.
- Trotter, P.J., Adamson, A.L., Ghrist, A.C., Rowe, L., Scott, L.R., Sherman, M.P., Stites, N.C., Sun, Y., Tawiah-Boateng, M.A., Tibbetts, A.S., Wadington, M.C., and West, A.C.** (2005). Mitochondrial transporters involved in oleic acid utilization and glutamate metabolism in yeast. *Arch. Biochem. Biophys.* **442**: 21–32.
- Tugal, H.B., Pool, M., and Baker, A.** (1999). Arabidopsis 22-kilodalton peroxisomal membrane protein. Nucleotide sequence analysis and biochemical characterization. *Plant Physiol.* **120**: 309–320.
- van Grinsven, K.W.A., van Hellemond, J.J., and Tielens, A.G.M.** (2009). Acetate:succinate CoA-transferase in the anaerobic mitochondria of *Fasciola hepatica*. *Mol. Biochem. Parasitol.* **164**: 74–79.
- van Hove, J.L.K., Saenz, M.S., Thomas, J.A., Gallagher, R.C., Lovell, M.A., Fenton, L.Z., Shanske, S., Myers, S.M., Wanders, R.J.A., Ruiten, J., Turkenburg, M., and Waterham, H.R.** (2010). Succinyl-CoA ligase deficiency: a mitochondrial hepatoencephalomyopathy. *Pediatr. Res.* **68**: 159–164.
- van Roermund, C.W., Hetteema, E.H., van Den Berg, M., Tabak, H.F., and Wanders, R.J.** (1999). Molecular characterization of carnitine-dependent transport of acetyl-CoA from peroxisomes to mitochondria in *Saccharomyces cerevisiae* and identification of a plasma membrane carnitine transporter, Agp2p. *EMBO J.* **18**: 5843–5852.
- Viscomi, C., Spinazzola, A., Maggioni, M., Fernandez-Vizarra, E., Massa, V., Pagano, C., Vettor, R., Mora, M., and Zeviani, M.** (2009). Early-onset liver mtDNA depletion and late-onset proteinuric nephropathy in Mpv17 knockout mice. *Hum. Mol. Genet.* **18**: 12–26.
- Visser, W.F., van Roermund, C.W.T., Ijlst, L., Waterham, H.R., and Wanders, R.J.A.** (2007). Metabolite transport across the peroxisomal membrane. *Biochem. J.* **401**: 365–375.
- Voza, A., Parisi G., De Leonardis F., Lasorsa F.M., Castegna A., Amorese D., Marmo R., Calcagnile V.M., Palmieri L., Ricquier D., Paradies E., Scarcia P., Palmieri F., Bouillaud F., and Fiermonte G.** (2014). UCP2 transports C4 metabolites out of mitochondria, regulating glucose and glutamine oxidation. *Proc. Natl. Acad. Sci. U.S.A.* **111**: 960–965.
- Wilson, W.A., Roach, P.J., Montero, M., Baroja-Fernández, E., Muñoz, F.J., Eydallin, G., Viale, A.M., and Pozueta-Romero, J.** (2010). Regulation of glycogen metabolism in yeast and bacteria. *FEMS Microbiol. Rev.* **34**: 952–985.

- You, K.M., Rosenfield C., Knipple D.C.** (2003). Ethanol tolerance in the yeast *Saccharomyces cerevisiae* is dependent on cellular oleic acid content. *Appl. Environ. Microbiol.* **69**(3):1499-1503.
- Zelenaya-Troitskaya, O., Perlman, P.S., and Butow, R.A.** (1995). An enzyme in yeast mitochondria that catalyzes a step in branched-chain amino acid biosynthesis also functions in mitochondrial DNA stability. *EMBO J.* **14**: 3268–3276.
- Zhu, J. and Zhang, M.Q.** (1999). SCPD: a promoter database of the yeast *Saccharomyces cerevisiae*. *Bioinformatics* **15**: 607–611.
- Zwacka, R.M., Reuter, A., Pfaff, E., Moll, J., Gorgas, K., Karasawa, M., and Weiher, H.** (1994). The glomerulosclerosis gene *Mpv17* encodes a peroxisomal protein producing reactive oxygen species. *EMBO J.* **13**: 5129–5134.
- Zwietering, M.H., Jongenburger, I., Rombouts, F.M., and van 't Riet, K.** (1990). Modeling of the bacterial growth curve. *Appl. Environ. Microbiol.* **56**: 1875–1881.

Supplemented Results

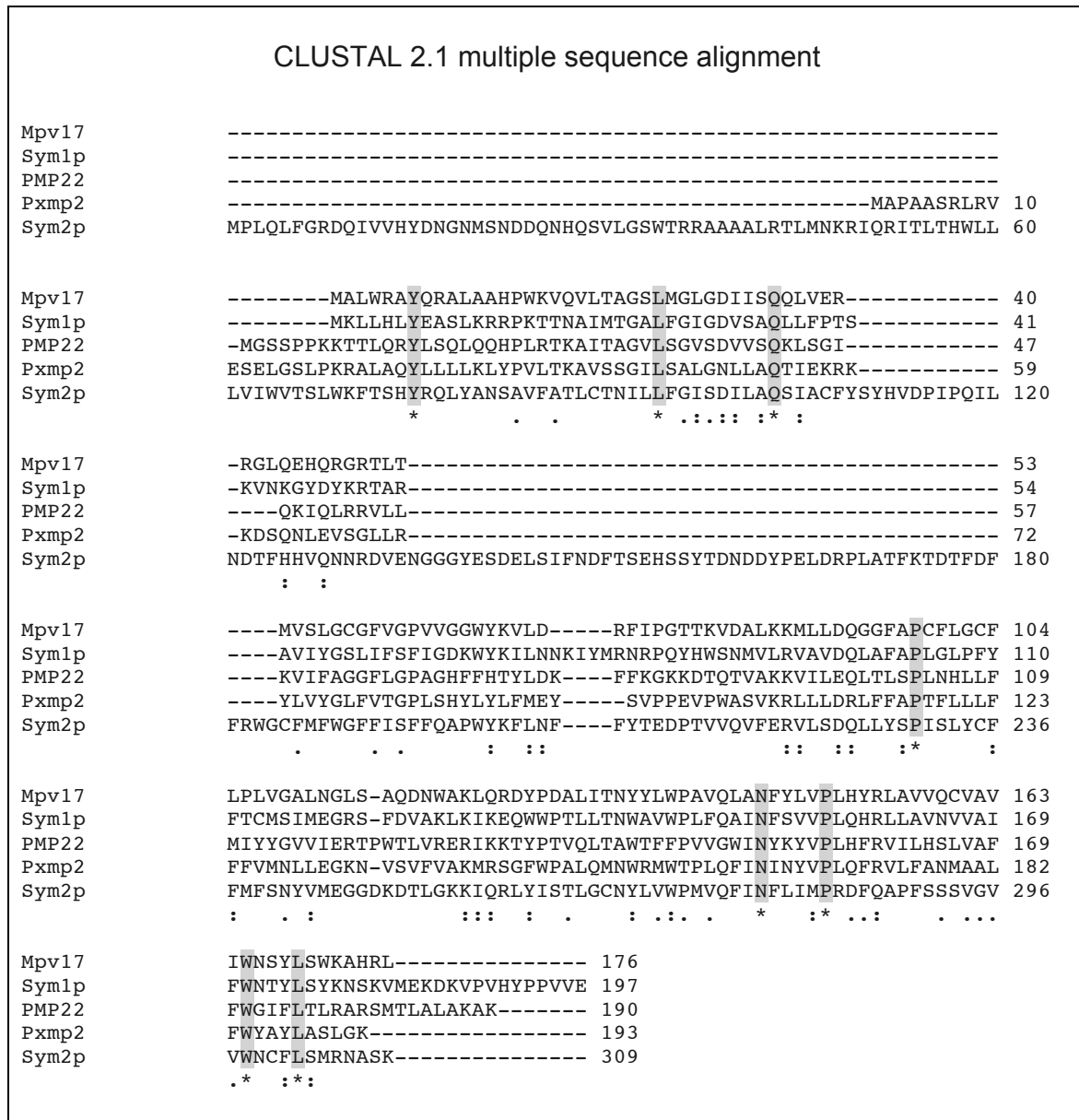
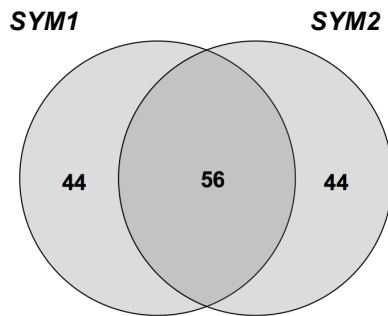
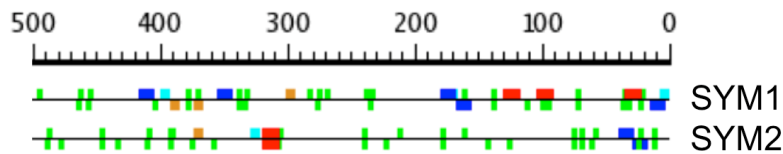


FIGURE S1. Multiple sequence alignment of *Saccharomyces cerevisiae* Sym1p (mitochondrial), Sym2p (peroxisomal), *Homo sapiens* MPV17 (mitochondrial), *Mus musculus* Pxmp2 (peroxisomal) and *Arabidopsis thaliana* PMP22 (peroxisomal). The alignment was generated with ClustalW2 (<http://www.ebi.ac.uk/Tools/msa/clustalw2/>). Highly conserved amino acid positions are shaded in grey.

A**B**

	Consensus Sequence	Count	Sig Value	Coverage
#1	ctatndbvvhgmta	5	8.411	100.00%
#2	tnsnaw	71	5.4976	100.00%
#3	actbwndnhdat	7	4.0066	100.00%
#4	actwnvtac	5	3.481	100.00%
#5	asastatr	5	3.3685	100.00%
#6	cnttwaa	10	3.1063	100.00%
#7	cctbtccc	3	0.77	100.00%
#8	cdcycc	7	0.3763	100.00%
#9	ctatc	7	0.1731	100.00%

**C**

	ABF1	ADR1	AP1	BAS2	ECB	GCN4	GCR1	HSTF	MCM1	PHO4	RAP1	SCB	STRE	SWI5	TBP
SYM1	-	2	-	2	1	7	-	1	-	-	-	1	-	-	-
SYM2	1	3	1	2	-	1	3	-	1	1	2	-	2	1	1

FIGURE S2. Co-regulation and promoter analysis of *Saccharomyces cerevisiae* SYM1/2
(A) Venn-Diagram of TOP100 coregulated genes of SYM1 and SYM2, data downloaded from the SPELL database (<http://imperio.princeton.edu:3000/yeast/>; Hibbs et al., 2007)
(B) Shared regulatory motifs in SYM1 and SYM2 promoter sequence. Data taken from the SCOPE project (<http://genie.dartmouth.edu/scope4/>; Carlson et al., 2007)
(C) Predicted binding sites of transcription factors in SYM1 and SYM2 promoter regions. Data according to the SCPD database (<http://cgsigma.cshl.org/jian>; Zhu and Zhang, 1999)

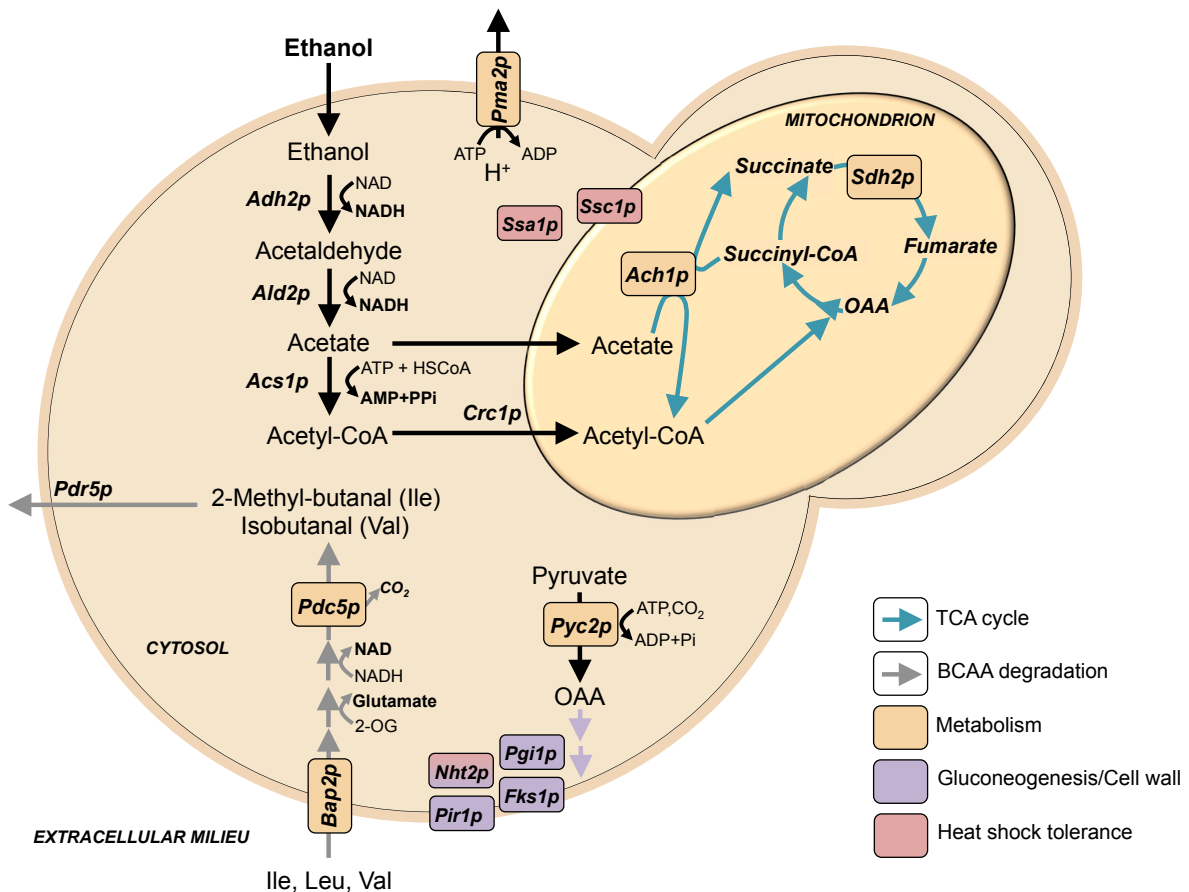


FIGURE S3. Model of the transcriptionally upregulated genes in *sym1Δ* cells in response to ethanol at 37°C. Data from Trott and Morano (2004).

Abbreviations: 2-OG: 2-oxoglutarate; Ach: acetyl-CoA hydrolase; Acs: acyl-CoA synthetase; Adh: alcohol dehydrogenase; Ald: aldehyde dehydrogenase; Bap: basic amino acid transport protein; BCAA: branched-chain amino acid; Crc: carnitine carrier; Fks: 1,3-β-D-glucan synthase; NAD: nicotinamide- dinucleotide; Nht: neutral trehalase; OAA: oxaloacetate; Pdc: pyruvate decarboxylase; Pdr: pleiotropic drug response; Pgi: phosphoglucose isomerase; Pir: protein containing internal repeats; Pma: plasma-membrane ATPase; Pyc: pyruvate carboxylase; Sdh: succinate dehydrogenase; Ssa/Ssc: stress-seventy subfamily A/C; TCA: tricarboxylic acid

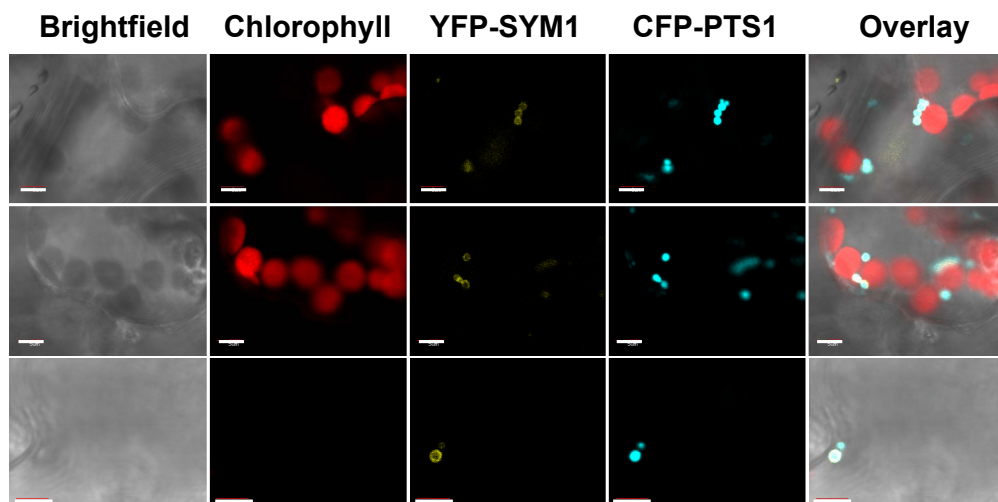


FIGURE S4. Confocal microscopic images of YFP-Sym1p localization taken from epidermis cells of four-week-old tobacco leaves co-expressing the peroxisomal marker CFP-PTS1. The YFP and CFP signal colocalized. Scale bar: 5 μm.

TABLE S1. BLAST identification of a methylmalonyl-CoA mutase in *S. cerevisiae*

Query: MutA, mitochondrial; Homo sapiens; 751 amino acids

Rank	Gene	Locus	Localization	Score	Cover	E -value	Ident
1	XDJ1	YLR090W	mito,N	30	14%	1.7	28%
2	RPL22-B	YFL034C	cyt	28.5	4%	2	42%
3	DSF1	YEL070W	n.d.	29.6	6%	2.4	30%
4	FMT	YBL013W	mito	28.9	13%	3.1	28%
5	TAZ1	YPR140W	mito	28.9	2%	3.5	50%

Localization information from <http://www.yeastgenome.org>

CLUSTAL 2.1 multiple sequence alignment

```

MutA      MLRAKNQLFLLSPHYLRQVKESGSRLLIQORLLHQOQPLHPEWAALAKKQLKGKNPEDLI 60
Xdj1p     -----MSGSDRGDRLYDVLGVTRDATVQEIKTAYRKLALKHHHPDKYVD 43
          .. ** : : : : : * * ** : : :

MutA      WHTPEG--ISIKPLYSKRDTMDLPEELPGVKPFTRGPYPTMYTFRPWTIRQYAGFSTVEE 118
Xdj1p     QDSKEVNEIKFKEITAAYEILSDPEKKSHYDLYGD-----DNGAASSGGANGFGDEDF 96
          .: * *:* : : : : . ** . . : . : ** . :

MutA      SNKFYKDNKAGQQGLSVAFDLATHRGYDSNPRVRGVDVGMAGVAIDTVEDTKILFDGIP 178
Xdj1p     MNFFNFFNNGSHDGNNFPGEYDAYEEGNSTSSKD-IDIDISLTLKDLYMGKLLKFD--- 152
          * * : :...:* ... : : : : * ... * : : : . * ..* : **

MutA      LEKMSVSMTMNGAVIPVLANFIVTGEEQGVPEKELTGTIQNDILKEFMVRNTYIFPPEPS 238
Xdj1p     LKRQVICIKCHGSGWPKPKRIHVTV---HDVECESCAGKSKERLKRFGPG-----LVAS 203
          * : : : . : * : : : : ** : * * . : * . : : ** * . *

MutA      MKIIADIFEYTAKHMPKFNSISISGYHMQEAGADAILELAYTLADGLEYSRTGLQAGLTI 298
Xdj1p     QWVVCEKCNKGKGYTKRPK--NPKNFCPDCAGLGLLSKKEIITVN--VAPGHHFNDVITV 259
          : : : : : . : * : : : . : : : * * . : : . : . : : : * :

MutA      DEFAPRLSFFWGIGMNFYMEIAKMRAGRRLWAHLIEKMFQPKNSKSLLLRAHCQTSGWSL 358
Xdj1p     KGMAD-----EEIDKTTCG-DLKFHLTEKQENLEQKQIFLKNFDDGAG---- 301
          . : * : : : : ** * . * * ** * : : : : * . . : .

MutA      TEQDPYNNIVRTAIEAMAAVFGGTQSLHTNSFDEALGLPTVKSARIARNTQIIIQEESGI 418
Xdj1p     -----EDLYTSITISLSEALTFGEKFLTKTFDDRLLTSLVKPGRVVRPGDTIKIANEGW 355
          : : : : : : : : * : : : * : : : * : * : * : * : * : * : *

MutA      PKVADPWGGSYMMELTNDVYDAALKLINEIEEMGGMAKAVAEGIPKLRIECAARRQAR 478
Xdj1p     PILDNPHG-----RCGD 367
          * : : * * * * * * * * * * * * * * * * * * * * * * * * * *

MutA      IDSGSEVIVGVNKYQLEKEDAVEVLAIDNTSVRNROIEKLKIKSSRDQALAERCLAALT 538
Xdj1p     LYVFVHIEFPPDNWFNEKS---ELLAIKTNLPSSSSCASHATVNTEDDSNLTN----- 417
          : . : . : : : ** . * : * * . . . . : : : . * * : :

MutA      ECAASGDGNILALAVDASRARCTVGEITDALKKVFGEHKANDRMVSGAYRQEFGESKEIT 598
Xdj1p     -----NETI 421
          : *

MutA      SAIKRNVHKFMEREGRRPRLLVAKMGQDGHDRGAKVIATGFADLGFVDVIGPLFQTPREVA 658
Xdj1p     SNFRIHTDDLPEGIRP-----FKPEAQDSAHQKARSSYCCIQ----- 459
          * : : * . ** ** : : : * . : : : : :

MutA      QQAVDADVHAVGISTLAAGHKTLPPELIKELNSLGRPDILVMCGGVIPPQDYEFLEFVGV 718
Xdj1p     -----

MutA      SNVFGPGTRIPKAAVQVLDIEKCLEKKQQSV 750
Xdj1p     -----

```

TABLE S2. BLAST identification of a methylmalonyl-CoA decarboxylase in *S. cerevisiae*

Query: Escherichia coli O145:H28 str. RM13514; 261 amino acids

Rank	Gene	Locus	Localization	Score	Cover	E -value	Ident
1	EHD3	YDR036C	mito	43.9	66%	1.00E-06	21%
2	SYG1	YIL047C	PM	26.6	10%	0.33	43%
3	MSB1	YOR188W	cyt	26.2	41%	0.5	21%
4	MSA1	YOR066W	cyt,N	25.4	9%	0.7	46%
5	UBP9	YER098W	cyt	25.4	9%	0.75	38%
6	MCX1	YBR227C	mito	25	17%	1.2	29%

Localization information from <http://www.yeastgenome.org>

CLUSTAL 2.1 multiple sequence alignment

```

MMCD      -----MSYQY-----VNVVTINKVAVIEFNYGRKLN 27
Ehd3p     MLRNTLKCAQLSSKYGFKTTTRTFMTTQPQLNVTDAPPVLFVQDTARVITLNRPKKLN 60
           :*  :*
           *  ...  :..  **  :*  :****

MMCD      LSKVFIDDLMQALSIDLNRPEIR-CIILRAPSGSKVFSAG-----HDIHELPSGGRDPLSY 81
Ehd3p     LNAEMSESMFKTLNEYAKSDTTLNLVILKSSNRPRSFCAAGDVATVAIFNFNKEFAKSIKF 120
           * .  :  : : : : * . :  : :  : * : * *  * : : : .  : : : :

MMCD      DDPLRQITRMIQKFPKPIISMVEGVSVWGGAFEMIMSSDLIIAASTSTFSMTPVNLGVPYN 141
Ehd3p     FTDEYSLNFQIATYLPKPIVTFMDGITMGGVGLSIHTPFRIATENTKWAMPEMDIGFFPD 180
           : . .  *  : .  * : : : : : : * . * * . : : : : * : : : : : * . : : * . :

MMCD      LVGIHNLTR-----DAGFHIVKELIFTASPIAQRALAVGILNHVVEVEELEDFTLQMAH 196
Ehd3p     VGSTFALPRIVTLANSNSQMALYLCLTGEVVTGADAYMLGLASHYVSENLDALQKRLGE 240
           : . .  * . *  : : .  : :  *  : * . .  : * .  * : : * . * .  * : : : : : : . .

MMCD      HIS--EKAP-----LAIAVIKEELRVLGEAHTMNSD----- 225
Ehd3p     ISPPFNNDPQSAYFFGMVNESIDFVSPLPKDYVFKYSNEKLNVEACFNLSKNGTIEDI 300
           .  : :  *  : :  : :  : :  : :  : * : * . * :  : : : : : :

MMCD      --EFERIQG-----MRRAVYDSE- 241
Ehd3p     MNNLRQYEGSAEGKAFQAQEIKTLLTKSPSSLQIALRLVQENSRDHIESAIKRDLYTAAN 360
           : : :  : *  : : : : : : : : : : : : : : : : : : : : : : : : : : :

MMCD      --DYQEGMNAFLEKRKPNFVGH----- 261
Ehd3p     MCMNQDSLVEFSEATKHKLIDKQRPYPWTKKEQLFVSQLTSITSPKPSLPMSLLRNTSN 420
           * : . :  *  *  *  *  : : : :

MMCD      -----
Ehd3p     VTWTQYPYHSKYQLPTEQEIAAYIEKRTNDDTGAKVTEREVLNHFANVIPSRRGKLGIQS 480

MMCD      -----
Ehd3p     LCKIVCERKCEEVNDGLRWK 500

```

Supplemented Material and Methods

TABLE M1. *Escherichia coli*, *Saccharomyces cerevisiae* and *Agrobacterium tumefaciens* strains used in this study.

Strain	Genotype	Reference
<i>E. coli</i> MACH1-T1R	F- Φ 80lacZ Δ M15 Δ lacX74 hsdR(rK-, mK+) Δ recA1398 endA1 tonA	Invitrogen, Life Technologies
<i>E. coli</i> ccdB survival 2 TI ^R	F- mcrA Δ (mrr-hsdRMS- mcrBC) Φ 80lacZ Δ M15 Δ lacX 74 recA1 ara Δ 139 Δ (ara- leu)7697galU galK rpsL (StrR) endA1 nupG fhu2::IS2	Invitrogen, Life Technologies
<i>S. cerevisiae</i> BY4741	Mat a his3 Δ leu2 Δ met15 Δ ura3 Δ	Euroscarf
<i>S. cerevisiae</i> BY4742	Mat α his3 Δ leu2 Δ lys2 Δ ura3 Δ	Euroscarf
<i>S. cerevisiae</i> sym1 Δ	Mat a his3 Δ leu2 Δ met15 Δ ura3 Δ YLR251w::kanMX4	Euroscarf
<i>S. cerevisiae</i> sym2 Δ	Mat α his3 Δ leu2 Δ lys2 Δ ura3 Δ YOR292c::kanMX4	Euroscarf
<i>S. cerevisiae</i> cit2 Δ	Mat a his3 Δ leu2 Δ met15 Δ ura3 Δ YCR005c::kanMX4	Euroscarf
<i>S. cerevisiae</i> cit3 Δ	Mat a his3 Δ leu2 Δ met15 Δ ura3 Δ YPR001w::kanMX4	Euroscarf
<i>S. cerevisiae</i> icl2 Δ	Mat a his3 Δ leu2 Δ met15 Δ ura3 Δ YPR006c::kanMX4	Euroscarf
<i>S. cerevisiae</i> cit2 Δ sym1 Δ	Mat a his3 Δ leu2 Δ met15 Δ ura3 Δ YCR005c::kanMX4 YLR251w::hygMX4	This study
<i>S. cerevisiae</i> cit3 Δ sym1 Δ	Mat a his3 Δ leu2 Δ met15 Δ ura3 Δ YPR001w::kanMX4 YLR251w::hygMX4	This study
<i>S. cerevisiae</i> icl2 Δ sym1 Δ	Mat a his3 Δ leu2 Δ met15 Δ ura3 Δ YPR006c::kanMX4 YLR251w::hygMX4	This study
<i>S. cerevisiae</i> ehd3 Δ	Mat a his3 Δ leu2 Δ met15 Δ ura3 Δ YDR036c::kanMX4	Euroscarf
<i>S. cerevisiae</i> xdj1 Δ	Mat a his3 Δ leu2 Δ met15 Δ ura3 Δ YLR090w::kanMX4	Euroscarf
<i>S. cerevisiae</i> gsy1 Δ gsy2 Δ	Mat α leu2 Δ trp1 Δ ura3 Δ gsy1::kanMX6 gsy2::natMX4	Baskaran et al., 2011
<i>A. tumefaciens</i> GV3101 pMP90	C58 Rif ^R , pMP90 (pTic58 Δ T-DNA, Gent ^R)	T-DNA transfer

TABLE M2. Oligonucleotides used in this study.

Name		Sequence (5'→3')	Target [Purpose]
Cloning			
UCP2F	F	AAGCTTACCATGGCGGATTTCAA	UCP2 (At5g58970) CDS w/o STOP [C-terminal fusion to His-tag]
UCP2R	R	GGATCCATCGTACAAGACTTGTCTT	
JW103	F	GGGGACAAGTTTGTACAAAAAAGCAGGCTTCGAAGGA GATAGAACCATGAAGTTATTGCATTTATATGAAGCG	SYM1 (YLR251W) CDS w/STOP [N-terminal fusion to YFP] (GW)
JW104	R	GGGGACCACCTTTGTACAAGAAAGCTGGGTCTTATTCG ACCACGGGTGG	
JW109	F	GGGGACAAGTTTGTACAAAAAAGCAGGCTTCGAAGGA GATAGAACCATGCCTCTTCAACTTTTTGGC	SYM2 (YOR292C) CDS w/o STOP [C-terminal fusion to YFP] (GW)
JW110	R	GGGGACCACCTTTGTACAAGAAAGCTGGGTCTTTAGAC GCATTTCTCATCGAA	
Genotyping (according to euroscarf instructions)			
P78	R	CTGCAGCGAGGAGCCGTAAT	Kan_A
P79	F	TGATTTTGATGACGAGCGTAAT	Kan_B
JW48	F	TGGTCTTTTCTCTCCGATGG	SYM1 YLR251W_A
JW49	R	ATTAGACCAGTGGTACTGAGGTCTG	SYM1 YLR251W_B
JW50	F	AGAGCAATGGTGGCCTACAC	SYM1 YLR251W_C
JW51	R	CGGTAGCTGAAGAACAACAGG	SYM1 YLR251W_D
JW114	F	AACCGGTGTAACCCCATACA	SYM2 YOR292C_A

JW115	R	TCTATAATGACTGGTAAATTTCCATAGG	SYM2 YOR292C_B
JW116	F	TACAAGTTCTTGAATTTCTTTTACTGA	SYM2 YOR292C_C
JW117	R	GCCATCGATAAAAGGTTGGT	SYM2 YOR292C_D
Deletion			
SYM1F	F	tctttgttactataggaagatagaattgatattaaaacagCGTACGC TGCAGGTCGAC	SYM1 (YLR251W) gene replacement
SYM1R	R	tctttgttactataggaagatagaattgatattaaaacagCGTACGC TGCAGGTCGAC	

Abbreviations: F: forward (sense) primer; GW: Gateway; R: reverse (antisense) primer;

IV.2 Manuscript 2

Participation of Arabidopsis Peroxisomal membrane protein of 22 kDa in fatty and branched-chain amino acid metabolism renders it crucial to peroxisome function and plant performance in abiotic stress conditions.

Jan Wiese¹, Martin G. Schroers¹, Henrik Tjellström², Cheng Peng², Robert L. Last^{2,3}, John B. Ohlrogge², Jianping Hu^{2,4}, Andreas P.M. Weber¹ and Nicole Linka^{1¶}

¹Department of Plant Biochemistry, Heinrich-Heine University Düsseldorf, 40225 Düsseldorf, Germany

²Department of Plant Biology, Michigan State University, East Lansing, MI 48824, USA

³Department of Biochemistry and Molecular Biology, Michigan State University, East Lansing, MI 48824, USA

⁴MSU-DOE Plant Research Laboratory, Michigan State University, East Lansing, MI 48824, USA

¶ Corresponding author

Abstract

Peroxisomal fatty acid β -oxidation and glyoxylate cycle activity are important to convert storage oil to respiratory substrates and gluconeogenic C-units for germination and seedling growth. During extended darkness β -oxidation and branched-chain amino acid (BCAA) catabolism are important to fuel plant respiratory metabolism, whereas in developmental senescence β -oxidation contributes to mobilize carbon reserves to seed sinks. Knowledge about transport across the peroxisomal membrane in these pathways is scarce. Here, we report on a putative transport function of the *Arabidopsis thaliana* Peroxisomal Membrane Protein of 22 kDa (PMP22) by analysis of loss-of-function mutants during seedling establishment, developmental senescence and abiotic stress conditions. *pmp22* mutants displayed inefficient storage oil mobilization and compromised adaptations to darkness-induced starvation, temperature variation and oxidative stress. Growth of *pmp22* mutants was sensitive to the presence of BCAA and associated catabolites (e.g. isobutyrate, propionate, and acrylate). In hypocotyls of *pmp22* mutants we observed peroxisome aggregates, which are suggested to represent non-functional, highly oxidized peroxisomes. Heterologous expression of PMP22 suppressed the growth phenotype of a yeast mutant defective in a metabolite channel. Due to similarities to BCAA catabolic mutants we discuss PMP22 function in export of the end product of peroxisomal BCAA conversion, 3-hydroxypropionate.

Introduction

Our knowledge of transport proteins residing in the peroxisomal membrane is scarce compared to the diverse range of metabolite translocators reported for plastidic and mitochondrial membranes (Linka and Weber, 2010; Linka and Esser, 2012; Linka and Theodoulou, 2013).

Plant peroxisomes are essential organelles and harbor pathways of central C metabolism. Most prominent roles are storage oil mobilization by fatty acid β -oxidation and glyoxylate cycle activity during early seedling establishment and glycolate detoxification in the photorespiratory C_2 cycle of photosynthetic leaves (Hu et al., 2012). In seedlings fatty acids are released from oil-body stored triacylglycerol (TAG), imported into peroxisomes and oxidized to acetyl-CoA units by β -oxidation. The glyoxylate cycle converts acetyl-CoA units to enable synthesis of carbohydrates or mitochondrial respiration. Therefore, malate synthase and citrate synthase produce C_4 and C_6 units by acetyl-CoA condensation to glyoxylate and oxaloacetate. Isocitrate lyase releases glyoxylate and succinate. Succinate is exported for consumption in the gluconeogenic pathway or respiration (Graham, 2008). In the photorespiratory C_2 cycle Ribulose-1,5-bisphosphate-carboxylase/oxygenase originated glycolate is converted to glyoxylate, which is transaminated to glycine and shuttled to mitochondria for decarboxylation (Reumann and Weber, 2006). Peroxisomes are involved in the recycling of Nitrogen from the N-source to sinks by an implication in purine degradation (Brychkova et al., 2008b; Werner and Witte, 2011). In addition to high mass flux, these processes comprise intra- and extraperoxisomal reactions (Fig. 1).

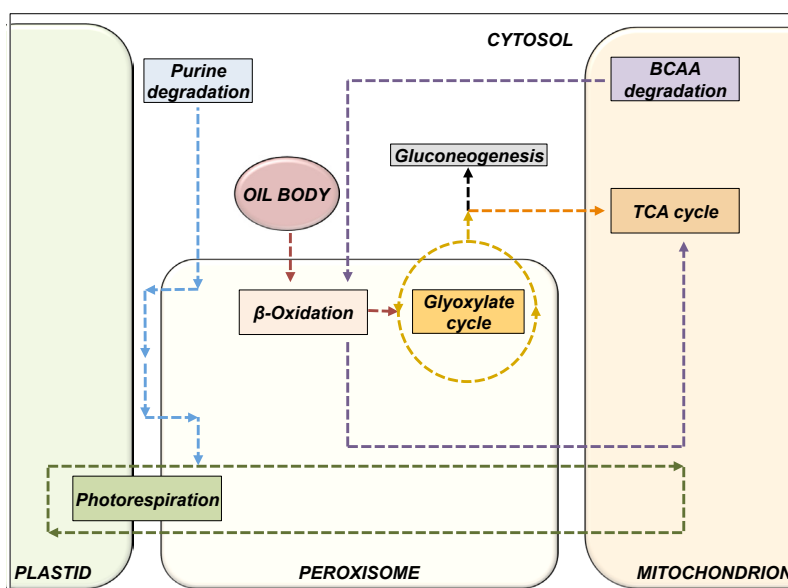


FIGURE 1. Network of Carbon and Nitrogen metabolic pathways implicated in transport of carboxylates or carboxylic-acid-CoA-esters across the peroxisomal membrane. BCAA: branched-chain amino acid; TCA: tricarboxylic acid.

Substantial channeling of both substrates and cofactors across the peroxisomal membrane is needed to meet the metabolic requirements (Visser et al., 2007; Rottensteiner and Theodoulou, 2006; Linka and Theodoulou, 2013).

Previously peroxisomal cofactor transport systems for ATP (Arai et al., 2008; Linka et al., 2008) and NAD/CoA (Bernhardt et al., 2012; Agrimi et al., 2012) were identified. The peroxisomal fatty acid ABC-transporter PXA1 was first identified due to 2,4-dichlorophenoxybutyric acid (2,4-DB) resistance (Hayashi et al., 1998) and has been implicated in import of C₂-C_{>22} monocarboxylic acids (Zolman et al., 2001b; Footitt et al., 2002; Nyathi et al., 2010; De Marcos Lousa et al., 2013). To date, other peroxisomal transport proteins are unknown.

β-oxidation of fatty acids and branched-chain amino acid (BCAA) catabolites is important for alternative respiration in stressed plants (Araújo et al., 2011; Kunz et al., 2009; Araújo et al., 2010). Photosynthetic assimilates are limited in extended darkness and natural senescence conditions, therefore fatty acid and amino acid respiration are devoted to compensate for low carbon and energy status (Pracharoenwattana et al., 2005; Buchanan-Wollaston et al., 2005; Usadel et al., 2008; Yang and Ohlrogge, 2009; Engqvist et al., 2011; 2009). The importance of β-oxidation in mature leaves has further been demonstrated by sensitivity to extended darkness of *pxa1* and mutants of peroxisomal 3-ketoacyl-CoA thiolase (KAT2; Kunz et al., 2009) and 3-hydroxyisobutyryl-CoA hydrolase (CHY1; Dong et al., 2009). CHY1 is needed for both fatty acid and valine catabolism (Zolman et al., 2001a). β-oxidation enzymes and peroxisomal citrate synthase were transcriptionally induced in extended darkness as well as in developmental senescence (van der Graaff et al., 2006; Breeze et al., 2011).

The *Arabidopsis* Peroxisomal Membrane Protein of 22 kDa (PMP22) was identified as one of the first plant peroxisomal membrane proteins by subcellular fractionation (Tugal et al., 1999). Later immunofluorescence imaging (Murphy et al., 2003) and experimental proteomics (Eubel et al., 2008; Reumann et al., 2009) confirmed this finding. A putative functional orthologue of PMP22, mammalian Peroxisomal Membrane Protein 2 (Pxmp2), formed a water filled, porin-like channel in artificial lipid bilayers (Rokka et al., 2009). *Pxmp2*^{-/-} peroxisomes displayed partial restriction of permeability to uric acid. *In vitro* characterization indicated Pxmp2 to be permeable to carboxylic acids such as pyruvate and 2-oxoglutarate (Rokka et al., 2009). Pore-

forming activities in peroxisomal membrane fractions have also been described for yeast, mammals and protozoa (Van Veldhoven et al., 1987; Antonenkov et al., 2005; 2009; Grunau et al., 2009; Gualdron-López et al., 2012). Reumann and coworkers (Reumann et al., 1995; 1996; 1997; 1998) described the presence of porin-like channels in spinach leaf peroxisomes and castor bean glyoxysomes. The postulated channel had a high-affinity binding site for small dicarboxylic anions and was proposed to facilitate flux through the photorespiratory and glyoxylate cycle.

Mitochondrial PMP22 homologues, human MPV17 and the stress-inducible yeast MPV17 protein 1 (Sym1p), are involved in mtDNA maintenance. Mutations in MPV17 cause the mitochondrial DNA depletion syndrome (MDSS), a genetically heterogeneous group of autosomal recessive disorders characterized by decreased mtDNA content, accompanied by reduction of mitochondrial respiration chain activity. Patients often die in infancy or early childhood. Baker's yeast Sym1p formed a channel in artificial bilayers (Reinhold et al., 2012). *sym1Δ* was compromised in growth on medium with non-fermentable carbon sources under heat stress conditions. Overexpression of yeast endogenous membrane proteins Ymc1p or Odc1p suppressed the phenotype (Dallabona et al., 2010). These proteins belong to the Mitochondrial Carrier Family (MCF) and counter-exchange 2-oxodicarboxylates across the inner mitochondrial membrane and enable anaplerotic flux into the tricarboxylic acid (TCA) cycle (Fiermonte et al., 2001; Trotter et al., 2005). Literature reports point to a high probability of a role for MPV17/PMP22 proteins in transmembrane transport.

Here, we describe PMP22 to genetically complement *sym1Δ* and propose PMP22 as plant peroxisomal pore-forming protein. We focus on the physiological importance of Arabidopsis PMP22 in seedling storage oil mobilization and alternative respiration in extended darkness. PMP22 was required for general peroxisome function. Furthermore PMP22 seemed to be required for optimal nutrient relocation in developmental senescence. We discuss whether PMP22 is a general diffusion pore for small solutes or specifically facilitates translocation of BCAA catabolites. Latter was indicated by similarity to *chy1* and led to the hypothesis that loss of 3-hydroxypropionate export in BCAA degradation could potentially cause pleiotropic phenotypes.

Results

Identification of a novel β -oxidation transport protein

We aimed to identify a protein that enables transport of small carboxylic acid across the peroxisomal membrane. To this end we screened microarray data for induced gene expression of membrane proteins in dark-treated and senescing leaf tissue, which are conditions of enhanced lipid catabolism and require export of peroxisomally generated dicarboxylates for cellular viability (Buchanan-Wollaston et al., 2005; Kunz et al., 2009; Yang and Ohlrogge, 2009; Troncoso-Ponce et al., 2013). We identified the Peroxisomal Membrane Protein of 22 kDa (PMP22) to exhibit the predicted pattern of upregulation in prolonged darkness, leaf ageing and natural senescence (Figure 2A).

The Arabidopsis genome encodes ten marginally studied PMP22-type proteins

BLAST analysis of the Arabidopsis proteome unraveled nine PMP22 paralogues (Figure 2B), hereafter referred to as PMP22-type proteins. The genes encode integral membrane proteins with at least four predicted transmembrane helices. With the exception of At1g52870 the proteins are characterized by the presence of the 57 aa MPV17/PMP22 superfamily domain spanning the last two C-terminal transmembrane helices (Punta et al., 2012). Combined BLASTP and HMMER (Finn et al., 2011) analysis revealed the MPV17/PMP22 domain to be restricted to PMP22-type genes in *A. thaliana*. The region with the highest sequence conservation in PMP22-type proteins aligns with the first transmembrane domain and the following hydrophilic part of PMP22 (Figure S1). This region harbors two conserved amino acids, R54 and G67, which were essential for MPV17 function (Spinazzola et al., 2006). Neighbour-Joining phylogenetic tree reconstruction revealed pairs of high sequence identity: At4g33905 and At2g14860 share 71 % identical aa residues, PMP22 and At4g14305 have 57 % sequence identity (thus hereafter referred to as PMP22-like) and At4g03410 is to 50 % identical to At1g52870. The overall identity of PMP22-type proteins averages 22 %.

PMP22-type proteins localize to plastids, mitochondria and peroxisomes

Experimental proteomics suggested At2g42770 and At5g19750 to localize to the chloroplast envelope and At3g24570 to reside in mitochondrial membranes (Ferro et al., 2003; Froehlich et al., 2003; Zybailov et al., 2008; Klodmann et al., 2011). Subcellular localization predictions by sequence comparison suggested At1g52870

and At4g03410 to reside in plastidic membranes and At2g14860, At4g33905, At5g43140 are expected to localize to mitochondrial membranes (Schwacke et al., 2003; Tanz et al., 2013).

Subcellular localization of PMP22-like (At4g14305) was addressed by transient expression of N- and C-terminal EYFP fusion proteins in tobacco and analyzed by *in vivo* fluorescence microscopy. The signals colocalized with the fluorescence of the CFP-PTS1 peroxisome marker (Figure 2C).

We revealed extraperoxisomal localization for mitochondria predicted At2g14860, At3g24570 and At5g43140 when the C-terminus was masked by EYFP fusion. At2g14860, At5g43140 signals displayed the mitochondrial fluorescence pattern of At3g24570, with a punctuate pattern of oval particles (ca. 1 μm in diameter, considerably smaller than peroxisomes) dispersed in the cell (Figure S2).

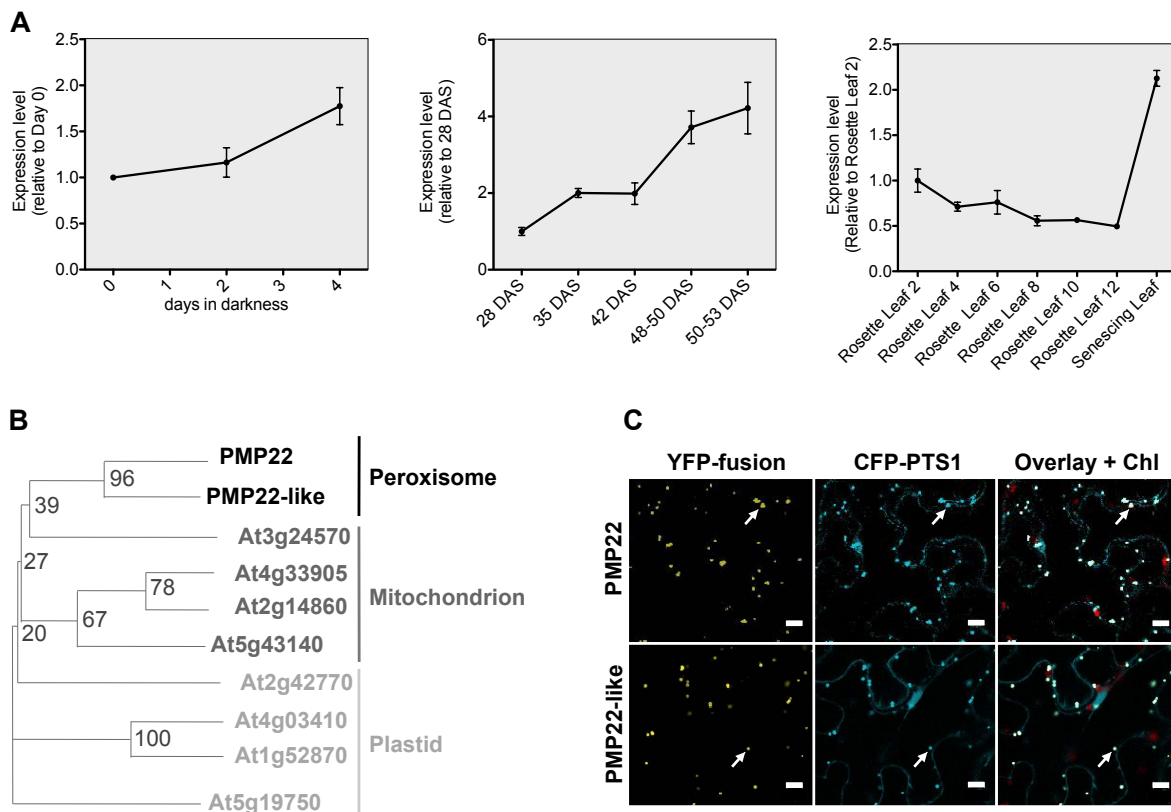


FIGURE 2. Analysis of PMP22 transcripts in response to dark and ageing, Phylogenetic reconstruction of PMP22-type proteins and colocalization of PMP22 and PMP22-like EYFP fusion proteins and CFP-PTS1 in tobacco epidermis cells.

(A) Plot of mean PMP22 expression. PMP22 was induced upon shift to darkness, natural senescence and leaf ageing. Data for darkness and natural senescence was derived from van der Graaff et al. (2006) and rosette leaf ageing data was taken from Schmid et al. (2005). DAS: days after sewing.

(B) Unrooted Neighbour Joining phylogenetic tree of *A. thaliana* PMP22-type family proteins including information on subcellular localization. Node labels represent Bootstrap values.

(C) Confocal microscopic images of PMP22-YFP and PMP22-like-YFP localization taken from epidermis cells of 4-week-old tobacco leaves co-expressing the C-terminal YFP fusion protein and the peroxisomal marker CFP-PTS1. Scale bar: 10 μm . Chl: Chlorophyll autofluorescence

Reciprocal BLAST analysis indicated the conservation of an organelle specific isoform in chlorophyte and streptophyte lineages (Figure S3). To date there is no report ascribing a molecular function neither to the MPV17/PMP22 domain nor any of the PMP22-type genes in *A. thaliana*. Recently, At2g42770 was proposed as a putative photorespiratory transporter by co-expression analysis (Bordych et al., 2013). Amino acid and cofactor metabolism co-regulation is shared within the PMP22-type family (Figure S3C).

Pathway network based searches with ATTED-II (Obayashi et al., 2011) identified PMP22 expression to correlate with BCAA degradation, glyoxylate and dicarboxylate metabolism, fatty acid β -oxidation, α -linolenic metabolism, pyridine nucleotide cycling and sulfite oxidation.

PMP22 interacts with PMP22-like

To elucidate the role of two peroxisomal PMP22-type proteins *in planta*, we first profiled the tissue-specific expression of both genes (Figure 3A). PMP22 and PMP22-like transcript were detectable in roots, seeds, seedlings, leaves, and flowers, but, compared to PMP22, reduced by up to three orders of magnitude. Both PMP22 and PMP22-like were transcriptionally induced 15- and 5-fold in senescing leaf tissue, when compared to vegetative rosette leaves.

Given the spatiotemporal co-existence of PMP22 and PMP22-like, we examined the physical interaction potential by *in vivo* bimolecular fluorescence complementation (Citovsky et al., 2006). Therefore intrinsically non-fluorescent split YFP protein sequences were translationally fused to the coding sequences of the candidate genes. nYFP and cYFP fusion-protein pairs were transiently coexpressed in *Nicotiana tabacum* along with the peroxisomal CFP-PTS1 marker. YFP fluorescence analysis showed that PMP22 and PMP22-like associate *in planta* as homo- and hetero-oligomers in the peroxisomal membrane, independent of a N- or C-terminal location of the split YFP entity (Figure 3B). Expression of nYFP or cYFP from the empty vector did not result in fluorescence complementation, though PMP22 membrane topology suggested the bait halves at the termini of PMP22 and PMP22-like to face cytosol (A. Meyer, unpublished).

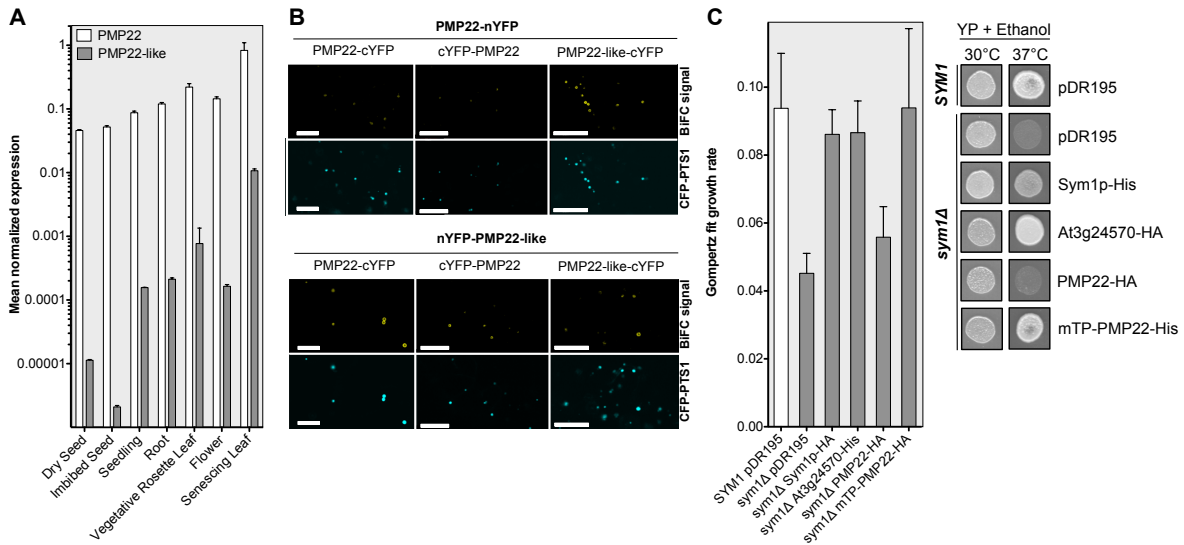


FIGURE 3. Analysis of tissue-specific abundance of PMP22 and PMP22-like transcripts, suppression of the *sym1Δ* growth phenotype by heterologous expression of At3g24570 and mtTP-PMP22 and bimolecular fluorescence complementation by interaction of PMP22 and PMP22-like *in vivo*

(A) Plot of mean normalized expression (+SE; n=3) of PMP22 and PMP22-like in different tissues. PMP22 and PMP22-like were constitutively expressed but reached highest levels in ageing leaves. PMP22-like is a low expressed gene and had highest expression in senescence.

(B) Microscopic images of bimolecular fluorescence complementation of split YFP pairs fused to C- and N-termini of PMP22 and PMP22-like. YFP fluorescence indicated hetero- and homo-oligomerisation of the proteins *in vivo*. Confocal microscopic images were taken from epidermis cells of 4-week-old tobacco leaves co-expressing the indicated split YFP fusion proteins and the peroxisomal marker CFP-PTS1. Scale bar: 10 μm. BiFC: bimolecular fluorescence (YFP) complementation

(C) (left) Plot of mean *sym1Δ* growth rate (+SD; n=4) upon introduction of the empty vector, SYM1, At3g24570, PMP22 or mTP-PMP22 as estimated by fitting growth in Yeast extract/Bacto-peptone/2 % (v/v) ethanol to the Gompertz-growth equation (Zwietering et al., 1990). (right) Photograph of *sym1Δ* cells grown at 30°C/37°C on Yeast extract/Bacto-peptone/ 2 % (v/v) ethanol upon transgenic introduction of the empty expression vector, SYM1, At3g24570, PMP22 or mTP-PMP22. Cells were grown in YPD, serially diluted and spotted. Mitochondria re-targeted PMP22 genetically suppressed the heat sensitive *sym1Δ* phenotype on ethanol containing medium, as shown by the calculated growth rate at restrictive growth (left) and the dilution patch assay. Cells transformed with the empty vector (pDR195) were used as control. His: Hexahistidine-tag; HA: Hemagglutinin-tag; mTP: mitochondrial targeting peptide; pDR195: empty expression vector (Control); YP: Yeast extract-Bacto-peptone

PMP22 suppresses the phenotype of yeast with a defect in a pore-forming protein

Two MPV17/PMP22 domain proteins were reported to form ion channels upon incorporation in artificial lipid bilayers: the peroxisomal Pmp2 in mammals (Rokka et al., 2009) and baker's yeast mitochondrial Sym1p (Reinhold et al., 2012). We assessed if pore-forming activity is an intrinsic feature of the PMP22 protein or requires association to PMP22-like. Pure fractions of recombinant PMP22-His were sufficient to detect channel-forming activity *in vitro* (Figure S4/S5). Furthermore, we aimed to restore *sym1Δ* growth by heterologous expression of PMP22. *sym1Δ* growth was shown to be compromised at 37°C with ethanol as sole carbon source

(Trott and Morano, 2004). Expression of the At3g24570 gene product (mitochondrial PMP22-type protein) suppressed this growth phenotype. PMP22 expression did not restore wild-type growth. Expression of the *A. thaliana* succinate-fumarate carrier (AtMSFC1; Catoni et al., 2003) mitochondrial targeting peptide translationally fused to PMP22 resulted in suppression of the *sym1Δ* phenotype (Figure 3C). Notably, the suppression was successful in absence of hetero-oligomerization with PMP22-like. This suggests PMP22 to form a pore in membranes as homo-oligomer and an involvement in metabolite channeling across the peroxisomal membrane.

Conventional *in vitro* Liposome uptake studies (Linka et al., 2008; Bernhardt et al., 2012) with import promoting substrate gradients across PMP22-proteoliposome membranes did not result in detectable uptake of labeled anions (Figure S7). Growth of an *E. coli* malate uptake mutant (Lo et al., 1972; Lee et al., 2008;) was not restored by inducing expression of PMP22 (Figure S8).

Characterization of *Arabidopsis pmp22* mutants

To investigate the role of PMP22 and PMP22-like *in planta* we established homozygous *A. thaliana* T-DNA insertion lines: *pmp22-1* (SALK_205443), *pmp22-like-1* (GABI-380B12) and *pmp22-like-2* (SALK_052461; Figure 4A). Sequencing of the plant T-DNA border flanking regions revealed none of the integration sites to hit exons. In RT-PCR analysis *pmp22-like-1* had no detectable full-length transcript (Figure 4B). *pmp22-like-2* and *pmp22-1* were knockdown lines with 10 % and 30 % residual transcript (Figure 4C).

Simultaneously we used an RNAi approach to repress the expression of PMP22 or PMP22-like. We retrieved artificial miRNA sequences from the Web microRNA Designer 3 (WMD3; Ossowski et al., 2008; Schwab et al., 2006) and transgenically introduced constitutive repression of PMP22 or PMP22-like in *Arabidopsis* under control of the cauliflower mosaic virus 35S promoter. Screening of independent transgenic lines (T_2) by quantitative RT-PCR detected up to ten-fold reduction of PMP22 or PMP22-like in rosette leaves, correlating with the presence of the respective miRNA (Figure 4C). Segregation analysis led to the identification of several homozygous lines.

In early plant growth we did not observe phenotypic growth differences of either *pmp22* or *pmp22-like* lines compared to wild types (Figure 5). Mature *pmp22-2*,

pmp22-6 and *pmp22-8* displayed a reduced rosette diameter, smaller leaves and symptoms of premature senescence of oldest rosette leaves (Figure 4D).

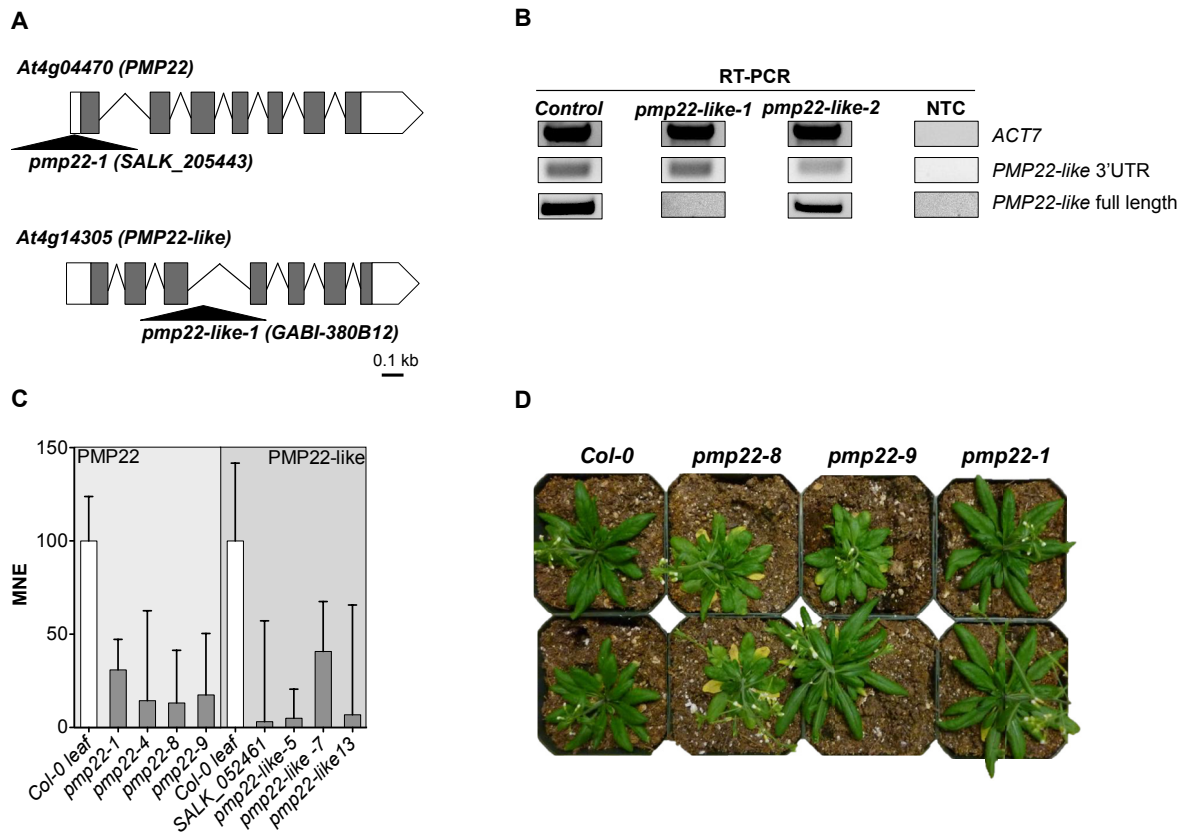


FIGURE 4. T-DNA insertion/RNAi mutants of PMP22(-like) have reduced or absent transcript.

(A) Gene structures of PMP22 and PMP22-like. (Open) boxes indicate (un-)translated regions. Triangles represent insertion sites of T-DNA lines for *pmp22-1* (5'UTR) and *pmp22-like-1* and *pmp22-like-2* (3rd Intron). The gene structure is based on information obtained from the TAIR database (<http://www.arabidopsis.org>).

(B) RT-PCR analysis of PMP22-like transcripts. *pmp22-like-1* had no detectable full length transcript in six-week-old rosette leaves, whereas *pmp22-like-2* still showed amplification of the full length transcript. NTC: non-template control

(C) Plot of mean normalized expression (+SE; n=9) of PMP22 and PMP22-like in 6-week-old rosette leaves in RNAi and T-DNA mutants of *pmp22* and *pmp22-like*. Lowest transcript of PMP22 was detected in *pmp22-8*: a miRNA line with ca. 10% residual transcript. The amount of cDNA template in each RT-PCR reaction was normalized to the signal from the ACT7. MNE: mean normalized expression

(D) Photograph of 9-week-old *pmp22* plants.

***PMP22* is vital in extended darkness and prevents cell death upon reillumination**

In extended darkness plant health depends on peroxisome function as shown for mutations in the 3-hydroxyisobutyrate hydrolase CHY1 and the fatty acid importer PXA1 (Dong et al., 2009; Kunz et al., 2009). A reduced maximum quantum yield (QY_{max}) reflects damage to Photosystem II (PSII), which is generally considered as the first manifestation of leaf stress and prompted by heterogeneous factors in response to environmental changes (Oxborough, 2004). In *chy1-3* and *pxa1-2* plants

PSII electron transport is sensitive to 50 h extended darkness (Figure 5, Figure S9; Dong et al., 2009; Kunz et al., 2009). We monitored PSII electron transport in four-week-old *pmp22* and *pmp22-like* plants after periods of prolonged darkness by Chlorophyll a fluorescence yield. First, we screened PSII activity in ten *pmp22* amiRNA lines exposed to 50 h darkness (Figure 5).

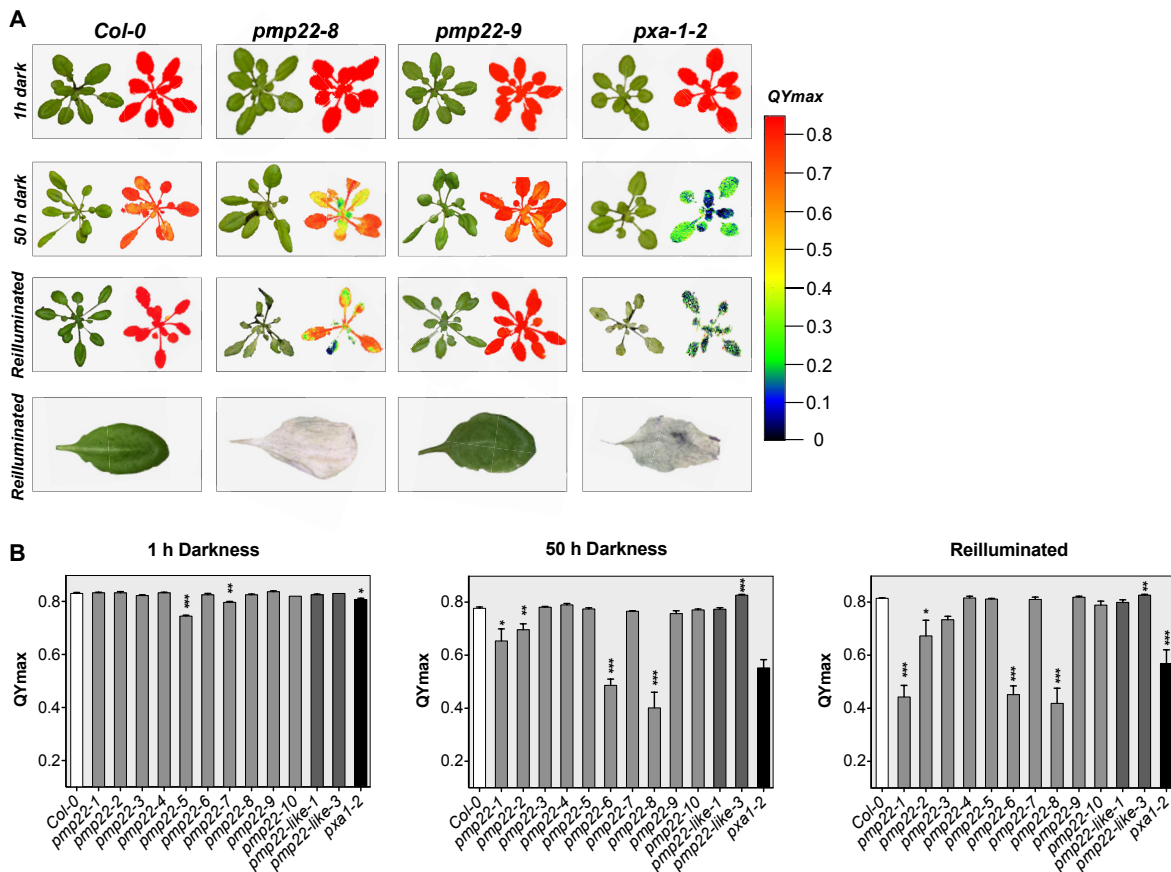


FIGURE 5. Morphology and PSII electron transport of *Col-0*, *pmp22*, *pmp22-like* and *pxa1-2* in extended darkness and reillumination.

(A) Photograph and false color images representing maximum quantum yield (QYmax) of *Col-0*, *pmp22-8*, *pmp22-9* and *pxa1-2* after the indicated duration dark exposure and 50 h darkness followed by 24 h reillumination.

(B) Mean of maximum quantum yield (+SE; n = 5) of 10-d-old *Col-0*, *pmp22*, *pmp22-like* and *pxa1-2* subjected to 1 h, 50 h of darkness and 24 h reillumination after 50 h darkness. Differences between the mean of biological replicates were marked as statistically significant (t-test) with the *Col-0* control by (*), (**) or (***) at respective significance levels of (P < 0.05), (P < 0.01) or (P < 0.001).

Three miRNA lines (*pmp22-2*, *pmp22-6* and *pmp22-8*) showed significantly reduced maximum quantum yields in extended night compared to the wild type (Figure S10). Upon reillumination these plants died; leaves dehydrated and bleached to a bluish-white color similar to the observation in the *pxa1-2* control. The T-DNA line *pmp22-1* did not show reduced PSII electron transport after 24 h extended darkness as *pmp22-8* and *pxa1-2*, but it showed frequent and reproducible quantum yield

reduction after extending the dark period to 50 h. Such a drastic effect has not been observed for other miRNA lines such as *pmp22-9*. Screening of wild type and *pmp22-like* lines did not reveal such an effect (Figure S10).

The reduction in chlorophyll contents in extended darkness confirmed the detected stress status for *pmp22* lines (Figure S11). Extending the dark period to six days further revealed sensitivity of *pmp22-3*, *pmp22-5* and *pmp22-like-1* to extended darkness (Figure S10B). To summarize, reduced PSII activities confirm the hypothesized role of PMP22 in darkness stressed plants.

Exploration of the GENEVESTIGATOR database (Zimmermann et al., 2004) revealed that PMP22 gene expression is upregulated upon cold stress, heat shock, low oxygen, drought, iron deficiency and nitrate starvation conditions. With respect to this finding we investigated PSII integrity in heat and cold stress conditions. We detected drastic reductions of maximum quantum yield for both abiotic stresses (Figure S12A). Furthermore, the heat shock resulted in large necrotic lesions dispersed across all rosette leaves of *pmp22-1* and *pmp22-8* plants (Figure S12B). These results accentuate the need of PMP22 function in dynamic environments in response to abiotic stress stimuli.

Absence of PMP22 leads to a defect in storage oil mobilization

Similar to PMP22, PXA1 is needed in the abiotic stress response of mature plants, but PXA1 is also indispensable for seedling growth (Zolman et al., 2001b). Next, we analyzed if PMP22 and PMP22-like support storage oil mobilization similar to PXA1. β -oxidation converts dichlorophenoxybutyric acid (2,4-DB) to the synthetic auxin 2,4-dichlorophenoxyacetic acid (2,4-D), which inhibits root elongation (Estelle and Somerville, 1987) and renders root elongation of β -oxidation mutants 2,4-DB-resistant (Hayashi et al., 1998). Hence, seedling primary root growth inhibition upon 2,4-DB exposure mirrors β -oxidation rates. As shown in Figure 6A/B, the *pmp22* root growth was less sensitive to 2,4-DB than the wild type. All mutant lines grew like the wild type or showed an even stronger response to the 2,4-D herbicide. *pmp22-like* lines did not exhibit 2,4-DB resistance (Figure 6C). Therefore, we dismiss PMP22-like from a hypothetical function in seedling establishment and further focus on the role of the seemingly more important PMP22 isoform. For subsequent experiments, we employed mainly the *pmp22-8* mutant, which displayed typical phenotypes.

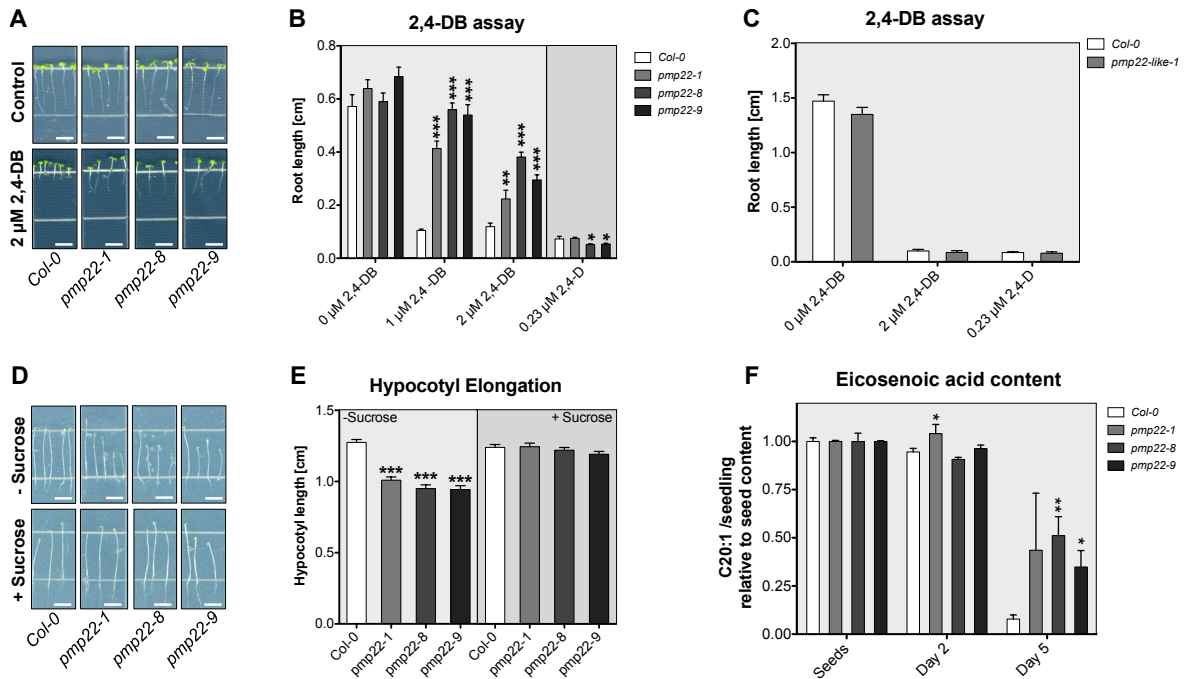


FIGURE 6. Mutants deficient in PMP22 are compromised in storage oil mobilization.

(A)/(B)/(C) Representative photograph and mean root lengths (+SE; $n > 30$) of 7-d-old wild type, *pmp22-1*, *pmp22-8*, *pmp22-9* and *pmp22-like-1* grown in short-day conditions on half strength MS medium (Mock) or the same medium supplemented with 2,4-dichlorophenoxybutyric acid (2,4-DB) or 2,4-dichlorophenoxyacetic acid (2,4-D)

(D)/(E) Photograph and mean hypocotyl lengths (+SE; $n > 30$; left) of 7-d-old dark-grown wild type, *pmp22-1*, *pmp22-8* and *pmp22-9* grown on half strength MS medium or the same medium supplemented with sucrose.

(F) Seed-oil specific eicosenoic acid content was measured in seeds and seedlings established in the absence of sucrose.

Differences between the mean (SE) of three biological replicates were marked as statistically significant (t-test) with the SYM1 control by (*), (**) or (***) at respective significance levels of ($P < 0.05$), ($P < 0.01$) or ($P < 0.001$).

Postgerminative growth of many β -oxidation mutants was shown to be “sucrose dependent”, because wild-type growth was reached upon provision of exogenous sucrose. We tested the requirement of exogenous sucrose in *pmp22* mutants by growing seedlings in the light or dark (Figure 6). *pmp22* seedlings did not exhibit a sucrose-dependent root elongation: 7-day-old seedlings vertically grown on agar plates without sucrose under short-day conditions were indistinguishable from the wild type. In contrast, hypocotyl elongation in the dark depended on sucrose, as only in presence of sucrose *pmp22* hypocotyls reached wild-type length.

We further analyzed the role of PMP22 in storage oil mobilization and measured the fatty acid contents in seeds and seedlings. Eicosenoic acid (C20:1) was determined to monitor TAG breakdown (Lemieux et al., 1990). In wild type seedlings, the level of eicosenoic acid dropped by 90 % five days after imbibition. In five-day-old *pmp22* seedlings, the eicosenoic acid level was only reduced by approximately 50 % (Figure

6F). This observation indicates *pmp22* mutants to be able to mobilize storage oil, but reduction of PMP22 delays this process.

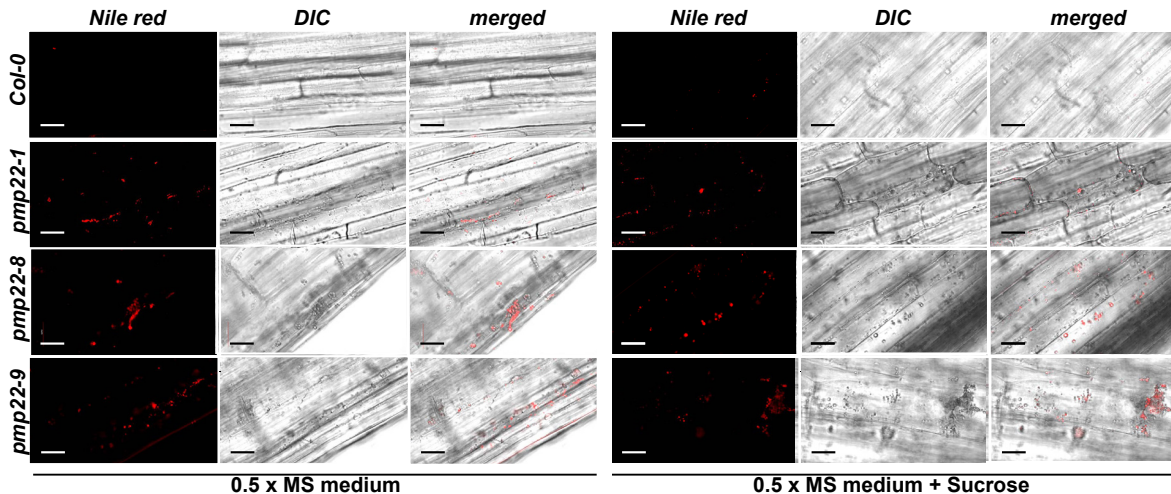


FIGURE 7. Absence of PMP22 causes retention of oil bodies.

Representative fluorescence images of 5-d-old dark grown hypocotyls of wild type, *pmp22-1*, *pmp22-8* and *pmp22-9* on half-strength MS agar plates (left) or medium with 1 % (w/v) sucrose (right) stained with Nile Red. Scale bar: 20 μ m. DIC: Differential Interference Contrast

Eicosenoic acid is stored in TAG lipids that are stored in oil-bodies. We stained 5-day-old etiolated seedlings with the neutral lipid dye Nile Red (Greenspan et al., 1985). Fluorescence imaging revealed prolonged oil body retention in the hypocotyls of all analyzed *pmp22* lines (Figure 7). To conclude, the reduced rate of peroxisomal β -oxidation in *pmp22* seedlings inhibits lipolysis during early seedling growth.

PMP22 is involved in acetate recycling during early seedling growth

Peroxisomes are implicated in the conversion of exogenous acetate provided during seedling growth. This occurs independently of β -oxidation core-components (Turner et al., 2005). PXA1 was suggested to facilitate acetate import (Hooks et al., 2007). Intraperoxisomal acetate will be activated to acetyl-CoA and subsequently glyoxylate cycle enzymes conjugate acetyl-CoA to glyoxylate or oxaloacetate to release malate or citrate (Allen et al., 2011).

Fluoroacetate (FAc) activation generates toxic fluoroacetyl-CoA, which undergoes transformation to the energy metabolism inhibitors fluoromalate or fluorocitrate (Proudfoot et al., 2006). Acyl-activating enzyme 7 mutants (*aae7*) and *pxa1-2* have been shown to be resistant to FAc treatment (Turner et al., 2005; Hooks et al., 2007). Here, we report on enhanced FAc resistance in root growth in *pmp22* and *chy1-3* (Figure 8), most likely due to reduced FAc conversion. This allows for the conclusion

that activity of PXA1, AAE7, malate synthase, or citrate synthase or export of fluoro-carboxylic acids is compromised.

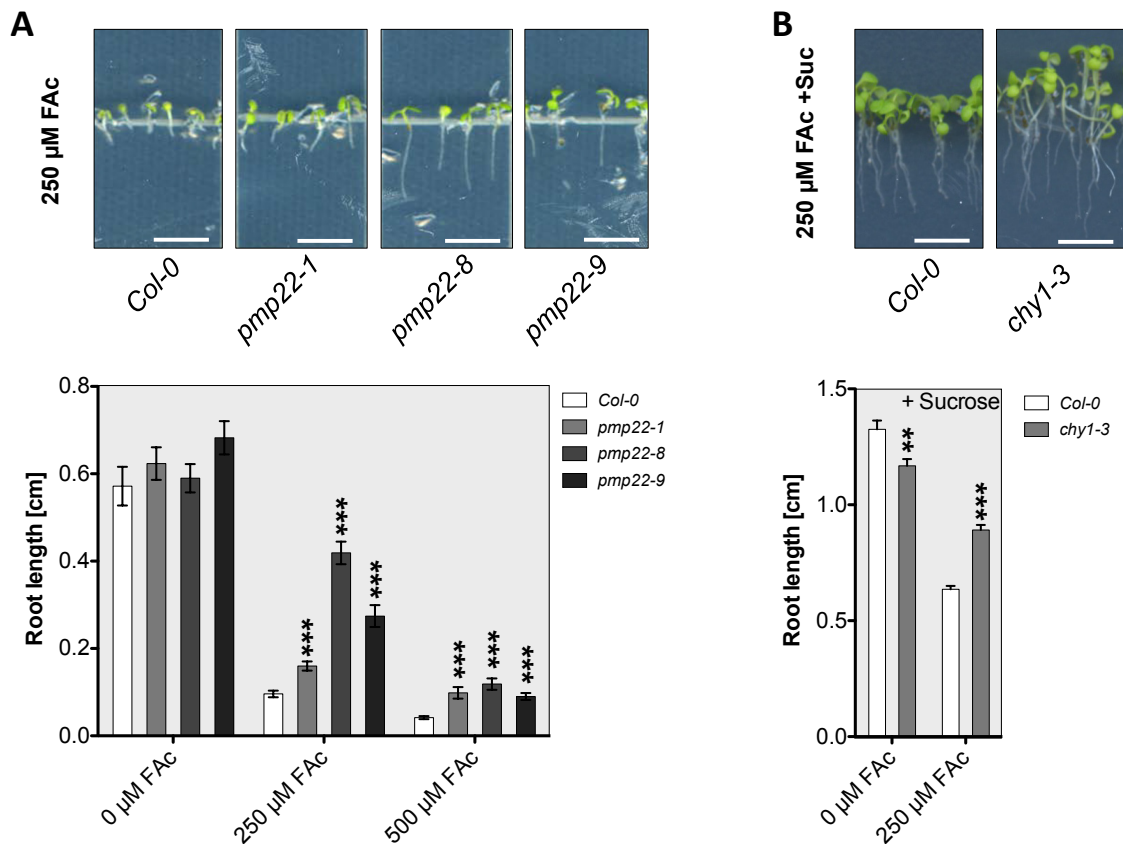


FIGURE 8. Fluoroacetate (FAC) resistance of *pmp22* and *chy1-3*.

(A) Photograph and mean root lengths (+SE; $n > 30$; lower panel) of seven-day-old wild type, *pmp22-1*, *pmp22-8*, and *pmp22-9* grown in short-day conditions on half strength MS medium (Mock) or the same medium supplemented with fluoroacetate (FAC).

(B) Photograph and mean root lengths (+SE; $n > 30$; lower panel) of 7-d-old wild type and *chy1-3* grown in short-day conditions on half strength MS medium (1 % (w/v) sucrose (Mock) or the same medium supplemented with fluoroacetate (FAC).

Differences between the mean (+SE) of each treatment were marked as statistically significant (t-test) with the *Col-0* control by (*), (**), or (***) at respective significance levels of ($P < 0.05$), ($P < 0.01$) or ($P < 0.001$). Scale bar: 5 mm.

Peroxisomes aggregate in pmp22 hypocotyls

It may be assumed that the defects in storage oil mobilization and fluoroacetate conversion are caused by a general dysfunctional peroxisome. Highly oxidized peroxisomes with inactive catalase and of general low catalytic capacity were shown to form aggregates prior to autophagic degradation (Shibata et al., 2013). This has also been reported for hypocotyls (Kim et al., 2013). Staining of *pmp22* peroxisomes with the fluorescent dye BODIPY but also TEM imaging revealed altered peroxisome morphology. Peroxisomes were not dispersed within the cell in *pmp22* hypocotyls but formed clusters (Figure 9A/B). Such an aggregation was not observed for the *Col-0*

control. This suggests peroxisomes to be damaged in the *pmp22* mutant. *pmp22* seedlings were sensitive to exogenous hydrogen peroxide (Figure 9C), when catalase was inhibited by 3-amino-triazole (Havir, 1992). The evidence points to a decrease in the high affinity reactive oxygen species (ROS) detoxification system of peroxisome membrane bound ascorbate peroxidase and monodehydroascorbate reductase (Del Río et al., 2002) Furthermore, reduced glycolate oxidase activity was measured in *pmp22-8* (Figure S13).

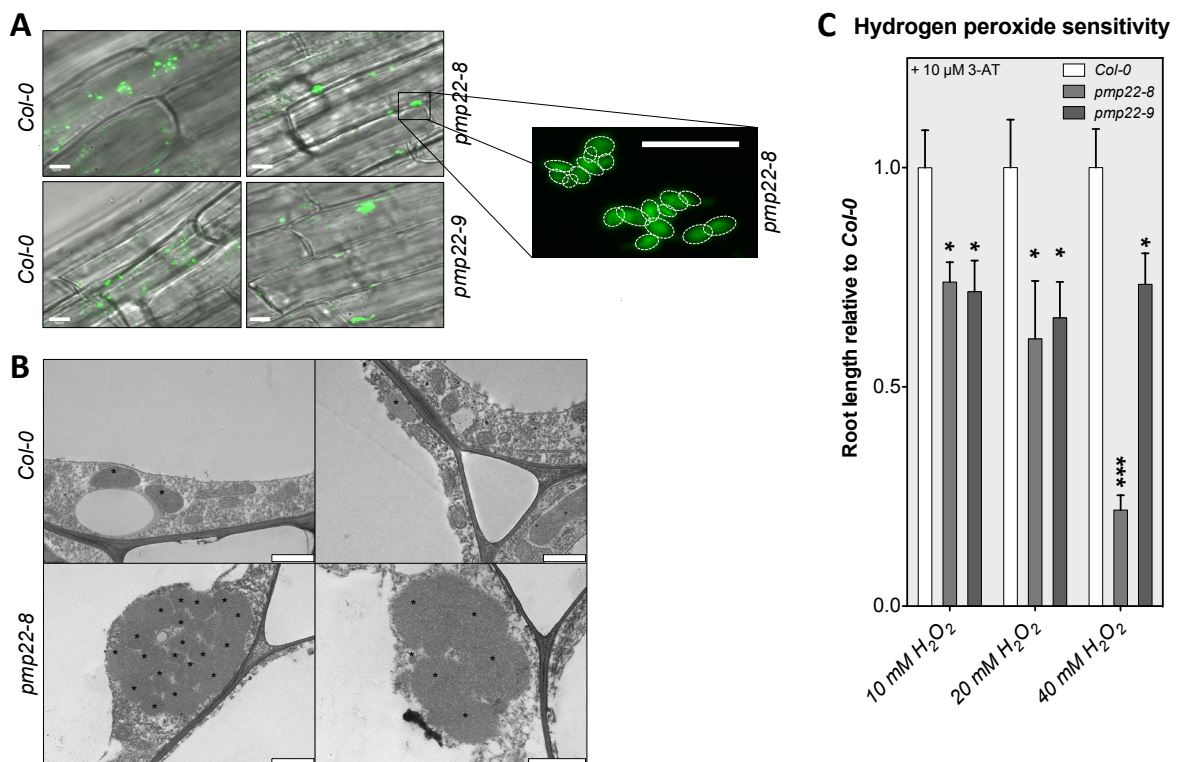


FIGURE 9. Aberrant peroxisome morphology in *pmp22* hypocotyls and hydrogen peroxide sensitive root growth.

(A) Microscopic image of BODIPY stained peroxisomes in 5-day-old *Col-0*, *pmp22-8*, and *pmp22-9* hypocotyls grown on half strength MS medium. Scale bar: 10 μ M.

(B) Transmission Electron microscopic observation of peroxisomes in 5-day-old *Col-0*, *pmp22-8*, and *pmp22-9* hypocotyls grown on half strength MS medium. Asterisks mark peroxisomes. Scale bar: 1 μ M.

(C) Root lengths (+SE; $n > 15$) of 14-d-old *pmp22-1*, *pmp22-8*, *pmp22-9* relative to wild type, grown in short-day conditions on half strength MS medium supplemented with hydrogen peroxide (H₂O₂). Differences between the mean (SE) were marked as statistically significant (t-test) with the SYM1 control by (*), (**), or (***) at respective significance levels of ($P < 0.05$), ($P < 0.01$) or ($P < 0.001$).

***pmp22* root elongation is sensitive to BCAA presence**

To further test activity of *pmp22* peroxisomes we transferred seedlings five days after radicle emergence to media supplemented with high levels of peroxisomal β -oxidation substrates. We analyzed primary root length elongation as indicator for plant fitness. Significant growth restrictions of *pmp22* in comparison to wild-type

plants were observed on: BCAA (isoleucine, leucine, valine), BCAA catabolites (3-hydroxyisocaproic acid, 4-methylvaleric acid, isobutyric acid, propionic acid, acrylic acid), α -linolenic acid and the chlorophyll catabolite phytol (Figure 10, Figure S14-S16). Reduced growth was also noted in presence of glycolate. In all aforementioned conditions *pmp22* seedlings remained small and pale green or bleached and died.

Peroxisomes are needed for nitrogen mobilization, due to action in purine-ring catabolism. Uric acid is converted to allantoin, a reaction that releases hydrogen peroxide in the peroxisome matrix (Parish, 1972; Harrison-Lowe and Olsen, 2006). Allantoin is then extraperoxisomally cleaved into ammonium and glyoxylate. Subsequently, glyoxylate enters the peroxisomal photorespiratory cycle. Provision of uric acid as sole N-source reduces *pmp22* growth in comparison to the wild type. This is an indication for either reduced peroxisomal enzymatic activity or reduced channeling of substrates across the peroxisomal membrane.

Notably, a few substrates of peroxisomal conversion did not lead to growth restrictions: glyoxylate, glycine, serine, lysine, malate and pimelic acid did not alter root length elongation (Reumann and Weber, 2006; Eisenhut et al., 2013; Engqvist et al., 2009; Magliano et al., 2011; Maruyama et al., 2012; Tanabe et al., 2011). Strongest sensitivity was detected upon exposure to BCAA catabolites, however not to 3-hydroxypropionate, the end product of peroxisomal BCAA conversion.

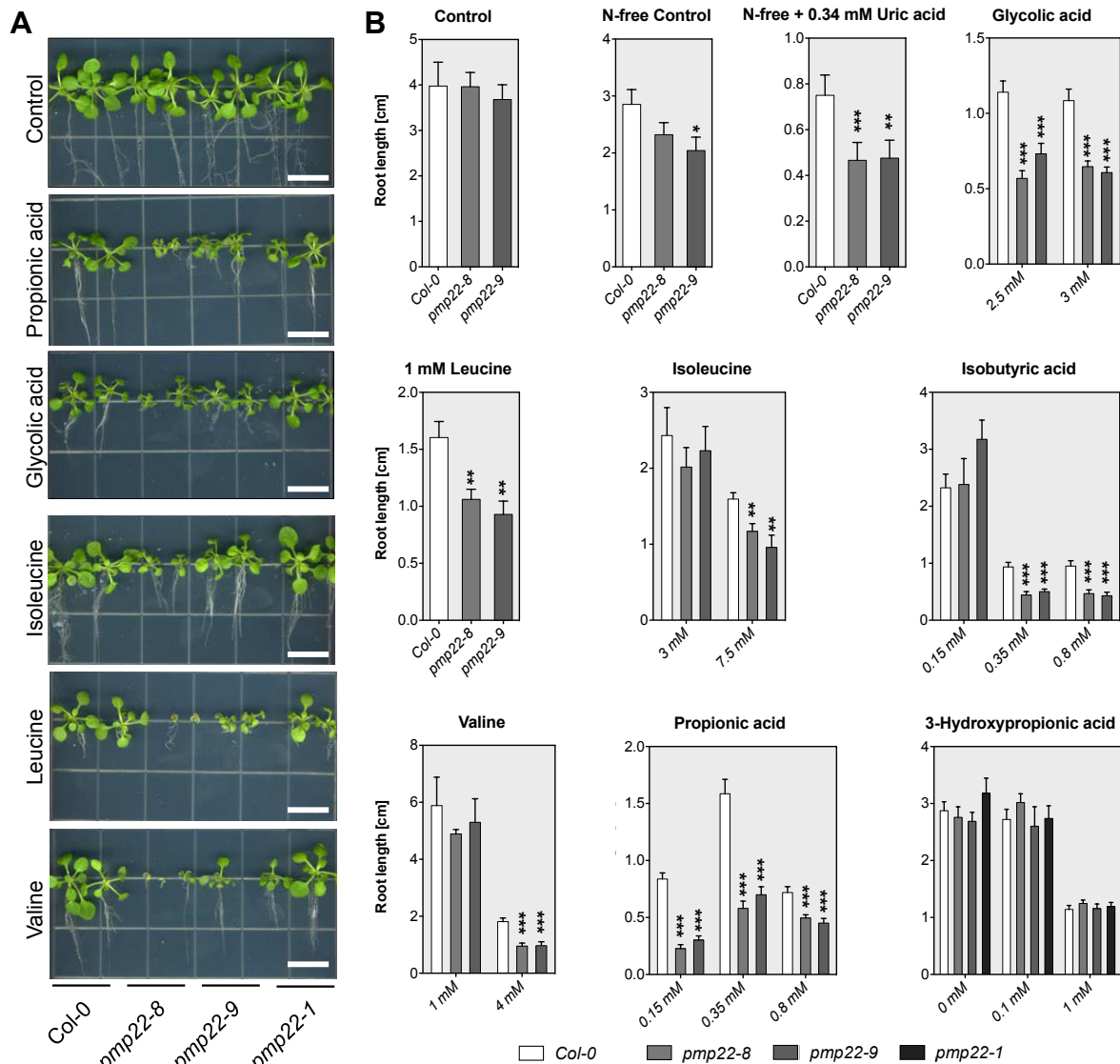


FIGURE 10. Reduction of PMP22 led to compromised growth on propionate, isobutyrate, glycolate, valine, leucine, isoleucine and uric acid as sole N-source.

(A) Photographs of 17-day-old *Col-0*, *pmp22-1*, *pmp22-8* and *pmp22-9* transferred (five days after radicle emergence) to half strength MS medium supplemented with 250 μ M propionic acid, 2.5 mM glycolic acid, 7.5 mM isoleucine, 1 mM leucine, 4 mM valine or without supplement (Control). Scale bar: 10 mm.

(B) Mean root lengths (\pm SE; $n > 15$) of 17-day-old *Col-0*, *pmp22-1*, *pmp22-8* and *pmp22-9* grown in short-day conditions transferred (5 days after radicle emergence) to half strength MS medium supplemented with the indicated amount of carboxylic or amino acid. Differences between the mean (\pm SE) of three biological replicates were marked as statistically significant (t-test) with the *Col-0* control by (*), (**) or (***) at respective significance levels of ($P < 0.05$), ($P < 0.01$) or ($P < 0.001$).

Peroxisomal BCAA degradation requires activity of the 3-hydroxybutyryl-CoA hydrolase CHY1 (Zolman et al., 2001a) and our analyses revealed *chy1* as sensitive to fluoroacetate and reillumination after prolonged darkness as *pmp22* (Figure S9).

Metabolite analysis reveals disturbed alternative respiration in stressed *pmp22* plants

BCAA catabolism partially comprises peroxisomal β -oxidation and is known to be important for energy metabolism in prolonged darkness (Dong et al., 2009; Kochevenko et al., 2012; Araújo et al., 2011). *pmp22* growth restriction to exogenous supply of BCAA and sensitivity to darkness indicated a role of PMP22 in BCAA catabolism. We profiled amino acids and carboxylic acids in dark stressed plants and compared *pmp22* mutants to wild type and *pxa1-2*. PXA1 has been implicated with the import of acetate (Hooks et al., 2007) and there is a strong possibility that PXA1 facilitates import of BCAA catabolites such as isobutyryl-CoA and propionyl-CoA (our own unpublished data). A principal component analysis (PCA) of amino acid levels revealed *pmp22* metabolite variations to be different from the *Col-0* control and in the same range as that of *pxa1-2* in extended darkness conditions (Figure 11). This confirmed the results of disrupted seedling storage oil mobilization and points towards a role of PMP22 in β -oxidation or acetyl-CoA conversion. There is no severe difference in amino acids levels for the weaker *pmp22* alleles (*pmp22-1*, *pmp22-9*) compared to the wild type in non-stress conditions, whereas a clear difference is apparent in the variations for the strong repressor line *pmp22-8*.

At the end of the regular night we did not detect significant changes in amino acid levels of wild type, *pxa1-2* and *pmp22* (e.g. aspartate; Figure 12). 50 h of darkness led to higher abundance of aspartate in *pxa1-2* and *pmp22* lines, whereas aspartate pools seemed largely depleted in nine days of darkness in comparison to the wild type. Identical patterns were observed for branched-chain and aromatic amino acids, which have been proposed to support mitochondrial respiration in dark stress (Engqvist et al., 2009; 2011; Araújo et al., 2010). Nine-week-old *pmp22-8* leaves displayed higher levels of BCAA and glycolate than the wild type. This was in line with the observation of premature senescence, as these molecules were reported for increase in senescing leaf tissue (Figure S17; Watanabe et al., 2013).

With respect to carboxylic acids, we noted significantly higher 2-oxoglutarate levels in extended darkness accompanied by low glutamate levels in *pxa1-2* and *pmp22*, which suggests respiratory dysfunction or deficiency in nitrogen remobilization by transamination to glutamate. In nine days of darkness leaf 2-oxoglutarate and glutamate levels of *pmp22-8* and *pxa1-2* were lower than in the wild type. The same held true for succinate levels in extended darkness. We must expect altered

respiratory metabolism in *pmp22* mutants and less ATP production. In a previous study *pxa1-2* displayed a lower ATP/ADP ratio than the wild type in prolonged darkness longer than 24 h (Kunz et al., 2009). Consistent with reduced glucose levels in *pmp22* it can be concluded that PMP22 is involved in provision of C-units anaplerotic to the TCA cycle.

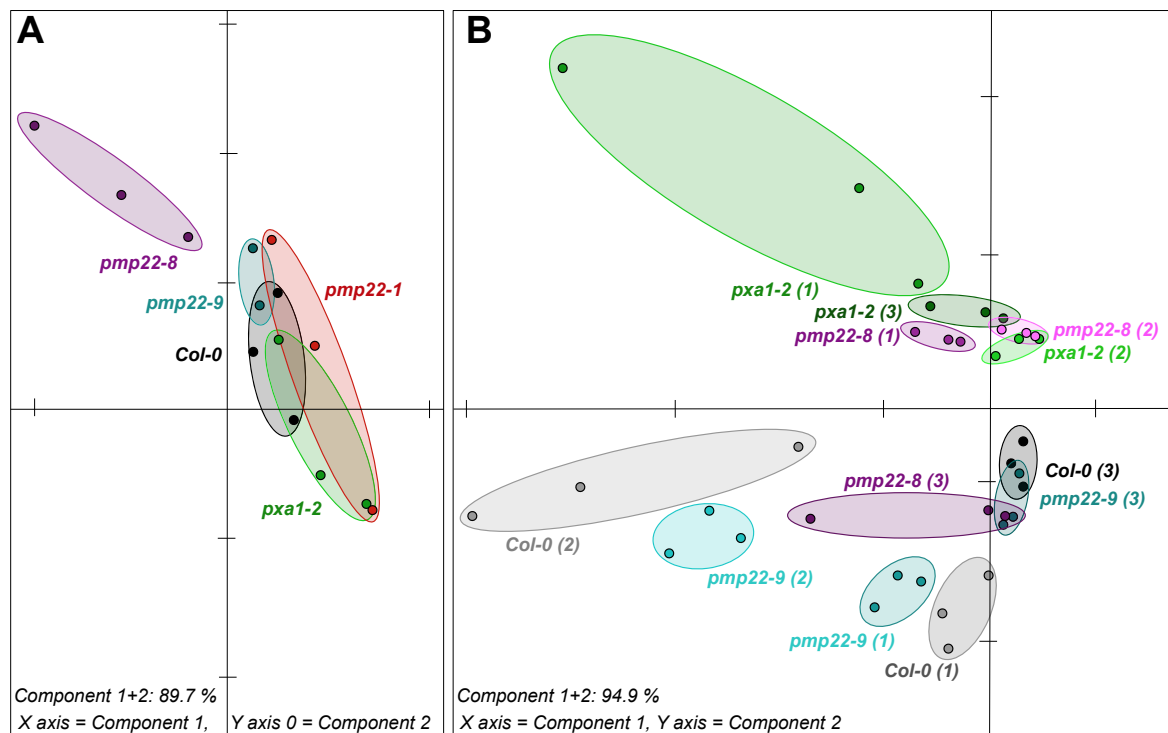


FIGURE 11. 2D-PCA score plot of amino acid levels. The plots were applied for the amino acids detected in *Arabidopsis* extract.

(A) End of the regular night amino acid data in a 2D-PCA score plot of *Col-0*, *pmp22-1*, *pmp22-8*, *pmp22-9* and *pxa1-2*. Amino acids were measured by HPLC-DAD.

(B) Extended darkness (50 h) (1), carbon starvation in 9 d darkness (2) and extended darkness (50 h) plus 24 h reillumination (3) amino acid data in a 2D-PCA score plot of *Col-0*, *pmp22-1*, *pmp22-8*, *pmp22-9* and *pxa1-2*. Amino acids were measured by GC-MS.

PCA was conducted by the MultiExperiment Viewer (Saeed et al., 2003). Biological replicates are encircled. PCA: Principal Component Analysis

***pmp22* seeds were filled with less nutrients**

In a simulated natural day with increasing light intensity the photosynthetic performance of three-week-old *pmp22* plants was decreased, as evident in Figure S18 the photochemical quantum yield was reduced by up to 25 %. We hypothesized that this reduced photosynthetic capacity and the observed premature senescence were detrimental to biomass production and seed filling. To this end we analyzed seed quantity and quality.

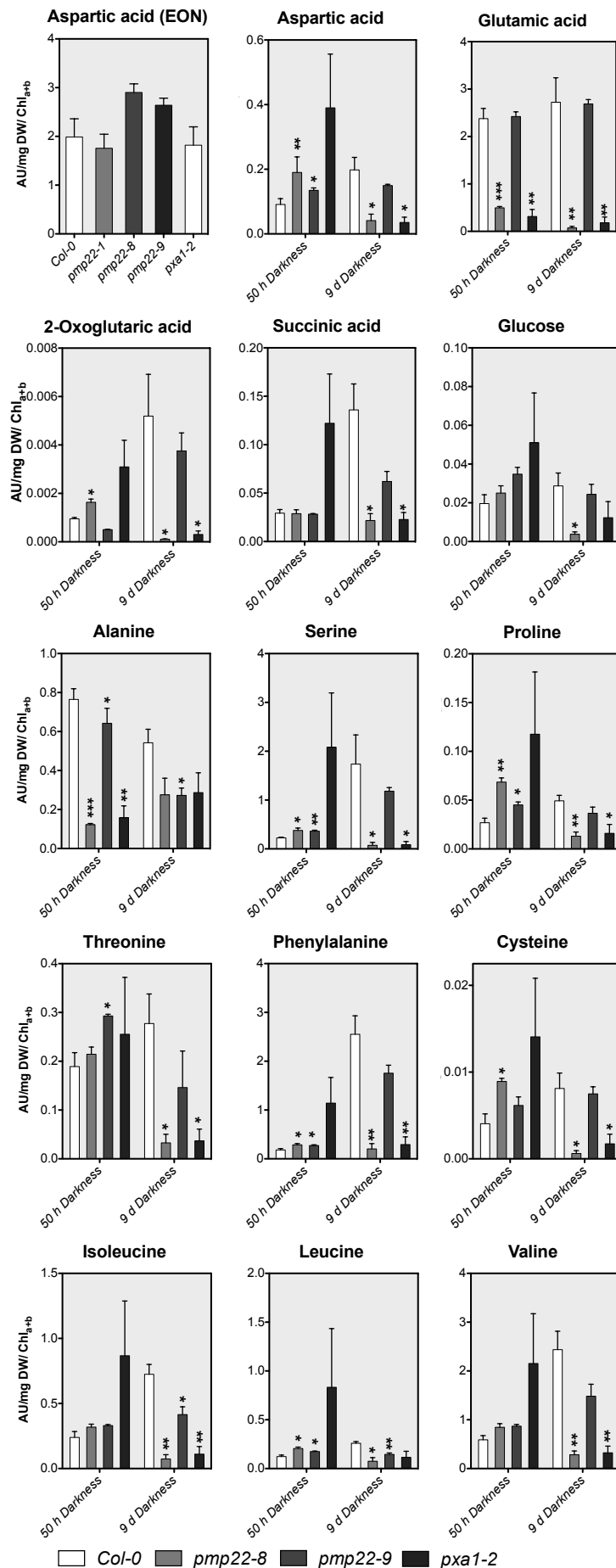


FIGURE 12. Means of amino acids and carboxylic acid contents (+SE) of *Col-0*, *pmp22-8*, *pmp22-9*, and *pxa1-2* at the end of the regulator night, 50 h darkness and nine days darkness. Leaf extracts of 4-week-old plants were subjected to GC-MS or HPLC-DAD analysis for metabolite quantification. The data is shown in an arbitrary unit normalized to mg dry weight. Chlorophyll_{a/b} contents were used to normalize biological replicates. Differences between the mean of three biological replicates were marked as statistically significant (t-test) with the *Col-0* control by (*), (**) or (***) at respective significance levels of ($P < 0.05$), ($P < 0.01$) or ($P < 0.001$). EON: end of night.

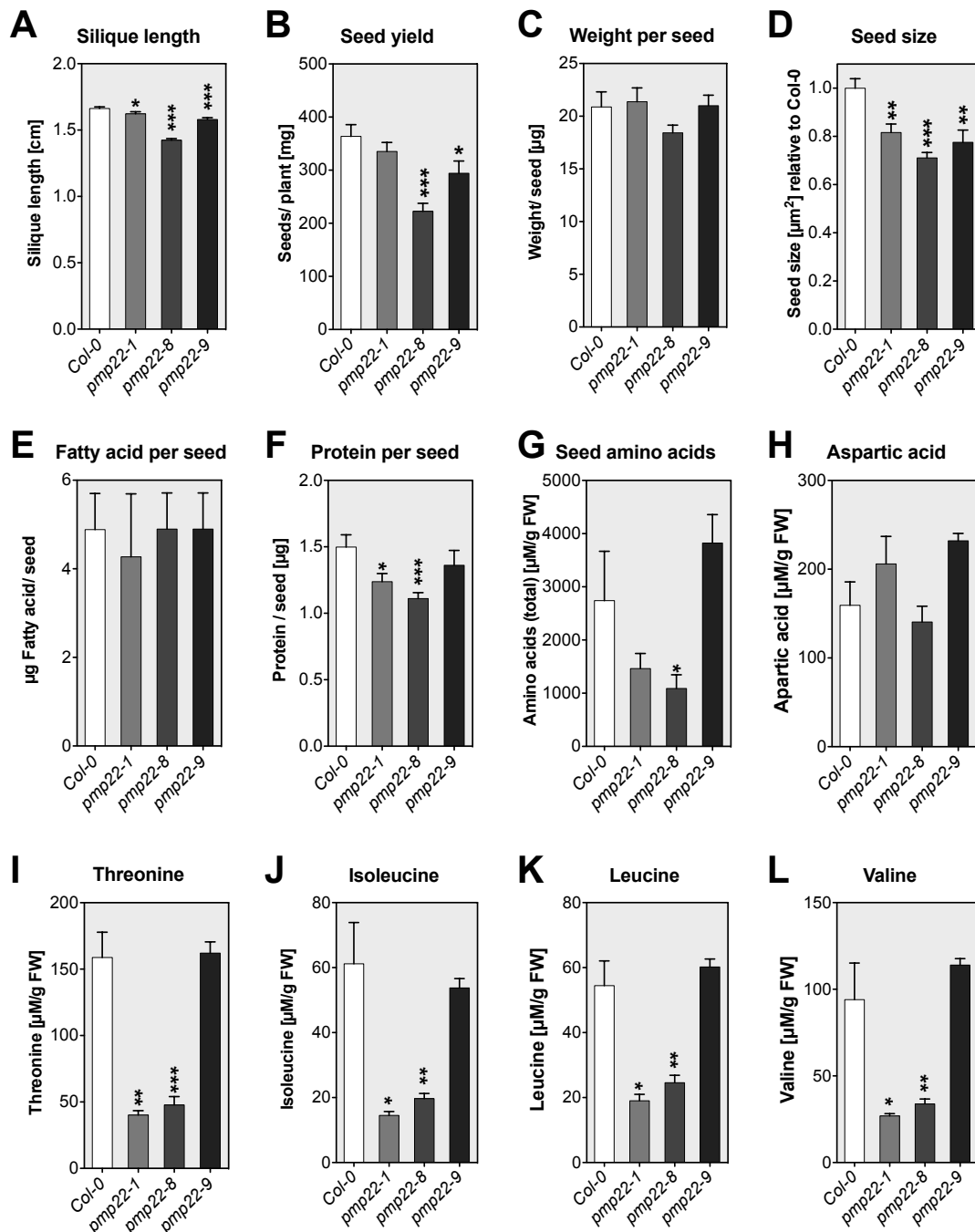


FIGURE 13. Impact of *PMP22* reduction on silique size, seed quantity and seed filling.

(A) Mean silique lengths (+SE; $n > 150$) of 10-w-old wild type, *pmp22-1*, *pmp22-8* and *pmp22-9* determined 14 day after flowering.

(B) Mean seed yield per plant (+SE; $n = 15$) of wild type, *pmp22-1*, *pmp22-8* and *pmp22-9*.

(C) Mean seed weight (+SE, $n > 3500$) of wild type, *pmp22-1*, *pmp22-8* and *pmp22-9*.

(D) Mean seed size (+SE, $n > 5000$) of wild type, *pmp22-1*, *pmp22-8* and *pmp22-9*.

(E)/(F) Mean of fatty acid and protein content per seed (+SE, $n = 4$) of wild type, *pmp22-1*, *pmp22-8* and *pmp22-9*.

(G) Mean of seed protein amino acids (+SE; $n=3$) of wild type, *pmp22-1*, *pmp22-8* and *pmp22-9* quantified by LC-MS

(H)-(L) Mean of aspartic acid, threonine, isoleucine, leucine and valine (+SE; $n=3$) of wild type, *pmp22-1*, *pmp22-8* and *pmp22-9* quantified by LC-MS.

Differences between the mean (SE) of at least three biological replicates were marked as statistically significant (t-test) with the *Col-0* control by (*), (**) or (***) at respective significance levels of ($P < 0.05$), ($P < 0.01$) or ($P < 0.001$).

Reduced reproductive success has already been reported for *pxa1* and the *kat2-1* allele of the core β -oxidation enzyme 3-ketoacyl-CoA-thiolase (Footitt et al., 2007a; 2007b). The *pxa1* alleles *cts-1* and *cts-2*, but also *kat2-1* displayed shorter siliques, which we also observed for *pmp22*. In case of *pxa1* silique size reduction was linked to reduced fertility, because pollen tube germination and growth depends on energy provision by β -oxidation. In case of *pmp22* shorter siliques size resulted in reduced seed biomass yield per plant (Figure 13A-C). Fatty acids levels were largely the same per seed but seeds displayed less protein, which corresponded to a reduced seed size (Figure 13D/E). Seed amino acids were significantly reduced for *pmp22-8* and *pmp22-1* and especially BCAA were reduced by more than half of the wild-type level, which indicates PMP22 to be needed for optimal nitrogen mobilization (Figure 13F-L).

Germination potential is not reduced by reduction in PMP22

To exclude the possibility that the observed hypocotyl elongation and storage oil-mobilization defect in the dark is a consequence of a developmental defect caused by lowered seed quality prior to and during seed germination, we compared the germination of *pmp22* seeds with that of the wild type. As detailed in Figure 14, germination rates were in the range of the wild type and the development of seedlings to emergence of true leaves was not delayed.

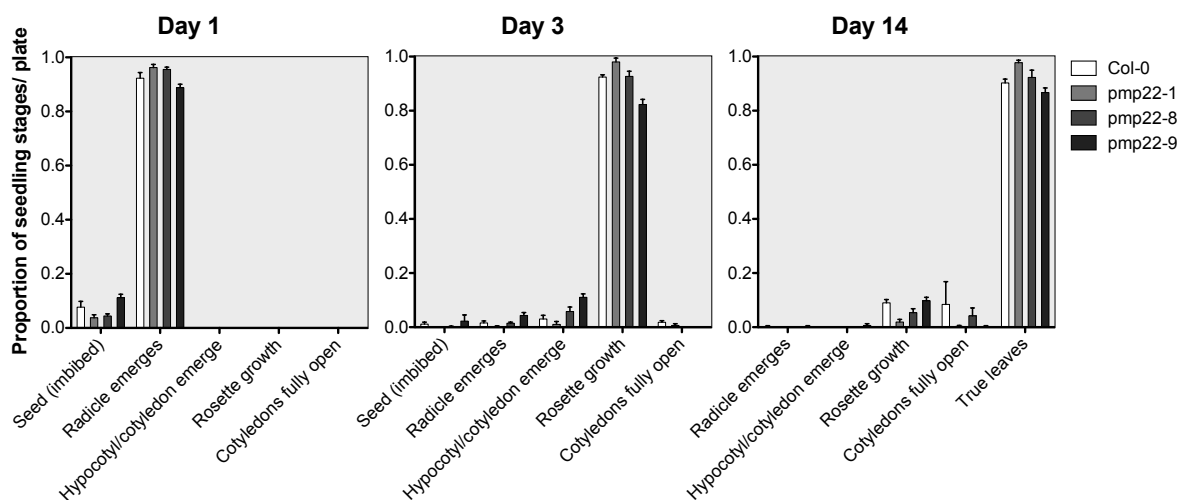


FIGURE 14. PMP22 germination potential and postgerminative developmental categories correspond to the wild type. Mean percentage (+SE; $n > 400$) of *Col-0*, *pmp22-1*, *pmp22-8*, and *pmp22-9* seeds/seedlings in the indicated developmental category per plate.

Discussion

This study aimed to expand the knowledge of peroxisomal transport proteins. We identified PMP22 as a candidate to be involved in peroxisomal carboxylic acid transport and characterized the role of PMP22 *in planta*. We could show that PMP22 activity provides protection from premature senescence and accumulation of harmful compounds or physiological states during extended darkness. Non-stressed, 3-week-old *pmp22* plants had mildly reduced PSII electron transport (Figure S18), whereas mature plants manifested premature senescence symptoms. In abiotic stress conditions PMP22 was required in both seedlings and adult plants for fatty acid β -oxidation, glyoxylate cycle activity, photorespiratory glycolate oxidation, purine catabolism, BCAA respiration and optimal efficiency of membrane bound ROS detoxification systems (Figure 5-12). A general defect in peroxisome function was further confirmed by visualization of peroxisome aggregates in *pmp22* mutants. Peroxisome clusters are suggested to represent highly oxidized organelles (Shibata et al., 2013; Kim et al., 2013). *pmp22* growth was particularly sensitive to the presence of BCAA catabolites and to a minor extent to glycolic acid, uric acid as sole nitrogen source and fatty acids. Both intracellular alternative respiration in extended darkness and whole plant C/N relocation from source (leaves) to (seed) sinks in developmental senescence were disturbed (Figure 13). The latter was demonstrated by reduced protein contents in the seeds. Also *pmp22* plants produced seeds filled with less BCAA.

Yeast complementation suggests PMP22 to form a porin-like channel

Reciprocal BLAST analysis unraveled two isoforms of Arabidopsis peroxisomal PMP22-type proteins in plant proteomes. Bimolecular fluorescence complementation indicated the capacity of these proteins to physically interact (Figure 3B), while *sym1* Δ phenotype suppression showed that hetero-oligomerisation is not prerequisite for functionality (Figure 3C). PMP22 might enable transport of metabolites through a porin-like channel.

The mouse peroxisomal channel Pxmp2 forms a homotrimeric complex and the pore size allows for permeation of small anionic metabolites, such as glycolate, pyruvate and 2-oxoglutarate, when used as electrolyte solution in planar lipid bilayer experiments (Rokka et al., 2009). We subjected PMP22 to electrophysiological characterization using the artificial lipid-bilayer incorporation technique (Bartsch et al., 2013; Harsman et al., 2011). PMP22-His was isolated in high purity and

incorporated in lipid bilayers did result in two measureable channel activities (Figure S6). Incubation of the bilayer with the reconstitution detergent did not result in these channel activities, but did render the lipid bilayer highly prone to disruption. Chloride ion transport activity could be detected for both channel activities. Reports conducted by S. Reumann (Reumann et al., 1998) describe plant peroxisomal channels (spinach and castor bean) with permeability coefficient ratios indicating 20-25 fold preference of anion over cation transport. According to the data generated by Reumann et al. (1998) plants constitute an exception for the permeability properties in the eukaryotic kingdom for possessing a highly anion selective peroxisomal channel. PMP22 conductance matches the data reported for yeast, protozoa and mammals, describing unspecific pore-forming activity, majorly preferring cations in *ex vivo* assays. PMP22 did not exhibit typical voltage-dependent anion channel gating properties: the current at different holding potentials did not undergo transitions from high conducting open states to low current conducting states (Homblé et al., 2012). The transport of dicarboxylates through peroxisomal porin-like channel has been suggested for *S. cerevisiae*. Here, channel activity similar to that of Pxmp2 has been described (Antonenkov et al., 2009; Grunau et al., 2009). *In vitro* liposome assays and *E. coli* complementation studies did not suggest dicarboxylate translocation for PMP22, probably because the experimental set-up was inappropriate to monitor the PMP22 transport or due to a lack of protein modifications that are required for functionality. To conclude, electrophysiological analysis and suppression of the *sym1Δ* phenotype point to a high probability of PMP22 to form a metabolite channel.

Loss of PMP22 function in planta influences photosynthesis in non-stress conditions

We obtained transgenic *pmp22* lines of diverse physiological readout. The reduction of the PMP22 amount sufficed to analyze potential functions, which indicates absence of analogous or redundant proteins. *pmp22* mutations resulted in premature senescence (Figure 4; Figure S17). Interestingly *pmp22-9* showed reduced peroxisomal activity in seedling-based assays. Treatment of adult *pmp22-9* plants with up to 50 h darkness followed by reillumination never caused severe damage, which might reflect the incomplete suppression of this gene in mature plants. Furthermore, we detected this line to resemble the wild type in seed traits, which further confirms a reduced repression with onset of age. The T-DNA insertion mutant *pmp22-1* frequently displayed darkness induced lethality, when kept in the dark for

50 h and also showed marked reduction of seed amino acid content. The measured reduced rate of photosynthesis of several lines might be due to reduced photorespiratory metabolism, as evidenced by reduced glycolate oxidation activity (Figure S13). Furthermore, *pmp22* plants had a reduced potential in ROS scavenging and it may be reasonable to suppose that PMP22 function is needed in the response to a diverse range of environmental stress.

PMP22 is required for storage oil mobilization due to implication in β -oxidation and glyoxylate cycle

pmp22 seedlings retained oil bodies but also showed more TAG derived eicosenoic acid (Figure 6/7). This phenotype is shared with other β -oxidation mutants and reflects defective lipolysis and reduced β -oxidation. Acyl-CoAs have been suggested to regulate lipolysis (Germain et al., 2001; Graham et al., 2002; Graham, 2008) pointing to a regulatory role of β -oxidation to lipolysis.

The *pmp22* plants are partially resistant to 2,4-DB root growth inhibition suggesting reduced conversion of the inactive precursor to the active auxin by β -oxidation. The degree of resistance is lower than that observed in known β -oxidation mutants, including *pxa1* (Hayashi et al., 1998; Zolman et al., 2000; 2001b). PXA1 seems to be involved in the import of 2,4-DB, but an export system for 2,4-D was not found (Strader and Bartel, 2011; Hu et al., 2012). Cell expansion in hypocotyls is driven by endogenous auxin, produced by peroxisomal β -oxidation of indole-butyric acid (Strader et al., 2010). The fact that *pmp22* hypocotyl elongation depends on exogenous sucrose rules out that a disturbed auxin metabolism leads to the defect in *pmp22* hypocotyl elongation.

Auxin levels increase with onset of senescence and extraperoxisomal indole acetic acid (IAA) biosynthetic genes are upregulated during age-dependent leaf senescence (van der Graaff et al., 2006) and IAA represses some senescence associated genes (Noh and Amasino, 1999), which implies that auxin is a negative regulator of leaf senescence. The impact of β -oxidation generated IAA on senescence has not yet been addressed, but it appears that reduced rates of β -oxidation would promote senescence, as seen for *pmp22*. Therefore, β -oxidation activity might not only delay senescence by minimizing of free fatty acid content and ROS induced stress (Kunz et al., 2009; Bieker et al., 2012) but potentially also by production of auxin. The observed premature senescence and hypocotyl elongation

could be explained by the requirement of PMP22 for functional β -oxidation, however this does not exclude the possibility that PMP22 is involved in export of IAA.

pmp22 hypocotyl elongation resembles findings for the glyoxylate cycle malate synthase (MLS1) mutant. *mls1* and *pmp22* have no defect in germination and postgerminative growth in the light. Dark incubation however leads to reduced performance. In case of *mls1* it is assumed that acetyl-CoA mobilization by citrate synthase is sufficient, when the photorespiratory pathway is instrumentalized for glyoxylate conversion (Cornah et al., 2004). Hypocotyl elongation defect and the resistance to FAc implicate PMP22 in preservation of activity of the glyoxylate or photorespiratory cycle or export of intermediates of these pathways to the cytosol.

In pmp22 dark starvation may lead to accumulation of toxic free fatty acids, pheophorbide a and reactive oxygen species

A reduced rate of lipid catabolism in extended darkness and natural senescence may be inferred in *pmp22* due to the observed compromise in storage oil mobilization in *pmp22* seedlings. Fatty acids serve as energy source in extended darkness (Usadel et al., 2008; Kunz et al., 2009) and natural senescence (Yang and Ohlrogge, 2009). In natural senescence and extended darkness lipase activity increases and releases free fatty acids (FFA; Buchanan-Wollaston et al., 2005; van der Graaff et al., 2006; Slocombe et al., 2009; Kunz et al., 2009). FFAs are detrimental to cells by mechanisms that eventually lead to energy deprivation and ROS production: FFA form protonophores, dissipate electrochemical gradients and interfere with activity of photosystems and the respiratory chain (Schönfeld and Wojtczak, 2008). We detected PSII damages in *pmp22* after prolonged darkness. This could be caused by accumulation of FFA as assumed for *pxa1-2* (Kunz et al. 2009). There is also evidence that the phototoxic chlorophyll catabolite pheophorbide a accumulates in *pxa1* and *kat2-1* (Kunz et al., 2009). The observed leaf damage and rapid photo-bleaching following reillumination of *pmp22* plants strongly resembles phenotypes of the pheophorbide a oxidase mutant (Pruzinská et al., 2003; Tanaka et al., 2003). Thus, *pmp22* might be essential in darkness to support β -oxidation in preventing the accumulation of FFA and pheophorbide a.

PMP22 supports optimal mobilization of C/N in extended darkness and senescence

Extended darkness and senescence shares the need of macromolecule degradation, nutrient salvage/translocation and detoxification of toxic catabolites (Lim et al., 2007). Production of citrate from fatty acids by combined action of β -oxidation and glyoxylate cycle has been postulated to support respiration (Buchanan-Wollaston et al., 2005; Pracharoenwattana et al., 2005; Kunz et al., 2009). In carbon starved *pmp22* plants, reduction of TCA cycle intermediates 2-oxoglutarate and succinate substantiates a lack of peroxisomal produced citrate to support respiration. TCA pools are depleted in *pmp22* and energy metabolism seems to be compromised by loss of Carbon supply by the fatty acid β -oxidation. Taken together the results from the FAc feeding and the lack of TCA intermediate availability indicate malfunctioning β -oxidation supported citrate synthesis. Either acetyl-CoA supply is shortened due to malfunctioning β -oxidation or reduced export of glyoxylate cycle compounds.

In end of night conditions mitochondrial respiration is largely dependent on carbohydrate oxidation (Stitt and Zeeman, 2012). In extended darkness it has been shown that plant mitochondria break down alternative respiratory substrates. Autophagic mechanisms and proteasome activity were shown to release amino acids when there is a lack in carbohydrates (Bassham, 2007; Xiong et al., 2007). Lysine, aromatic and branched-chain amino acids donate electrons to the mitochondrial ubiquinone pool for oxidative phosphorylation. In *pmp22* BCAA and aromatic amino acid pools are much lower than in the wild type, indicating enhanced proteolysis in the wild type or premature consumption for alternative respiration in *pmp22*.

Amino acid respiration is linked to nitrogen recycling and requires cooperation of peroxisomes, mitochondria, chloroplasts and the cytosol (Araújo et al., 2011). Less activity in nitrogen mobilization was observed in *pmp22* as seen by an increased 2-oxoglutarate/glutamate ratio, reduced seed protein or amino acid content. Wild types displayed more glutamate, the major N transport metabolite (Potel et al., 2009).

Another macromolecule that is degraded in senescence is DNA. Peroxisomes are involved in nucleic acid breakdown via the conversion of urate to (S)-allantoin and this requires exchange of urate and allantoin across the peroxisomal membrane is required (Werner and Witte, 2011). An involvement in this transport process was reported for Pxmp2 (Rokka et al., 2009). Enzymes involved in this pathway share

phenotypes with *pmp22*, e.g. a xanthine dehydrogenase (XDH) mutant is sensitive to cold and extended darkness (Brychkova et al., 2008a). In plants the activity of XDH is enhanced with age (Hesberg et al., 2004; Nakagawa et al., 2007) and catabolic products of purine, the ureides, are considered as long-distance transport nitrogen metabolites (Tegeder, 2014). We observed reduced growth of *pmp22* with uric acid as sole nitrogen source and less nitrogen stored in the form of proteins and amino acids in *pmp22* seeds.

After peroxisomal uric acid conversion, the last steps of ureide breakdown take place in the ER, resulting in the formation of glyoxylate, which is thought to be converted by peroxisomal enzymes of the photorespiratory pathway to glycine or serine (Winkler et al., 1987). In bacteria aminotransferase activity couples purine degradation to amino acid recycling as a source of nitrogen and carbon (Ramazzina et al., 2010). Alanine-glyoxylate aminotransferase (AGT) isoforms of *Arabidopsis* could adopt a comparable role *in planta*. One of three described AGT isoforms has been proven to be localized to peroxisomes; the other two carry at their C-terminal end canonical PTS1 sequences SKM> and SRI> (Liepman and Olsen, 2001; 2003). The substrate specificities of these enzymes have not been extensively studied.

A putative involvement of PMP22 in uric acid import or allantoin export function would be in accordance with the observed premature senescence and defects in seed filling but also with the co-expression networks. PMP22 shows strong co-expression with transaminase activity, glyoxylate, dicarboxylate, and amino acid metabolism.

Natural senescence is the final stage of plant development and has been shown to substantially limit plant biomass and seed yield (Gregersen et al., 2013). *pmp22* displayed premature senescence and reduced reproductive features, which is why we propose PMP22 to be a negative regulator of senescence. A longer duration of senescence has been proposed to enhance seed yield and seed filling with nutrients (Egli, 2011). *pmp22* seeds revealed reduced contents of amino acids and lacked especially BCAA. We hypothesize this to be due to consumption of amino acids in respiration but also due defective C/N mobilization. Interestingly the finding of shorter siliques was already shown for the β -oxidation mutant *kat2-1* and *pxa1* (Footitt et al., 2007a; 2007b). It was shown that siliques are shortened due to a lack in fertility, because male gametophytes rely on β -oxidation for germination and pollen tube elongation. This indicates β -oxidation to govern reproductive fitness by energy provision.

Toxicity of feeding and autophagic degradation of peroxisomes

In *pmp22* high levels of amino acids led to growth inhibition, which has not been observed for wild types. *pmp22* was sensitive to feeding of a wide variety of substrates that harbor the potential to peroxisomally release acrylyl-CoA.

A similar phenotype has been reported for mutants in 3-hydroxyisobutyryl-CoA hydrolase CHY1 (Zolman et al., 2001a; Lange et al., 2004; Dong et al., 2009). Also *pmp22* and *chy1* share impaired storage oil mobilization and sensitivity to cold and dark stress. It was assumed that in *chy1* toxic methylacrylyl-CoA molecules are sequestered in the peroxisome or leak to the cytosol. *chy1* mutants exhibit reduced KAT activity (Lange et al., 2004), which is thought to arise from methylacrylyl-CoA inhibition. KAT structure analysis revealed KAT activity to be regulated by a redox switch (Pye et al., 2010). *chy1* displays high ROS levels (Dong et al., 2009) and these might also account for KAT inhibition. Probably analysis of *chy1* will also reveal highly oxidized peroxisomes in aggregates and *chy1* might as well display heat sensitivity, as heat is known to trigger ROS formation (Larkindale et al., 2005).

Comparison of *pmp22* and *chy1* led to development of a model of PMP22 function in BCAA catabolism (Figure 15). This model would allow for explanation of the probably pleiotropic phenotypes that were seen. The model proposes PMP22 to export 3-hydroxypropionate and prevent peroxisomes from accumulation of toxic enoyl-CoA and supports respiration of amino acids by converting generation of reduction equivalents and carbon units that can enter the TCA cycle. Also this would require channeling of substrates across the mitochondrial membrane and suggests a function of mitochondrial PMP22-type proteins in this pathway. Notably, expression of At3g24570 led to suppression of *sym1Δ* and could facilitate 3-hydroxypropionate import into the mitochondrial matrix.

Conclusion

In contrast to mammals, where P_{xmp2} knockout has a very mild phenotype plant metabolism is highly dependent on PMP22 function. PXA1 has been shown to import a wide range of metabolites, which are broken down to acetyl-CoA and propionyl-CoA units, which are further metabolized to dicarboxylates or 3-hydroxypropionate (Graham, 2008). Here, we identified PMP22 to potentially contribute to export of short-chain carboxylic acids. Future research will reveal if PMP22 is specific for

export of BCAA catabolites or facilitates translocation of a wide variety of carboxylic acids across the peroxisomal membrane. Here, we provide evidence that PMP22 is needed for optimal storage oil mobilization, survival of extended darkness and degradation of BCAA oxidation products and optimal seed filling.

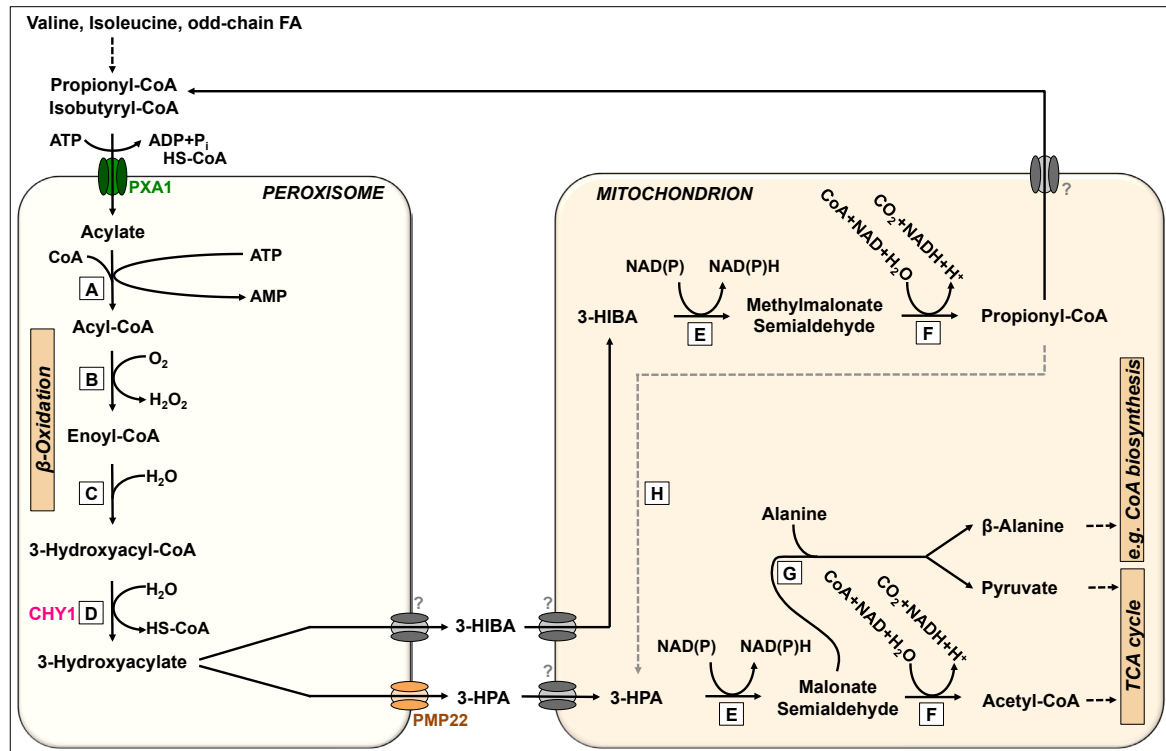


FIGURE 15. Hypothetical model of PMP22 function in propionyl-CoA degradation mediated by 3-hydroxypropionate export. The acylic acid propionate or more specifically its CoA ester (propionyl-CoA) derived from odd-chain fatty acids or isoleucine and isobutyryl-CoA derived from valine catabolism are metabolized to 3-hydroxypropionate (3-HPA) and 3-hydroxyisobutyrate (3-HIBA) respectively by peroxisomal β -oxidation. In the model intermediates are simplified (Acyl-CoA: propionyl-CoA/isobutyryl-CoA; Enoyl-CoA: Acrylyl-CoA and Methylacrylyl-CoA; 3-Hydroxyacyl-CoA: 3-Hydroxypropionyl-CoA/3-Hydroxyisobutyryl-CoA; 3-Hydroxyacylate: 3-HPA and 3-HIBA). Inside mitochondria 3-HIBA is converted to propionyl-CoA, which reenters peroxisomes to be oxidized to 3-HPA. The 3-HPA is converted to acetyl-CoA by mitochondrial enzymes, fueling the TCA cycle or converted to pyruvate. Enzymes: (A) Acyl-CoA synthetase, (B) Acyl-CoA oxidase, (C) Enoyl-CoA hydratase, (D) Hydroxyacyl-CoA hydrolase, (E) Hydroxyacid dehydrogenase, (F) (Methyl) malonate semialdehyde dehydrogenase, (G) β -Alanine aminotransferase

In field conditions mutations in PMP22 are likely to be selected against, because glyoxylate cycle action would be vital for the successful establishment of buried seedlings and adaption to abiotic stress is a prerequisite to survive in a changing environment. It will be interesting to see if PMP22 represents a bottleneck in the proposed implications and if overexpression will then lead to optimized responses to abiotic stress responses and prevent stress-induced senescence to enhance plant productivity.

Material and Methods

Chemicals were purchased from Sigma-Aldrich. Reagents and enzymes for recombinant DNA techniques were obtained from Clontech, Invitrogen, New England Biolabs and Promega.

Cloning procedures and generation of pmp22 miRNA mutants

For cloning sequences were retrieved from TAIR10 (www.arabidopsis.org) or SGD (www.yeastgenome.org). Arabidopsis genes were amplified from cDNA. *S. cerevisiae* genes were amplified from gDNA. miRNA target sites were identified by following the instructions on <http://wmd3.weigelworld.org>. 35S:amiRNA constructs were cloned as described by Schwab et al. (2006) with primers NL412-419 (Table S1). The PCR amplification product, including the specific miRNA, was cloned into the pHannibal vector (Wesley et al., 2001) and the expression cassette was subsequently ligated into the *NotI* site of the T-DNA binary vector pART27 (Gleave, 1992). DNA sequences were verified by DNA sequencing (GATC Biotech AG). Transformation of Arabidopsis was conducted according to the floral-dip method (Clough and Bent, 1998) with *Agrobacterium tumefaciens* GV3101 pMP90 (Koncz et al., 1989). Transgenic plants were selected based on kanamycin resistance (50 µg/mL) conferred by the *nptII* gene present in pART27.

Isolation of T-DNA insertion lines

Arabidopsis thaliana mutants were obtained from the Nottingham Arabidopsis Stock Centre: SALK_205443 (pmp22-1), SALK_052461 (pmp22-like-2) and SALK_019234 (pxa1-2) and the GABI-Kat project of the Bielefeld University: GABI_380B12 (pmp22-like-1). *chy1-3* (Zolman et al. 2001) was provided by Bethany Zolman. To identify homozygous T-DNA insertion lines, genomic DNA was isolated by the method of Edwards et al. (1991) and genotyped using gene-specific primer pairs and a primer pair for the T-DNA/gene junction (Table S1). The T-DNA position was verified by sequencing.

(quantitative) Reverse transcriptase-polymerase chain reaction

RNA was isolated from different *A. thaliana* tissues after a protocol developed by (Chomczynski and Sacchi, 1987). RNA integrity was determined on a 1 % agarose gel. Prior to cDNA synthesis, RNA was treated with RNase-free RQ1-DNase

(Promega) as recommended by the manufacturer. The PMP22(-like) transcripts were examined via quantitative reverse transcription PCR (qRT-PCR). For this analysis the messenger RNAs (mRNAs) of the total RNA were transcribed into complementary DNAs (cDNAs) using the Superscript III RNase H- Reverse Transcriptase (Invitrogen, Life Technologies GmbH). The cDNA synthesis was performed according to the manufacturers' instructions. The resulted cDNA pools were used as template for PCR or Real-time PCR with gene-specific primers (listed in Table S1). Transcript levels in Arabidopsis were determined by qRT-PCR with the MESA-SYBR-Green II Kit without ROX (Eurogentec Germany GmbH) according to the manuals instructions, run with the Standard SYBR-Green protocol of the StepOnePlus™ Real-Time PCR System (Applied Biosystems, Life technologies Corporation). The BLACK oligonucleotides published by Czechowski et al. (2005) were used as reference primer pair.

Plant cultivation

Seeds were surface sterilized, stratified for 4-7 days at 4°C and germinated on 0.8 % (w/v) agar-solidified half-strength MS medium (Duchefa) (with 1 % (w/v) sucrose, if indicated). Plants were incubated in a 16-h-light/8-h- dark cycle (22/18°C) in growth chambers (100 $\mu\text{mol m}^{-2} \text{s}^{-1}$ light intensity).

For the analysis of seedling growth, plants were grown on half-strength MS agar plates supplemented with or without sucrose in constant darkness or in short-day conditions (8-h light/16-h dark cycles). After the indicated period, seedlings were photographed or scanned and roots or hypocotyls were measured using IMAGEJ (<http://rsbweb.nih.gov/ij>). Plate additives were added from solutions adjusted to pH 5.6. For extended darkness treatments, 25-30 day old plants were subjected to prolonged night conditions at the start of the regular night for the time indicated. To determine seed parameters plants were grown randomized and the position of plant trays was systematically rotated to minimize light effects.

Yeast complementation studies

The *sym1* Δ knockout mutant deficient in the Stress inducible yeast MPV17 protein 1 (Sym1p) was purchased from euroscarf Frankfurt (Acc no. Y05160; Table S2). For complementation studies, the ORFs of At5g24570 and At4g04770 were integrated into pAG426 (Alberti et al., 2007, Addgene) or a modified pDR195 (Rentsch et al.,

1995) containing the *Arabidopsis* MSFC1 (At5g01340) mitochondrial targeting peptide CDS (Table S1) after in between promoter and multiple cloning site was fused to PMP22 by ligation of a synthetic adapter. In addition, the coding sequence of SYM1 was PCR-amplified from genomic DNA of the lab yeast strain INVSc1 (Invitrogen) and a pAG423 yeast expression construct was obtained.

Yeast was cultivated using standard YPD media and transformed with the expression constructs using the lithium acetate method (Schiestl and Gietz, 1989). The transformants were selected on synthetic complete minimal medium lacking uracil (SC-Ura). For yeast complementation studies, the transformed knockout mutants were analyzed on SC-Ura agar plates using lauric acid as the sole carbon source (Palmieri et al., 2001).

Localization studies by transient tobacco transformation

PMP22(-like) coding sequences were cloned into pUB series vectors (Grefen et al., 2010). Transient expression for localization studies in *Nicotiana benthamiana* and *Nicotiana tabacum* was done as described in Breuers et al. (2012). Three days after co-infiltration epidermal cells were analyzed with a Laser scanning microscope Zeiss 510 Meta or Olympus Fluoview1000.

Oil-body staining

Lipid bodies of 4-day-old etiolated seedlings were stained with Nile Red, as previously described by Linka et al. (2008) and images were recorded with a Olympus Fluoview1000 Laser scanning microscope.

BODIPY visualization of peroxisomes

Peroxisomes were stained and visualized in five-day-old seedlings with the BODIPY fluorescent dye as described by Landrum et al. (2010).

TEM Imaging

Ultrastructure of organelles in hypocotyl cells of 5-day-old hypocotyls by TEM analysis was done as described in Aung and Hu (2011).

PAM fluometry

In vivo chlorophyll a fluorescence assays were performed using the FluorCam FC 800-C (Photon Systems Instruments). 25-30 day-old dark-treated plants were taken

directly out of the growth cabinet and used for fluorescence measurements. To investigate defects in the photosynthetic apparatus standard settings of the manufacturer's software were used.

Fatty acid profiling

Fatty acids were analyzed following conversion to methyl esters after Browse et al. (1986). Fatty acid methyl esters were analyzed by gas chromatography on a DB23 column (30 m × 0.25 mm × 0.2 mm; J&W Scientific) and detected by flame ionization. Fatty acid content is expressed relative to the internal standard C17:0. The samples were analyzed with three independent biological replicates of each five pooled seeds/seedlings. Plants were stratified for five days and transferred to an 8-h/16-h light/dark cycle at $100 \mu\text{E m}^{-2} \text{s}^{-1}$ at 22°C/18°C. Plant material was harvested in the middle of the light period.

Leaf metabolite analysis

Preparation of samples for metabolic analysis was performed as described in Fiehn (2006). Samples were harvested by shock freezing rosette leaves in liquid nitrogen. Leaves were ground in liquid nitrogen, freeze dried and 5 mg of leaf powder was used for extraction with 1.5 ml of pre-chilled (−20°C) mixture of H₂O/methanol/CHCl₃ (1:2.5:1) containing 50 μM ribitol. Following incubation under gentle agitation for 6 min at 4°C on a rotating device, samples were centrifuged for 2 min at 20,000 g. 50 μL of the supernatant were dried and used for further analysis by gas chromatography/electron-impact time-of-flight mass spectrometry, as previously described (Lee and Fiehn, 2008). Extracts were additionally subjected to amino acid analysis by high-performance liquid chromatography (ZORBAX Rapid Resolution HT Eclipse Plus C18, 2.1 x 50 mm, 1.8 μm column) coupled to a diode array detector (DAD). Metabolite content is expressed relative to the internal standard ribitol. Chlorophyll was quantified from methanol extract according to Lichtenthaler and Wellburn (1983) and used for normalization of biological replicates. All samples were analyzed with three independent biological replicates.

Seed amino acid quantification

Seed amino acids were analyzed as described in Gu et al. (2012).

Protein quantification

Seed protein was isolated by grinding in extraction buffer (10 % (v/v) glycerol, 1 % (v/v) β -mercaptoethanol, 100 mM Tris, 1 mM phenylmethanesulfonylfluoride, 0.1 % (v/v) Troton-X-100). After centrifugation the seed protein supernatant was purified and quantified with the Compat-Able BCA protein Assay Kit (Thermo-Scientific).

Bioinformatic and statistical analyses

Phylogenetic trees were constructed with the MEGA5 software (Tamura et al., 2011). PCA score plots were generated with the Multiple Experiment Viewer (Saeed et al., 2003). Statistical analyses and Gompertz-growth rate fit were performed with GraphPad Prism 5.0. Quantitative analysis results are presented as means +SE from repeated experiments as indicated in the figure legends. Pairwise Student's t test was used to analyze statistical significance.

Supplemented data

- Fig. S1** ClustalW2 multiple sequence alignment of *Arabidopsis thaliana* PMP22-type family proteins
- Fig. S2** Extraperoxisomal localization of mitochondria predicted PMP22-type family proteins encoded by At3g25570, At5g43140 and At2g14860
- Fig. S3** Analysis of PMP22-type sequence conservation in selected plant proteomes.
- Fig. S4** Co-regulation categories of Arabidopsis PMP22-type genes PMP22 (At4g04470), At2g42770, At5g19750 and At5g43140
- Fig. S5** Purification and structure analysis by CD-spectroscopy of recombinant PMP22-His in DDM micelles and PMP22-His proteoliposome flotation assay
- Fig. S6** Electrophysiological characterization of planar lipid bilayer incorporated PMP22-His
- Fig. S7** *In vitro* PMP22-His proteoliposome transport assays with radiolabeled 2-oxoglutarate, malate and sulfate.
- Fig. S8** *E. coli* CBT315 growth phenotype suppression assay by heterologous expression of PMP22
- Fig. S9** Analysis of *chy1-3* in prolonged darkness and upon reillumination
- Fig. S10** Photosystem II electron transport monitored by chlorophyll fluorescence

in *Col-0*, *pmp22* and *pmp22-like* after dark treatment.

- Fig. S11** Chlorophyll contents in *Col-0*, *pmp22-1*, *pmp22-8*, *pmp22-9* and *pxa1-2* after exposure to darkness.
- Fig. S12** Photosystem II electron transport monitored by chlorophyll fluorescence and leaf morphology in *Col-0*, *pmp22-1*, *pmp22-8*, *pmp22-9* and *pxa1-2* after changes in the temperature.
- Fig. S13** Glycolate oxidase activity (+SE; n=3) in seedlings of *Col-0*, *pmp22-1* and *pmp22-8*
- Fig. S14** Mean root length (+SE) of *Col-0*, *pmp22-8* and *pmp22-9* after exposure to Glycine, lactic acid, malic acid, glyoxylic acid, pimelic acid, 3-hydroxyisocaproic acid, 4-methylvaleric acid and lysine.
- Fig. S15** Growth of *Col-0*, *pmp22-1*, *pmp22-8* and *pmp22-9* on half strength MS medium with acrylic acid.
- Fig. S16** Growth of *Col-0*, *pmp22-1*, *pmp22-8* and *pmp22-9* on half strength MS medium with Phytol
- Fig. S17** Levels of isoleucine, leucine, valine, glycolic acid and uric acid in natural senescent leaves of *Col-0* and *pmp22-8*
- Fig. S18** Photosynthetic capacity of *Col-0*, *pmp22-1*, *pmp22-2* and *pmp22-8* monitored by chlorophyll fluorescence (photochemical quantum yield, Phi2) with light intensity of a simulated natural day (highest light intensity by midday)

Supplemented Material

Table S1 Oligonucleotides used in this study

Table S2 *Escherichia coli*, *Agrobacterium tumefaciens* and *Saccharomyces cerevisiae* strains used in this study

Supplemented Methods

Supplemented References

Acknowledgements

The authors thank Bethany Zolman for sending *chy1-3* seeds. BODIPY was kindly provided by Alison Baker. Jan Wiese gratefully acknowledges Ronghui Pan for help with confocal microscopy, Alicia Withrow for help with TEM-imaging, Navneet Kaur, Jiying Li and Gaëlle Cassin are appreciated for helping with plant care. Sarah Keßel-Vigelius, Canan Külahoglu, Alisandra Denton and Samanta Kurz are appreciated for helpful discussion. Elisabeth Klemp and Katrin Weber helped with amino acid and carboxylic acid analysis. Philipp Bartsch, Anke Harsmann and Richard Wagner helped with electrophysiological analyses. Judith Paulus, Patricia Robel and Georg Groth gave advice on protein purification. Florian Hahn and Lars Lüers helped with CD-spectroscopy. Linda Savage and Jeffrey Cruz assisted with photosynthesis measurements. Michael Thomashow provided plant growth space.

Author contributions

Jan Wiese performed all experiments and wrote the manuscript. Henrik Tjellström assisted with fatty acid measurement. Martin Schroers assisted with darkness experiments. Cheng Peng helped with seed amino acid extraction and quantification. Nicole Linka helped with *in vitro* uptake studies. Jianping Hu, Robert Last, John Ohlrogge, Andreas Weber and Nicole Linka provided lab space and helpful discussions. Jan Wiese and Nicole Linka designed the experiments.

References

- Agrimi, G., Russo, A., Pierri, C.L., and Palmieri, F.** (2012). The peroxisomal NAD⁺ carrier of *Arabidopsis thaliana* transports coenzyme A and its derivatives. *J. Bioenerg. Biomembr.* **44**: 333–340.
- Alberti, S., Gitler, A.D., and Lindquist, S.** (2007). A suite of Gateway cloning vectors for high-throughput genetic analysis in *Saccharomyces cerevisiae*. *Yeast* **24**: 913–919.
- Allen, E., Moing, A., Wattis, J.A.D., Larson, T., Maucourt, M., Graham, I.A., Rolin, D., and Hooks, M.A.** (2011). Evidence that ACN1 (acetate non-utilizing 1) prevents carbon leakage from peroxisomes during lipid mobilization in *Arabidopsis* seedlings. *Biochem. J.* **437**: 505–513.
- Antonenkov, V.D., Mindthoff, S., Grunau, S., Erdmann, R., and Hiltunen, J.K.** (2009). An involvement of yeast peroxisomal channels in transmembrane transfer of glyoxylate cycle intermediates. *Int. J. Biochem. Cell Biol.* **41**: 2546–2554.
- Antonenkov, V.D., Rokka, A., Sormunen, R.T., Benz, R., and Hiltunen, J.K.** (2005). Solute traffic across mammalian peroxisomal membrane—single channel conductance monitoring reveals pore-forming activities in peroxisomes. *Cell. Mol. Life Sci.* **62**: 2886–2895.
- Arai, Y., Hayashi, M., and Nishimura, M.** (2008). Proteomic identification and characterization of a novel peroxisomal adenine nucleotide transporter supplying ATP for fatty acid beta-oxidation in soybean and *Arabidopsis*. *Plant Cell* **20**: 3227–3240.
- Araújo, W.L., Ishizaki, K., Nunes-Nesi, A., Larson, T.R., Tohge, T., Krahnert, I., Witt, S., Obata, T., Schauer, N., Graham, I.A., Leaver, C.J., and Fernie, A.R.** (2010). Identification of the 2-hydroxyglutarate and isovaleryl-CoA dehydrogenases as alternative electron donors linking lysine catabolism to the electron transport chain of *Arabidopsis* mitochondria. *Plant Cell* **22**: 1549–1563.
- Araújo, W.L., Tohge, T., Ishizaki, K., Leaver, C.J., and Fernie, A.R.** (2011). Protein degradation - an alternative respiratory substrate for stressed plants. *Trends Plant Sci.* **16**: 489–498.
- Bartsch, P., Harsman, A., and Wagner, R.** (2013). Single channel analysis of membrane proteins in artificial bilayer membranes. *Methods Mol. Biol.* **1033**: 345–361.
- Bassham, D.C.** (2007). Plant autophagy—more than a starvation response. *Curr. Opin. Plant Biol.* **10**: 587–593.
- Bernhardt, K., Wilkinson, S., Weber, A.P.M., and Linka, N.** (2012). A peroxisomal carrier delivers NAD⁺ and contributes to optimal fatty acid degradation during storage oil mobilization. *Plant J.* **69**: 1–13.
- Bieker, S., Riester, L., Stahl, M., Franzaring, J., and Zentgraf, U.** (2012). Senescence-specific alteration of hydrogen peroxide levels in *Arabidopsis thaliana* and oilseed rape spring variety *Brassica napus* L. cv. Mozart. *J Integr Plant Biol* **54**: 540–554.
- Bordych, C., Eisenhut, M., Pick, T.R., Kuelahoglu, C., and Weber, A.P.M.** (2013). Co-expression analysis as tool for the discovery of transport proteins in photorespiration. *Plant Biol (Stuttg)* **15**: 686–693.
- Breeze, E. et al.** (2011). High-resolution temporal profiling of transcripts during *Arabidopsis* leaf senescence reveals a distinct chronology of processes and regulation. *Plant Cell* **23**: 873–894.
- Breuers, F.K.H., Bräutigam, A., Geimer, S., Welzel, U.Y., Stefano, G., Renna, L., Brandizzi, F., and Weber, A.P.M.** (2012). Dynamic Remodeling of the Plastid Envelope Membranes - A Tool for Chloroplast Envelope in vivo Localizations. *Front Plant Sci* **3**: 7.
- Browse, J., McCourt, P.J., and Somerville, C.R.** (1986). Fatty acid composition of leaf lipids determined after combined digestion and fatty acid methyl ester formation from fresh tissue. *Anal. Biochem.* **152**: 141–145.
- Brychkova, G., Alikulov, Z., Fluhr, R., and Sagi, M.** (2008a). A critical role for ureides in dark and senescence-induced purine remobilization is unmasked in the *Atxdh1* *Arabidopsis* mutant. *Plant J.* **54**: 496–509.
- Brychkova, G., Fluhr, R., and Sagi, M.** (2008b). Formation of xanthine and the use of purine metabolites as a nitrogen source in *Arabidopsis* plants. *Plant Signal Behav* **3**:

- 999–1001.
- Buchanan-Wollaston, V., Page, T., Harrison, E., Breeze, E., Lim, P.O., Nam, H.G., Lin, J.-F., Wu, S.-H., Swidzinski, J., Ishizaki, K., and Leaver, C.J.** (2005). Comparative transcriptome analysis reveals significant differences in gene expression and signalling pathways between developmental and dark/starvation-induced senescence in *Arabidopsis*. *Plant J.* **42**: 567–585.
- Catoni, E., Schwab, R., Hilpert, M., Desimone, M., Schwacke, R., Flügge, U.-I., Schumacher, K., and Frommer, W.B.** (2003). Identification of an *Arabidopsis* mitochondrial succinate-fumarate translocator. *FEBS Lett.* **534**: 87–92.
- Chomczynski, P. and Sacchi, N.** (1987). Single-step method of RNA isolation by acid guanidinium thiocyanate-phenol-chloroform extraction. *Anal. Biochem.* **162**: 156–159.
- Citovsky, V., Lee, L.-Y., Vyas, S., Glick, E., Chen, M.-H., Vainstein, A., Gafni, Y., Gelvin, S.B., and Tzfira, T.** (2006). Subcellular localization of interacting proteins by bimolecular fluorescence complementation in planta. *J. Mol. Biol.* **362**: 1120–1131.
- Clough, S.J. and Bent, A.F.** (1998). Floral dip: a simplified method for *Agrobacterium*-mediated transformation of *Arabidopsis thaliana*. *Plant J.* **16**: 735–743.
- Cornah, J.E., Germain, V., Ward, J.L., Beale, M.H., and Smith, S.M.** (2004). Lipid utilization, gluconeogenesis, and seedling growth in *Arabidopsis* mutants lacking the glyoxylate cycle enzyme malate synthase. *J. Biol. Chem.* **279**: 42916–42923.
- Czechowski, T., Stitt, M., Altmann, T., Udvardi, M.K., and Scheible, W.-R.** (2005). Genome-wide identification and testing of superior reference genes for transcript normalization in *Arabidopsis*. *Plant Physiol.* **139**: 5–17.
- Dallabona, C., Marsano, R.M., Arzuffi, P., Ghezzi, D., Mancini, P., Zeviani, M., Ferrero, I., and Donnini, C.** (2010). Sym1, the yeast ortholog of the MPV17 human disease protein, is a stress-induced bioenergetic and morphogenetic mitochondrial modulator. *Hum. Mol. Genet.* **19**: 1098–1107.
- De Marcos Lousa, C., van Roermund, C.W.T., Postis, V.L.G., Dietrich, D., Kerr, I.D., Wanders, R.J.A., Baldwin, S.A., Baker, A., and Theodoulou, F.L.** (2013). Intrinsic acyl-CoA thioesterase activity of a peroxisomal ATP binding cassette transporter is required for transport and metabolism of fatty acids. *Proc. Natl. Acad. Sci. U.S.A.* **110**: 1279–1284.
- Del Río, L.A., Corpas, F.J., Sandalio, L.M., Palma, J.M., Gómez, M., and Barroso, J.B.** (2002). Reactive oxygen species, antioxidant systems and nitric oxide in peroxisomes. *J. Exp. Bot.* **53**: 1255–1272.
- Dong, C.-H., Zolman, B.K., Bartel, B., Lee, B.-H., Stevenson, B., Agarwal, M., and Zhu, J.-K.** (2009). Disruption of *Arabidopsis* CHY1 reveals an important role of metabolic status in plant cold stress signaling. *Mol Plant* **2**: 59–72.
- Edwards, K., Johnstone, C., and Thompson, C.** (1991). A simple and rapid method for the preparation of plant genomic DNA for PCR analysis. *Nucleic Acids Res.* **19**: 1349.
- Egli, D.B.** (2011). Time and the Productivity of Agronomic Crops and Cropping Systems. *Agronomy Journal* **103**: 743–750.
- Eisenhut, M., Pick, T.R., Bordych, C., and Weber, A.P.M.** (2013). Towards closing the remaining gaps in photorespiration--the essential but unexplored role of transport proteins. *Plant Biol (Stuttg)* **15**: 676–685.
- Engqvist, M., Drincovich, M.F., Flügge, U.-I., and Maurino, V.G.** (2009). Two D-2-hydroxy-acid dehydrogenases in *Arabidopsis thaliana* with catalytic capacities to participate in the last reactions of the methylglyoxal and beta-oxidation pathways. *J. Biol. Chem.* **284**: 25026–25037.
- Engqvist, M.K.M., Kuhn, A., Wienstroer, J., Weber, K., Jansen, E.E.W., Jakobs, C., Weber, A.P.M., and Maurino, V.G.** (2011). Plant D-2-hydroxyglutarate dehydrogenase participates in the catabolism of lysine especially during senescence. *J. Biol. Chem.* **286**: 11382–11390.
- Estelle, M.A. and Somerville, C.** (1987). Auxin-resistant mutants of *Arabidopsis thaliana* with an altered morphology. *Mol Gen Genet* **206**: 200–206.
- Eubel, H., Meyer, E.H., Taylor, N.L., Bussell, J.D., O'Toole, N., Heazlewood, J.L., Castleden, I., Small, I.D., Smith, S.M., and Millar, A.H.** (2008). Novel proteins, putative

- membrane transporters, and an integrated metabolic network are revealed by quantitative proteomic analysis of Arabidopsis cell culture peroxisomes. *Plant Physiol.* **148**: 1809–1829.
- Ferro, M., Salvi, D., Brugière, S., Miras, S., Kowalski, S., Louwagie, M., Garin, J., Joyard, J., and Rolland, N.** (2003). Proteomics of the chloroplast envelope membranes from Arabidopsis thaliana. *Mol. Cell Proteomics* **2**: 325–345.
- Fiehn, O.** (2006). Metabolite profiling in Arabidopsis. *Methods Mol. Biol.* **323**: 439–447.
- Fiermonte, G., Dolce, V., Palmieri, L., Ventura, M., Runswick, M.J., Palmieri, F., and Walker, J.E.** (2001). Identification of the human mitochondrial oxodicarboxylate carrier. Bacterial expression, reconstitution, functional characterization, tissue distribution, and chromosomal location. *J. Biol. Chem.* **276**: 8225–8230.
- Finn, R.D., Clements, J., and Eddy, S.R.** (2011). HMMER web server: interactive sequence similarity searching. *Nucleic Acids Res.* **39**: W29–37.
- Footitt, S., Cornah, J.E., Pracharoenwattana, I., Bryce, J.H., and Smith, S.M.** (2007a). The Arabidopsis 3-ketoacyl-CoA thiolase-2 (*kat2-1*) mutant exhibits increased flowering but reduced reproductive success. *J. Exp. Bot.* **58**: 2959–2968.
- Footitt, S., Dietrich, D., Fait, A., Fernie, A.R., Holdsworth, M.J., Baker, A., and Theodoulou, F.L.** (2007b). The COMATOSE ATP-binding cassette transporter is required for full fertility in Arabidopsis. *Plant Physiol.* **144**: 1467–1480.
- Footitt, S., Slocombe, S.P., Larner, V., Kurup, S., Wu, Y., Larson, T., Graham, I., Baker, A., and Holdsworth, M.** (2002). Control of germination and lipid mobilization by COMATOSE, the Arabidopsis homologue of human ALDP. *EMBO J.* **21**: 2912–2922.
- Froehlich, J.E., Wilkerson, C.G., Ray, W.K., McAndrew, R.S., Osteryoung, K.W., Gage, D.A., and Phinney, B.S.** (2003). Proteomic study of the Arabidopsis thaliana chloroplastic envelope membrane utilizing alternatives to traditional two-dimensional electrophoresis. *J. Proteome Res.* **2**: 413–425.
- Germain, V., Rylott, E.L., Larson, T.R., Sherson, S.M., Bechtold, N., Carde, J.P., Bryce, J.H., Graham, I.A., and Smith, S.M.** (2001). Requirement for 3-ketoacyl-CoA thiolase-2 in peroxisome development, fatty acid beta-oxidation and breakdown of triacylglycerol in lipid bodies of Arabidopsis seedlings. *Plant J.* **28**: 1–12.
- Gleave, A.P.** (1992). A versatile binary vector system with a T-DNA organisational structure conducive to efficient integration of cloned DNA into the plant genome. *Plant Mol. Biol.* **20**: 1203–1207.
- Graham, I.A.** (2008). Seed storage oil mobilization. *Annu Rev Plant Biol* **59**: 115–142.
- Graham, I.A., Li, Y., and Larson, T.R.** (2002). Acyl-CoA measurements in plants suggest a role in regulating various cellular processes. *Biochem. Soc. Trans.* **30**: 1095–1099.
- Greenspan, P., Mayer, E.P., and Fowler, S.D.** (1985). Nile red: a selective fluorescent stain for intracellular lipid droplets. *J. Cell Biol.* **100**: 965–973.
- Grefen, C., Donald, N., Hashimoto, K., Kudla, J., Schumacher, K., and Blatt, M.R.** (2010). A ubiquitin-10 promoter-based vector set for fluorescent protein tagging facilitates temporal stability and native protein distribution in transient and stable expression studies. *Plant J.* **64**: 355–365.
- Gregersen, P.L., Culetic, A., Boschian, L., and Krupinska, K.** (2013). Plant senescence and crop productivity. *Plant Mol. Biol.* **82**: 603–622.
- Grunau, S., Mindthoff, S., Rottensteiner, H., Sormunen, R.T., Hiltunen, J.K., Erdmann, R., and Antonenkov, V.D.** (2009). Channel-forming activities of peroxisomal membrane proteins from the yeast *Saccharomyces cerevisiae*. *FEBS J.* **276**: 1698–1708.
- Gu, L., Jones, A.D., and Last, R.L.** (2012). Rapid LC–MS/MS Profiling of Protein Amino Acids and Metabolically Related Compounds for Large-Scale Assessment of Metabolic Phenotypes.: 1–11.
- Gualdron-López, M., Vapola, M.H., Miinalainen, I.J., Hiltunen, J.K., Michels, P.A.M., and Antonenkov, V.D.** (2012). Channel-forming activities in the glycosomal fraction from the bloodstream form of *Trypanosoma brucei*. *PLoS ONE* **7**: e34530.
- Harrison-Lowe, N. and Olsen, L.J.** (2006). Isolation of glyoxysomes from pumpkin cotyledons. *Curr Protoc Cell Biol* **Chapter 3**: Unit 3.19.
- Harsman, A., Bartsch, P., Hemmis, B., Krüger, V., and Wagner, R.** (2011). Exploring

- protein import pores of cellular organelles at the single molecule level using the planar lipid bilayer technique. *Eur. J. Cell Biol.* **90**: 721–730.
- Havir, E.A.** (1992). The in Vivo and in Vitro Inhibition of Catalase from Leaves of *Nicotiana sylvestris* by 3-Amino-1,2,4-Triazole. *Plant Physiol.* **99**: 533–537.
- Hayashi, M., Toriyama, K., Kondo, M., and Nishimura, M.** (1998). 2,4-Dichlorophenoxybutyric acid-resistant mutants of *Arabidopsis* have defects in glyoxysomal fatty acid beta-oxidation. *Plant Cell* **10**: 183–195.
- Hesberg, C., Hänsch, R., Mendel, R.R., and Bittner, F.** (2004). Tandem orientation of duplicated xanthine dehydrogenase genes from *Arabidopsis thaliana*: differential gene expression and enzyme activities. *J. Biol. Chem.* **279**: 13547–13554.
- Homblé, F., Krammer, E.-M., and Prévost, M.** (2012). Plant VDAC: facts and speculations. *Biochim. Biophys. Acta* **1818**: 1486–1501.
- Hooks, M.A., Turner, J.E., Murphy, E.C., Johnston, K.A., Burr, S., and Jarosławski, S.** (2007). The *Arabidopsis* ALDP protein homologue COMATOSE is instrumental in peroxisomal acetate metabolism. *Biochem. J.* **406**: 399–406.
- Hu, J., Baker, A., Bartel, B., Linka, N., Mullen, R.T., Reumann, S., and Zolman, B.K.** (2012). Plant peroxisomes: biogenesis and function. *Plant Cell* **24**: 2279–2303.
- Kim, J., Lee, H., Lee, H.N., Kim, S.-H., Shin, K.D., and Chung, T.** (2013). Autophagy-related proteins are required for degradation of peroxisomes in *Arabidopsis* hypocotyls during seedling growth. *Plant Cell* **25**: 4956–4966.
- Klodmann, J., Senkler, M., Rode, C., and Braun, H.-P.** (2011). Defining the protein complex proteome of plant mitochondria. *Plant Physiol.* **157**: 587–598.
- Kochevenko, A., Araújo, W.L., Maloney, G.S., Tieman, D.M., Do, P.T., Taylor, M.G., Klee, H.J., and Fernie, A.R.** (2012). Catabolism of branched chain amino acids supports respiration but not volatile synthesis in tomato fruits. *Mol Plant* **5**: 366–375.
- Koncz, C., Martini, N., Mayerhofer, R., Koncz-Kalman, Z., Körber, H., Redei, G.P., and Schell, J.** (1989). High-frequency T-DNA-mediated gene tagging in plants. *Proc. Natl. Acad. Sci. U.S.A.* **86**: 8467–8471.
- Kunz, H.-H., Scharnewski, M., Feussner, K., Feussner, I., Flügge, U.-I., Fulda, M., and Gierth, M.** (2009). The ABC transporter PXA1 and peroxisomal beta-oxidation are vital for metabolism in mature leaves of *Arabidopsis* during extended darkness. *Plant Cell* **21**: 2733–2749.
- Landrum, M., Smertenko, A., Edwards, R., Hussey, P.J., and Steel, P.G.** (2010). BODIPY probes to study peroxisome dynamics in vivo. *Plant J.* **62**: 529–538.
- Lange, P.R., Eastmond, P.J., Madagan, K., and Graham, I.A.** (2004). An *Arabidopsis* mutant disrupted in valine catabolism is also compromised in peroxisomal fatty acid beta-oxidation. *FEBS Lett.* **571**: 147–153.
- Larkindale, J., Hall, J.D., Knight, M.R., and Vierling, E.** (2005). Heat stress phenotypes of *Arabidopsis* mutants implicate multiple signaling pathways in the acquisition of thermotolerance. *Plant Physiol.* **138**: 882–897.
- Lee, M., Choi, Y., Burla, B., Kim, Y.-Y., Jeon, B., Maeshima, M., Yoo, J.-Y., Martinoia, E., and Lee, Y.** (2008). The ABC transporter AtABCB14 is a malate importer and modulates stomatal response to CO₂. *Nat. Cell Biol.* **10**: 1217–1223.
- Lemieux, B., Miquel, M., Somerville, C., and Browse, J.** (1990). Mutants of *Arabidopsis* with alterations in seed lipid fatty acid composition. *Theor. Appl. Genet.* **80**: 234–240.
- Lichtenthaler, H.K. and Weellburn, A.R.** (1983). Determinations of total carotenoids and chlorophylls a and b of leaf extracts in different solvents. *Biochem. Soc. Trans.* **11**: 591–592.
- Liepmann, A.H. and Olsen, L.J.** (2003). Alanine aminotransferase homologs catalyze the glutamate:glyoxylate aminotransferase reaction in peroxisomes of *Arabidopsis*. *Plant Physiol.* **131**: 215–227.
- Liepmann, A.H. and Olsen, L.J.** (2001). Peroxisomal alanine : glyoxylate aminotransferase (AGT1) is a photorespiratory enzyme with multiple substrates in *Arabidopsis thaliana*. *Plant J.* **25**: 487–498.
- Lim, P.O., Kim, H.J., and Nam, H.G.** (2007). Leaf senescence. *Annu Rev Plant Biol* **58**: 115–136.

- Linka, N. and Esser, C.** (2012). Transport proteins regulate the flux of metabolites and cofactors across the membrane of plant peroxisomes. *Front Plant Sci* **3**: 3.
- Linka, N. and Theodoulou, F.L.** (2013). Metabolite transporters of the plant peroxisomal membrane: known and unknown. *Subcell. Biochem.* **69**: 169–194.
- Linka, N. and Weber, A.P.M.** (2010). Intracellular metabolite transporters in plants. *Mol Plant* **3**: 21–53.
- Linka, N., Theodoulou, F.L., Haslam, R.P., Linka, M., Napier, J.A., Neuhaus, H.E., and Weber, A.P.M.** (2008). Peroxisomal ATP import is essential for seedling development in *Arabidopsis thaliana*. *Plant Cell* **20**: 3241–3257.
- Lo, T.C., Rayman, M.K., and Sanwal, B.D.** (1972). Transport of succinate in *Escherichia coli*. I. Biochemical and genetic studies of transport in whole cells. *J. Biol. Chem.* **247**: 6323–6331.
- Lucas, K.A., Filley, J.R., Erb, J.M., Graybill, E.R., and Hawes, J.W.** (2007). Peroxisomal metabolism of propionic acid and isobutyric acid in plants. *J. Biol. Chem.* **282**: 24980–24989.
- Magliano, P., Flippi, M., Arpat, B.A., Delessert, S., and Poirier, Y.** (2011). Contributions of the peroxisome and β -oxidation cycle to biotin synthesis in fungi. *J. Biol. Chem.* **286**: 42133–42140.
- Maruyama, J.-I., Yamaoka, S., Matsuo, I., Tsutsumi, N., and Kitamoto, K.** (2012). A newly discovered function of peroxisomes: involvement in biotin biosynthesis. *Plant Signal Behav* **7**: 1589–1593.
- Murphy, M.A., Phillipson, B.A., Baker, A., and Mullen, R.T.** (2003). Characterization of the targeting signal of the *Arabidopsis* 22-kD integral peroxisomal membrane protein. *Plant Physiol.* **133**: 813–828.
- Nakagawa, A., Sakamoto, S., Takahashi, M., Morikawa, H., and Sakamoto, A.** (2007). The RNAi-mediated silencing of xanthine dehydrogenase impairs growth and fertility and accelerates leaf senescence in transgenic *Arabidopsis* plants. *Plant Cell Physiol.* **48**: 1484–1495.
- Noh, Y.S. and Amasino, R.M.** (1999). Identification of a promoter region responsible for the senescence-specific expression of SAG12. *Plant Mol. Biol.* **41**: 181–194.
- Nyathi, Y., De Marcos Lousa, C., van Roermund, C.W., Wanders, R.J.A., Johnson, B., Baldwin, S.A., Theodoulou, F.L., and Baker, A.** (2010). The *Arabidopsis* peroxisomal ABC transporter, comatose, complements the *Saccharomyces cerevisiae* pxa1 pxa2Delta mutant for metabolism of long-chain fatty acids and exhibits fatty acyl-CoA-stimulated ATPase activity. *J. Biol. Chem.* **285**: 29892–29902.
- Obayashi, T., Nishida, K., Kasahara, K., and Kinoshita, K.** (2011). ATTED-II updates: condition-specific gene coexpression to extend coexpression analyses and applications to a broad range of flowering plants. *Plant Cell Physiol.* **52**: 213–219.
- Ossowski, S., Schwab, R., and Weigel, D.** (2008). Gene silencing in plants using artificial microRNAs and other small RNAs. *Plant J.* **53**: 674–690.
- Oxborough, K.** (2004). Imaging of chlorophyll a fluorescence: theoretical and practical aspects of an emerging technique for the monitoring of photosynthetic performance. *J. Exp. Bot.* **55**: 1195–1205.
- Palmieri, L., Rottensteiner, H., Girzalsky, W., Scarcia, P., Palmieri, F., and Erdmann, R.** (2001). Identification and functional reconstitution of the yeast peroxisomal adenine nucleotide transporter. *EMBO J.* **20**: 5049–5059.
- Parish, R.W.** (1972). Urate oxidase in peroxisomes from maize root tips. *Planta* **104**: 247–251.
- Potel, F., Valadier, M.-H., Ferrario-Méry, S., Grandjean, O., Morin, H., Gaufichon, L., Boutet-Mercey, S., Lothier, J., Rothstein, S.J., Hirose, N., and Suzuki, A.** (2009). Assimilation of excess ammonium into amino acids and nitrogen translocation in *Arabidopsis thaliana*—roles of glutamate synthases and carbamoylphosphate synthetase in leaves. *FEBS J.* **276**: 4061–4076.
- Pracharoenwattana, I., Cornah, J.E., and Smith, S.M.** (2005). *Arabidopsis* peroxisomal citrate synthase is required for fatty acid respiration and seed germination. *Plant Cell* **17**: 2037–2048.

- Proudfoot, A.T., Bradberry, S.M., and Vale, J.A.** (2006). Sodium fluoroacetate poisoning. *Toxicol Rev* **25**: 213–219.
- Pruzinská, A., Tanner, G., Anders, I., Roca, M., and Hörtensteiner, S.** (2003). Chlorophyll breakdown: pheophorbide a oxygenase is a Rieske-type iron-sulfur protein, encoded by the accelerated cell death 1 gene. *Proc. Natl. Acad. Sci. U.S.A.* **100**: 15259–15264.
- Punta, M. et al.** (2012). The Pfam protein families database. *Nucleic Acids Res.* **40**: D290–301.
- Pye, V.E., Christensen, C.E., Dyer, J.H., Arent, S., and Henriksen, A.** (2010). Peroxisomal plant 3-ketoacyl-CoA thiolase structure and activity are regulated by a sensitive redox switch. *J. Biol. Chem.* **285**: 24078–24088.
- Ramazzina, I., Costa, R., Cendron, L., Berni, R., Peracchi, A., Zanotti, G., and Percudani, R.** (2010). An aminotransferase branch point connects purine catabolism to amino acid recycling. *Nat. Chem. Biol.* **6**: 801–806.
- Reinhold, R., Krüger, V., Meinecke, M., Schulz, C., Schmidt, B., Grunau, S.D., Guiard, B., Wiedemann, N., van der Laan, M., Wagner, R., Rehling, P., and Dudek, J.** (2012). The channel-forming Sym1 protein is transported by the TIM23 complex in a presequence-independent manner. *Mol. Cell. Biol.* **32**: 5009–5021.
- Rentsch, D., Laloi, M., Rouhara, I., Schmelzer, E., Delrot, S., and Frommer, W.B.** (1995). NTR1 encodes a high affinity oligopeptide transporter in Arabidopsis. *FEBS Lett.* **370**: 264–268.
- Reumann, S. and Weber, A.P.M.** (2006). Plant peroxisomes respire in the light: some gaps of the photorespiratory C2 cycle have become filled--others remain. *Biochim. Biophys. Acta* **1763**: 1496–1510.
- Reumann, S., Bettermann, M., Benz, R., and Heldt, H.W.** (1997). Evidence for the Presence of a Porin in the Membrane of Glyoxysomes of Castor Bean. *Plant Physiol.* **115**: 891–899.
- Reumann, S., Maier, E., Benz, R., and Heldt, H.W.** (1996). A specific porin is involved in the malate shuttle of leaf peroxisomes. *Biochem. Soc. Trans.* **24**: 754–757.
- Reumann, S., Maier, E., Benz, R., and Heldt, H.W.** (1995). The membrane of leaf peroxisomes contains a porin-like channel. *J. Biol. Chem.* **270**: 17559–17565.
- Reumann, S., Maier, E., Heldt, H.W., and Benz, R.** (1998). Permeability properties of the porin of spinach leaf peroxisomes. *Eur. J. Biochem.* **251**: 359–366.
- Reumann, S., Quan, S., Aung, K., Yang, P., Manandhar-Shrestha, K., Holbrook, D., Linka, N., Switzenberg, R., Wilkerson, C.G., Weber, A.P.M., Olsen, L.J., and Hu, J.** (2009). In-depth proteome analysis of Arabidopsis leaf peroxisomes combined with in vivo subcellular targeting verification indicates novel metabolic and regulatory functions of peroxisomes. *Plant Physiol.* **150**: 125–143.
- Rokka, A., Antonenkov, V.D., Soininen, R., Immonen, H.L., Pirilä, P.L., Bergmann, U., Sormunen, R.T., Weckström, M., Benz, R., and Hiltunen, J.K.** (2009). Pxmp2 is a channel-forming protein in Mammalian peroxisomal membrane. *PLoS ONE* **4**: e5090.
- Rottensteiner, H. and Theodoulou, F.L.** (2006). The ins and outs of peroxisomes: co-ordination of membrane transport and peroxisomal metabolism. *Biochim. Biophys. Acta* **1763**: 1527–1540.
- Saeed, A.I. et al.** (2003). TM4: a free, open-source system for microarray data management and analysis. *BioTechniques* **34**: 374–378.
- Schiestl, R.H. and Gietz, R.D.** (1989). High efficiency transformation of intact yeast cells using single stranded nucleic acids as a carrier. *Curr. Genet.* **16**: 339–346.
- Schmid, M., Davison, T.S., Henz, S.R., Pape, U.J., Demar, M., Vingron, M., Schölkopf, B., Weigel, D., and Lohmann, J.U.** (2005). A gene expression map of Arabidopsis thaliana development. *Nat. Genet.* **37**: 501–506.
- Schönfeld, P. and Wojtczak, L.** (2008). Fatty acids as modulators of the cellular production of reactive oxygen species. *Free Radic. Biol. Med.* **45**: 231–241.
- Schwab, R., Ossowski, S., Riester, M., Warthmann, N., and Weigel, D.** (2006). Highly specific gene silencing by artificial microRNAs in Arabidopsis. *Plant Cell* **18**: 1121–1133.
- Schwacke, R., Schneider, A., van der Graaff, E., Fischer, K., Catoni, E., Desimone, M., Frommer, W.B., Flügge, U.-I., and Kunze, R.** (2003). ARAMEMNON, a novel database

- for Arabidopsis integral membrane proteins. *Plant Physiol.* **131**: 16–26.
- Shibata, M., Oikawa, K., Yoshimoto, K., Kondo, M., Mano, S., Yamada, K., Hayashi, M., Sakamoto, W., Ohsumi, Y., and Nishimura, M.** (2013). Highly oxidized peroxisomes are selectively degraded via autophagy in Arabidopsis. *Plant Cell* **25**: 4967–4983.
- Slocombe, S.P., Cornah, J., Pinfield-Wells, H., Soady, K., Zhang, Q., Gilday, A., Dyer, J.M., and Graham, I.A.** (2009). Oil accumulation in leaves directed by modification of fatty acid breakdown and lipid synthesis pathways. *Plant Biotechnol. J.* **7**: 694–703.
- Spinazzola, A. et al.** (2006). MPV17 encodes an inner mitochondrial membrane protein and is mutated in infantile hepatic mitochondrial DNA depletion. *Nat. Genet.* **38**: 570–575.
- Stitt, M. and Zeeman, S.C.** (2012). Starch turnover: pathways, regulation and role in growth. *Curr. Opin. Plant Biol.* **15**: 282–292.
- Strader, L.C. and Bartel, B.** (2011). Transport and metabolism of the endogenous auxin precursor indole-3-butyric acid. *Mol Plant* **4**: 477–486.
- Strader, L.C., Culler, A.H., Cohen, J.D., and Bartel, B.** (2010). Conversion of endogenous indole-3-butyric acid to indole-3-acetic acid drives cell expansion in Arabidopsis seedlings. *Plant Physiol.* **153**: 1577–1586.
- Tamura, K., Peterson, D., Peterson, N., Stecher, G., Nei, M., and Kumar, S.** (2011). MEGA5: molecular evolutionary genetics analysis using maximum likelihood, evolutionary distance, and maximum parsimony methods. *Mol. Biol. Evol.* **28**: 2731–2739.
- Tanabe, Y., Maruyama, J.-I., Yamaoka, S., Yahagi, D., Matsuo, I., Tsutsumi, N., and Kitamoto, K.** (2011). Peroxisomes are involved in biotin biosynthesis in *Aspergillus* and Arabidopsis. *J. Biol. Chem.* **286**: 30455–30461.
- Tanaka, R., Hirashima, M., Satoh, S., and Tanaka, A.** (2003). The Arabidopsis-accelerated cell death gene ACD1 is involved in oxygenation of pheophorbide a: inhibition of the pheophorbide a oxygenase activity does not lead to the “stay-green” phenotype in Arabidopsis. *Plant Cell Physiol.* **44**: 1266–1274.
- Tanz, S.K., Castleden, I., Hooper, C.M., Vacher, M., Small, I., and Millar, H.A.** (2013). SUBA3: a database for integrating experimentation and prediction to define the SUBcellular location of proteins in Arabidopsis. *Nucleic Acids Res.* **41**: D1185–91.
- Tegeer, M.** (2014). Transporters involved in source to sink partitioning of amino acids and ureides: opportunities for crop improvement. *J. Exp. Bot.*
- Troncoso-Ponce, M.A., Cao, X., Yang, Z., and Ohlrogge, J.B.** (2013). Lipid turnover during senescence. *Plant Sci.* **205-206**: 13–19.
- Trott, A. and Morano, K.A.** (2004). SYM1 is the stress-induced *Saccharomyces cerevisiae* ortholog of the mammalian kidney disease gene Mpv17 and is required for ethanol metabolism and tolerance during heat shock. *Eukaryotic Cell* **3**: 620–631.
- Trotter, P.J., Adamson, A.L., Ghrist, A.C., Rowe, L., Scott, L.R., Sherman, M.P., Stites, N.C., Sun, Y., Tawiah-Boateng, M.A., Tibbetts, A.S., Wadington, M.C., and West, A.C.** (2005). Mitochondrial transporters involved in oleic acid utilization and glutamate metabolism in yeast. *Arch. Biochem. Biophys.* **442**: 21–32.
- Tugal, H.B., Pool, M., and Baker, A.** (1999). Arabidopsis 22-kilodalton peroxisomal membrane protein. Nucleotide sequence analysis and biochemical characterization. *Plant Physiol.* **120**: 309–320.
- Turner, J.E., Greville, K., Murphy, E.C., and Hooks, M.A.** (2005). Characterization of Arabidopsis fluoroacetate-resistant mutants reveals the principal mechanism of acetate activation for entry into the glyoxylate cycle. *J. Biol. Chem.* **280**: 2780–2787.
- Usadel, B., Bläsing, O.E., Gibon, Y., Retzlaff, K., Höhne, M., Günther, M., and Stitt, M.** (2008). Global transcript levels respond to small changes of the carbon status during progressive exhaustion of carbohydrates in Arabidopsis rosettes. *Plant Physiol.* **146**: 1834–1861.
- van der Graaff, E., Schwacke, R., Schneider, A., Desimone, M., Flügge, U.-I., and Kunze, R.** (2006). Transcription analysis of arabidopsis membrane transporters and hormone pathways during developmental and induced leaf senescence. *Plant Physiol.* **141**: 776–792.
- Van Veldhoven, P.P., Just, W.W., and Mannaerts, G.P.** (1987). Permeability of the

- peroxisomal membrane to cofactors of beta-oxidation. Evidence for the presence of a pore-forming protein. *J. Biol. Chem.* **262**: 4310–4318.
- Visser, W.F., van Roermund, C.W.T., Ijlst, L., Waterham, H.R., and Wanders, R.J.A.** (2007). Metabolite transport across the peroxisomal membrane. *Biochem. J.* **401**: 365–375.
- Watanabe, M., Balazadeh, S., Tohge, T., Erban, A., Giavalisco, P., Kopka, J., Mueller-Roeber, B., Fernie, A.R., and Hoefgen, R.** (2013). Comprehensive dissection of spatiotemporal metabolic shifts in primary, secondary, and lipid metabolism during developmental senescence in Arabidopsis. *Plant Physiol.* **162**: 1290–1310.
- Werner, A.K. and Witte, C.-P.** (2011). The biochemistry of nitrogen mobilization: purine ring catabolism. *Trends Plant Sci.* **16**: 381–387.
- Wesley, S.V. et al.** (2001). Construct design for efficient, effective and high-throughput gene silencing in plants. *Plant J.* **27**: 581–590.
- Winkler, R.G., Blevins, D.G., Polacco, J.C., and Randall, D.D.** (1987). Ureide Catabolism of Soybeans : II. Pathway of Catabolism in Intact Leaf Tissue. *Plant Physiol.* **83**: 585–591.
- Xiong, Y., Contento, A.L., Nguyen, P.Q., and Bassham, D.C.** (2007). Degradation of oxidized proteins by autophagy during oxidative stress in Arabidopsis. *Plant Physiol.* **143**: 291–299.
- Yang, Z. and Ohlrogge, J.B.** (2009). Turnover of fatty acids during natural senescence of Arabidopsis, Brachypodium, and switchgrass and in Arabidopsis beta-oxidation mutants. *Plant Physiol.* **150**: 1981–1989.
- Zimmermann, P., Hirsch-Hoffmann, M., Hennig, L., and Gruissem, W.** (2004). GENEVESTIGATOR. Arabidopsis microarray database and analysis toolbox. *Plant Physiol.* **136**: 2621–2632.
- Zolman, B.K., Monroe-Augustus, M., Thompson, B., Hawes, J.W., Krukenberg, K.A., Matsuda, S.P., and Bartel, B.** (2001a). chy1, an Arabidopsis mutant with impaired beta-oxidation, is defective in a peroxisomal beta-hydroxyisobutyryl-CoA hydrolase. *J. Biol. Chem.* **276**: 31037–31046.
- Zolman, B.K., Silva, I.D., and Bartel, B.** (2001b). The Arabidopsis pxa1 mutant is defective in an ATP-binding cassette transporter-like protein required for peroxisomal fatty acid beta-oxidation. *Plant Physiol.* **127**: 1266–1278.
- Zolman, B.K., Yoder, A., and Bartel, B.** (2000). Genetic analysis of indole-3-butyric acid responses in Arabidopsis thaliana reveals four mutant classes. *Genetics* **156**: 1323–1337.
- Zwietering, M.H., Jongenburger, I., Rombouts, F.M., and van 't Riet, K.** (1990). Modeling of the bacterial growth curve. *Appl. Environ. Microbiol.* **56**: 1875–1881.
- Zybailov, B., Rutschow, H., Friso, G., Rudella, A., Emanuelsson, O., Sun, Q., and van Wijk, K.J.** (2008). Sorting signals, N-terminal modifications and abundance of the chloroplast proteome. *PLoS ONE* **3**: e1994.

Supplemental Results

PMP22	-----	
PMP22-like	-----	
At2g14860	-----MSRALFRNV	9
At3g24570	-----	
At4g33905	-----MTGALFRNA	9
At5g43140	-----MNIVGLSKRF	10
At2g42770	-----	
At5g19750	-----MLNSI	5
At1g52870	MAAASLHTSISPRSLFPLSKPSLKPHRSQILLRNKQRCVSCALIRDEIDLIPVQSRDRT	60
At4g03410	MAAL---CCPFTTIIVSGKVSSRIKTAGPLPR-----INPFKNQKRL	39
PMP22	-----	
PMP22-like	-----	
At2g14860	AVDTARLIRRNAASTDQYGKTG-----VAQSRP-----YFR	41
At3g24570	-----	
At4g33905	ASDAARIFRLQRATMTNFFGKLDPLPIGGNIQRLQSRP-----FYR	50
At5g43140	FSDRRLSHGINNALLKTVFTGRKPILG---FSGRSIH-----ELR	47
At2g42770	-----MDALGGCGGAGGFVGWNGFDQRKKKSSG-----DRG	32
At5g19750	TLTRKPLPFFNSVGFSGNHSSSFGRRTITEGSSSKALSFGYKKNVGLKCRSNWPGRSGT	65
At1g52870	DHEEGSVVMSTETAVDGNESVVVGFSAATSEGQLSLEGFSSSSSGADLGDEKRENEE	120
At4g03410	ITERNLIVKS---IIEDREADVKNDNFKAEELSED-----KVED	78
PMP22	-----MGSSPPKKTTLQ-----RYLSLQOQH	21
PMP22-like	-----MSDLAKDAWR-----KYLIQLQAH	19
At2g14860	SRQLLERAKETGVSPSPSLGFSSSSPSRIGFVG-----WYLG MVKSH	84
At3g24570	MLKLRWYQRCLTVHPVKTQVISSGFLWGFQDVT-----AQYIHTSTAK	44
At4g33905	TPQFLGKAKETGVSGFCSSSSSSSTVSTAGFIG-----WYLG MVKSR	93
At5g43140	KTGNFVIPRVFSVRNLTTKASSSSS-KQPAFLR-----WYLRKLESH	89
At2g42770	KKRNSSGSDSDVSRDAGGYRFPKQAVTAGALT-----FTGDTIA	73
At5g19750	AFGHLVVRVSAVPGNSGGSGGLGGSGGGGGGGSDGKGGKWSLLSWYQALLSNS	125
At1g52870	MEKMDIRTNATIVLAAGSYAITKLLTIDHDYWHGWTLFEILRYAPQHNWIAYEEALKQN	180
At4g03410	TDRLMSRGINAAIVLAAGTVAVTKLLTIDHDYWGWTLYEILRYAPEHNWFAYEQILKTN	138
PMP22	PLRTRKAITAGVLSGVSDVVSQKLS--GIQKIQLRRVLLKVI FAGGFLGPAGHFFHTYLDK	79
PMP22-like	PLRTRKAITAGVLAGCSDAIAQKIS--GVKRIQFRRLLLMLYGFAYGPPGHFFHKLMDT	77
At2g14860	PVVTKSVTSSLIYAADLSSQTI AKTSSESYDLVVRTARMGGYGLFVLGPTLHYWFFMFSR	144
At3g24570	RRLRLRLTETNKDADADAEIKVKWKQDAEFKVNWRKVAITSMFGFVGFPVGHFWYEGLDK	104
At4g33905	PVLTKSVTSSLIYAADLSSQTI PQASVDSYDLVVRTARMGGYGLLILGPTLHYWFFNLMS	153
At5g43140	PFMTKSIITTSVIYMAADLTSQMITMEPTGSFDLIRTARMASFGILFGLGPSQHLWFSYLSK	149
At2g42770	QLSGRWKRTALKQSSSELDEGELWNIFSEHDWIRALRMSYGFELLYPGGSYAWYQFLDH	133
At5g19750	FVLTKAVTAALLNLVGDLICQLTIN-KTSSLDKKRLLTFFLGLGLVGPPTLHFYLYLSK	184
At1g52870	PVLAQMVISGVVYVGDWIAQCYEGKPLFEIDRARTLRSGLVGFTHLHSLSHFYQFCEE	240
At4g03410	PVLAQMAISGIVYSLGDWIAQCYEGKPLFEFDRTRVLRSLVGFTHLHSLSHYFYQFCEA	198
PMP22	FFKG-----KKTDTQVAKKIVILEQLTSLPLNHLLFMIYYGVVIERTPWTLVRERIKKTY	134
PMP22-like	IFKG-----KKGNSTVAKKIVILEQLTSSPWNNFLFMSYGLVVEGRPWKLKVKHKLKDY	132
At2g14860	LFP-----KQDLITTFKKMAMGQTIYGPIMTVIFFSLN-ASLQGERGSVILARLKRDL	197
At3g24570	FTKLKLRYVPKSTRFVAAKVAMDGLIFGPVDLLVFFTYM-GFATGKNTAEVKEGLKRDFL	163
At4g33905	LFP-----KRDLIITTFKKMAMGQTVYGPAMNVVFFSLN-AALQGENGSEIVARLKRDL	206
At5g43140	IILP-----KRDVLTTFKKIMMGQVLFQPVSNVFFYSYN-AALQGENSEIVARLKRDL	202
At2g42770	SLP-----KPTATNLVLKVLNQLVILGSPVIAVIFAWN--NLWLKGLSELGNKYQKDAL	185
At5g19750	VVT-----ASGLSGAVIRLLDQFVFAPIFVGVFLSAV-VTLEGKP-SNVIPKLQOEW	236
At1g52870	LFP-----FDQWVVPKVAFDQTVWSAIWNSIYFTVL-GFLRFESPISIFKELKATFL	293
At4g03410	LFP-----FQEWVVPKVAFDQTVWSAIWNSIYFTVL-GLLRFQSPADIFSEIKTFL	251
PMP22	TVQLTAWTFFFPVGVWVINYKIVPLHFRVILHSLVAFFWGFIFLTLRARSMTLALAKA	190
PMP22-like	TIQLTAWKFWPIVGVWVNYQYVPLQFRVLFSSFVASCWSIFLNLKARSPVIGN	184
At2g14860	PALFNGVMYWPLCDFITFRFPVHLQPLVSNFSYVWTIYMTYMANREKPVIAIST	252
At3g24570	PALALEGGAWPLLQIANFRYVPVQYQLLYNIFCLVDSAFLSWVEQQDAAWKQWFTSSF	223
At4g33905	PTMLNGVMYWPLCDFITFKFCPVYLQPLVSNFSYLTWITITYMASRATPTAIEI	261
At5g43140	PTLKNGLMYWVPCDFVTFKYVPVHLQPLMNSSCAYIWTIYLTYMANQTKADS	254
At2g42770	PTLLYGFREFVFPVSIILNFWVPLQARVAFMSGVSVFVNFYLSSTMSK	232
At5g19750	GAMIANWQLWIPFQFLNFRFVPQNYQVLASNVALAWNVLISFAHKEVVAK	287
At1g52870	PMLTVG---SFGHLI-----	306
At4g03410	PMLTAGWKLWPLAHLVTYGIVPDQRLWVDCIELIWTILSTYSNEKAEQAASETNS	311
PMP22	-----	
PMP22-like	-----	
At2g14860	-----	
At3g24570	QPLKERGGQGV	235
At4g33905	-----	
At5g43140	-----	
At2g42770	-----	
At5g19750	-----	
At1g52870	-----	
At4g03410	SHSSED-----	317

FIGURE S1. Pairwise ClustalW2 multiple sequence alignment of *A. thaliana* PMP22-type family proteins. Predicted membrane spanning regions were underlined (*Tm consens*, Schwacke et al. 2003). Asterisks mark highly conserved amino acid positions.

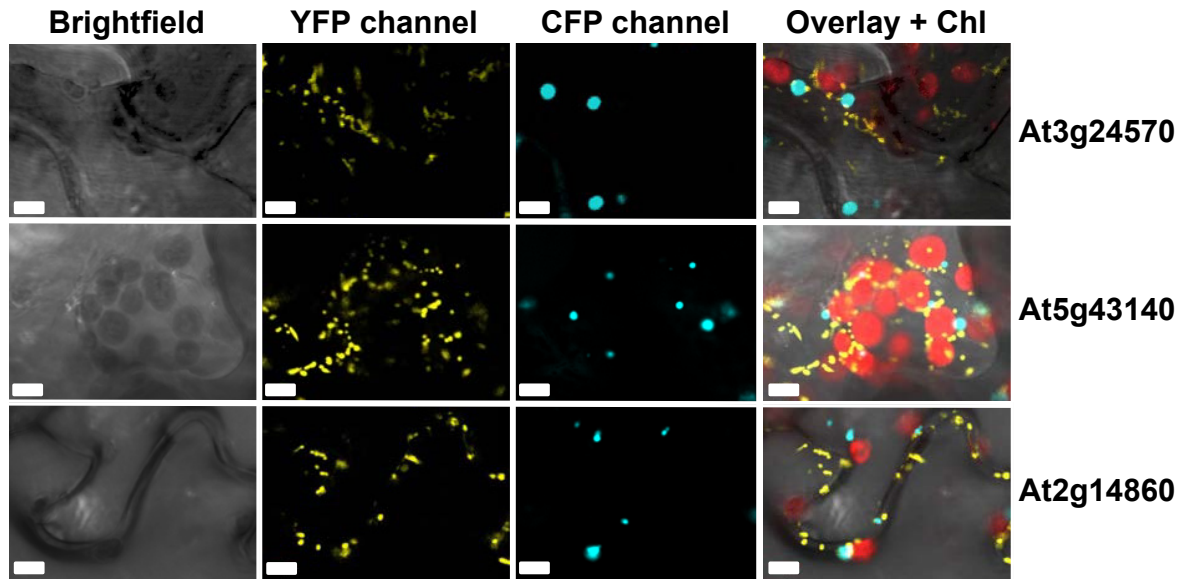


FIGURE S2. Microscopy images showing extraperoxisomal localization of YFP fused mitochondria predicted PMP22-type family proteins encoded by At3g25570, At5g43140 and At2g14860. YFP fusion proteins display punctate fluorescence signals (C-terminus masked by EYFP) that did not colocalize with the peroxisome CFP-PTS1 marker (Linka et al. 2008). Confocal images were taken from epidermis cells of 4-week-old tobacco leaves co-expressing the peroxisomal marker and target gene-EYFP fusion proteins. Scale bar: 5 μ m.

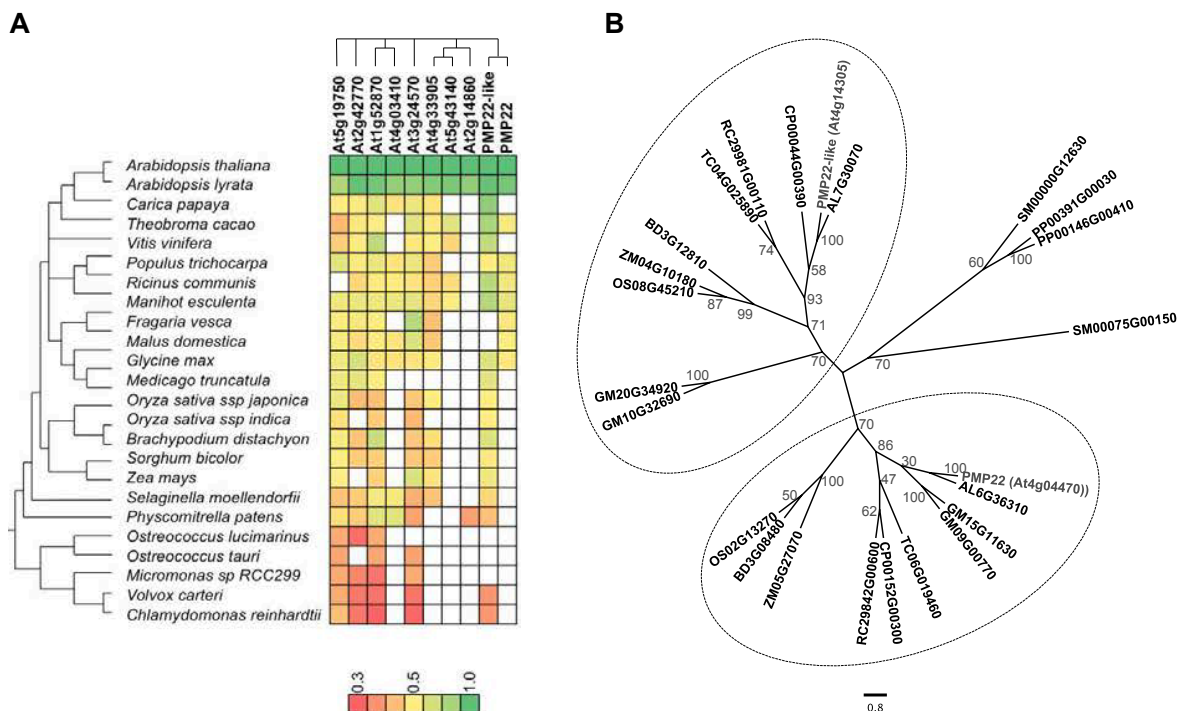


FIGURE S3. Analysis of PMP22-type sequence conservation in selected plant proteomes.

(A) Reciprocal BLASTP analysis of PMP22-type family protein in proteomes of sequenced plants and algae downloaded from the PLAZA website (<http://bioinformatics.psb.ugent.be/plaza/>; Proost et al. 2009). Primary sequence similarity of positive reciprocal best blast hits is represented by a colored field, which follows the indicated code.

(B) Neighbour joining tree of the two best BLASTP hits of PMP22 and PMP22-like in *Physcomitrella patens*, *Selaginella moellendorffii*, *Oryza sativa*, *Brachypodium distachyon*, *Zea mays*, *Ricinus communis*, *Carica papaya*, *Theobroma cacao*, *Glycine max* and *Arabidopsis lyrata*. PMP22 and PMP22-like clades are marked by dashed circles. Node labels represent bootstrap values.

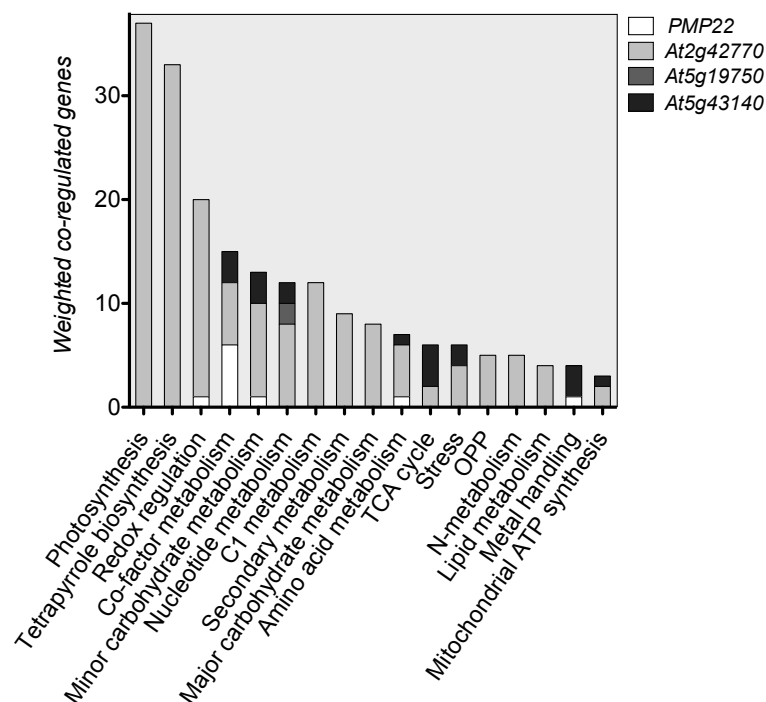


FIGURE S4. Co-regulation categories of Arabidopsis PMP22-type genes PMP22 (At4g04470), At2g42770, At5g19750 and At5g43140. Data was downloaded from the AthCoR@CSB.DB database (Steinhauser et al., 2004). OPPP: oxidative pentose-phosphate pathway; TCA: tricarboxylic acid

FIGURE S5 (next page). Purification and structure analysis by CD-spectroscopy of recombinant PMP22-His in DDM micelles and PMP22-His proteoliposome flotation assay.

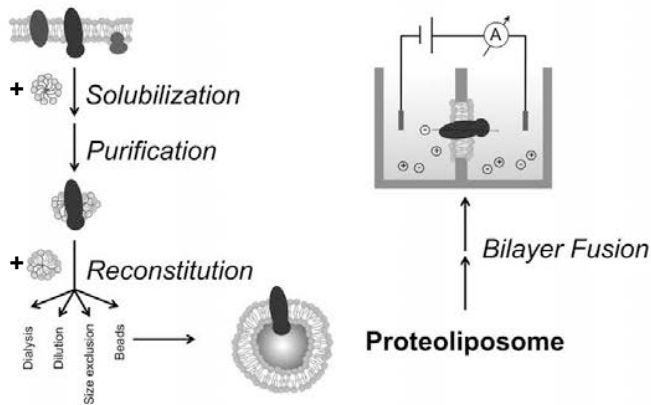
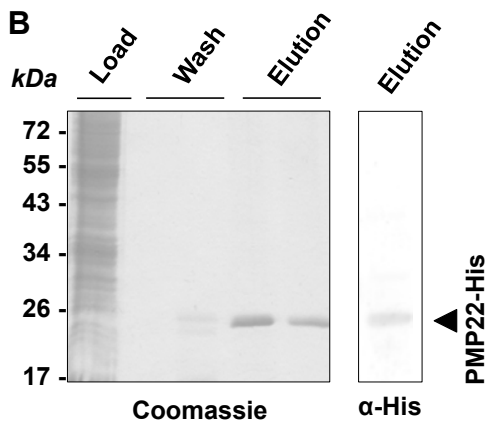
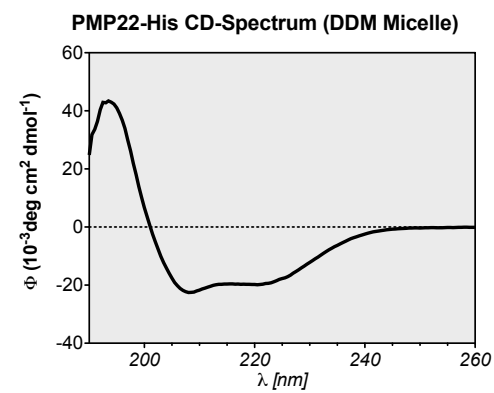
(A) Workflow of purification and setup of planar lipid bilayer measurements. Detergent treatment solubilizes membrane proteins from native membranes and enables affinity chromatographic isolation of proteins. Purified proteins are reconstituted in small unilamellar vesicles by dialysis, dilution, size-exclusion chromatography or bead addition to minimize interference of detergent in planar lipid bilayer experiments. Proteoliposomes are added to a lipid-bilayer separated measurement chamber and fused to the artificial lipid-bilayer. Electrophysiological properties can be determined upon fusion of the liposomes to the bilayer membrane.

(B) Coomassie stained SDS-PAGE analysis of PMP22-His FPLC purification from DDM solubilized *S. cerevisiae* FGY217 membranes (*load*). Non-specifically bound protein was washed from the Ni-NTA matrix with up to 100 mM imidazole (*wash*). PMP22-His eluted at high purity from the columns with a concentration of 250 mM imidazole in the buffer (*elution*). Hexahistidine-tag specific antiserum confirmed the predominant protein in the eluate to be full length PMP22-His. PMP22-His degradation were not observed.

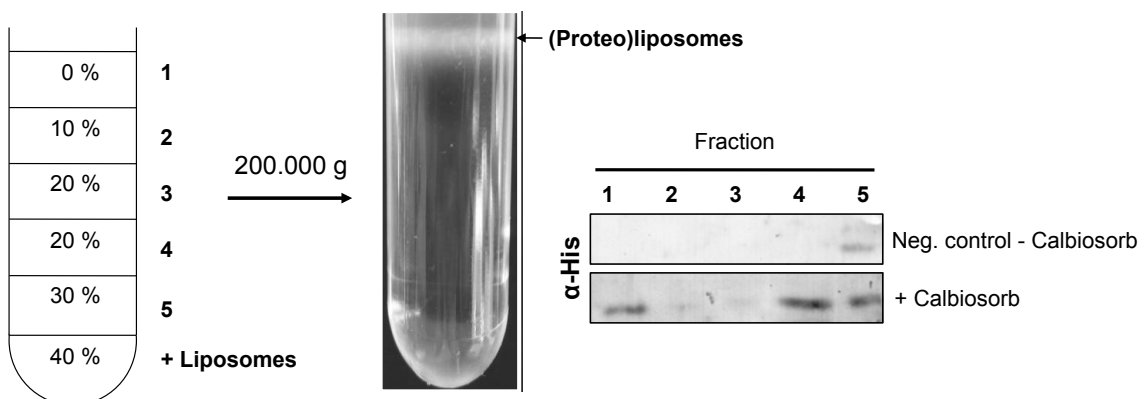
(C) Far-UV circular dichroism (CD) spectrum of PMP22-His in DDM micelles (in 10 mM Tris-NaOH (pH 8), 500 mM $(\text{NH}_4)_2\text{SO}_4$, 0.1 % (w/v) DDM). The background spectrum of the buffer was subtracted.

(D) CD spectrum analysis revealed a predominantly α -helical conformation of PMP22-His in DDM micelles.

(E) Nycodenz gradient flotation analysis to verify successful incorporation of PMP22-His into proteoliposomes by Calbisorb detergent removal. Calbisorb detergent removal originated (PMP22-His Proteo-)Liposomes were mixed with 80% Nycodenz and a step gradient with decreasing Nycodenz concentration was prepared on top. Upon centrifugation a turbid ring was observed at the interphase between 0 and 10% Nycodenz. Proteins in the fractions were precipitated and subjected to immunoblot analysis, showing that the addition of Calbisorbs leads to detection of PMP22-His in the liposome fraction. As negative control detergent solubilized protein and mixed Triton-X-100 phosphatidylcholine micelles were incubated in the absence of Calbisorbs: upon density gradient centrifugation PMP22-His was not found in the upper fraction.

A native membrane**Single channel recording****B****C****D****PMP22-His Far UV Circular-Dichroism spectrum analysis**

α -helix	β -strand	Reference
87.59 %	0.48 %	Perez-Iratxeta and Andrade-Navarro et al. 2008
56.14 %	6.05 %	Louis-Jeune et al. 2011
44.1 %	7.5 %	Raussens et al. 2003

E

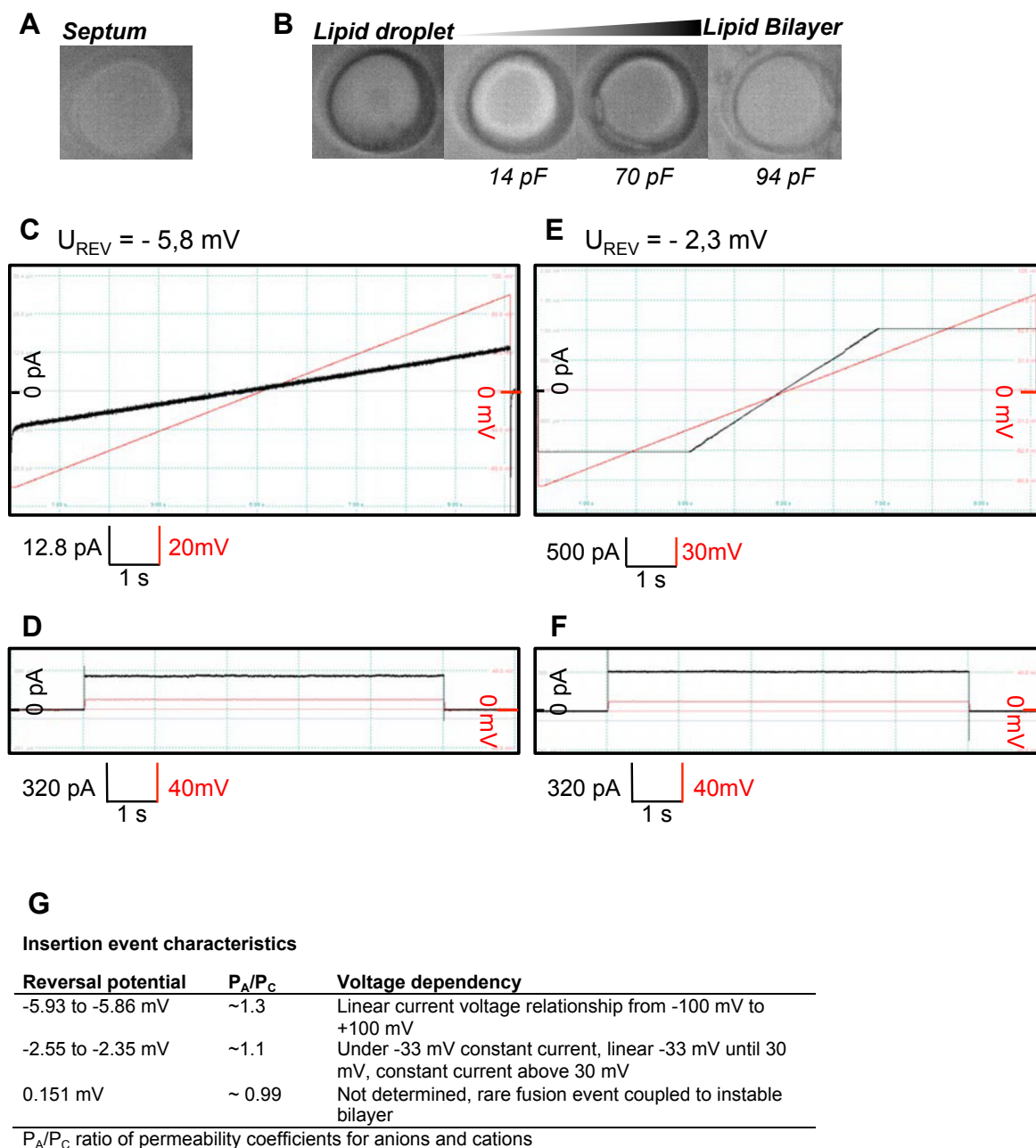


FIGURE S6. Electrophysiological characterization of planar lipid bilayer incorporated PMP22-His. **(A)** Image of the septum (approximately 100 μ m) in a polytetrafluorethylene foil of an Ionovation compact lipid bilayer measurement chamber in an aqueous environment. **(B)** Images of the process of lipid bilayer formation in the Ionovation compact system. Organic solvent dissolved lipid was applied to the septum with a Hamilton syringe. Subsequent lifting and lowering of the buffer level led to reduction of the annulus surrounding the bilayer. A bilayer suitable for electrophysiological analysis had a capacitance above 30 pF. **(C)/(E)** Current vs. voltage plots of single insertion events after addition of PMP22-His proteoliposomes. PMP22-His incubation led to two measureable channel activities (left panel and right panel). The reversal potential (U_{REV}) of the activity is indicated above the plot. **(D)/(F)** Recordings of the above-described insertion events at 0 and 10 mV holding potential. Recordings were performed at asymmetric electrolyte solution conditions (250 mM KCl in *cis* and 20 mM KCl in *trans*). **(G)** Description of the insertions events upon addition of PMP22-His proteoliposomes to the lipid bilayer. P_A/P_C ratio of anion over cation permeability coefficient.

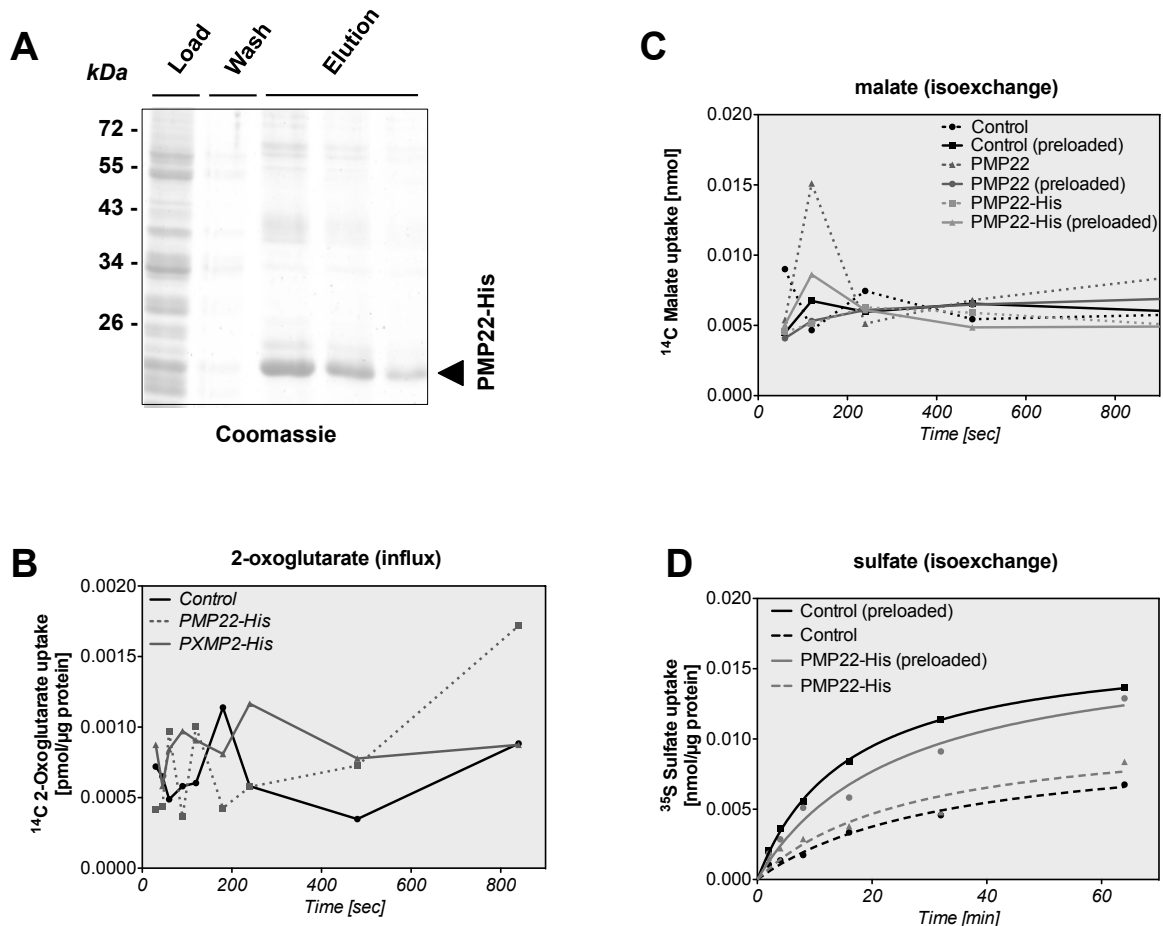


FIGURE S7. *In vitro* PMP22-His transport assays with radiolabeled 2-oxoglutarate, malate and sulfate. **(A)** Coomassie stained SDS-PAGE analysis of PMP22-His by Ni-NTA batch purification upon Brij-35 solubilization. Wheat germ extract expressed protein (*Load*) was bound to Ni-NTA beads, unspecifically bound protein was removed by washing with 100 mM imidazole (*Wash*) and PMP22-His was eluted with 250 mM imidazole (*Elution*). The enriched PMP22 protein was subsequently integrated in liposomes by detergent dilution and freeze-thaw cycling. **(B)** Influx studies of ^{14}C -labelled 2-Oxoglutarate in the 4 mM in the extraliposomal medium into PMP22-His or PXMP2 proteoliposomes. Ni-NTA was purified from Wheat germ extract expressed protein. As control IMAC purified wheat germ extract incubated with the empty vector was reconstituted as well as Wheat germ extract purified PXMP2. **(C)** ^{14}C Malate antiport studies with 30 mM malate inside liposomes and 300 μM malate in the outside medium. Protein derived from desalted wheat germ extracts. **(D)** ^{35}S sulfate antiport studies with 20 mM sulfate inside liposomes and 1 mM sulfate in the outside medium. Proteoliposomes were produced from yeast membrane (FGY217) isolations.

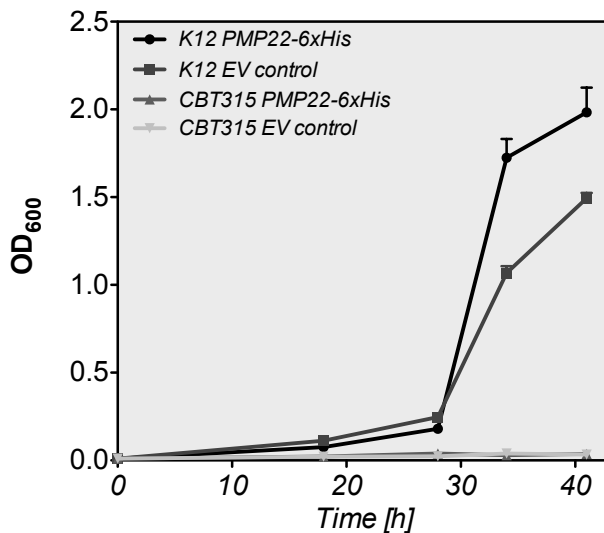


FIGURE S8. Plot of *E. coli* CBT315 growth in M9 minimal medium with malate (2% w/v) as sole carbon source. The CBT315 strain is unable to grow in the medium. The wild-type strain (K12) grew, the derivative CBT315 strain did neither grow with the PMP22-His expression vector nor when transformed with the empty vector (EV control). PMP22-His expression was induced in the cells by addition of 1mM IPTG.

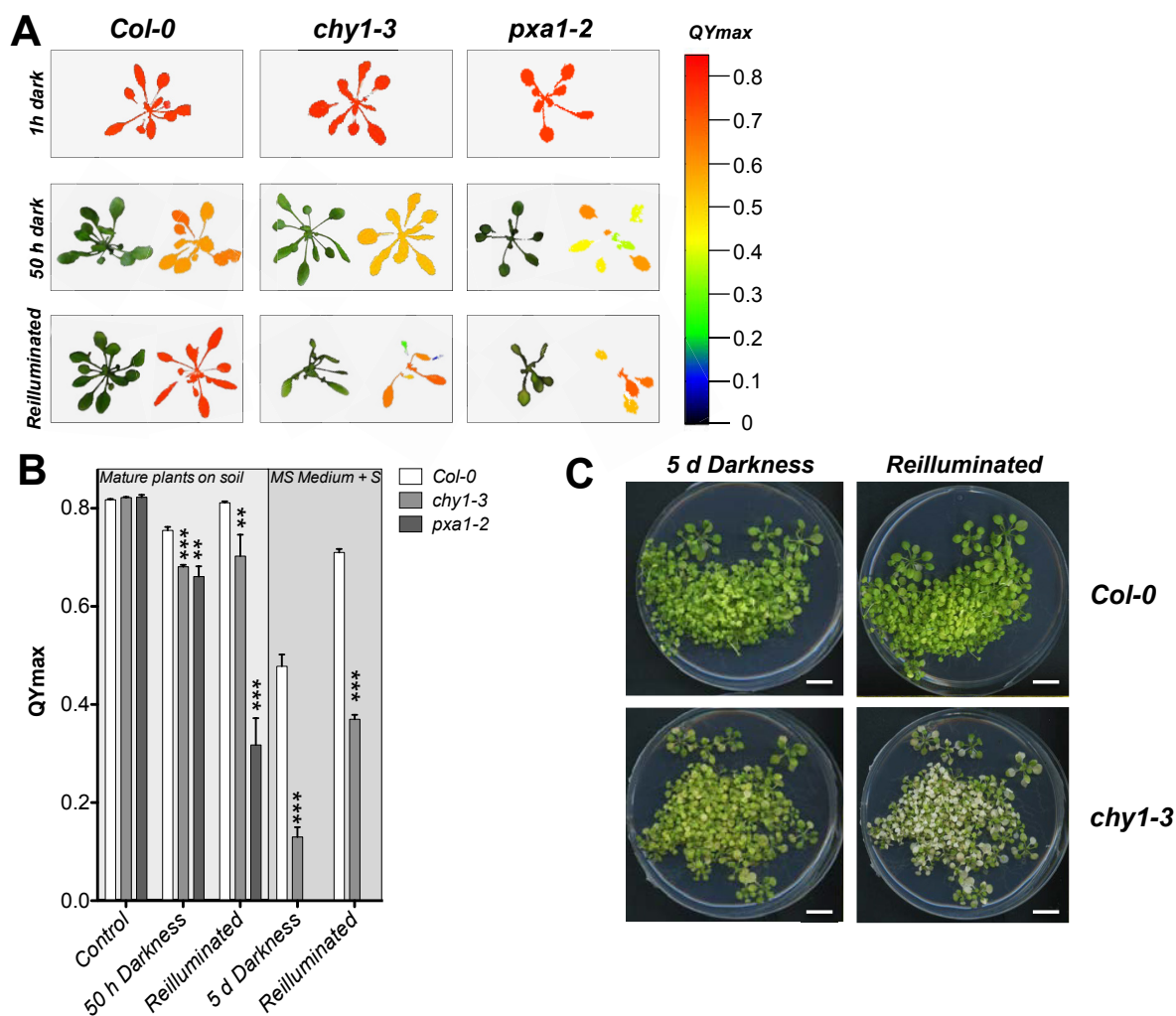


FIGURE S9. Morphology and PSII electron transport of *Col-0*, *chy1-3* and *pxa1-2* in extended darkness and reillumination.

(A) Photograph and false color images representing maximum quantum yield (QYmax) of 3-week-old *Col-0*, *chy1-3* and *pxa1-2* after the indicated duration of darkness exposure and 50 h darkness followed by 24 h reillumination.

(B) Mean of maximum quantum yield (+SE; $n = 3$) of three-week-old *Col-0*, *chy1-3* and *pxa1-2* subjected to 1 h, 50 h of darkness and 10 h reillumination after 50 h darkness. Differences between the mean of biological replicates were marked as statistically significant (t-test) with the *Col-0* control by (*), (**) or (***) at respective significance levels of ($P < 0.05$), ($P < 0.01$) or ($P < 0.001$).

(C) Photograph of 14-d-old *Col-0* and *chy1-3* in half strength MS medium with 1% (w/v) sucrose incubated for five days in the dark and reilluminated for 10 h.

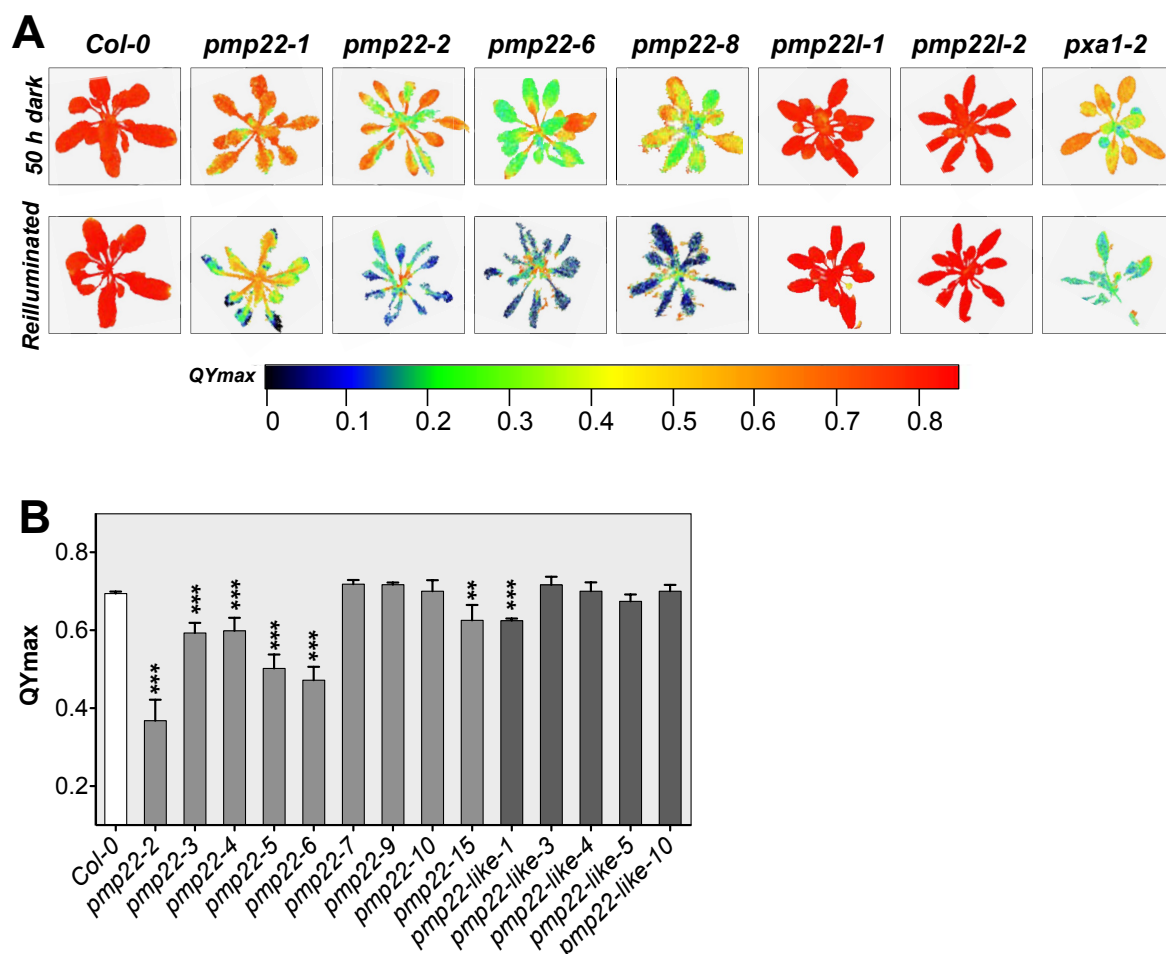


FIGURE S10. Photosystem II electron transport monitored by chlorophyll fluorescence in *Col-0*, *pmp22* and *pmp22-like* after dark treatment.

(A) False color image representing maximum quantum yield (QYmax) of *Col-0*, *pmp22*, *pmp22-like* and *pxa1-2* in response to darkness (50 h) and 24 h reillumination after 50 h darkness.

(B) Mean of maximum quantum yield (+SE; n>15) of 10-day-old *Col-0*, *pmp22* and *pmp22-like* subjected to 6 days of darkness. Differences between the mean (+SE; n>3) of at least three biological replicates were marked as statistically significant (t-test) with the *Col-0* control by (*), (**) or (***) at respective significance levels of (P < 0.05), (P < 0.01) or (P < 0.001).

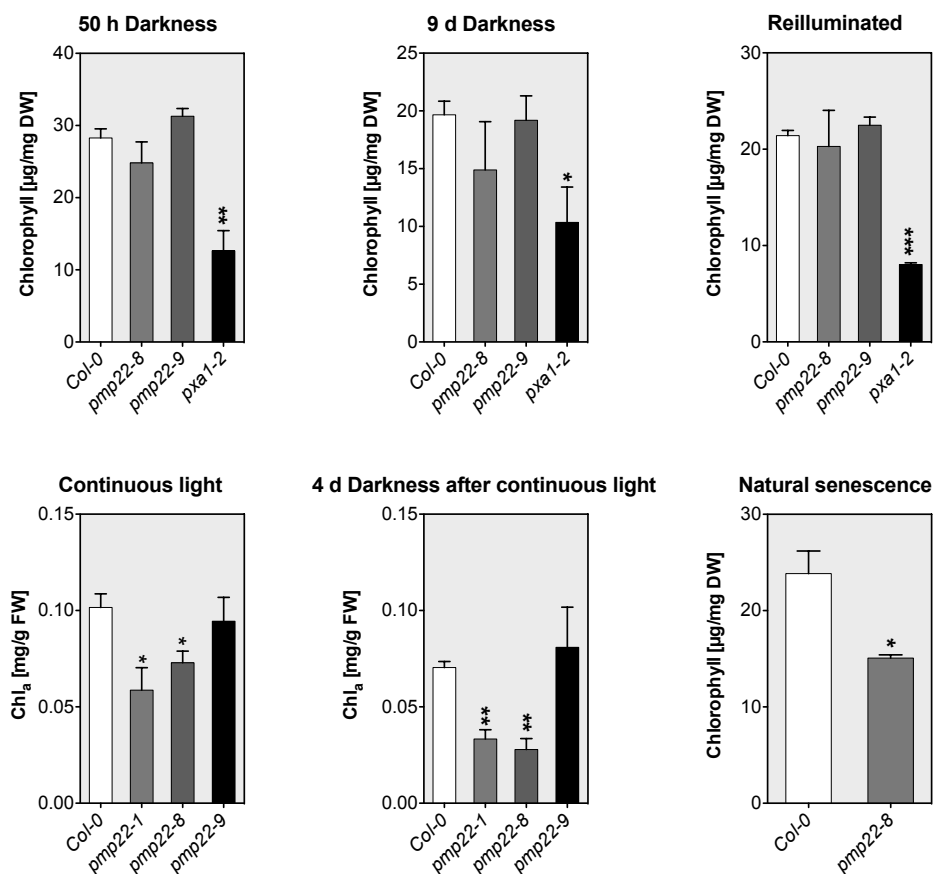


Figure S11. Mean chlorophyll concentration (+SE; $n = 3$) of 3-week-old and 9-week-old (Natural senescence) *Col-0*, *pmp22-1*, *pmp22-8*, *pmp22-9* and *pxa1-2* after exposure to darkness. Differences between the mean (SE) of three biological replicates were marked as statistically significant (t-test) with the *Col-0* control by (*), (**) or (***) at respective significance levels of ($P < 0.05$), ($P < 0.01$) or ($P < 0.001$).

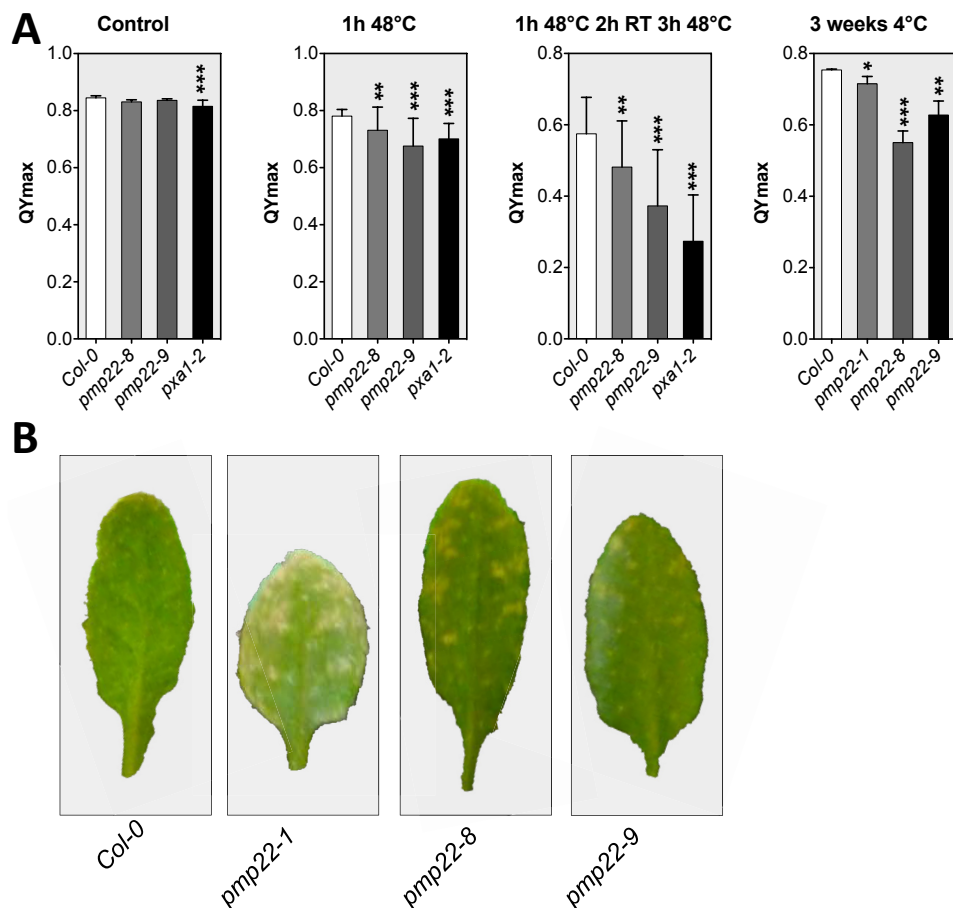


FIGURE S12. Photosystem II electron transport monitored by chlorophyll fluorescence and leaf morphology in *Col-0*, *pmp22-1*, *pmp22-8*, *pmp22-9* and *pxa1-2* after changes in the temperature.

(A) Mean of maximum quantum yield (+SE, $n = 4$) of *Col-0*, *pmp22-1*, *pmp22-8*, *pmp22-9* and *pxa1-2* after heat or cold treatment. Differences between the mean (SE) of at least three biological replicates were marked as statistically significant (t-test) with the *Col-0* control by (*), (**) or (***) at respective significance levels of ($P < 0.05$), ($P < 0.01$) or ($P < 0.001$).

(B) Photograph of leaves 24 h after application of last heat stress (1 h 48°C, 2 h RT, 3 h 48°C). Necrotic lesions were visible.

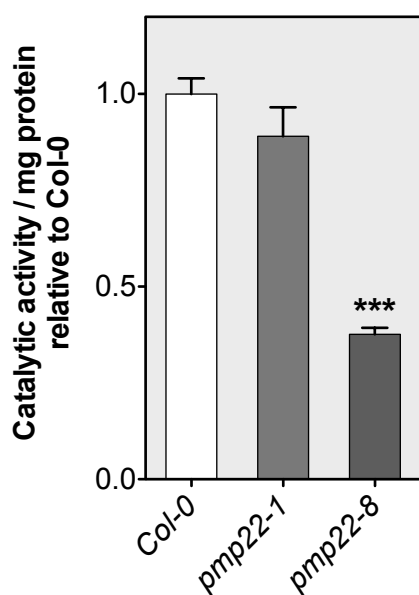


FIGURE S13. Mean glycolate oxidase activity (+SE, $n = 3$) relative to the *Col-0* control of *pmp22-1* and *pmp22-8*. Protein was extracted from 6-d-old seedlings. Differences between the mean (SE) of three biological replicates were marked as statistically significant (t-test) with the *Col-0* or 0 μ M control by (*), (**) or (***) at respective significance levels of ($P < 0.05$), ($P < 0.01$) or ($P < 0.001$).

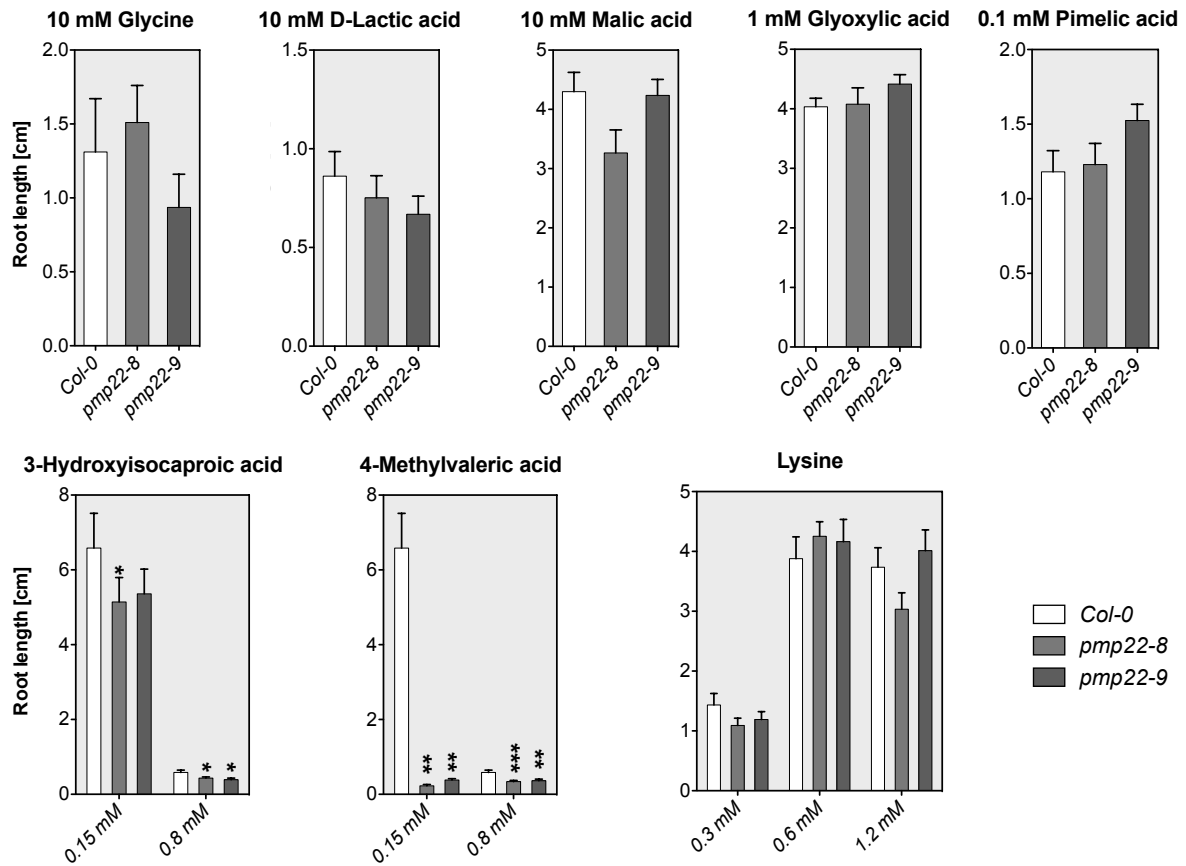


FIGURE S14. Mean root length (+SE, $n > 15$) of 17-d-old *Col-0*, *pmp22-8* and *pmp22-9* grown in short-day conditions transferred (5 days after radicle emergence) to half strength MS medium supplemented with the indicated amount of glycine, lactic acid, malic acid, glyoxylic acid, pimelic acid, 3-hydroxyisocaproic acid, 4-methylvaleric acid and lysine. Differences between the mean (SE) of three biological replicates were marked as statistically significant (t-test) with the *Col-0* control by (*), (**) or (***) at respective significance levels of ($P < 0.05$), ($P < 0.01$) or ($P < 0.001$).

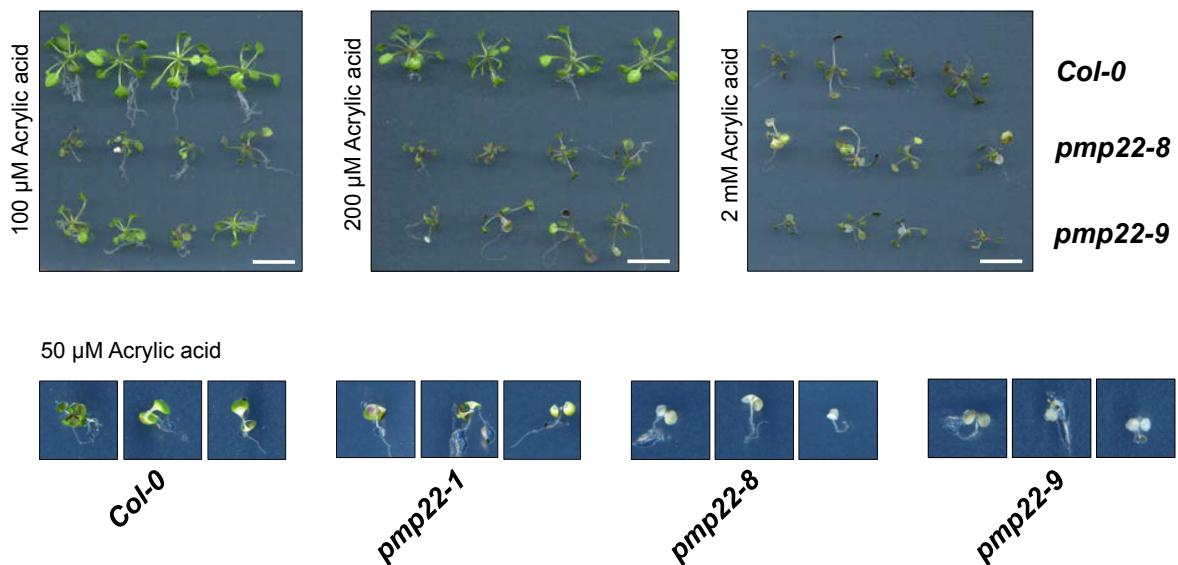


FIGURE S15. Photographs of 14-day-old *Col-0*, *pmp22-1*, *pmp22-8* and *pmp22-9* grown in short day conditions transferred (5 days after radicle emergence) to half strength MS medium supplemented with the indicated amount of acrylic acid (upper panel) or seven-day-old seedling germinated on half strength MS medium with 50 μ M acrylic acid (lower panel). Scale bar: 10 mm.

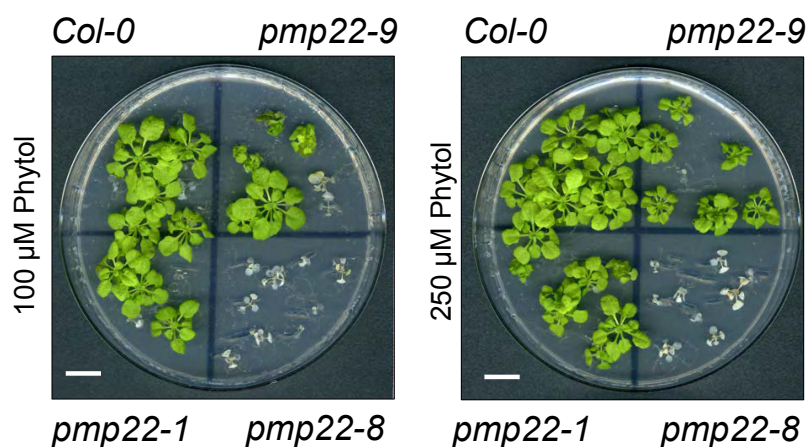
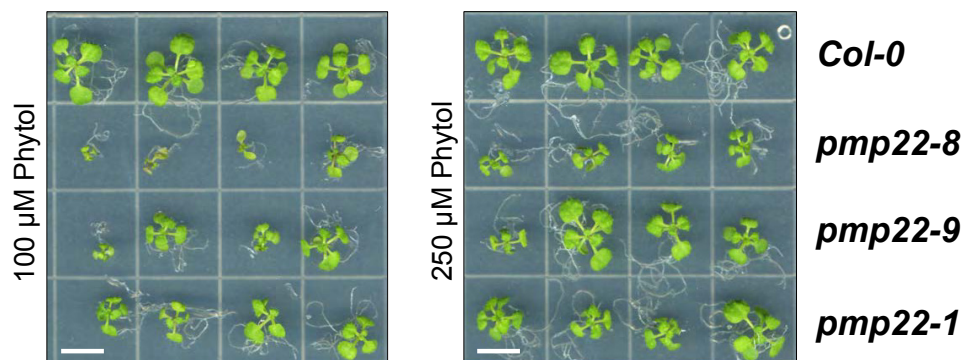


FIGURE S16. Photographs of 12-day-old (upper panel) and 24-day-old *Col-0*, *pmp22-1*, *pmp22-8* and *pmp22-9* transferred (5 days after radicle emergence) to half strength MS medium supplemented with the indicated amount of Phytol in 0.25 % ethanol. Scale bar: 10 mm.

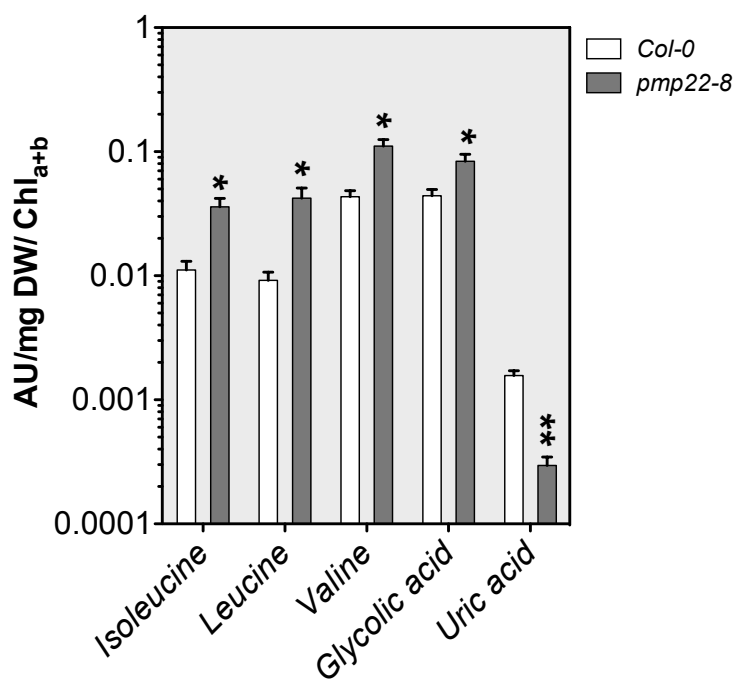


FIGURE S17. Mean levels (+SE; n =3) of isoleucine, leucine, valine, glycolic acid and uric acid in natural senescent leaves of *Col-0* and *pmp22-8*. Leaf extracts of 9-week-old plants were subjected to GC-MS analysis for metabolite quantification. The data is shown in an arbitrary unit normalized to mg dry weight. Chlorophyll_{a+b} contents were used to normalize biological replicates. Differences between the mean (SE) of three biological replicates were marked as statistically significant (t-test) with the SYM1 control by (*), (**) or (***) at respective significance levels of (P < 0.05), (P < 0.01) or (P < 0.001).

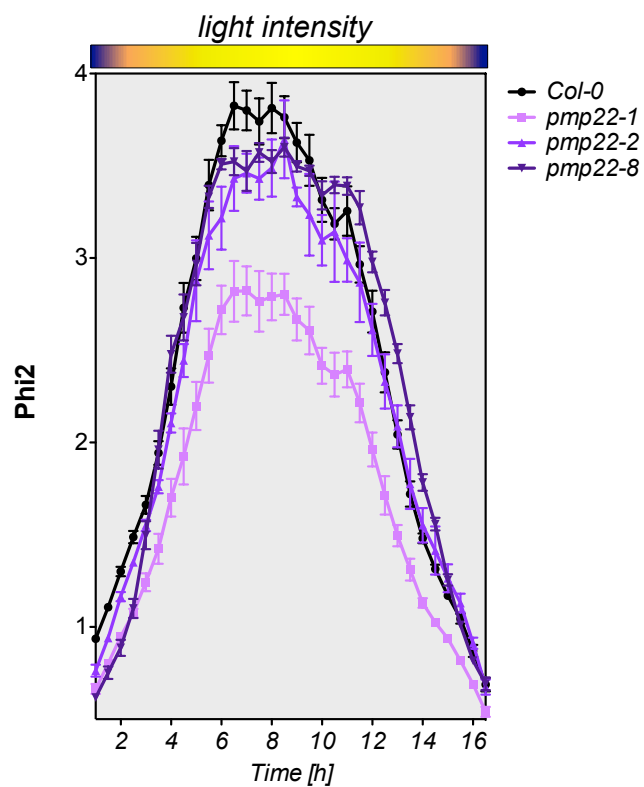


FIGURE S18. Photosynthetic capacity of *Col-0*, *pmp22-1*, *pmp22-2* and *pmp22-8* monitored by chlorophyll fluorescence (photochemical quantum yield, Phi2) with light intensity of a simulated natural day (highest light intensity by midday).

Supplemented Material

TABLE S1. Oligonucleotides used in this study.

Name		Sequence (5'→3')	Target [Purpose]
Cloning			
JW1	F	GGGGACAAGTTTGTACAAAAAAGCAGGCTTCGAAG GAGATAGAACCATGGGATCTTCACCACCGA	PMP22 (At4g04470) CDS (GW)
JW2	R	GGGGACCACTTTGTACAAGAAAGCTGGGTCTTAGC CTTTGCCAAAGCTAGTG	PMP22 (At4g04470) CDS w/o STOP (GW) [C-terminal fusion to (split)YFP, His or HA tag]
JW3	R	GGGGACCACTTTGTACAAGAAAGCTGGGTCTACTT AGCCTTTGCCAAAGCTAGTG	PMP22 (At4g04470) CDS w/ STOP (GW) [N-terminal (split)YFP fusion, protein expression]
NL425	F	CACACAAGCTTACCATGGGATCTTCACCACCGAAG	PMP22 (At4g04470) CDS
NL411	R	CACACGGATCCCTTAGCCTTTGCCAAAGCTAGTG	[Inducible Yeast expression with C-terminal His-tag]
JW39	F	NNNCGCGGCCGCATGGGATCTTCACCACCGA	PMP22 (At4g04470) CDS [Constitutive Yeast expression amplified from pIVEX1.3::PMP22-His]
NL408	F	CACACATGGGATCTTCACCACCGAAG	PMP22 (At4g04470) CDS w/ STOP [Wheat germ extract expression]
NL450	R	CACACGAGCTCTCACTTAGCCTTTGCCAAAGCT	
NL408	F	CACACACCATGGGATCTTCACCACCGAAG	PMP22 (At4g04470) CDS w/o STOP [Wheat germ extract expression with C-terminal His tag]
NL411	R	CACACGGATCCCTTAGCCTTTGCCAAAGCTAGTG	
JW44	F	NNNCTCGAGATGGGATCTTCACCACCGA	
JW71	R	NNNAGATCTTTAATGATGATGATGATGATGCTGC TGCCTTAGCCTTTGCCAAAGCTAGTG	PMP22 (At4g04470) CDS [E. coli expression with C-terminal His-tag]
JW4	F	GGGGACAAGTTTGTACAAAAAAGCAGGCTTCGAAG GAGATAGAACCATGGCGGATCTTGCTAAAGACGC	Cloning of PMP22-like (At4g14305) CDS (GW)
JW5	R	GGGGACCACTTTGTACAAGAAAGCTGGGTCCGCGT TTTTGATCACCGG	Cloning of PMP22-like (At4g14305) CDS w/o STOP [C-terminal fusion to (split)YFP, His or HA tag] (GW)
JW6	R	GGGGACCACTTTGTACAAGAAAGCTGGGTCTACG CGTTTTGATCACCGG	Cloning of PMP22-like (At4g14305) CDS w/ STOP [N-terminal (split)YFP fusion] (GW)
JW7	F	NNNCCATGGCACCTGCGCGTCC	Cloning of <i>Mus musculus</i> Pxpmp2 CDS
JW9	R	NNNCCGGGGCTACTTCCCCAGAGACGCCAGGT	[Wheat germ extract expression]
JW10	F	GGGGACAAGTTTGTACAAAAAAGCAGGCTTCGAAG GAGATAGAACCATGGTGAAGCTTTGGAGATGGTAC	Cloning of At3g24570 CDS w/o STOP [C-terminal fusion to YFP, Yeast expression] (GW)
JW11	R	GGGGACCACTTTGTACAAGAAAGCTGGGTCTACTCC GCCTTGGCCAC	
JW96	F	GGGGACAAGTTTGTACAAAAAAGCAGGCTTCGAAG GAGATAGAACCATGAGCAGAGCATTGTTCAAG	Cloning of At2g14860 w/o STOP [C-terminal fusion to YFP] (GW)
JW97	R	GGGGACCACTTTGTACAAGAAAGCTGGGTCCGTTG AAATTGCGACTGGTT	
JW100	F	GGGGACAAGTTTGTACAAAAAAGCAGGCTTCGAAG GAGATAGAACCATGAATATCGTTGGATTGAGCA	Cloning of At5g43140 w/o STOP [C-terminal fusion to YFP] (GW)
JW101	R	GGGGACCACTTTGTACAAGAAAGCTGGGTCCGCTGT CAGCTTTCGTCTGGT	
JW102	F	GGGACAAGTTTGTACAAAAAAGCAGGCTTCGAAGGA GATAGAACCATGAAGTTATTGCATTTATATGAAGCG	Cloning of SYM1 (YLR251W) w/o STOP [Yeast expression] (GW)
JW103	R	GGGGACCACTTTGTACAAGAAAGCTGGGTCTTCGAC CACGGGTGGATAAT	
JW37	F	tcgaAGCTTACCATGGCGACGAGAACGGAATCGAAGA AGCAGATTCCGCCGGAGCTGTCGACTCTCGAG	MSFC1 (At5g01340) mitochondrial targeting peptide adapter ligated into <i>Xho</i> I site of pDR195
JW38	R	tcgaCTCGAGAGTGCAGCTCCGGCGGAATCTGCTT CTTCGATTCCGTTCTCGTCCCATGGTAAGCT	
miRNA cloning			
NL412	F	gaTAATGCGACCAGGCTGTCCAActctctttgtattcca	PMP22 (At4g04470) I miR-s
NL413	R	agTTGGACAGCCTGGTCCGATTAtcaaagagaatcaatga	PMP22 (At4g04470) II miR-a
NL414	F	agTTAGACAGCCTGGACGCATTTcacaggtcgtgatatg	PMP22 (At4g04470) III miR*s
NL415	R	gaAAATGCGTCCAGGCTGTCTAAactacatatattccta	PMP22 (At4g04470) IV miR*a
NL416	F	gaTACATACTGATAAATTAGCCCActctctttgtattcca	PMP22-like (At4g14305) I miR-s
NL417	R	agTGGGCTAATTATCAGTATGTAtcaaagagaatcaatga	PMP22-like (At4g14305) II miR-a
NL418	F	agTGAGCTAATTATCTGTATGTTTcacaggtcgtgatatg	PMP22-like (At4g14305) III miR*s
NL419	R	gaAACATACAGATAAATTAGCTCAactacatatattccta	PMP22-like (At4g14305) IV miR*a
Genotyping & (quantitative) RT PCR			
P46	R	TGGTTCACGTAGTGGGCCATCG	SALK T-DNA Left border (LBa1)
JW31	R	CCCATTGGACGTGAATGTAGACAC	GABI_KAT T-DNA Left border
JW131	F	CTCCTGTGACGGTTTTTGGT	<i>pmp22-1</i> SALK_205443 gene specific
JW132	R	ACCACCGGGAAAAACTGTGA	
JW124	F	GTATGGCTTTGCTTATGGAGG	<i>pmp22-like-1</i> GABI380B12 gene specific
JW125	R	CCATGCGGTTAACTGGATAG	
NL452	F	GAGAGACTGCAATGTTTCTGTGA	<i>pmp22-like-2</i> SALK_052641C gene specific
NL453	R	TTTTTCAGGCGATCACTGC	
P67	F	TTCAATGTCCCTGCCATGTA	At5g09810 cDNA/gDNA positive control gDNA test /
P68	R	TGAACATCGATGGACCTGA	RT-PCR

JW69	F	GTGAAAACGTGTTGGAGAGAAGCAA	qPCR transcript normalization ("BLACK" Czechowski et al. 2005)
JW70	R	TCAACTGGATACCCTTTTCGCA	
JW78	F	AGTTAAAGCAAATCAAACAGCTCTG	PMP22 (At4g04470) 3'UTR (q)RT-PCR
JW79	R	CCCTCGTTTTTATATGATGTTTGTG	
JW89	F	GGAGGAAACAAGAATGGATCTC	PMP22-like (At4g14305) 3'UTR (q)RT-PCR
JW90	R	CGTAATTGTGAGAGACTGCAATG	

Abbreviations: F: forward (sense) primer; GW: Gateway; R: reverse (antisense) primer;

TABLE S2. *Escherichia coli*, *Agrobacterium tumefaciens* and *Saccharomyces cerevisiae* strains used in this study.

Strain	Genotype	Purpose	Reference
<i>E. coli</i> MACH1-T1R	F- Φ 80lacZ Δ M15 Δ lacX74 hsdR(rK-, mK+) Δ recA1398 endA1 tonA	Cloning	Invitrogen Life Technologies
<i>E. coli</i> ccdB survival 2 TI ^R	F- mcrA Δ (mrr-hsdRMS- mcrBC) Φ 80lacZ Δ M15 Δ lacX 74 recA1 ara Δ 139 Δ (ara- leu)7697galU galK rpsL (StrR) endA1 nupG fhu2::IS2	Cloning (Gateway vector propagation)	Invitrogen Life Technologies
<i>E. coli</i> K12	Wild type	Complementation assay (Control)	Bachmann, 1972; Lee et al., 2008
<i>E. coli</i> CBT 315	sdh-2, λ -, rpsL129(strR), dctA5, thi-1	Complementation assay	Lo et al., 1972; Lee et al., 2008
<i>A. tumefaciens</i> GV3101 pMP90	C58 Rif ^R , pMP90 (pTic58 Δ T-DNA, Gent ^R)	T-DNA transfer	Koncz and Schell, 1986
<i>S. cerevisiae</i> BY4741	<i>Mat a his3Δ leu2Δ met15Δ ura3Δ</i>	Complementation assay (Control)	Euroscarf
<i>S. cerevisiae</i> <i>sym1Δ</i>	<i>BY4741; Mat a his3Δ leu2Δ met15Δ ura3Δ YLR251w::kanMX4</i>	Complementation assay	Euroscarf
<i>S. cerevisiae</i> FGY217	<i>MATα ura3-52 lys2Δ201 pep4Δ</i>	Protein Expression	Kota et al. 2007

Supplemented Methods

SDS-PAGE and immunoblot protein sample analysis

Protein gel electrophoresis and Western Blot analysis was performed under standard conditions (Russel and Sambrook, 2001). Immunoblots incubated with the first antiserum were developed with anti-rabbit alkaline phosphatase conjugated antibodies with the BCIP/NBT Color Development substrate (Promega). Alternatively horseradish peroxidase conjugated antibodies were used and developed with the Immobilon Western Chemiluminescence Kit (Merck-Millipore) and the Fujifilm LAS-4000 Imaging device (Fujifilm Life Science). Antibodies were purchased from Promega.

Protein quantification

Protein quantification was performed with the Pierce BCA protein assay kit (used for samples with up to 20mM imidazole, high amounts of lipid or detergent; Thermo Fisher Scientific Inc., Rockford, IL, USA) or the Quick Start Bradford Protein Assay (samples with more than 20 mM imidazole, Bio-Rad Laboratories Inc., Hercules, CA, USA).

Wheat germ extract protein expression and purification

Wheat germ extract cell free expression was performed with the RTS-100 Wheat Germ CECF Kit (5 Prime GmbH, Hamburg, Germany). Expression was performed as described in the manual's instructions. Three μg of RNase free plasmid DNA was added to the reaction mix. PMP22 and PXMP2 were inserted into pIVEX1.3 after amplification with the primers listed in Table S1. For uptake studies lipid and detergent was added to allow functional folding of the expressed membrane protein (Nozawa et al., 2007). Phospholipids were supplied as TRIS (pH=7.5, HCl) buffered liposomes produced by sonication (f.c. 1% (w/v) Soybean-Phosphatidylcholine, Lipoid GmbH, Ludwigshafen, Germany) and Brij-35 (f.c. 0.04% w/v) were added to the wheat germ extract.

Recombinant membrane protein was collected by ultracentrifugation (100,000 g, 4°C, 1h), with PNI (100 mM NaH_2PO_4 pH=7.6, 250 mM NaCl, 20-150 mM Imidazole, 0.5 – 0.05% w/v Brij-35) and the pellet was homogenized with a 21-Gauge needle. The detergent Brij-35 was then added and protein was solubilized at 4°C by magnetic stirring for 30 min. PNI pre-equilibrated Ni^{2+} -NTA (QIAGEN, Hilden, Germany) was

added and the purification was performed in batch according to the manuals instructions. For washing and elution Brij-35 concentration was reduced to 1x CMC.

***Saccharomyces cerevisiae* protein expression and purification**

PMP22-His protein was heterologously produced in yeast. The coding sequence was amplified from *A. thaliana* cDNA with the primers NL425/NL411 and inserted in the *HindIII/BamHI* pYES2/NTa backbone for in-frame fusion to the hexahistidine tag. The protein was expressed as described in by Drew et al. (2008). Briefly, the preculture was diluted to an OD₆₀₀ of 0.12 and aerobically grown in minimal medium with 0.01% (w/v) glucose. At an OD₆₀₀ of 0.6 the expression was induced with galactose (f.c. 2% w/v) and DMSO (f.c. 2.5% v/v) was added as molecular chaperone. Cells were harvested after 22 h and resuspended in CRB (50 mM Tris, 1 mM EDTA, 0.6 M sorbitol (pH 7.6); 1 g cells per 3 mL buffer). Cell disruption was performed sequentially with increasing pressure of 25, 30 and 35 kpsi at 4°C with the Constant Systems Limited (Northants, United Kingdom) one shot model heavy duty cell disruption device. Cell debris was pelleted by centrifugation at 10,000 g (4°C, 10 min) and the supernatant was used for ultracentrifugation (120,000 g, 4°C, 2 h), the membrane pellet was resuspended in TNI-10 (10 mM Tris, 300 mM NaCl, 10 mM imidazole (pH 8.0)) with a 21-Gauge needle to a homogenous suspension and adjusted to a protein concentration of 3.5 mg/mL. Then detergent powder was added (DDM f.c. 1% w/v) and the membrane protein was solubilized by magnetic stirring at 4°C for 60 minutes. The solution was then ultracentrifuged (100,000 g, 1 h, 4°C) and loaded onto 1 mL Protino® - Ni²⁺-NTA FPLC column (Macherey-Nagel GmbH and Co. KG, Düren, Germany) which was pre-equilibrated with TNI-10 (+ Detergent) by using the ÄKTA prime plus chromatography system. The column was washed with 20 mM – 100 mM Imidazole (f.c.) and subsequently eluted in TNI-250 (10 mM Tris, 300 mM NaCl, 250 mM imidazole (pH 8.0)) containing detergent in the critical micelle concentration. Purification was conducted at 4°C.

Circular dichroism analysis of PMP22-His

Circular dichroism spectra were measured with a JASCO J-815 spectrometer (Jasco International, Tokyo, Japan) at 20°C using a quartz cell with 0.1 cm path length. PMP22-His was expressed and purified from yeast and dialyzed against 10 mM Tris-NaOH, pH 8, 500 mM (NH₄)₂SO₄, 0.1 % N-dodecyl beta-maltoside (DDM, GLYCON

Biochemicals GmbH, Luckenwalde, Germany). For the measurement, 0.5 mg/ml PMP22-His were used. Secondary structure prediction was performed with the indicated web tools.

Electrophysiological measurements in planar lipid bilayers

For electrophysiological experiments IMAC purified PMP22-6xHis was reconstituted in small unilamellar phosphatidylcholine (Soybean L- α -phosphatidylcholine, Lipoid GmbH, Ludwigshafen, Germany) liposomes. The lipid:protein ratio was adjusted to 20:1 in MTK20 buffer (20 mM KCl, 10 mM MOPS pH=7.0 (Tris)). Lipids were solubilized with Triton-X-100 to mixed micelles (Carl Roth GmbH and Co. KG, Karlsruhe, Germany). Mixed micelles and Brij-35 solubilized PMP22-6xHis were combined and mixed over night at 4°C by stirring. Brij-35 and Triton-X-100 were removed by binding to Calbiosorbs (Calbiochem, Merck-Millipore, Schwalbach, Germany). This led to proteoliposome formation, visible by the whitish color of the solution. Proteoliposome aliquots were shock frozen in liquid nitrogen and stored in -80°C. Incorporation of PMP22-His into proteoliposomes was confirmed by Nycodenz flotation (Step gradient 40% - 0%, Liposomes added to the bottommost fraction, Centrifugation 200,000 g, 4°C, 1h). After centrifugation the protein in the fractions was precipitated by trichloroacetic acid, washed with acetone, resuspended in SDS-loading dye and analyzed by SDS-PAGE and immunoblotting.

For electrophysiological characterization the proteoliposomes were subjected to planar lipid bilayer fusion with the Ionovation compact instrument (Ionovation GmbH, Osnabrück, Germany). The functional incorporation of the membrane proteins led to the transfer of ions across the bilayer. Ion currents were measured with the HEKA EPC10 USB amplifier. Liposome fusion and measurements were conducted as described in the manufacturer's manual. Electrode contact to the solution in the measurement compartments was established with 2 % (v/v) agarose-bridges in 2 M KCl. The bilayer lipid was applied by the painting technique and measurements were performed with the bilayer capacitance exceeding 30 pF.

1-5 μ L proteoliposome suspension was added to the *cis* chamber (250 mM KCl, 10 mM MOPS pH=7.0 (Tris)). Ca^{2+} -ions were added to mediate the adsorption of the proteoliposomes to the bilayer and the osmotic gradient across the bilayer (*trans*

chamber with 20 mM KCl, 10 mM MOPS pH=7.0 (Tris)) favors liposome swelling which is beneficial for fusion events.

Intrinsic ion channel features lead to permeability differences and selectivity for certain ions. This ion selectivity was measured under asymmetric conditions. If the channel prefers an ion, an electrochemical potential across the bilayer will be build up, which can be reversed by applying a holding potential. At the reversal potential no net flux across the pore will be observed. With a known reversal potential the relation of the permeability coefficients can be calculated with the Goldman-Hodgkin-Katz-potential equation:

$$\frac{P_C}{P_A} = \frac{[A]_{\text{trans}} - e^{\frac{U_{\text{rev}}F}{RT}} \times [A]_{\text{cis}}}{e^{\frac{U_{\text{rev}}F}{RT}} \times [C]_{\text{trans}} - [C]_{\text{cis}}}$$

[A]_{cis/trans} = Anion concentration

[C]_{cis/trans} = Cation concentration

F = Faradaykonstante

P_A = Anion permeability coefficient

P_C = Cation permeability coefficient

R = universal gas constant

T = Temperature

U_{rev} = Reversal potential

Analysis of protein transport function in an in vitro liposome system

Transport proteins were integrated in artificial hydrophobic lipid environments for biochemical studies. To examine the transport properties of PXMP2 and PMP22, recombinant proteins were reconstituted into liposomes by using the freeze-thaw method (Rigaud and Levy, 2003). The reconstitution of artificial liposomes was used to insert proteins in lipid vesicles simulating a natural environment. For the reconstitution of in vitro translated proteins 8 % (w/v) phospholipid suspension of phosphatidylcholine was prepared; 500 µl of Ni-NTA purified or gel-filtrated protein sample, both produced via *in vitro* translation was mixed with 500 µl 8% (w/v) phospholipid suspension (final lipid concentration = 4% w/v).

For the reconstitution of PMP22-His residing in yeast membranes 3% (w/v) phospholipid suspension was prepared; 50 - 100 µl of the resuspended yeast membrane pellet was reconstituted in 900 - 950 µl 3% (w/v) phospholipid suspension (final lipid concentration = ~ 3% w/v).

The liposomes were prepared from acetone-washed L-α-phosphatidylcholine from soybean and stored at -20°C. For antiport studies internal substrate was provided to

drive the uptake of external substrate. Phospholipids were dissolved in the counter-exchange substrate in buffer B (20 mM potassium gluconate, 100 mM Tricine, 30 mM counter exchange substrate (pH 7.5)) by sonication on ice with a micro-tip (Output 3, 30%). As a control lipid suspension without an internal substrate was prepared in buffer A (50 mM potassium gluconate, 100 mM Tricine (pH 7.5)). Recombinant protein was added to the liposome suspension, immediately mixed by vortexing and frozen in liquid nitrogen (storage in -80°C). Rapid freezing led to an opening of the vesicles and the subsequent thawing process at RT leads to the insertion of the transport protein into the lipid vesicles. Proteoliposomes were pulse sonicated ten times to generate uniform proteoliposomes and to seal them. The residual counter exchange substrate, which was not incorporated into proteoliposomes, was removed by gel filtration using pre-equilibrated Sephadex PD-10 column (GE Healthcare Munich). According to the handbook, columns were equilibrated eight times with PD-10 buffer (40 mM potassium gluconate; 100 mM Sodium gluconate; 10 mM Tricine (pH 7.5)). The eluates (1 ml) containing the proteoliposomes were then collected and stored on ice for uptake experiments.

The transport activity was assayed by measuring the uptake of radioactive substrate in unlabeled substrate containing proteoliposomes (forward exchange). The uptake experiment itself was started when 1 mL proteoliposomes was added to the transport mix (40 mM potassium gluconate, 100 mM sodium gluconate, 10 mM Tricine, 4.2 mM Transport substrate; 5 μCi radioactive substrate (pH 7.5)) containing the labeled substrate. The reaction was stopped at a certain time point by the addition of the proteoliposomes on pre-equilibrated Dowex anion-exchange columns. The columns were filled with AG1-X8 Resin 100-200 mesh, acetate form (Bio-Rad Laboratories Inc., Hercules, CA, USA) and equilibrated seven times with 150 mM sodium acetate (pH 7.5). The negatively charged substrate, which was not incorporated into the proteoliposomes was removed by anion exchange. The liposomal flow-through, eluted with 1.2 mL 150 mM sodium acetate, was collected in scintillation vials filled with 3 mL Rotiszint eco (Carl Roth GmbH). The uptake of radiolabeled substrate was measured in a scintillation counter after inverting the scintillation vials three times. The nanomoles of substrate taken up were calculated as $\text{cpm}/\text{specific radioactivity}$ (cpm, counts per minutes). The specific radioactivity is given by the ratio between cpm and nmoles of substrate and obtained by measuring the cpm of a transport medium aliquot that contains a known amount of substrate.

***E. coli* complementation**

The dicarboxylate transport mutant CBT315 (CGSC no.:5269) and its isogenic wild type, K12 (CGSC no.:4401) were obtained from the *E. coli* Genetic Resources Center of Yale University (<http://cgsc.biology.yale.edu>). A PMP22 PCR fragment (Primer listed in Table S1) was inserted into the *XhoI/BglII* opened pTAC-MAT-TAG-2 (Sigma-Aldrich). For functional complementation tests a modified pRARE (Novagen) vector (Gentamycin resistance encoded in pDONR207 (Invitrogen) *DraIII/PvuI* fragment was inserted into *ScaI* site of pRARE) was co-transformed into *E. coli* with the empty vector or *the PMP22 construct*. Cells were grown on M9 medium containing 2% (w/v) L-malic acid (pH adjusted to 6.6 with NaOH) at 37 °C. Expression was induced by addition of 1 mM IPTG.

Chlorophyll quantification

Rosette leaves were snap-frozen in liquid nitrogen, and homogenized by grinding in a mortar. The fresh weight was determined and the chlorophyll concentration was determined as described previously (Porra et al., 1989).

Glycolate oxidase activity measurement

100 mg six-day-old Arabidopsis seedlings were homogenized in 1mL 20 mM Tris-HCl, 0.5 mM DTT, 5 % (w/v) Glycerol, 5% PVPP50, Roche Protease inhibitor cocktail. The homogenate was clarified by centrifugation. The reaction medium contained 50 µL extract (ca. 50 µg total protein), 50 mM Tris-HCl (pH 8.2) and 10 mM phenylhydrazine. The reaction was started by the addition of 1 mM sodium glycolate and followed spectrophotometrically at 320 nm. Activity was calculated as the absorption/time slope in the linear initial period.

Supplemented References

- Drew D., Newstead S., Sonoda Y., Kim H., von Heijne G., Iwata S.** (2008) GFP-based optimization scheme for the overexpression and purification of eukaryotic membrane proteins in *Saccharomyces cerevisiae*. *Nat Protoc* **3**: 784-798.
- Koncz, C., Martini, N., Mayerhofer, R., Koncz-Kalman, Z., Körber, H., Redei, G.P., and Schell, J.** (1989). High-frequency T-DNA-mediated gene tagging in plants. *Proc. Natl. Acad. Sci. U.S.A.* **86**: 8467–8471.
- Kota, J., Gilstring, C.F., and Ljungdahl, P.O.** (2007). Membrane chaperone Shr3 assists in folding amino acid permeases preventing precocious ERAD. *J. Cell Biol.* **176**: 617–628.
- Lee, M., Choi, Y., Burla, B., Kim, Y.-Y., Jeon, B., Maeshima, M., Yoo, J.-Y., Martinoia, E., and Lee, Y.** (2008). The ABC transporter AtABCB14 is a malate importer and modulates stomatal response to CO₂. *Nat. Cell Biol.* **10**: 1217–1223.
- Lo, T.C., Rayman, M.K., and Sanwal, B.D.** (1972). Transport of succinate in *Escherichia coli*. I. Biochemical and genetic studies of transport in whole cells. *J. Biol. Chem.* **247**: 6323–6331.
- Louis-Jeune, C., Andrade-Navarro, M.A., and Perez-Iratxeta, C.** (2011). Prediction of protein secondary structure from circular dichroism using theoretically derived spectra. *Proteins* **80**: 374–381.
- Perez-Iratxeta, C. and Andrade-Navarro, M.A.** (2008). K2D2: estimation of protein secondary structure from circular dichroism spectra. *BMC Struct. Biol.* **8**: 25.
- Proost, S., Van Bel, M., Sterck, L., Billiau, K., Van Parys, T., Van de Peer, Y., and Vandepoele, K.** (2009). PLAZA: a comparative genomics resource to study gene and genome evolution in plants. *Plant Cell* **21**: 3718–3731.
- Raussens, V., Ruyschaert, J.-M., and Goormaghtigh, E.** (2003). Protein concentration is not an absolute prerequisite for the determination of secondary structure from circular dichroism spectra: a new scaling method. *Anal. Biochem.* **319**: 114–121.
- Rigaud, J.-L. and Lévy, D.** (2003). Reconstitution of membrane proteins into liposomes. *Meth. Enzymol.* **372**: 65–86.
- Russell, D.W. and Sambrook, J.** (2001). *Molecular cloning. A laboratory manual.*
- Schwacke, R., Schneider, A., van der Graaff, E., Fischer, K., Catoni, E., Desimone, M., Frommer, W.B., Flügge, U.-I., and Kunze, R.** (2003). ARAMEMNON, a novel database for *Arabidopsis* integral membrane proteins. *Plant Physiol.* **131**: 16–26.
- Steinhauser, D., Usadel, B., Luedemann, A., Thimm, O., and Kopka, J.** (2004). CSB.DB: a comprehensive systems-biology database. *Bioinformatics* **20**: 3647–3651.

IV.3 Manuscript 3

The implication of peroxisomal metabolite transport in propionic and isobutyric acid metabolism is important for amino acid respiration

Jan Wiese^{*}, Martin G. Schroers^{*}, Andreas P.M. Weber and Nicole Linka[¶]

Department of Plant Biochemistry, Heinrich-Heine University Düsseldorf, 40225 Düsseldorf, Germany

^{*}Co-first authors

[¶]Corresponding author

Abstract

Defects in metabolic conversion of propionic and isobutyric acid have been associated with severe diseases in humans. Little is known about the fate of propionic acid and isobutyric acid in plants. In leaf tissue these molecules are released during the degradation of branched-chain amino acids, phytol and odd-chain fatty acids. Here we report evidences that these molecules are metabolized via peroxisomal β -oxidation. The performance of *Arabidopsis thaliana* mutant plants, defective in peroxisomal metabolite or cofactor transport crucial for functional β -oxidation, was analyzed during dark-induced leaf stress. Under this condition, high levels of propionic acid and isobutyric acid are produced. We showed that the peroxisomal ABC transporter, catalyzing the uptake of fatty acids, was also involved in the import of these short monocarboxylic acids. Together with the peroxisomal carrier proteins supplying β -oxidation with ATP and NAD/CoA, they play a role in the detoxification of propionate and isobutyrate. An impaired function of peroxisomal transport resulted in sensitivity to extended darkness, premature senescence and reduced reproductive fitness. β -oxidation could be connected to amino acid homeostasis. Finally we propose a model of solute transport steps at the peroxisomal membrane for the conversion of propionic acid and isobutyric acid.

Introduction

In *Arabidopsis thaliana* storage oil is broken down to gluconeogenic and respiratory carbon units with implication of peroxisomal β -oxidation in the transition from seeds to seedlings. Fatty acids released from storage oil are imported as acyl-CoA esters into peroxisomes via the peroxisomal ABC transporter, hereafter referred to as PXA1 (also known as AtABCD1, CTS, PED3, ACN2; reviewed in Hu et al., 2012). During this transport process the CoA moiety is cleaved off and the fatty acids are re-esterified with Coenzyme A (CoA) in an ATP-dependent manner (De Marcos Lousa et al., 2013). *A. thaliana* peroxisomes possess two ATP carrier proteins (called PNC1 and PNC2; Arai et al., 2008; Linka et al., 2008) to fuel ATP dependent reactions such as fatty acid activation. The NAD/CoA transporter (called PXN; Agrimi et al., 2012; Bernhardt et al., 2012) was implicated in supplying β -oxidation with cofactors for β -oxidation. Mutations in these peroxisomal transport proteins cause an inhibition in β -oxidation, resulting in *A. thaliana* plants restricted in seedling development.

Respiration of fatty acids that are derived from lipid turnover via β -oxidation is required for survival of extended darkness to overcome the low carbon and energy status (Kunz et al., 2009; Slocombe et al., 2009). In senescing leaves β -oxidation is important for the mobilization of membrane lipids, which are thereby converted for relocation of carbon units to sink tissues (Yang and Ohlrogge, 2009; Troncoso-Ponce et al., 2013). β -oxidation plays a general role in fertilization. Mobilization of lipids in both pollen and female tissues are essential as shown for *pxa1* and β -oxidation core enzyme 3-ketoacyl-coA thiolase mutant *kat2-1* (Footitt et al., 2007a; 2007b).

Carbohydrate oxidation primarily supports plant respiration in non-photosynthetic tissue, while turnover of intracellular proteins occurs at times when plant cells are carbon limited, for example during extended periods of darkness, leaf senescence, and under conditions of environmental and developmental stress (Araújo et al., 2011). In stressed *A. thaliana* rosette leaves proteolysis releases amino acids that can be mobilized for use in other parts of the plant, but also provide alternative substrates for the mitochondrial electron transport chain. The branched-chain amino acids (BCAA), aromatic amino acids and lysine can provide electrons both directly to electron transfer flavoprotein (ETF) complex as well as indirectly because their catabolic products are fed directly into the tricarboxylic acid (TCA) cycle (Engqvist et al., 2009; Araújo et al., 2010; Engqvist et al., 2011). In case of BCAA breakdown,

isovaleryl-CoA dehydrogenase dehydrogenase provides electrons to the ubiquinol pool via the ETF/ETFQO complex (Araújo et al., 2010;). During the degradation of valine and isoleucine isobutyryl-CoA and propionyl-CoA are released in mitochondria. It was assumed that these short-chain fatty acids are further converted to 3-hydroxy-acids involving enzymes of the peroxisomal β -oxidation machinery (Zolman et al., 2001a; Lange et al., 2004; Lucas et al., 2007; Zolman et al., 2008). Propionyl-CoA can also be derived from degradation of odd-numbered fatty acids (Lucas et al. 2007). A link between peroxisomal β -oxidation and amino acid catabolism has been established by the analysis of 3-hydroxybutyryl-CoA hydrolase mutant *chy1*. This mutant is involved in valine breakdown and displays impaired β -oxidation probably due to accumulation of the toxic valine catabolite methylacrylyl-CoA (Zolman et al., 2001a).

Since the BCAA degradation is initiated in the mitochondria, the intermediates, such as propionic acid and isobutyric acid, have to be shuttled to peroxisomes for further conversion via β -oxidation. Here, we address the role of transport proteins known to be associated with peroxisomal fatty acid oxidation for a requirement in BCAA degradation.

In this work we showed that the peroxisomal ABC transporter, catalyzing the uptake of fatty acids, was involved in the import of these short monocarboxylic acids. Together with the peroxisomal carrier proteins supplying β -oxidation with ATP and NAD/CoA, they play a role in the detoxification of propionic acid and isobutyric acid under stress conditions such as extended darkness. Furthermore, we identified PNC, PXN and PXA1 as negative regulators of developmental senescence. The loss of these transport proteins resulted in less seed biomass, implicating a defect in the relocation of C and N from leave sources to seed sinks.

Results

Feeding of BCAA and intermediate catabolites inhibits growth of β -oxidation transport mutants.

The 3-hydroxyisobutyryl-CoA hydrolase CHY1 was previously described as a link between valine catabolism and fatty acid β -oxidation (Zolman et al. 2001a). To obtain further insight in the role of peroxisomal β -oxidation in BCAA degradation, we performed feeding experiments with leucine, isoleucine, valine and their catabolites including propionic acid and acrylic acid. We analyzed *Arabidopsis thaliana* T-DNA Insertion lines in the *Columbia-0* (*Col-0*) background. To gain *in vivo* information about peroxisomal ATP translocation, we constructed a double mutant *pnc1/2* (*pnc1-1*: SAIL_303H02; *pnc2-1*: SALK014579; Linka et al., 2008; Kessel-Vigelius et al., in preparation) of the two ATP/AMP carriers PNC1 and PNC2. Furthermore, *pxn-1* (GABI-046D01; Bernhardt et al., 2012) and *pxa1-2* (SALK_019334; Kunz et al., 2009) were included in the performed assays. We assessed growth performance upon provision of high levels of BCAA or the catabolic products isobutyrate, propionate or acrylate. These were added during postgerminative growth to nine-day-old seedlings. Growth assays were performed on vertically placed half strength MS-plates containing sucrose. We quantified growth rate of the seedling plants by measuring the primary root length. Primary root length was documented on the day of transfer and after 10 days of growth (Figure 1C). *pnc1/2* and *pxa1-2* mutants transferred to propionic acid medium did not show root elongation, indicating a growth inhibition by this molecule at the given concentration. Root growth of *pxn-1* and the wild type was not affected. Addition of isobutyric acid inhibited root growth in all plants tested within the 10-day growth period, but after three weeks rosette development of *Col-0* and *pxn-1* indicated less sensitivity to this compound for *pnc1/2* and *pxa1-2*, which displayed smaller rosettes and deformed leaves (Figure S3) compared to the wild type. Feeding of acrylic acid led to a growth arrest in the wild type and mutants. However, wild type and *pxn-1* displayed increased tolerance, because degreening of seedlings was progressing more slowly. In contrast *pnc1/2* and *pxa1-2* plants were extremely impaired in growth and leaves quickly bleached to a white color within the 10-day period.

The presence of BCAA negatively affected root elongation of the β -oxidation transporter mutants. Leucine presence for example caused reduced root elongation of *pnc1/2* and *pxa1-2* in comparison to *Col-0* and *pxn-1*. Especially with regard to leaf

morphology these plants did not reach the size of the respective *Col-0* control. Differences between the *Col-0* control and *pxn-1* root elongation were not detected.

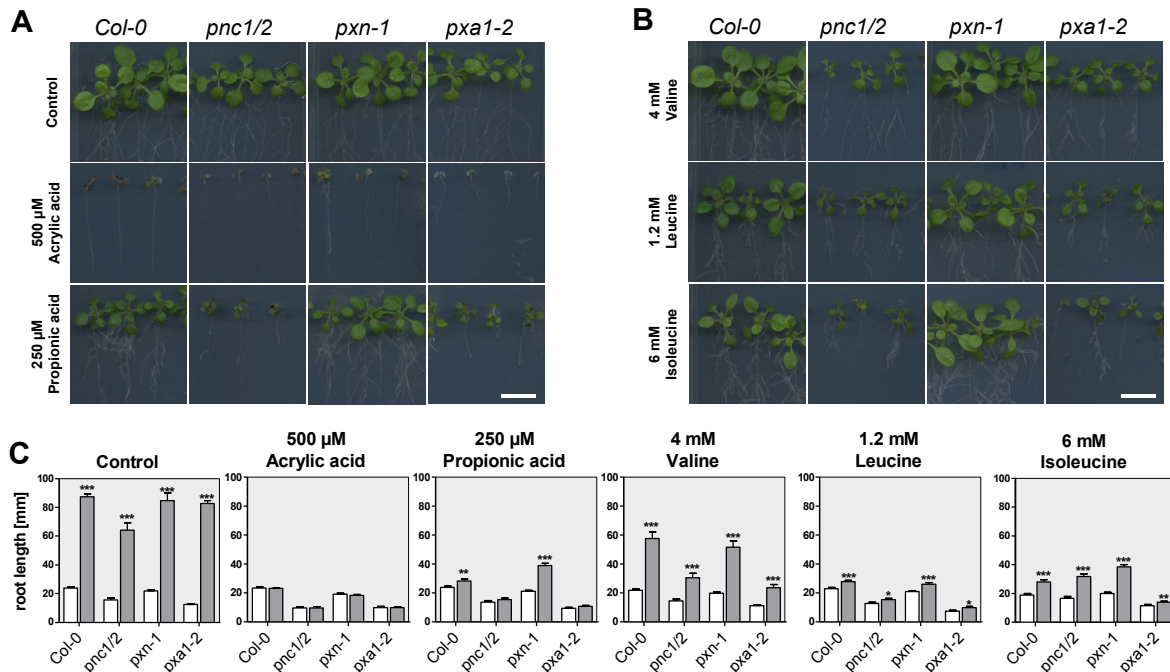


FIGURE 1. Exogenous supply of small carboxylic acids or branched-chain amino acids reduces primary root growth in peroxisomal transporter mutants. Images were taken and analyzed after 1 day and 11 days. Primary root growth was statistically compared for each line and condition. Plants were germinated on plates containing 0.5x MS medium supplied with 1% (w/v) sucrose and transferred to the supplemented or control plates after nine days.

(A) Photograph of *Col-0*, *pnc1/2*, *pxn-1* and *pxa1-2* moved to plates containing half strength MS medium and an addition of either 0.25 mM propionic acid or 0.5 mM acrylic acid.

(B) Photograph of *Col-0*, *pnc1/2*, *pxn-1* and *pxa1-2* moved to plates containing half strength MS medium and an addition of 4 mM valine, 1.2 mM leucine or 6 mM isoleucine

(C) Mean primary root length (+SE) measured 1 day and 11 days (grey bars) after transfer to the feeding plates. Data presents the primary root length in mm, visualized is the mean of seven to 22 replicates with SE. Asterisks indicate statistical differences in root length between the 20 hour and the 11 days measurement (* P < 0.05, ** P < 0.01, *** P < 0.001; Student's t-test). Scale bar: 10 mm.

PNC and PXA1 activity were needed to enable growth in the presence of high levels of BCAA, propionate and acrylate. These findings confirmed the need for peroxisomal β -oxidation in conversion of BCAA. BCAA catabolism was shown to be important in stressed plants (Araújo et al., 2011). Mutants of the 3-hydroxyisobutyryl-CoA hydrolase CHY1 have been shown to be impaired in extended darkness and cold (Dong et al., 2009), indicating an increased need for BCAA degradation during these stress conditions. Peroxisomal β -oxidation is important throughout the plant life cycle (Theodoulou et al., 2006) and consequently the transport proteins supplying β -oxidation are also required. We asked if the β -oxidation transporter genes show induced expression in cellular stress conditions, that depend on alternative oxidation, as described for extended darkness and natural senescence (Buchanan-Wollaston et al., 2005; Engqvist et al., 2011; Araújo et al., 2010).

Transport genes are dynamically expressed

A drastic increase of expression in developmental senescence and after shift to darkness was detected for PNC1, PNC2, PXA1 and PXN (Figure 2). This reflects knowledge that extended darkness eventually elicits a senescence similar program, which demands high β -oxidation rates for lipid turnover and BCAA degradation (Buchanan-Wollaston et al., 2005; Kunz et al., 2009; Yang and Ohlrogge 2009; Troncoso-Ponce et al., 2013). Peroxisomal transporter transcripts also increased in response to several abiotic stimuli (Figure S1), hence we proposed these to be required for stress tolerance.

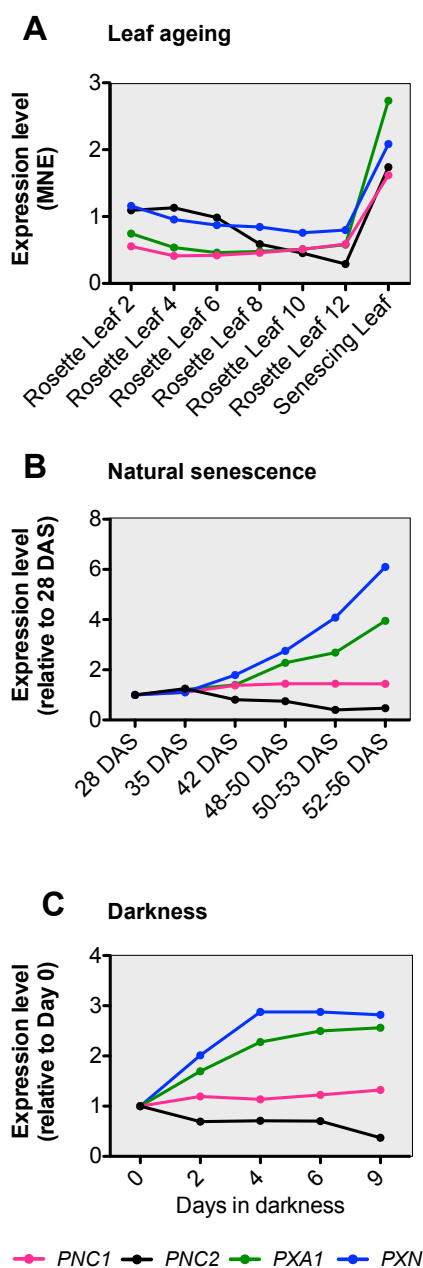


FIGURE 2. Mean normalized transcript abundance of *PXA1*, *PXN*, *PNC1*, and *PNC2* in *Arabidopsis thaliana* rosette leaves in developmental senescence and after shift to darkness.

(A) Mean transcript level in plant ageing. Data was taken from AtGenExpress (Schmid et al., 2005; Kilian et al., 2007)

(B) Mean transcript level in rosette leaves relative to day 28 days after sowing. Data taken from van der Graaff et al. (2006).

(C) Mean transcript level relative to day 0 in rosette leaves after shift to darkness. Data taken from van der Graaff et al. (2006).

Transport mutants are stressed in extended darkness

Transcriptional activation implied β -oxidation transport to be required in stressed plants. Therefore, we investigated if ablation of β -oxidation transport functions induces stress in mature rosette leaves of *pnc1/2*, *pxa1-2*, and *pxn-1* plants. We measured chlorophyll fluorescence parameters and evaluated the flow of electrons through photosystem II (PSII), which expresses overall photosynthetic capacity. Damage to PSII is considered as one of the first indications of stress in a leaf. Hence, maximum quantum yield expresses to which extent PSII is damaged by applied environmental changes and consequently, if a plant can tolerate that stress (Maxwell and Johnson, 2000).

Four-week-old *Col-0*, *pnc1/2*, *pxa1-2*, and *pxn-1* plants were transferred to the dark for periods up to 50 h and reilluminated for 24 h or kept in the dark for nine days. Nine days of darkness deplete cells of carbon and require mobilization of stored carbon in lipid and proteins (Araújo et al. 2010). *pxa1* displayed a mild reduction in PSII activity after one hour of darkness (Figure 3A). The other mutants displayed phenotypic differences to the wild type only after shift to darkness. The loss of PSII electron transport depended on the duration of darkness (Figure 3A). Similar to *pxa1-2*, *pnc1/2* plants bleached to a bluish to brown color and quickly dehydrated upon reillumination after at least 32 h darkness within a few hours of light (Figure 3B).

Keeping the plant in darkness for nine days resulted in increased PSII damage for *pxn-1* compared to the wild type. The observed dark induced damage also depended on leaf age, because older leaves appeared to be more susceptible upon reillumination than younger leaves. Lethality upon reillumination was not observed for *Col-0* or *pxn-1*. *pxn-1* displayed significantly reduced PSII electron flow only after nine days of incubation in the dark. The findings of PSII damage was further supported by reduced chlorophyll content of *pnc1/2*, *pxa1*, and *pxn-1* after nine days of darkness (Figure S2). In summary, restrictions in β -oxidation transport led to enhanced stress in extended darkness.

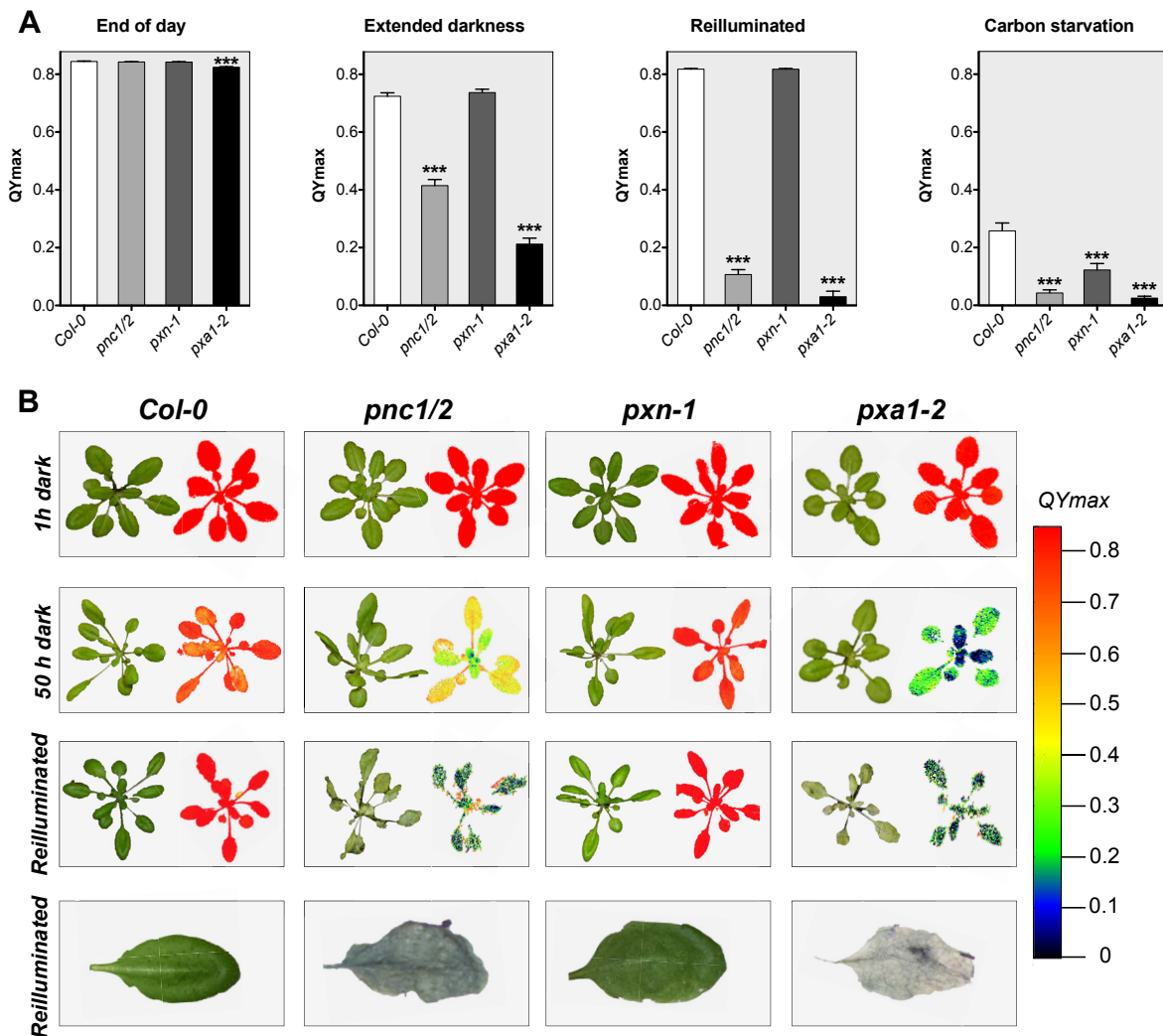


FIGURE 3. Response of 4-week-old *Col-0*, *pnc1/2*, *pxn-1* and *pxa1-2* plants to extended darkness. **(A)** Mean (+SE) of maximum quantum yield of rosette leaves of 4-week-old *Col-0*, *pnc1/2*, *pxn-1* and *pxa1-2* at the end of day, extended darkness (50h), reillumination for 24 h after 50 h darkness and incubation in the dark for nine days (Carbon starvation). Results are representative for eight independent experiments each performed with at least three biological replicates. Differences between the mean of each treatment were marked as statistically significant (t-test) with the *Col-0* control by (*), (**), or (***) at respective significance levels of ($P < 0.05$), ($P < 0.01$) or ($P < 0.001$). **(B)** Photographs and false-color images representing maximum quantum yield (QYmax; as indicated) of 4-week-old *Col-0*, *pnc1/2*, *pxn-1* and *pxa1-2* at the end of day, extended darkness (50h), reillumination for 24 h after 50 h darkness.

In extended darkness amino acid profiles are affected by loss of β -oxidation transporters

Dark-induced senescence phenotypes have been described for mutants deficient in *PXA1* (Kunz et al., 2009), *ACX1/2*, *LACS6/7* (Yang and Ohlrogge, 2009) in respect to fatty acid catabolism. We addressed if compromised β -oxidation influences alternative respiration through alterations in BCAA and aromatic amino acid metabolism, as these are known to serve as alternative respiratory sources. A link between β -oxidation and BCAA degradation has been established for *CHY1*, which is

sensitive to extended darkness due to accumulation of the toxic intermediate methylacrylyl-CoA (Zolman et al., 2001a) and has been confirmed by feeding experiments conducted in this study. We analyzed the effect of darkness on peroxisomal transport mutants on metabolite level. Therefore selected sugars, hydrophilic carboxylic acids and amino acids were profiled by GC-MS and HPLC-DAD.

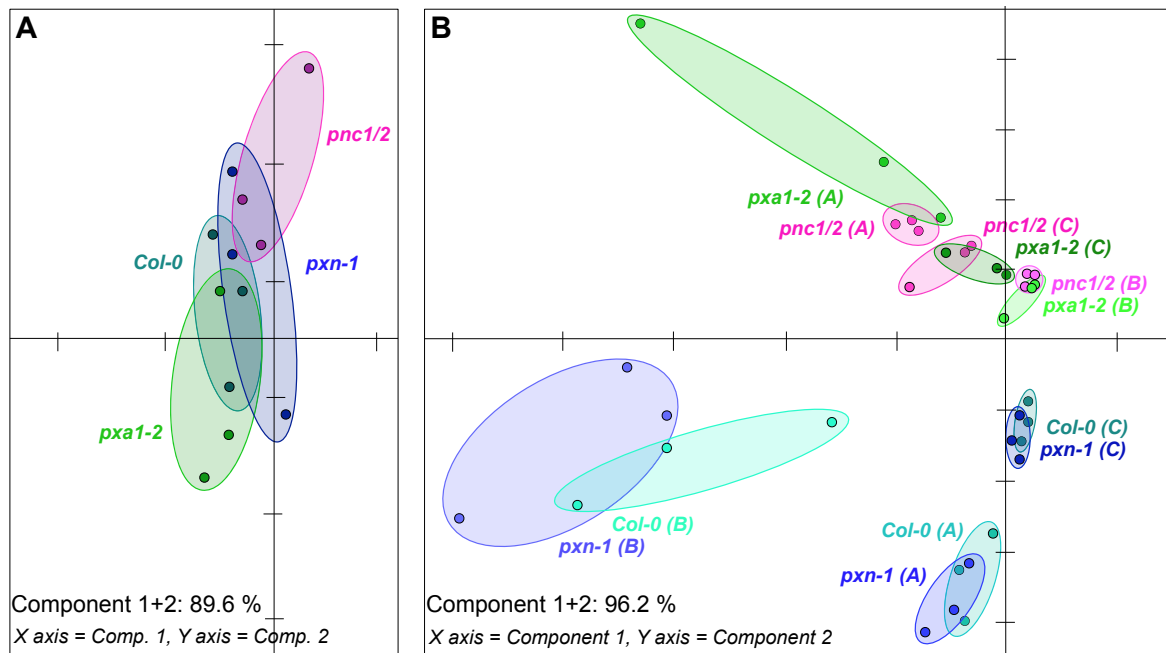


FIGURE 4. Principal Component Analysis (PCA) of amino acid data of 4-week-old *Col-0*, *pnc1/2*, *pxn-1* and *pxa1-2* to extended darkness.

(A) PCA score plot of proteinogenic amino acids in non-stressed plants (End of night)

(B) PCA score plot of amino acids extract from Wild type (*Col-0*) plants and the peroxisomal transporter mutants *pnc1/2*, *pxn-1*, and *pxa1-2* either exposed to 50 h of darkness (A), nine days of darkness (B) or 50 h of darkness followed by 24 h illumination (C) subjected to GC-MS analysis. PCA conducted with the MultiExperiment Viewer (Saeed et al., 2003). Biological replicates are encircled.

First, we subjected amino acid contents to principal component analysis (PCA) to abstract the amino acid status for each mutant plant extract. In non-stress condition (end of regular night) PCA variations were largely the same and actual levels confirmed that amino acid metabolism is not significantly altered. In response to darkness *pnc1/2* and *pxa1-2* amino acid variations contrasted to *Col-0* and *pxn-1* (Figure 4). Both pairs showed partially overlapping variation patterns, but grouped particularly in the 2D plot. Even though not all of the metabolite fingerprint pools differed, each mutant represented a conditions specific pattern, thus we can conclude that PXA1 and PNC activity is required for maintenance of amino acid homoeostasis in extended darkness.

The interconversion between glutamate and 2-oxoglutarate catalyzed by glutamate dehydrogenase (GDH) fuels the TCA cycle in stress conditions and is a key reaction in plant C and N metabolism. *gdh* mutants do not survive dark treatment due to restrictions in amino acid metabolism (Miyashita and Good, 2008). A closer look at metabolism in extended darkness (50 h) revealed a change in glutamate and 2-oxoglutarate pools. *pnc1/2* and *pxa1-2* exhibited decreased glutamic acid pools compared to the wild type in extended darkness, while the same extracts displayed increased 2-oxoglutarate levels. In contrast to *pnc1/2* and *pxa1-2*, *Col-0* appears to produce glutamate by amination of 2-oxoglutarate. 2-oxoglutarate reached lowest levels in *pnc1/2* and *pxa1-2* carbon starved plants. Upon reillumination 2-oxoglutarate levels were in the magnitude of 50 h dark-treated *pnc1/2* and *pxa1-2* in wild type and *pxn-1*. The TCA intermediate (iso-)citrate levels differed significantly in carbon starved *pnc1/2* and *pxa1-2* plants, exhibiting strongly reduced pool sizes, while here wild type and *pxn-1* displayed higher levels.

It may be reasonable to assume that carbon starved *Col-0* and *pxn-1* plants disposed of a C-source that was not available to *pnc1/2* and *pxa1-2*. Amino acids can be used as respiratory substrates and this process was negatively affected in *pnc1/2* and *pxa1-2* plants during dark-induced carbon starvation: plants could not efficiently use amino acids as energy source and thus the pools of TCA cycle intermediates, like isocitrate and 2-oxoglutarate, were depleted.

pnc1/2 and *pxa1-2* showed differences in BCAA contents, which have been suggested to be preferably consumed to support respiratory growth in carbon starvation (Araújo et al., 2010). The comparison to *Col-0* showed higher BCAA levels in reilluminated transport mutants and reduced levels in carbon starvation. Again, *pxn-1* exhibited almost wild-type contents. In *Col-0* BCAA accumulate in the leaves from 50 h darkness to 9d darkness, indicating that protein turnover was elevated under these conditions (Araújo et al., 2011). *pnc1/2* and *pxa1* could not use fatty acids or BCAA as carbon sources due to a block of β -oxidation, protein turnover/amino acid catabolism was decelerated in these mutants in comparison to *Col-0*, as demonstrated by lower levels of valine, leucine and isoleucine in nine days of darkness. The aromatic amino acid phenylalanine also showed the pattern of branched-chain amino acids (Figure 6).

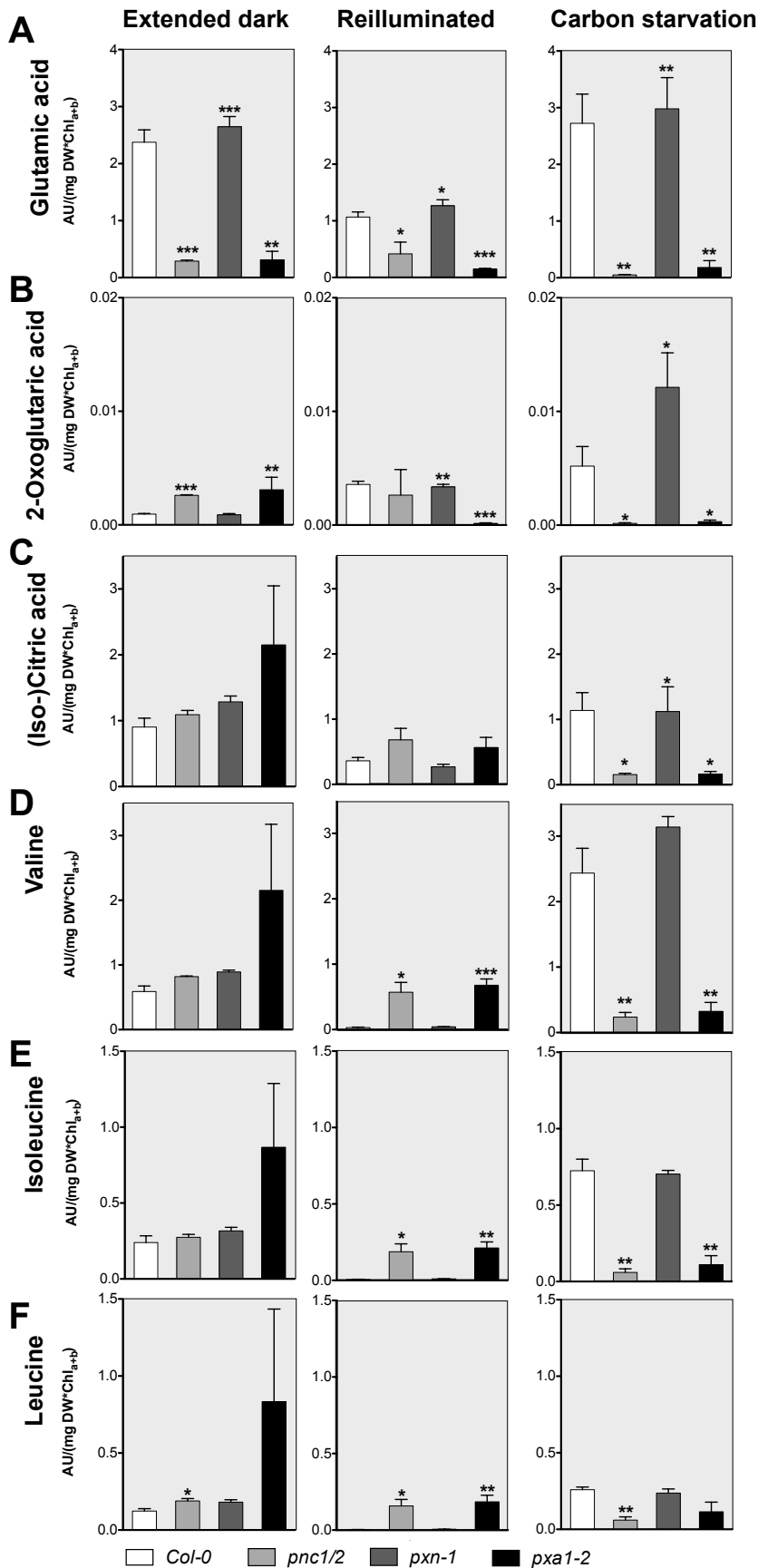


FIGURE 5. Extended darkness influences respiratory metabolites as well as BCAA in peroxisomal β -oxidation transport mutants.

(A)-(F) Mean levels of indicated metabolite content (+SE) of 4-week-old *Col-0*, *pnc1/2*, *pxn-1* and *pxa1-2* in response to extended darkness (50h darkness), reillumination (50h darkness + 24h light) and carbon starvation (9 days darkness). Leaf extracts were subjected to GC-MS analysis for metabolite quantification. Data represent the mean of three biological replicates. Asterisks indicate statistical significance versus the *Col-0* control in each diagram (* $P < 0.05$, ** $P < 0.01$, *** $P < 0.001$; Student's t-test). The data is shown in an arbitrary unit normalized to mg dry weight. Chlorophyll_{a/b} contents were used for normalization of biological replicates.

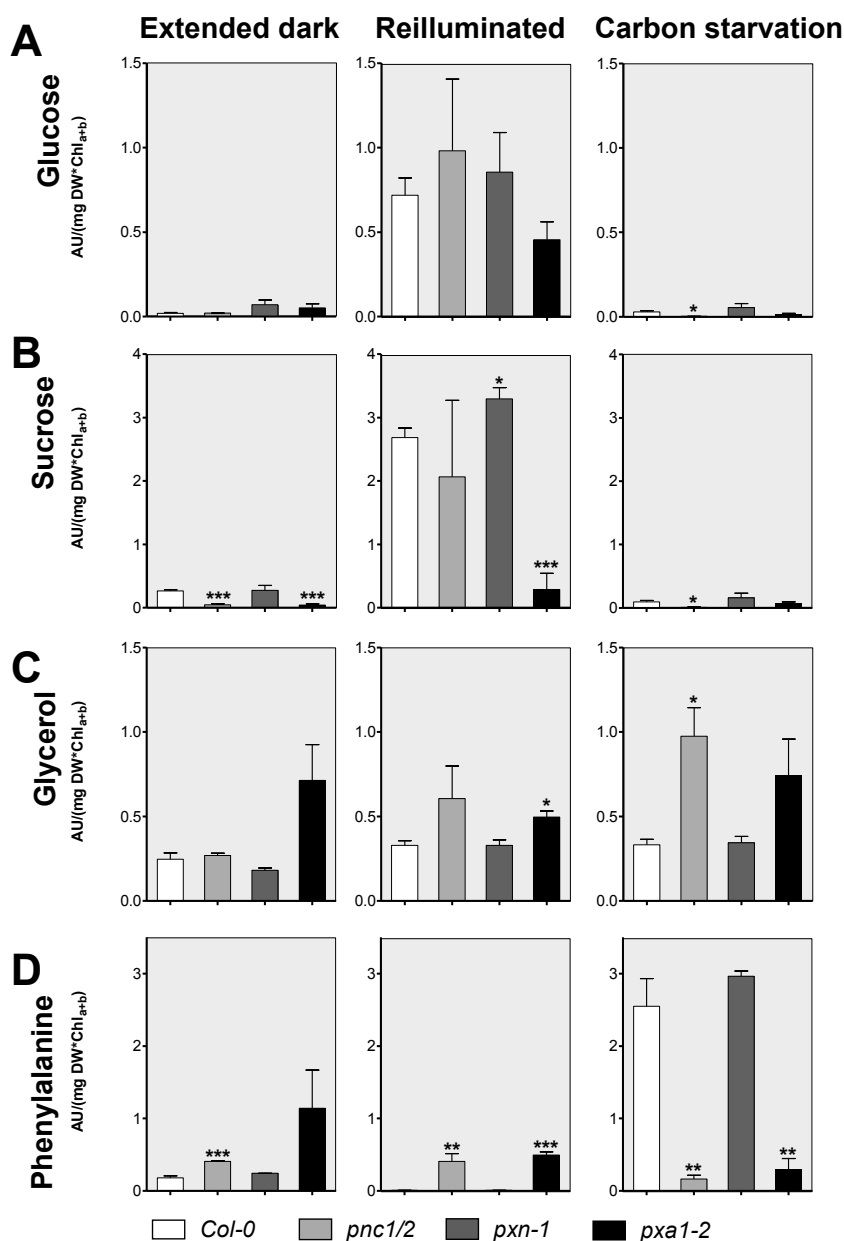


FIGURE 6. Extended darkness influences aromatic amino acids as well as carbohydrates in peroxisomal β -oxidation transport mutants.

(A)-(D) Mean levels of indicated metabolite content (+SE) of 4-week-old *Col-0*, *pnc1/2*, *pxn-1* and *pxa1-2* in response to extended darkness (50h darkness), reillumination (50h darkness + 24h light) and carbon starvation (9 days darkness). Leaf extracts were subjected to GC-MS analysis for metabolite quantification. Data represent the mean of three biological replicates. Asterisks indicate statistical significance versus the *Col-0* control in each diagram (* P < 0.05, ** P < 0.01, *** P < 0.001; Student's t-test). The data is shown in an arbitrary unit normalized to mg dry weight. Chlorophyll_{a/b} contents were used for normalization of biological replicates.

Carbohydrates contents (e.g. glucose or sucrose) were depleted in all lines after 50 hours and nine days of darkness, indicating that wild type and mutant plants were carbon starved under these conditions, but *pnc1/2* showed lowest levels of glucose and sucrose. In reilluminated leaves glucose and sucrose levels were unexpectedly not only increased in the wild type and *pxn-1*, but in all lines, suggesting restoration of photoautotrophic metabolism and synthesis of glucose and sucrose from photosynthetic CO₂ fixation.

Unexpectedly *pnc1/2* displayed a higher content of glycerol in carbon starvation. Glycerol and fatty acids are released during lipolysis. The released fatty acids undergo peroxisomal breakdown and glycerol enters respiration. Increased glycerol

in *pnc1/2* and *pxa1* could be explained by a decreased flux via the TCA cycle, since also intermediates of the TCA cycle were depleted.

Reduced β -oxidation transport leads to altered nutrient relocation in the final stage of leaf development

This altered mobilization of amino acids and carboxylic acids as respiratory substrates in carbon-starved β -oxidation transport mutants raised the question, whether this affects nutrient remobilization and relocation in developmental senescence. We grew plants in a chamber with 50-60% relative humidity and plants were watered regularly. In these growth conditions premature leaf ageing was observed for *pnc1/2* and *pxn-1* by degreening of oldest leaves (Figure S4). This was also reflected in chlorophyll contents measured for mature green leaves (Figure S4). In comparison to the wild type, profiling of late senescence marker SAG12 (Balazadeh et al., 2008) revealed higher variation in the β -oxidation transporter mutants in quantitative Real-Time PCR analysis (Figure 7A). *Col-0* showed SAG12 expression below that of the normalization control (0.0055 ± 0.0018), in contrast to *pnc1/2* (28.98 ± 27.15), *pxn-1* (8.791 ± 7.527) and *pxa1-2* ($6,135 \pm 3,471$). This accelerated leaf senescence indicated that peroxisomal β -oxidation transporters negatively regulate senescence, probably by preventing the induction by metabolic stress (Wingler and Roitsch, 2008; Abbasi et al., 2009).

This finding led to the hypothesis that a β -oxidation defect befalls the next generation, because altered energy availability might lead to reduced nutrient relocation and reduced seed quality. We observed a reduced silique size of 12-week-old plants (Figure 7B), which had already been reported for the core-component β -oxidation 3-Ketoacyl-CoA thiolase (*kat2-1*; Footitt et al., 2007a; 2007b). Authors suspected compromised β -oxidation to be cause of the defect due to impaired pollen tube elongation, leading to a reduced seed number per plant. In contrast our analyses showed seeds of all three mutants to be smaller in size (Figure 7D). Seed weight was reduced for the nucleotide carrier mutants, whereas not for *pxa1-2*, but the same trend was apparent. We quantified seed protein content to test for the hypothesized inability of C and N mobilization and relocation to seeds sinks. The analysis revealed that the seeds are equipped with significantly less protein and might mirror next to a defect in fatty acid breakdown the incompetence in BCAA metabolism.

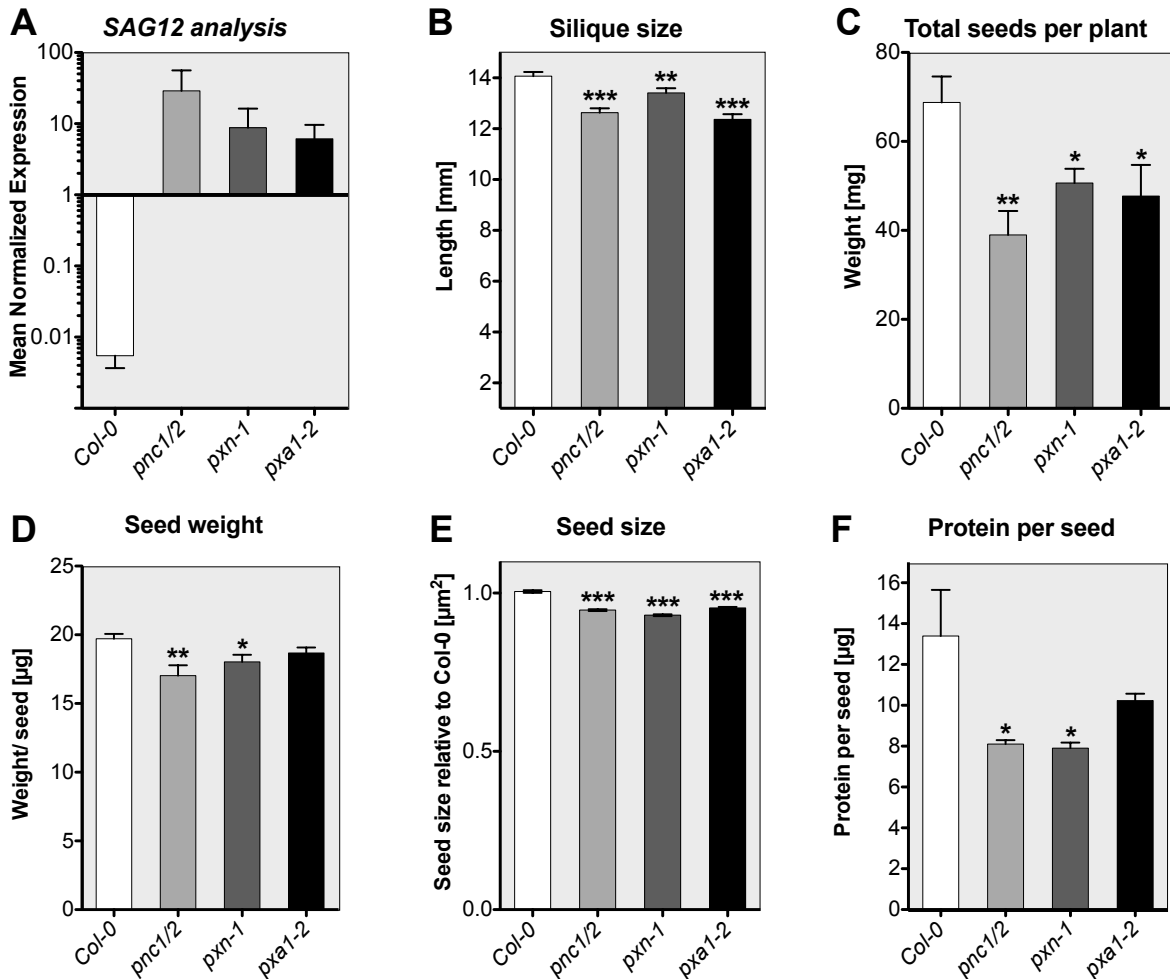


FIGURE 7. Senescence and reproductive fitness features of *Col-0*, *pnc1/2*, *pxn-1* and *pxa1-2*.
(A) Mean normalized expression (+SE) of the senescence marker gene *SAG12* analyzed by qRT-PCR. Plant material was taken from 10-week-old rosette leaves.
(B) Mean silique size (+SE; $n > 40$) in mm measured for 12 week old plants.
(C) Mean of seed yield mean (+SE; $n = 12$) per plant in mg.
(D) Mean of seed weight (+SE; $n = 6$). > 500 Seeds were counted automatically using the ImageJ distribution Fiji (Schindelin et al., 2012) and weighed.
(E) Mean seed size (+SE; $n > 500$) relative to *Col-0*. 2500-6500 seeds were measured with ImageJ.
(F) Mean protein content (+SE; $n = 4$) per seed. Proteins were isolated from 4 samples per line containing 500-1300 seeds. The protein amount was determined using a bicinchoninic acid (BCA) assay. Data shows the protein amount per seed in μ g as mean with SE.
Differences between the mean of each mutant versus the wild type in each diagram are marked as statistically significant (t-test) by (*), (**) or (***) at respective significance levels of ($P < 0.05$), ($P < 0.01$) or ($P < 0.001$).

Discussion

Our work addressed the importance of β -oxidation transporter beyond fatty acid catabolism. We described the role of peroxisomal transport in carbon starvation with respect to amino acid turnover and propionic acid metabolism. Our findings enabled us to integrate PXA1, PNC and PXN in the pathway of branched-chain amino acid (BCAA) degradation. This is the first report with a focus on BCAA catabolism related to transport across the peroxisomal membrane. We demonstrated that an impaired substrate and cofactor supply of β -oxidation disturbed the intracellular carbon mobilization, resulting in cellular stress. As a consequence developmental senescence and nutrient relocation was disrupted on an organism level and passed on the next generation by reduced seed quality and quantity.

Abiotic stress induced expression of β -oxidation transporters

The increased transcript of β -oxidation transporters in response to abiotic stress revealed the transporters to be important in a dynamic environment (Figure 2). A few previous reports highlighted the importance of peroxisomes in oxidative, heat, cold, dark, and salt stress (Shi et al., 2001; Cornah et al., 2004; Ma et al., 2006; Dong et al., 2009; Kunz et al., 2009; Taylor et al., 2009; Mitsuya et al., 2011). Our results confirmed that peroxisomes are needed for thermotolerance as monitored by PSII electron transport in heat stress conditions (Figure S5). We assume peroxisomes and peroxisomal transport to indirectly confer thermotolerance by preventing FFA accumulation and preventing ROS imbalance and oxidation of cellular macromolecules (Falcone et al., 2004; Queval et al., 2007; Mhamdi et al., 2012)

β -oxidation is needed to survive extended darkness

In extended darkness energy equivalents have to be generated independently of photosynthesis. Carbon-starved plants are bound to grow or sustain metabolic processes heterotrophically and trigger the degradation of cellular macromolecules, such as membrane lipids and proteins. This process releases free fatty acids and amino acids, which can both be used as respiratory substrates to generate energy in the form of ATP (Araújo et al., 2011). *pxa1-2* mutants were depicted as incapable to degrade membrane lipids and displayed a lowered ATP/ADP ratio after >24 hours of darkness (Kunz et al., 2009). The importance of β -oxidation proteins, e. g. KAT2, CHY1, but also the peroxisomal citrate synthase in mature plants subjected to

darkness has been previously addressed (Castillo and León, 2008; Dong et al., 2009; Kunz et al., 2009). Our study expands this knowledge and presents the impact of the two remaining transport proteins: the ATP transporter PNC (encoded by PNC1 and PNC2; Arai et al., 2008; Linka et al., 2008) and the NAD/CoA carrier PXN (Agrimi et al., 2012; Bernhardt et al. 2012).

Exposure of the transport mutants to extended darkness led to decreased maximum quantum yield of PSII (Figure 3). While *pnc1/2* and *pxa1-2* showed a strong reduction already after 50 hours of darkness, *pxn-1* was distinguishable from wild types only after nine days of darkness. This reflected findings on the role of PXN in seedlings, because *pxn-1* displayed a delay rather than a block in fatty acid breakdown. Unlike *pxa1-2* and *pnc1/2*, *pxn-1* was able to grow wild-type-like and seedling growth was not “sucrose-dependent” (Zolman et al., 2001b; Linka et al., 2008; Kessel-Vigelius et al., unpublished). *pxn-1* only showed a mild resistance to root growth inhibition by 2,4-DB compared to *pxa1-2* or *chy1* (Bernhardt et al., 2012).

Malfunctional β -oxidation entails the risk of an increase in free fatty acid and pheophorbide a levels

The effect of extended darkness was described for *pxa1-2* on accumulation of pheophorbide a (PhA) and FFA (Kunz et al., 2009). In *pxa1-2* the chloroplast membrane is damaged by the chlorophyll catabolite PhA. PhA is phototoxic, which explains the rapid bleaching of *pnc1/2* and *pxa1-2* leaves upon reillumination (Tanaka et al., 2003; Pruzinská et al., 2003); Figure 3B). Pheophorbide a oxygenase (PaO) catalyzes the oxidation of PhA. Plants lacking PaO show the same rapid bleaching of leaves, when transferred to light after darkness induced chlorophyll degradation (Tanaka et al., 2003).

The same effect of FFA accumulation seems to appear during heat stress, where adjustments of membrane lipid composition necessitates increased fatty acid turnover (Falcone et al., 2004; Larkindale et al., 2005). The FFA increase was thought to lead to membrane damage due to membrane permeabilization (Schönfeld and Wojtczak, 2008). This could also be the cause of PSII electron transport reduction in *pxa1-2* and *pnc1/2*. *pxn-1* proposedly does not accumulate fatty acids and therefore did not show the drastic photobleaching phenotype. Heat stress led to increased damage in membrane bound photosystems in *pnc1/2*, *pxa1-2* and *pxn-1* probably due to ROS formation (Kipp and Boyle, 2013); enhanced ROS production

might also explain the necrotic lesions observed for *pnc1/2*, *pxa1-2* and *pxn-1* plants after exposure to high temperature (Figure S5B). In conditions of high ROS peroxisomal catalase is inactivated (Williams, 1928; Kono and Fridovich, 1982) and a membrane bound complex of ascorbate peroxidase (APX) and monodehydroascorbate reductase accounts for prevention of peroxisomal ROS leakage: APX reduces H₂O₂ to water using ascorbate as electron donor, oxidizing it to monodehydroascorbate (MDA). MDA regeneration comes along with NADH oxidation in the process (Del Río et al., 2006). This ROS detoxification pathway might explain the observed reduced quantum yield obtained for the NAD(H) transporter mutant *pxn-1* in the basal heat stress assay, where *pnc1/2* plants demonstrate wild-type behavior (Figure S5A). Furthermore, heat denaturated proteins need to be degraded, leading to enhanced amino acid concentrations (Araújo et al., 2011). BCAA degradation gives rise to propionyl-CoA and isobutyryl-CoA, which require conversion to prevent toxic effects. Propionyl-CoA has been described as a potent inhibitor of many CoA dependent enzymes (Schwab et al., 2006).

Peroxisomes are implicated in amino acid metabolism

Our data suggests that β -oxidation activity affects amino acid pools (Figure 4/5) as previously described for the peroxisomal β -oxidation enzyme 3-hydroxyisobutyryl-CoA hydrolase CHY1 (Zolman et al., 2001). Mutants lacking CHY1 were hypersensitive to extended darkness as well as cold (Dong et al., 2009). β -oxidation is involved in the breakdown of BCAA (Lucas et al., 2007; Dong et al., 2009). The degradation is initiated in the mitochondrion and accompanied by the reduction of the ubiquinone pool and releases isobutyryl-CoA, propionyl-CoA, and probably methylacrylyl-CoA (Däschner et al., 2001). The importance of BCAA breakdown during extended darkness is also shown by the sensitivity of mutants for mitochondrial BCAA catabolic enzyme isovaleryl-CoA dehydrogenase (IVD1; Araújo et al., 2010). IVD1 has strongest activity towards the leucine catabolite isovaleryl-CoA, five times less activity towards the valine catabolite isobutyryl-CoA (Däschner et al., 2001). This implies that not only propionyl-CoA but also isobutyryl-CoA needs to enter peroxisomes for β -oxidation and leave it as 3-hydroxy acids. This was confirmed by analysis of *chy1* (Lucas et al., 2007). In mitochondria the 3-hydroxy acids were proposed to be converted to acetyl-CoA to fuel the TCA cycle (Lucas et al., 2007). In extended darkness we observed more 2-oxoglutarate and less

glutamate in *pxa1-2* and *pnc1/2*, which is indicative for reduced available nitrogen. The result of this could be an explanation for the reduced protein content in the seeds. The 2-oxoglutarate and glutamate levels declined after 9 days of darkness (Figure 5) and are likely to be respired in the TCA cycle. In carbon starvation we also noted less (iso-)citric acid, which suggested reduced flux through the TCA cycle. A potential cause could be reduced supply of fatty acids and amino acids for respiration (9 days darkness). The wild type and *pxn-1* had increased BCAA pools in nine days darkness, which was not observed for *pnc1/2* and *pxa1-2* (Figure 5D-F). Proteolysis could serve as BCAA source (Araùjo et al., 2011). Reilluminated *pnc1/2* and *pxa1-2* plants were heavily impaired and did not mobilize amino acids into protein synthesis as wild types and *pxn-1* did in this conditions (Figure 5D-F,6D). Our data shows less available sucrose and glucose in *pxa1-2* and *pnc1/2*, which reflected a general carbon depletion due to loss of β -oxidation. A defect in fatty acid catabolism and depleted TCA pool might lead to the increased glycerol levels detected (Figure 6). Future research will need to address if there is a feedback inhibition in BCAA degradation due to a buildup of propionyl-CoA or isobutyryl-CoA and if this influences proteolysis as the source of amino acids. Another interesting point will be to analyze if loss of β -oxidation induces proteolysis as a source of energy.

Feeding of carboxylic acids to β -oxidation transport mutants results in growth inhibition

Exogenous supply of propionic acid, acrylic acid (Figure 1) or isobutyric acid (Figure S3) led to a severe growth inhibition for *pnc1/2* and *pxa1-2*, indicating the importance of peroxisomal β -oxidation for degradation of small carboxylic acids. We redefined the model proposed by Lucas et al. (2007) describing the catabolism of propionic and isobutyric acid (Figure 8). We propose propionyl-CoA and isobutyryl-CoA as novel substrates of the peroxisomal ABC transporter PXA1 (De Marcos Lousa et al., 2013). The fact that the wild type appears to be less sensitive to the catabolites suggests that acrylate was mainly detoxified by peroxisomal implication. The strong defect of *pnc1/2* plants in the degradation of these compounds reflects the necessity of intraperoxisomal ATP, as a cosubstrate of short chain carboxylic CoA synthesis (Figure 1). PXN is indirectly linked to these processes by provision of NADH for H_2O_2 detoxification. PXN also provides NAD for β -oxidation. The fact that *pxn-1* did not differ from the wild type in the feeding experiments indicated sufficient ROS

degradation, either by peroxisomal catalase and/or the peroxisomal glutathione-ascorbate cycle with NADH supply by the malate/oxaloacetate shuttle (Reumann et al., 1996; Figure 1).

Seedling growth of *pnc1/2* and *pxa1-2* mutants was affected in the presence of exogenous leucine, although leucine catabolism is thought to be restricted to mitochondria, where leucine is metabolized to acetyl-CoA and acetoacetate (Däschner et al., 2001). The last step is catalyzed by a hydroxymethylglutaryl-CoA lyase, which was reported to be dually localized to mitochondria and peroxisomes and links leucine degradation to peroxisomal metabolism (Reumann et al., 2004). The leucine feeding results could also be explained by interference of high BCAA concentration with amino acid biosynthetic pathways and interconversion of BCAA.

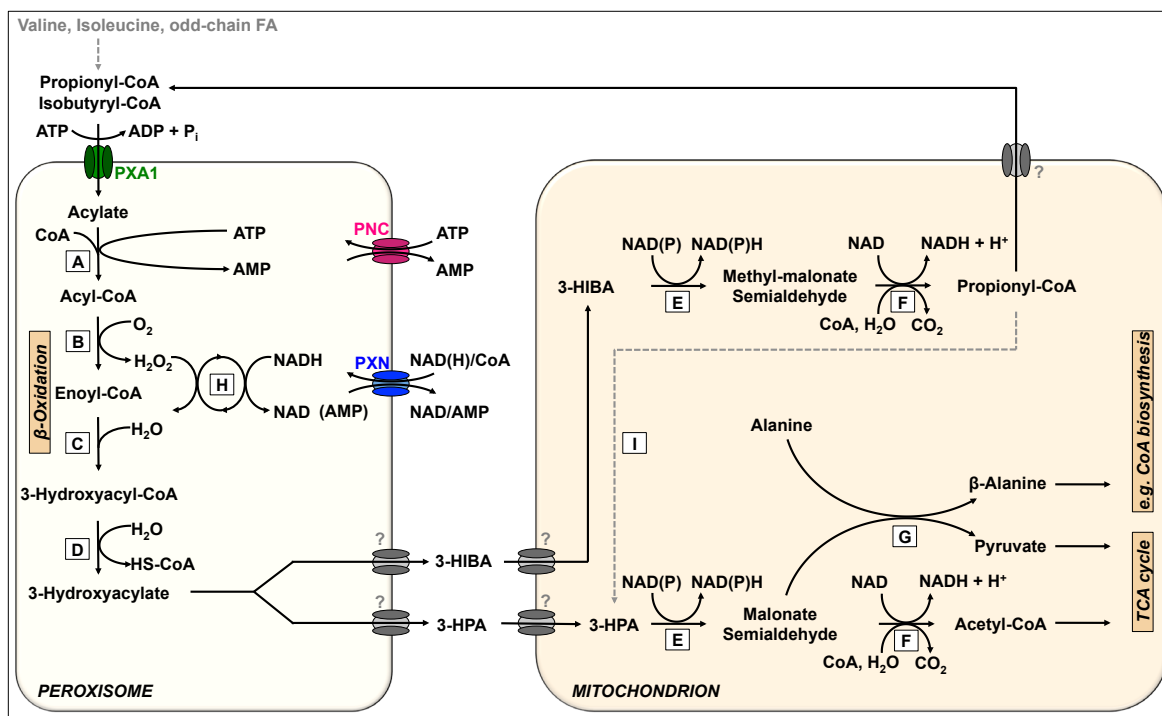


FIGURE 9. Redefined model of propionyl- and isobutyryl-CoA metabolism.

The acyclic acid propionate or more specifically its CoA ester (propionyl-CoA) derived from odd-chain fatty acids or isoleucine and isobutyryl-CoA derived from valine catabolism are metabolized to 3-hydroxypropionate (3-HPA) and 3-hydroxyisobutyrate (3-HIBA) respectively by peroxisomal β -oxidation. In the model intermediates are simplified (Acyl-CoA: propionyl-CoA/isobutyryl-CoA; Enoyl-CoA: Acrylyl-CoA and Methylacrylyl-CoA; 3-Hydroxyacyl-CoA: 3-Hydroxypropionyl-CoA/3-Hydroxyisobutyryl-CoA; 3-Hydroxyacylate: 3-HPA and 3-HIBA). Inside mitochondria 3-HIBA is converted to propionyl-CoA, which reenters peroxisomes to be oxidized to 3-HPA. The 3-HPA is converted to acetyl-CoA by mitochondrial enzymes, fueling the TCA cycle or converted to pyruvate. Enzymes: (A) Acyl-CoA synthetase, (B) Acyl-CoA oxidase, (C) Enoyl-CoA hydratase, (D) Hydroxyacyl-CoA hydrolase, (E) Hydroxyacid dehydrogenase, (F) (Methyl) malonate semialdehyde dehydrogenase, (G) β -Alanine aminotransferase, (H) Glutathione-Ascorbate cycle H₂O₂ detoxification.

β-oxidation contributes to optimal seed filling

That β -oxidation has an effect on development was already demonstrated by the *aim1* phenotype (Richmond and Bleecker, 1999). In our analysis of *pnc1/2*, *pxa1-2*, and *pxn-1* developmental senescence was accelerated compared to *Col-0*, as observed by earlier expression of the late senescence marker transcript *SAG12* (Figure 7A) and due to earlier chlorophyll breakdown (Figure S4). PXA1, PXN and PNC might therefore be negative regulators of leaf senescence. A wide variety of abiotic but also biotic stresses are known to induce senescence (Wingler and Roitsch 2008; Abbasi et al., 2009). Also hydrogen peroxide promote senescence and is part of the complex regulatory network of senescence (Bieker et al., 2012). Malfunctioning β -oxidation was already shown to be a source of ROS (Dong et al., 2009).

Extended natural senescence can lead to increased plant productivity (Egli et al., 2011). Therefore, we assumed that premature senescence negatively impacts seed yield per plant and seed quality. β -oxidation was previously shown to be important for fertility and wild-type silique size (Footitt et al., 2007a; 2007b). We observed the same reduction in silique size for *pxa1-2*, *pnc1/2* and *pxn-1*. This was probably due to compromised pollen tube elongation, which relies on β -oxidation activity. But not only overall seed biomass per plant was reduced, because we also observed a reduction in seed size, seed weight, and seed protein content. It was shown that fatty acids are degraded during natural leaf senescence (Yang and Ohlrogge, 2009) and the carbon is transported to seed-sinks to serve seed filling. In senescence organic nitrogen is relocated to reproductive tissue by phloem mediated long distance transport of e.g. glutamate to seed sink tissue (Zhang et al., 2011). Glutamate is synthesized by 2-oxoglutarate amination. Potentially all amino acids serve as N-donors. In dark treated leaf tissue catabolic pathways of isoleucine and valine have been shown to support ATP production, but the role as N-donor was previously not addressed. Glutamate, aspartate and ureides, but not BCAA have been proposed to be long distance N-transport substrates. BCAA degradation is required to recover nitrogen into the glutamate pools and consequently seed sinks.

Conclusion

β -oxidation is more deeply integrated in plant primary metabolism in vegetative and reproductive tissue than previously anticipated. Especially in stress-conditions we

could show that amino acid and fatty acid respiration were coordinated. β -oxidation seems to contribute to optimal photosynthesis not only by fatty acid degradation but also detoxification of amino acid catabolites. Especially in field conditions with occasional high light, drought, heat or cold stress, we would expect decreased β -oxidation flux, by reduced transport activity, to have a drastic effect on biomass production.

Material and Methods

Chemicals were purchased from Sigma-Aldrich. Reagents and enzymes for recombinant DNA techniques were obtained from New England Biolabs and Promega.

Isolation of T-DNA Insertion lines

pnc1-1 (SAIL_303H02), *pnc2-1* (SALK014579) and *pxa1-2* (SALK_019334) *Arabidopsis thaliana* mutants were obtained from the Nottingham Arabidopsis Stock Centre. We constructed the *pnc1/2* mutant by crossing of *pnc1-1* and *pnc2-1* (Kessel-Vigelius et al., unpublished). *pxn-1* was obtained from the GABI-Kat project of the Bielefeld University (GABI-046D01; Bernhardt et al., 2012).

Plant cultivation

Seeds were surface sterilized, stratified for 4-7 days at 4°C and germinated on 0.8% (w/v) agar-solidified half-strength MS medium (Duchefa) (with 1% (w/v) sucrose, if indicated). Plants were incubated in a 16-h-light/8-h- dark cycle (22/18°C) in growth chambers (100 $\mu\text{mol m}^{-2} \text{s}^{-1}$ light intensity).

For the analysis of seedling growth, plants were grown on half-strength MS agar plates supplemented with or without sucrose in constant darkness or in short-day conditions (8-h light/16-h dark cycles). After the indicated period, seedlings were photographed or scanned and roots or hypocotyls were measured using IMAGEJ (<http://rsbweb.nih.gov/ij>). Plate additives were added from solutions adjusted to pH 5.6. For extended darkness treatments, 25-30 day old plants were subjected to prolonged night conditions at the start of the regular night for the time indicated. To determine seed parameters plants were grown randomized and the position of plant trays was systematically rotated to minimize light effects.

PAM fluometry

In vivo chlorophyll a fluorescence assays were performed using the FluorCam FC 800-C (Photon Systems Instruments). 25-30 day-old dark-treated plants were taken directly out of the growth cabinet and used for fluorescence measurements. To investigate defects in the photosynthetic apparatus standard settings of the manufacturer's software were used.

Leaf metabolite analysis

Preparation of samples for metabolic analysis was performed as described in Fiehn (2006). Samples were harvested by shock freezing rosette leaves in liquid nitrogen. Leaves were ground in liquid nitrogen, freeze dried and 5 mg of leaf powder was used for extraction with 1.5ml of pre-chilled (-20°C) mixture of H_2O /methanol/ CHCl_3 (1:2.5:1) containing 50 μM ribitol. Following incubation under gentle agitation for 6 min at 4°C on a rotating device, samples were centrifuged for 2 min at 20.000 g. 50 μL of the supernatant was dried and used for further analysis by gas chromatography/electron-impact time-of-flight mass spectrometry, as previously described (Lee and Fiehn, 2008). Metabolite content is expressed relative to the internal standard ribitol. Extracts were additionally subjected to amino acid analysis by high-performance liquid chromatography (ZORBAX Rapid Resolution HT Eclipse Plus C18, 2.1 x 50 mm, 1.8 μm column) coupled to a diode array detector (DAD). Chlorophyll was quantified from methanol extract according (Lichtenthaler and Wellburn, 1983) and used for normalization of the three independent biological replicates.

Total seed protein quantification

Total protein content of *Col-0*, *pnc1/2*, *pxn-1*, and *pxa1-2* seeds was measured in six replicates. 10 – 25 mg (500 – 1300) seeds were homogenized with 1 ml extraction buffer (10% w/v Glycerol, 0.8 mM DTT, 1 mM PMSF 0.5% w/v, 100 mM Tris; pH: 8) using steel beads and a bead mill. The aqueous phase was purified 3 times by centrifugation (table centrifuge, 20.000 g). Protein concentrations were measured in 4 technical replicates using Pierce BCA Protein Assay Kit (Thermo Scientific).

Quantitative reverse transcriptase-polymerase chain reaction (qRT-PCR)

RNA was isolated from 10-week-old *A. thaliana* rosette leaves after a protocol developed by (Chomczynski and Sacchi, 1987). RNA integrity was determined on a 1% Agarose gel. Prior to cDNA synthesis, RNA was treated with RNase-free RQ1-DNase (Promega) as recommended by the manufacturer. The *Arabidopsis thaliana* senescence associated gene 12 (SAG12; At5g45890) transcript was examined via quantitative reverse transcription PCR (qRT-PCR). For this analysis the messenger RNAs (mRNAs) of the total RNA were transcribed into complementary DNAs (cDNAs) using the Superscript III RNase H- Reverse Transcriptase (Invitrogen, Life

Technologies). The cDNA synthesis was performed according to the manufacturers' instructions. The resulted cDNA pools were used as template for Real-time PCR with *A. thaliana* SAG12 specific oligonucleotides JW149 (TGCGGTAAATCAGTTTGCTG) and JW150 (ACGGCGACATTTTAGTTTGG). Transcript levels in *A. thaliana* were determined by quantitative RT-PCR with the MESA-SYBR-Green II Kit without ROX (Eurogentec Germany GmbH) according to the manuals instructions, run with the Standard SYBR-Green protocol of the StepOnePlus™ Real-Time PCR System (Applied Biosystems). The BLACK Oligonucleotides published by Czechowski et al. (2005) were used as reference primer pair.

Bioinformatic and statistical analysis

Pearson correlation analysis and PCA score plots were performed with the Multiple Experiment Viewer (Saeed et al., 2003). Statistical analyses were performed with GraphPad Prism 5.0. Quantitative analysis results are presented as means +SE from repeated experiments as indicated in the figure legends. Pairwise Student's t test was used to analyze statistical significance.

Supplemented data

- Fig. S1** Mean normalized transcript abundance of *PNC1*, *PXA1* and *PXN* in *Arabidopsis thaliana* rosette leaves in abiotic stress conditions
- Fig. S2** Mean of chlorophyll concentration (+SE; n=3) of 4-week-old old *Col-0*, *pnc1/2*, *pxn-1* and *pxa1-2* at the end of day, extended darkness (50 h), reillumination for 24 h after 50 h darkness and incubation in the dark for nine days (carbon starvation).
- Fig. S3** Effect of exogenous isobutyric acid supply on *Col-0*, *pnc1/2*, *pxa1-2* and *pxn-1* growth.
- Fig. S4** *pnc1/2* and *pxn-1* display accelerated leaf senescence
- Fig. S5** Heat stress treatment of 4-week-old *Col-0*, *pnc1/2*, *pxn-1* and *pxa1-2*

Acknowledgements

We thank Sarah Keßel-Vigelius for providing us with *pnc1/2* seeds. Elisabeth Klemp and Katrin Weber are acknowledged for help with GC-MS and HPLC-DAD analysis of plant extracts.

Author contributions

Jan Wiese and Martin Schroers performed the experiments. Jan Wiese, Martin Schroers, and Nicole Linka wrote the manuscript. Andreas Weber and Nicole Linka provided lab space and helpful discussions. Jan Wiese, Martin Schroers and Nicole Linka designed the experiments.

References

- Abbasi, A.-R., Saur, A., Hennig, P., Tschiersch, H., Hajirezaei, M., Hofius, D., Sonnewald, U., and Voll, L.M.** (2009). Tocopherol deficiency in transgenic tobacco (*Nicotiana tabacum* L.) plants leads to accelerated senescence. *Plant Cell Environ.* **32**: 144–157.
- Adham, A.R., Zolman, B.K., Millius, A., and Bartel, B.** (2005). Mutations in Arabidopsis acyl-CoA oxidase genes reveal distinct and overlapping roles in beta-oxidation. *Plant J.* **41**: 859–874.
- Agrimi, G., Russo, A., Pierri, C.L., and Palmieri, F.** (2012). The peroxisomal NAD⁺ carrier of Arabidopsis thaliana transports coenzyme A and its derivatives. *J. Bioenerg. Biomembr.* **44**: 333–340.
- Arai, Y., Hayashi, M., and Nishimura, M.** (2008). Proteomic identification and characterization of a novel peroxisomal adenine nucleotide transporter supplying ATP for fatty acid beta-oxidation in soybean and Arabidopsis. *Plant Cell* **20**: 3227–3240.
- Araújo, W.L., Ishizaki, K., Nunes-Nesi, A., Larson, T.R., Tohge, T., Krahnert, I., Witt, S., Obata, T., Schauer, N., Graham, I.A., Leaver, C.J., and Fernie, A.R.** (2010). Identification of the 2-hydroxyglutarate and isovaleryl-CoA dehydrogenases as alternative electron donors linking lysine catabolism to the electron transport chain of Arabidopsis mitochondria. *Plant Cell* **22**: 1549–1563.
- Araújo, W.L., Tohge, T., Ishizaki, K., Leaver, C.J., and Fernie, A.R.** (2011). Protein degradation - an alternative respiratory substrate for stressed plants. *Trends Plant Sci.* **16**: 489–498.
- Baker, A., Graham, I.A., Holdsworth, M., Smith, S.M., and Theodoulou, F.L.** (2006). Chewing the fat: beta-oxidation in signalling and development. *Trends Plant Sci.* **11**: 124–132.
- Balazadeh, S., Parlitz, S., Mueller-Roeber, B., and Meyer, R.C.** (2008). Natural developmental variations in leaf and plant senescence in Arabidopsis thaliana. *Plant Biol (Stuttg)* **10 Suppl 1**: 136–147.
- Bernhardt, K., Wilkinson, S., Weber, A.P.M., and Linka, N.** (2012). A peroxisomal carrier delivers NAD⁺ and contributes to optimal fatty acid degradation during storage oil mobilization. *Plant J.* **69**: 1–13.
- Bieker, S., Riestler, L., Stahl, M., Franzaring, J., and Zentgraf, U.** (2012). Senescence-specific alteration of hydrogen peroxide levels in Arabidopsis thaliana and oilseed rape spring variety Brassica napus L. cv. Mozart. *J Integr Plant Biol* **54**: 540–554.
- Buchanan-Wollaston, V., Page, T., Harrison, E., Breeze, E., Lim, P.O., Nam, H.G., Lin, J.-F., Wu, S.-H., Swidzinski, J., Ishizaki, K., and Leaver, C.J.** (2005). Comparative transcriptome analysis reveals significant differences in gene expression and signalling pathways between developmental and dark/starvation-induced senescence in Arabidopsis. *Plant J.* **42**: 567–585.
- Castillo, M.C. and León, J.** (2008). Expression of the beta-oxidation gene 3-ketoacyl-CoA thiolase 2 (KAT2) is required for the timely onset of natural and dark-induced leaf senescence in Arabidopsis. *J. Exp. Bot.* **59**: 2171–2179.
- Chomczynski, P. and Sacchi, N.** (1987). Single-step method of RNA isolation by acid guanidinium thiocyanate-phenol-chloroform extraction. *Anal. Biochem.* **162**: 156–159.
- Cornah, J.E., Germain, V., Ward, J.L., Beale, M.H., and Smith, S.M.** (2004). Lipid utilization, gluconeogenesis, and seedling growth in Arabidopsis mutants lacking the glyoxylate cycle enzyme malate synthase. *J. Biol. Chem.* **279**: 42916–42923.
- Czechowski, T., Stitt, M., Altmann, T., Udvardi, M.K., and Scheible, W.-R.** (2005). Genome-wide identification and testing of superior reference genes for transcript normalization in Arabidopsis. *Plant Physiol.* **139**: 5–17.
- Däschner, K., Couée, I., and Binder, S.** (2001). The mitochondrial isovaleryl-coenzyme a dehydrogenase of Arabidopsis oxidizes intermediates of leucine and valine catabolism. *Plant Physiol.* **126**: 601–612.
- De Marcos Lousa, C., van Roermund, C.W.T., Postis, V.L.G., Dietrich, D., Kerr, I.D., Wanders, R.J.A., Baldwin, S.A., Baker, A., and Theodoulou, F.L.** (2013). Intrinsic

- acyl-CoA thioesterase activity of a peroxisomal ATP binding cassette transporter is required for transport and metabolism of fatty acids. *Proc. Natl. Acad. Sci. U.S.A.* **110**: 1279–1284.
- Del Rio, L.A., Sandalio, L.M., Corpas, F.J., Palma, J.M., and Barroso, J.B.** (2006). Reactive oxygen species and reactive nitrogen species in peroxisomes. Production, scavenging, and role in cell signaling. *Plant Physiol.* **141**: 330–335.
- Do Y Lee and Fiehn, O.** (2008). High quality metabolomic data for *Chlamydomonas reinhardtii*. *Plant Methods* **4**: 7.
- Dong, C.-H., Zolman, B.K., Bartel, B., Lee, B.-H., Stevenson, B., Agarwal, M., and Zhu, J.-K.** (2009). Disruption of *Arabidopsis* CHY1 reveals an important role of metabolic status in plant cold stress signaling. *Mol Plant* **2**: 59–72.
- Egli, D.B.** (2011). Time and the Productivity of Agronomic Crops and Cropping Systems. *Agronomy Journal* **103**: 743–750.
- Engqvist, M., Drincovich, M.F., Flügge, U.-I., and Maurino, V.G.** (2009). Two D-2-hydroxy-acid dehydrogenases in *Arabidopsis thaliana* with catalytic capacities to participate in the last reactions of the methylglyoxal and beta-oxidation pathways. *J. Biol. Chem.* **284**: 25026–25037.
- Engqvist, M.K.M., Kuhn, A., Wienstroer, J., Weber, K., Jansen, E.E.W., Jakobs, C., Weber, A.P.M., and Maurino, V.G.** (2011). Plant D-2-hydroxyglutarate dehydrogenase participates in the catabolism of lysine especially during senescence. *J. Biol. Chem.* **286**: 11382–11390.
- Falcone, D.L., Ogas, J.P., and Somerville, C.R.** (2004). Regulation of membrane fatty acid composition by temperature in mutants of *Arabidopsis* with alterations in membrane lipid composition. *BMC Plant Biol.* **4**: 17.
- Fiehn, O.** (2006). Metabolite profiling in *Arabidopsis*. *Methods Mol. Biol.* **323**: 439–447.
- Footitt, S., Cornah, J.E., Pracharoenwattana, I., Bryce, J.H., and Smith, S.M.** (2007a). The *Arabidopsis* 3-ketoacyl-CoA thiolase-2 (*kat2-1*) mutant exhibits increased flowering but reduced reproductive success. *J. Exp. Bot.* **58**: 2959–2968.
- Footitt, S., Dietrich, D., Fait, A., Fernie, A.R., Holdsworth, M.J., Baker, A., and Theodoulou, F.L.** (2007b). The COMATOSE ATP-binding cassette transporter is required for full fertility in *Arabidopsis*. *Plant Physiol.* **144**: 1467–1480.
- Footitt, S., Slocombe, S.P., Larner, V., Kurup, S., Wu, Y., Larson, T., Graham, I., Baker, A., and Holdsworth, M.** (2002). Control of germination and lipid mobilization by COMATOSE, the *Arabidopsis* homologue of human ALDP. *EMBO J.* **21**: 2912–2922.
- Fulda, M., Shockey, J., Werber, M., Wolter, F.P., and Heinz, E.** (2002). Two long-chain acyl-CoA synthetases from *Arabidopsis thaliana* involved in peroxisomal fatty acid beta-oxidation. *Plant J.* **32**: 93–103.
- Hu, J., Baker, A., Bartel, B., Linka, N., Mullen, R.T., Reumann, S., and Zolman, B.K.** (2012). Plant peroxisomes: biogenesis and function. *Plant Cell* **24**: 2279–2303.
- Ishizaki, K., Larson, T.R., Schauer, N., Fernie, A.R., Graham, I.A., and Leaver, C.J.** (2005). The critical role of *Arabidopsis* electron-transfer flavoprotein:ubiquinone oxidoreductase during dark-induced starvation. *Plant Cell* **17**: 2587–2600.
- Khan, B.R., Adham, A.R., and Zolman, B.K.** (2012). Peroxisomal Acyl-CoA oxidase 4 activity differs between *Arabidopsis* accessions. *Plant Mol. Biol.* **78**: 45–58.
- Kilian, J., Whitehead, D., Horak, J., Wanke, D., Weinl, S., Batistic, O., D'Angelo, C., Bornberg-Bauer, E., Kudla, J., and Harter, K.** (2007). The AtGenExpress global stress expression data set: protocols, evaluation and model data analysis of UV-B light, drought and cold stress responses. *Plant J.* **50**: 347–363.
- Kipp, E. and Boyle, M.** (2013). The Effects of Heat Stress on Reactive Oxygen Species Production and Chlorophyll Concentration in *Arabidopsis thaliana*. *Research in Plant Sciences* **1**: 20–23.
- Kono, Y. and Fridovich, I.** (1982). Superoxide radical inhibits catalase. *J. Biol. Chem.* **257**: 5751–5754.
- Kunz, H.-H., Scharnewski, M., Feussner, K., Feussner, I., Flügge, U.-I., Fulda, M., and Gierth, M.** (2009). The ABC transporter PXA1 and peroxisomal beta-oxidation are vital for metabolism in mature leaves of *Arabidopsis* during extended darkness. *Plant Cell* **21**:

- 2733–2749.
- Lange, P.R., Eastmond, P.J., Madagan, K., and Graham, I.A.** (2004). An Arabidopsis mutant disrupted in valine catabolism is also compromised in peroxisomal fatty acid beta-oxidation. *FEBS Lett.* **571**: 147–153.
- Larkindale, J., Hall, J.D., Knight, M.R., and Vierling, E.** (2005). Heat stress phenotypes of Arabidopsis mutants implicate multiple signaling pathways in the acquisition of thermotolerance. *Plant Physiol.* **138**: 882–897.
- Lichtenthaler, H.K. and Weellburn, A.R.** (1983). Determinations of total carotenoids and chlorophylls a and b of leaf extracts in different solvents. *Biochem. Soc. Trans.* **11**: 591–592.
- Linka, N., Theodoulou, F.L., Haslam, R.P., Linka, M., Napier, J.A., Neuhaus, H.E., and Weber, A.P.M.** (2008). Peroxisomal ATP import is essential for seedling development in Arabidopsis thaliana. *Plant Cell* **20**: 3241–3257.
- Lucas, K.A., Filley, J.R., Erb, J.M., Graybill, E.R., and Hawes, J.W.** (2007). Peroxisomal metabolism of propionic acid and isobutyric acid in plants. *J. Biol. Chem.* **282**: 24980–24989.
- Ma, C., Haslbeck, M., Babujee, L., Jahn, O., and Reumann, S.** (2006). Identification and characterization of a stress-inducible and a constitutive small heat-shock protein targeted to the matrix of plant peroxisomes. *Plant Physiol.* **141**: 47–60.
- Maxwell, K. and Johnson, G.N.** (2000). Chlorophyll fluorescence—a practical guide. *J. Exp. Bot.* **51**: 659–668.
- Mhamdi, A., Noctor, G., and Baker, A.** (2012). Plant catalases: peroxisomal redox guardians. *Arch. Biochem. Biophys.* **525**: 181–194.
- Mitsuya, S., Kuwahara, J., Ozaki, K., Saeki, E., Fujiwara, T., and Takabe, T.** (2011). Isolation and characterization of a novel peroxisomal choline monooxygenase in barley. *Planta* **234**: 1215–1226.
- Miyashita, Y. and Good, A.G.** (2008). NAD(H)-dependent glutamate dehydrogenase is essential for the survival of Arabidopsis thaliana during dark-induced carbon starvation. *J. Exp. Bot.* **59**: 667–680.
- Obayashi, T., Hayashi, S., Saeki, M., Ohta, H., and Kinoshita, K.** (2009). ATTED-II provides coexpressed gene networks for Arabidopsis. *Nucleic Acids Res.* **37**: D987–91.
- Pruzinská, A., Tanner, G., Anders, I., Roca, M., and Hörtensteiner, S.** (2003). Chlorophyll breakdown: pheophorbide a oxygenase is a Rieske-type iron-sulfur protein, encoded by the accelerated cell death 1 gene. *Proc. Natl. Acad. Sci. U.S.A.* **100**: 15259–15264.
- Queval, G., Issakidis-Bourguet, E., Hoerberichts, F.A., Vandorpe, M., Gakière, B., Vanacker, H., Miginiac-Maslow, M., Van Breusegem, F., and Noctor, G.** (2007). Conditional oxidative stress responses in the Arabidopsis photorespiratory mutant cat2 demonstrate that redox state is a key modulator of daylength-dependent gene expression, and define photoperiod as a crucial factor in the regulation of H₂O₂-induced cell death. *Plant J.* **52**: 640–657.
- Reumann, S., Ma, C., Lemke, S., and Babujee, L.** (2004). AraPeroX. A database of putative Arabidopsis proteins from plant peroxisomes. *Plant Physiol.* **136**: 2587–2608.
- Reumann, S., Maier, E., Benz, R., and Heldt, H.W.** (1996). A specific porin is involved in the malate shuttle of leaf peroxisomes. *Biochem. Soc. Trans.* **24**: 754–757.
- Richmond, T.A. and Bleecker, A.B.** (1999). A defect in beta-oxidation causes abnormal inflorescence development in Arabidopsis. *Plant Cell* **11**: 1911–1924.
- Saeed, A.I. et al.** (2003). TM4: a free, open-source system for microarray data management and analysis. *BioTechniques* **34**: 374–378.
- Schmid, M., Davison, T.S., Henz, S.R., Pape, U.J., Demar, M., Vingron, M., Schölkopf, B., Weigel, D., and Lohmann, J.U.** (2005). A gene expression map of Arabidopsis thaliana development. *Nat. Genet.* **37**: 501–506.
- Schönfeld, P. and Wojtczak, L.** (2008). Fatty acids as modulators of the cellular production of reactive oxygen species. *Free Radic. Biol. Med.* **45**: 231–241.
- Schwab, M.A., Sauer, S.W., Okun, J.G., Nijtmans, L.G.J., Rodenburg, R.J.T., van den Heuvel, L.P., Dröse, S., Brandt, U., Hoffmann, G.F., Laak, Ter, H., Kölker, S., and Smeitink, J.A.M.** (2006). Secondary mitochondrial dysfunction in propionic aciduria: a

- pathogenic role for endogenous mitochondrial toxins. *Biochem. J.* **398**: 107–112.
- Shi, W.M., Muramoto, Y., Ueda, A., and Takabe, T.** (2001). Cloning of peroxisomal ascorbate peroxidase gene from barley and enhanced thermotolerance by overexpressing in *Arabidopsis thaliana*. *Gene* **273**: 23–27.
- Tanaka, R., Hirashima, M., Satoh, S., and Tanaka, A.** (2003). The *Arabidopsis*-accelerated cell death gene *ACD1* is involved in oxygenation of pheophorbide a: inhibition of the pheophorbide a oxygenase activity does not lead to the “stay-green” phenotype in *Arabidopsis*. *Plant Cell Physiol.* **44**: 1266–1274.
- Taylor, N.L., Tan, Y.-F., Jacoby, R.P., and Millar, A.H.** (2009). Abiotic environmental stress induced changes in the *Arabidopsis thaliana* chloroplast, mitochondria and peroxisome proteomes. *J Proteomics* **72**: 367–378.
- Tegeder, M.** (2014). Transporters involved in source to sink partitioning of amino acids and ureides: opportunities for crop improvement. *J. Exp. Bot.*
- Troncoso-Ponce, M.A., Cao, X., Yang, Z., and Ohlrogge, J.B.** (2013). Lipid turnover during senescence. *Plant Sci.* **205-206**: 13–19.
- Williams, J.** (1928). The decomposition of hydrogen peroxide by liver catalase. *J. Gen. Physiol.* **11**: 309–337.
- Wingler, A. and Roitsch, T.** (2008). Metabolic regulation of leaf senescence: interactions of sugar signalling with biotic and abiotic stress responses. *Plant Biol (Stuttg)* **10 Suppl 1**: 50–62.
- Yang, Z. and Ohlrogge, J.B.** (2009). Turnover of fatty acids during natural senescence of *Arabidopsis*, *Brachypodium*, and switchgrass and in *Arabidopsis* beta-oxidation mutants. *Plant Physiol.* **150**: 1981–1989.
- Zhang, X., Ju, H.-W., Chung, M.-S., Huang, P., Ahn, S.-J., and Kim, C.S.** (2011). The R-R-type MYB-like transcription factor, *AtMYBL*, is involved in promoting leaf senescence and modulates an abiotic stress response in *Arabidopsis*. *Plant Cell Physiol.* **52**: 138–148.
- Zolman, B.K., Martinez, N., Millius, A., Adham, A.R., and Bartel, B.** (2008). Identification and characterization of *Arabidopsis* indole-3-butyric acid response mutants defective in novel peroxisomal enzymes. *Genetics* **180**: 237–251.
- Zolman, B.K., Monroe-Augustus, M., Thompson, B., Hawes, J.W., Krukenberg, K.A., Matsuda, S.P., and Bartel, B.** (2001a). *chy1*, an *Arabidopsis* mutant with impaired beta-oxidation, is defective in a peroxisomal beta-hydroxyisobutyryl-CoA hydrolase. *J. Biol. Chem.* **276**: 31037–31046.
- Zolman, B.K., Silva, I.D., and Bartel, B.** (2001b). The *Arabidopsis* *pxa1* mutant is defective in an ATP-binding cassette transporter-like protein required for peroxisomal fatty acid beta-oxidation. *Plant Physiol.* **127**: 1266–1278.

Supplemented Results

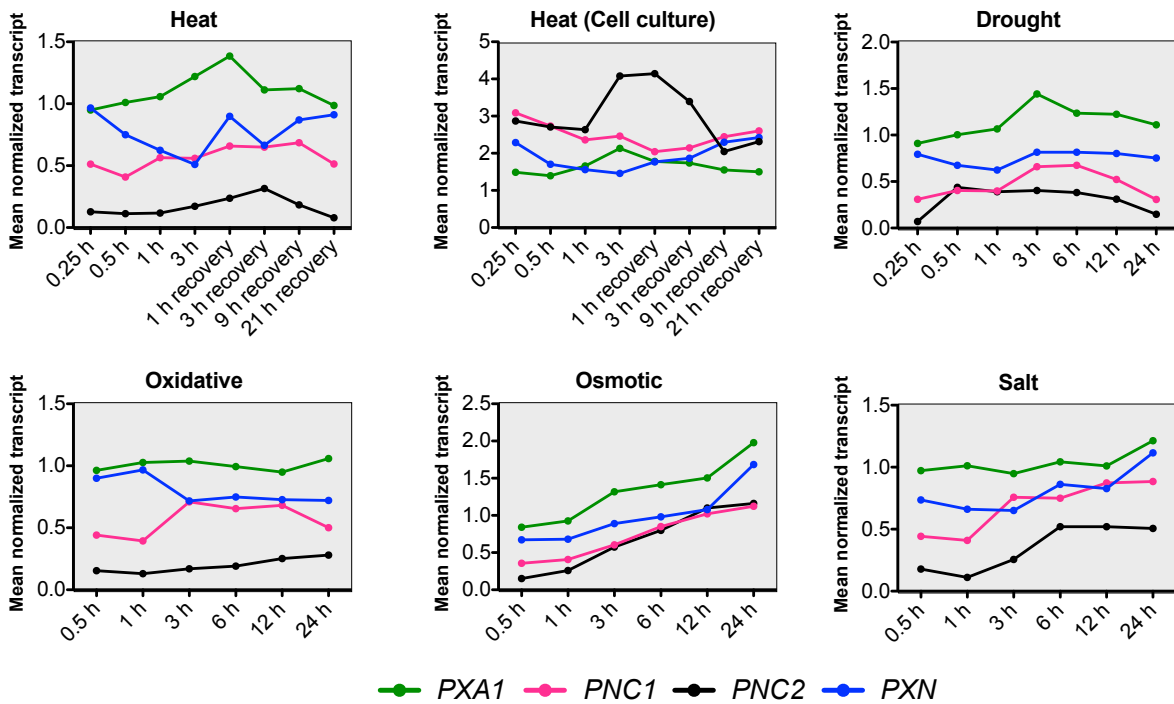


FIGURE S1. Mean normalized transcript abundance of *PXA1*, *PNC1*, *PNC2*, and *PXN* in *Arabidopsis thaliana* rosette leaves in the indicated abiotic stress conditions. Data derived from Kilian et al. (2007).

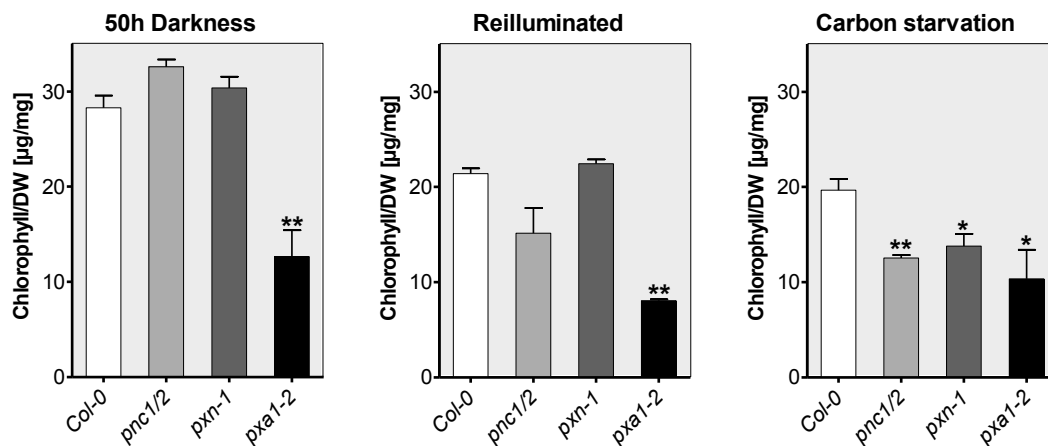


FIGURE S2. Mean of chlorophyll concentration (+SE; n=3) of 4-week-old *old Col-0*, *pnc1/2*, *pxn-1* and *pxa1-2* at the end of day, extended darkness (50 h), reillumination for 24 h after 50 h darkness and incubation in the dark for nine days (Carbon starvation). Differences between the mean of biological replicates of each measurement were marked as statistically significant (t-test) with the *Col-0* control by (*), (**), or (***) at respective significance levels of ($P < 0.05$), ($P < 0.01$) or ($P < 0.001$).

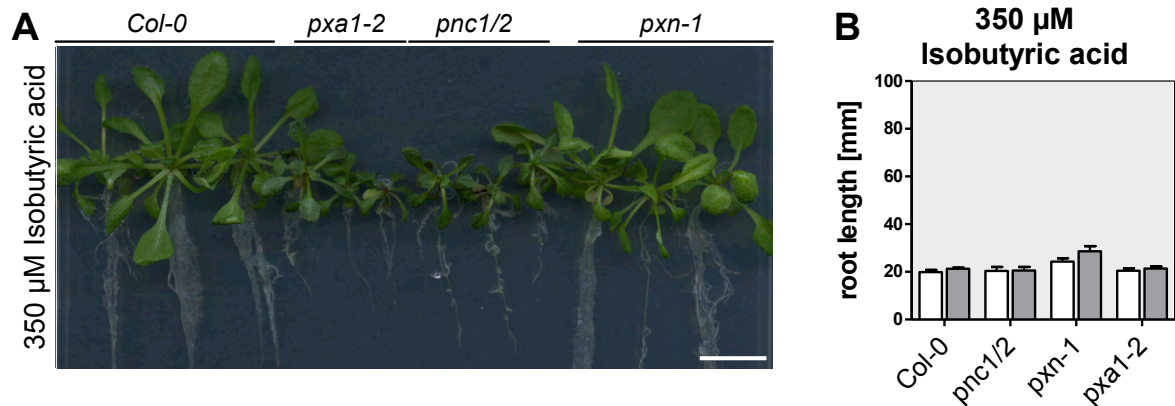


FIGURE S3. Effect of exogenous isobutyric acid supply on growth of *Col-0*, *pnc1/2*, *pxa1-2* and *pxn-1*. **(A)** Photograph of 30-d old seedling grown on 350 μ M isobutyric acid. Seeds were germinated on 0.5x MS medium supplied with 1% (w/v) sucrose and transferred to the supplemented plates. Scale bar: 10 mm.

(B) Mean primary root length (+SE) measured 1 day and 14 days (grey bars) after transfer to the feeding plates. Data presents the primary root length in mm, visualized is the mean of seven to 16 replicates with SE. There was no statistical difference for $P < 0.05$ detected (Student's t-test).

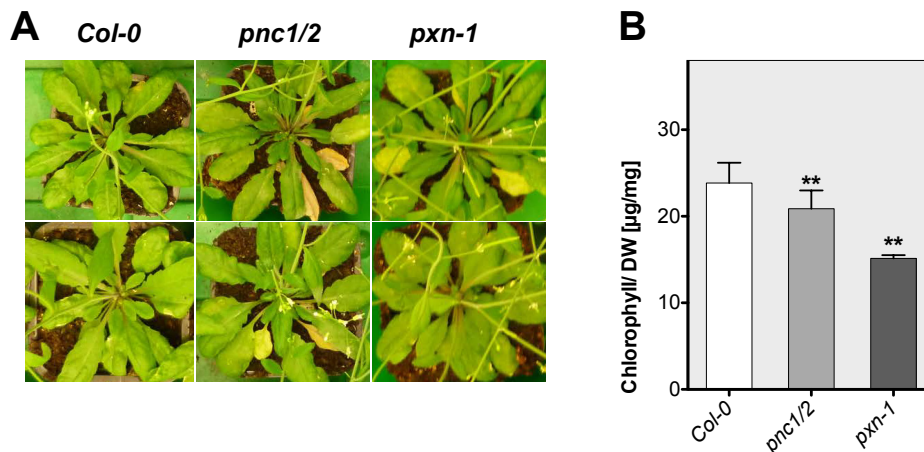


FIGURE S4. *pnc1/2* and *pxn-1* display accelerated leaf senescence.

(A) In green aged rosette leaves chlorophyll contents of *pnc1/2* and *pxn-1* are reduced in comparison to the wild-type.

(B) Differences between the mean of at least three biological replicates (SE) of each measurement were marked as statistically significant (t-test) with the *Col-0* control by (*), (**) or (***) at respective significance levels of ($P < 0.05$), ($P < 0.01$) or ($P < 0.001$).

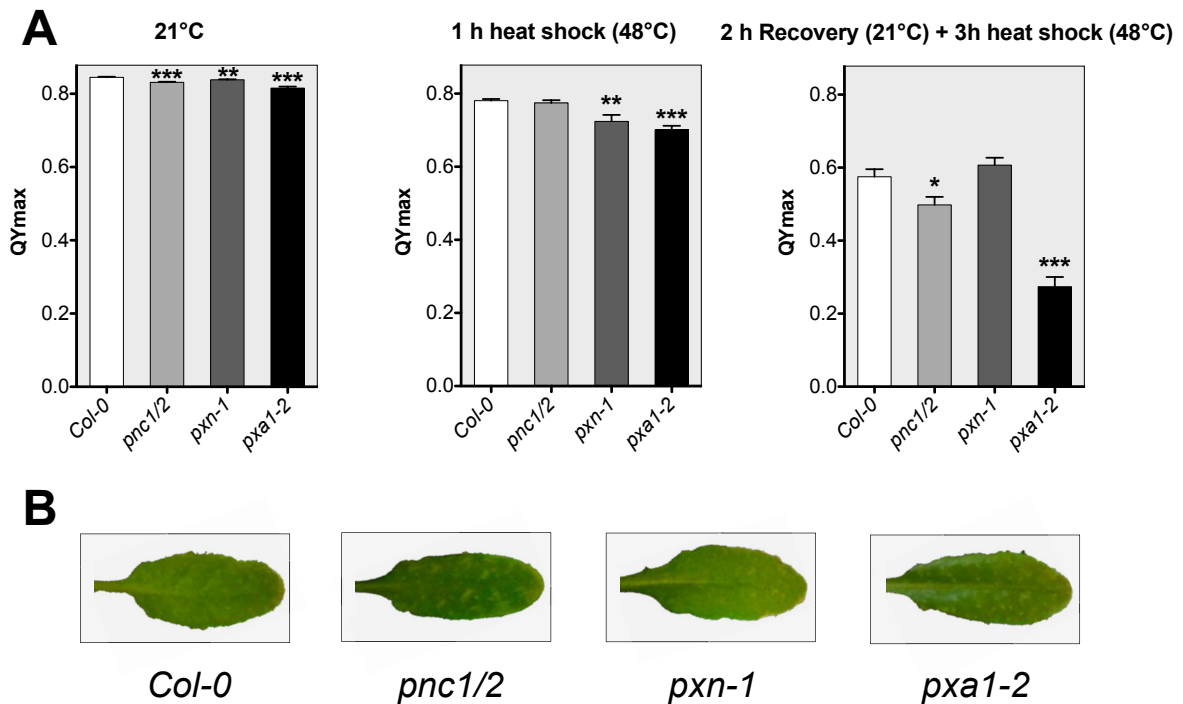


FIGURE S5. Heat stress treatment of 4-week-old *Col-0*, *pnc1/2*, *pxn-1* and *pxa1-2*.

(A) Mean of maximum quantum yield (+SE; n=3) of 4-week-old *Col-0*, *pnc1/2*, *pxn-1* and *pxa1-2* after exposure to 1 hour darkness (21°C), 1 h heat shock (48°C) and 2 h recovery at 21°C and 3 h heat shock (48°C). Differences between the mean (+SE) of each treatment were marked as statistically significant (t-test) with the *Col-0* control by (*), (**) or (***) at respective significance levels of ($P < 0.05$), ($P < 0.01$) or ($P < 0.001$). FAc: Fluoroacetic acid. Scale bar: 10 mm.

(B) Photograph of heat stressed leaves 24 h after the treatment. Necrotic lesions are more abundant for *pxa1-2*, *pnc1/2* and *pxn-1*.

V. Concluding remarks and outlook

This thesis set out to address physiological implications of MPV17/PMP22 proteins in the mitochondrial and peroxisomal membranes of *Saccharomyces cerevisiae* (Manuscript 1) and *Arabidopsis thaliana* (Manuscript 2). Experimental evidence points to a role of mitochondrial Sym1p (Trott and Morano, 2004; Spinazzola et al., 2006; Dallabona et al., 2010) and peroxisomal PMP22 (Tugal et al., 1999; Murphy et al., 2003) to form aqueous-pores in lipid bilayers that enable selective diffusion of small solutes. Channel forming activity was previously described for Sym1p (Reinhold et al., 2012) and the mammalian MPV17/PMP22-type protein peroxisomal membrane protein 2 (Pmp2; Rokka et al., 2009), but also for plant peroxisome membrane fractions (Reumann et al., 1995; 1996; 1997). Heterologous expression of mitochondria-targeted PMP22 suppressed the growth phenotype of the *sym1Δ* yeast mutant, indicating Sym1p and PMP22 to have analogous functions. Future research will need to determine if these proteins are general diffusion pores or if the translocation is restricted to certain molecular species, such as 3-hydroxypropionate.

Studies of *sym1Δ* revealed Sym1p to be important for the availability of TCA cycle intermediates at restrictive growth conditions as well as a role of Sym1p in preventing the accumulation of metabolites originating from mitochondrial pyruvate. Feeding of TCA and glyoxylate cycle intermediates restored wild-type growth at 37°C. Previously, it was assumed that *S. cerevisiae* cannot grow on propionate as sole carbon source (Graybill et al., 2007). However, we showed that propionate-sustained growth was possible at 37°C and depended on 2-methylcitrate-cycle activity to use propionate and methylmalonate as sole carbon source. Yeast metabolism was revealed to be more flexible than previously anticipated. Mutant analysis showed that the growth on propionate and methylmalonate was facilitated through Sym1p. Genetic evidence confirmed the necessity of *SYM1* in the 2-methylcitrate cycle and revealed that the 2-methylcitrate cycle is needed for methylmalonate degradation.

Dysfunctional TCA cycle and mtDNA depletion in *sym1Δ* pointed towards the possibility that Sym1p is needed to maintain Succinyl-CoA synthetase function (Chinnery, 2007). In humans the mutation of Succinyl-CoA synthetase leads to similar clinical symptoms as *Mpv17* (Viscomi et al., 2008; Ostergaard, 2008; Kölker and Okun, 2005; Fenton and Gravel, 2001; Suomalainen and Isohanni, 2010). Mutations in mitochondrial genes display numerous clinical phenotypes and in the

past yeast was used successfully to model human mitochondrial disease (Baile and Claypool, 2013). To this end *sym1Δ* should to be further investigated to fully understand *Mpv17* function. Future research could target Succinyl-CoA synthetase activity in *sym1Δ* and elucidate the bottleneck in *sym1Δ* mitochondrial function by measurement of flux through the TCA cycle and anaplerotic reactions after feeding of labeled substrates. In this study *XDJ1* and *EHD3* gene products were proposed to be involved in methylmalonyl-CoA conversions and corresponding activities should be verified by *in vitro* enzyme activity measurements.

SYM2 was identified due to structural and regulatory similarities to *SYM1*. Similar to Sym1p, Sym2p was needed to support growth on ethanol at 37°C. To elucidate *SYM2* function in glyoxylate cycle intermediate shuttling a *cat2Δ sym2Δ* could be generated to potentially reveal an oleic acid growth defect. Another interesting point would also be to further analyze the function of *CIT2*. This gene is involved in glyoxylate cycle and propionyl-CoA metabolism (Graybill et al., 2007) and has recently been reported to be indispensable for thermotolerance (Gibney et al., 2013).

The plant peroxisomal protein of 22 kDa (PMP22) was shown to be important for general peroxisome function, as indicated by formation of peroxisome clusters in *pmp22* hypocotyls. This was previously described for highly oxidized peroxisomes (Shibata et al., 2013). We established *pmp22* T-DNA and miRNA mutants that had compromised growth of seedling hypocotyls by a block of fatty acid β-oxidation and glyoxylate cycle activity. PMP22 was needed for conversion of storage oil into respiratory substrates and gluconeogenic Carbon units, which became visible in *pmp22* mutants by chlorophyll degradation after extended darkness and in natural senescence. Growth of *pmp22* mutants was sensitive to the presence of branched-chain amino acids (BCAA) and associated catabolites (isobutyrate, propionate and acrylate). Phenotypic similarities to a peroxisomal mutant in valine catabolism led to the discussion that PMP22 catalyzes the export of 3-Hydroxypropionate, the end product of peroxisomal BCAA conversion.

Our study unraveled the presence of ten PMP22-type genes in *A. thaliana* and future research ought address the roles of the plastidic and mitochondrial proteins to fully understand the biology of plastids and mitochondria. This study provides evidence that At3g24570 is a metabolite channel by suppression of the *sym1Δ* phenotype and could be involved in propionate export from the mitochondrion.

Similar roles as for PMP22 in extended darkness were revealed for PXA1 previously (Kunz et al., 2009). We showed that also the activity of PXN and PNC is needed for resistance to extended darkness (*Manuscript 3*). PXA1 and PNC1 are needed for propionate and isobutyrylate metabolism. Defects in metabolic conversion of isobutyryl-CoA and propionyl-CoA have been associated with severe diseases in humans and are well characterized. In plants these molecules are released in the degradation of BCAA, phytol and odd-chain fatty acids. BCAA degradation has recently attracted attention: in stressed plants BCAA have been shown to reduce the mitochondrial ubiquinone pool and support respiration (Araujo et al., 2010). However, the fate of the mitochondrial generated propionyl-CoA or defects in propionyl-CoA metabolism were neglected. Here we reported by analysis of β -oxidation mutants, that peroxisomes are essential to degrade propionate. PXA1 was implicated in the import of the short monocarboxylic acids. Future research should analyze a possible feedback inhibition of initial mitochondrial reaction of BCAA breakdown by propionate or propionyl-CoA as this could partially account for reduced N-mobilization to seeds in the β -oxidation mutants.

Leaf senescence and seed filling are synchronized processes (Pottier et al., 2014). *pmp22*, *pnc1/2*, *pxa1* and *pxn-1* *A. thaliana* mutants had reduced seed yield and seeds were filled with less nutrients. The plants might be disturbed on whole plant nutrient relocation efficiency. Natural senescence is the final stage of plant development and has been shown to substantially limit plant biomass and seed yield (Gregersen et al., 2013). Our work implies that peroxisomal β -oxidation could be used as a target of engineering to ameliorate natural senescence and increase plant productivity.

References

- Araujo, W.L., Ishizaki, K., Nunes-Nesi, A., Larson, T.R., Tohge, T., Krahnert, I., Witt, S., Obata, T., Schauer, N., Graham, I.A., Leaver, C.J., and Fernie, A.R.** (2010). Identification of the 2-Hydroxyglutarate and Isovaleryl-CoA Dehydrogenases as Alternative Electron Donors Linking Lysine Catabolism to the Electron Transport Chain of Arabidopsis Mitochondria. *The Plant Cell* **22**: 1549–1563.
- Baile, M.G. and Claypool, S.M.** (2013). The power of yeast to model diseases of the powerhouse of the cell. *Front Biosci (Landmark Ed)* **18**: 241–278.
- Chinnery, P.F.** (2007). Mutations in SUCLA2: a tandem ride back to the Krebs cycle. *Brain* **130**: 606–609.
- Dallabona, C., Marsano, R.M., Arzuffi, P., Ghezzi, D., Mancini, P., Zeviani, M., Ferrero, I., and Donnini, C.** (2010). Sym1, the yeast ortholog of the MPV17 human disease protein, is a stress-induced bioenergetic and morphogenetic mitochondrial modulator. *Human Molecular Genetics* **19**: 1098–1107.
- Fenton, W.A. and Gravel, R.A.** (2001). Disorders of propionate and methylmalonate metabolism. *The metabolic and molecular bases of inherited disease* **8**: 2165–2193.
- Gibney, P.A., Lu, C., Caudy, A.A., Hess, D.C., and Botstein, D.** (2013). Yeast metabolic and signaling genes are required for heat-shock survival and have little overlap with the heat-induced genes. *Proceedings of the National Academy of Sciences* **110**: E4393–402.
- Graybill, E.R., Rouhier, M.F., Kirby, C.E., and Hawes, J.W.** (2007). Functional comparison of citrate synthase isoforms from *S. cerevisiae*. *Archives of Biochemistry and Biophysics* **465**: 26–37.
- Gregersen, P.L., Culetic, A., Boschian, L., and Krupinska, K.** (2013). Plant senescence and crop productivity. *Plant Mol Biol* **82**: 603–622.
- Kölker, S. and Okun, J.G.** (2005). Methylmalonic acid — an endogenous toxin? *Cell. Mol. Life Sci.* **62**: 621–624.
- Kunz, H.-H., Scharnewski, M., Feussner, K., Feussner, I., Flügge, U.-I., Fulda, M., and Gierth, M.** (2009). The ABC transporter PXA1 and peroxisomal beta-oxidation are vital for metabolism in mature leaves of Arabidopsis during extended darkness. *The Plant Cell* **21**: 2733–2749.
- Murphy, M.A., Phillipson, B.A., Baker, A., and Mullen, R.T.** (2003). Characterization of the targeting signal of the Arabidopsis 22-kD integral peroxisomal membrane protein. *Plant Physiology* **133**: 813–828.
- Ostergaard, E.** (2008). Disorders caused by deficiency of succinate-CoA ligase. *J Inherit Metab Dis* **31**: 226–229.
- Pottier, M., Masclaux-Daubresse, C., Yoshimoto, K., and Thomine, S.** (2014). Autophagy as a possible mechanism for micronutrient remobilization from leaves to seeds. *Front Plant Sci* **5**: 11.
- Reinhold, R., Krüger, V., Meinecke, M., Schulz, C., Schmidt, B., Grunau, S.D., Guiard, B., Wiedemann, N., van der Laan, M., Wagner, R., Rehling, P., and Dudek, J.** (2012). The channel-forming Sym1 protein is transported by the TIM23 complex in a presequence-independent manner. *Molecular and Cellular Biology* **32**: 5009–5021.
- Reumann, S., Bettermann, M., Benz, R., and Heldt, H.W.** (1997). Evidence for the Presence of a Porin in the Membrane of Glyoxysomes of Castor Bean. *Plant Physiology* **115**: 891–899.
- Reumann, S., Maier, E., Benz, R., and Heldt, H.W.** (1996). A specific porin is involved in the malate shuttle of leaf peroxisomes. *Biochem. Soc. Trans.* **24**: 754–757.
- Reumann, S., Maier, E., Benz, R., and Heldt, H.W.** (1995). The membrane of leaf peroxisomes contains a porin-like channel. *J. Biol. Chem.* **270**: 17559–17565.
- Rokka, A., Antonenkov, V.D., Soininen, R., Immonen, H.L., Pirilä, P.L., Bergmann, U., Sormunen, R.T., Weckström, M., Benz, R., and Hiltunen, J.K.** (2009). Pxmp2 Is a Channel-Forming Protein in Mammalian Peroxisomal Membrane. *PLoS ONE* **4**: e5090.
- Shibata, M., Oikawa, K., Yoshimoto, K., Kondo, M., Mano, S., Yamada, K., Hayashi, M., Sakamoto, W., Ohsumi, Y., and Nishimura, M.** (2013). Highly Oxidized Peroxisomes

- Are Selectively Degraded via Autophagy in Arabidopsis. *The Plant Cell*.
- Spinazzola, A. et al.** (2006). MPV17 encodes an inner mitochondrial membrane protein and is mutated in infantile hepatic mitochondrial DNA depletion. *Nat. Genet.* **38**: 570–575.
- Suomalainen, A. and Isohanni, P.** (2010). Mitochondrial DNA depletion syndromes--many genes, common mechanisms. *Neuromuscul. Disord.* **20**: 429–437.
- Trott, A. and Morano, K.A.** (2004). SYM1 is the stress-induced *Saccharomyces cerevisiae* ortholog of the mammalian kidney disease gene Mpv17 and is required for ethanol metabolism and tolerance during heat shock. *Eukaryotic Cell* **3**: 620–631.
- Tugal, H.B., Pool, M., and Baker, A.** (1999). Arabidopsis 22-kilodalton peroxisomal membrane protein. Nucleotide sequence analysis and biochemical characterization. *Plant Physiology* **120**: 309–320.
- Viscomi, C., Spinazzola, A., Maggioni, M., Fernandez-Vizarra, E., Massa, V., Pagano, C., Vettor, R., Mora, M., and Zeviani, M.** (2008). Early-onset liver mtDNA depletion and late-onset proteinuric nephropathy in Mpv17 knockout mice. *Human Molecular Genetics* **18**: 12–26.

VI.1 Manuscript 4

Agrobacterium-mediated *Arabidopsis thaliana* transformation: an overview of T-DNA binary vectors, floral dip and screening for homozygous lines.

Kristin Bernhardt*, Sarah Vigelius*, Jan Wiese*, Nicole Linka
and Andreas P.M. Weber[†]

Department of Plant Biochemistry, Heinrich-Heine University Düsseldorf, 40225
Düsseldorf, Germany

* Co-first authors

[†] Corresponding author

Technical note**Agrobacterium-mediated *Arabidopsis thaliana* transformation: an overview of T-DNA binary vectors, floral dip and screening for homozygous lines****Kristin Bernhardt¹, Sarah K. Vigelius¹, Jan Wiese¹, Nicole Linka, and Andreas P.M. Weber^{2,*}**^{1,2} Institute of Plant Biochemistry, Heinrich-Heine University Düsseldorf, 40225 Düsseldorf, Germany; ¹ First authors; these authors contributed equally to this manuscript. ² Correspondence to: andreas.weber@uni-duesseldorf.de

For more than two decades *Agrobacterium*-mediated stable genetic transformation of plant cells is a routine laboratory method to generate transgenic plants. The natural capability of *Agrobacterium tumefaciens* to infect plants is thereby exploited for transferring foreign genes into plant cells. During stable transformation engineered DNA fragments are integrated into the plant genome and can be passed on to the next generations. The host specificity of *Agrobacteria* to plant species is limited and the genetic mechanisms underlying host specificity are complex. Besides *Arabidopsis thaliana*, *Agrobacterium tumefaciens* is also capable of successfully transforming a large variety of other plant species, such as maize or rice.

Using *Agrobacteria* to transform *Arabidopsis* is straightforward, requiring only standard laboratory equipment. Transformation by floral dip is easy and can be performed by non-specialists. Due to its small size, short generation time, high seed production and easy handling, *Arabidopsis*, which has emerged as model organism for plant biology research, is frequently chosen to generate transgenic plants.

This review focuses on the generation of transgenic *Arabidopsis* plants by *Agrobacteria* using the floral dip method. Besides a simplified protocol for the *Agrobacterium*-mediated transformation, we here describe common *Agrobacterium* strains and suitable binary T-DNA vectors. Further, we focus on plant selection to finally isolate homozygous transgenic mutant lines.

Journal of Endocytobiosis and Cell Research (2012) 19-28

Category: technical notes

Keywords: Transgenic plant, transformation technology, *Agrobacteria*, *Arabidopsis*, floral dip method, binary vectors

Received: 20 February 2012; Accepted: 09 March 2012

Introduction

An important step in plant science was taken when Marc van Montagu and Jeff Schell discovered the genetic transfer

mechanism between *Agrobacteria* and plants (Van Larebeke et al. 1974). Later, this finding enabled researchers to perform controlled expression of transgenes in plants. In early experiments tissue cultures were transformed, though regenerating plant tissue is difficult and laborious (Lloyd et al. 1986; Valvekens et al. 1988). In 1987, Marks and Feldman established a technique, which did not require tissue culture. Instead, transgenic plants were generated by co-cultivation of *Arabidopsis* seeds with *Agrobacteria* (Feldman and Marks 1987). However, the reproducibility of this method proved difficult and generation of transgenic lines took several years. Plant transformation was improved when Pelletier and colleagues succeeded in transforming *Arabidopsis* plants by vacuum infiltration (Bechtold et al. 1993). In the late 1990s protocols were further simplified. Transgenic plants were gained by dipping inflorescences into *Agrobacteria* solution (Clough and Bent 1998). Although other transformation methods, like particle bombardment, protoplast bombardment or direct gene transfer into protoplasts (Negrutiu et al. 1987) are available, *Agrobacterium*-mediated plant transformation remains the most frequently used method (Vain 2007).

Genetically altered plants are important experimental tools to both basic and applied molecular research, allowing the investigation of functions of a gene-of interest (GOI) *in planta* by either silencing or mis-expression. Loss-of-function can be accomplished by creating hairpin RNA molecules, which evoke the formation of small interfering RNAs (siRNAs). These molecules were shown to down-regulate gene functions (Smith et al. 2000; Small 2007). Today, artificial micro RNAs (amiRNAs) are more commonly used to silence genes. This is because amiRNAs, generated from endogenous precursors, do more specifically hit target genes than siRNAs (Schwab et al. 2005; Alvarez et al. 2006; Schwab et al. 2006). Ectopic over-expression of genes is achieved by placing the GOI downstream of a strong heterologous promoter, like the cauliflower mosaic virus 35S promoter (p35S) or the ubiquitin10 promoter (pUB10). To determine its subcellular localisation or to purify the GOI, it can be translationally fused to a fluorescent protein or purification tag, either controlled by its endogenous or a heterologous promoter (Karimi et al. 2007). The activity of a promoter can be analyzed by cloning its sequence upstream of a reporter gene, such as β -glucuronidase (GUS) (Jefferson et al. 1987). Further applications of transgenic plants in basic research are for example mapping of genes (Clough et al. 2000) or genetic screening for desired phenotypes (Bent 2000). In applied agricultural and horticultural research, plant genetic engineer-

ing is used to generate useful plant phenotypes, which are unachievable by conventional plant breeding (Vain 2007). In the following chapters we describe different *Agrobacterium* strains, which can be used for transformation, we show binary vectors that can be used for different purposes (Table 1) and we provide a simplified floral dip protocol (Box). Furthermore we delineate the selection of transgenic plants to gain homozygous mutants for phenotypic analyses. In Figure 2 we sum up all steps from the preparation to the homozygous mutant plants.

The Method

Agrobacteria strains

Agrobacteria are soil-dwelling plant pathogens that integrate bacterial transfer DNA (T-DNA) into the plant genome (Chilton et al. 1977). The T-DNA is transferred to plant cells, transported to the nucleus and expressed when inserted in the host's nuclear genome. The T-DNA encodes for enzymes that either induce tumor formation or produce opines. These nitrogen-rich molecules serve as energy source for the Agrobacteria, but cannot be metabolized by the plant (McCullen and Binns 2006).

The tumor-inducing plasmid (Ti-plasmid) encodes for the T-DNA and virulence effector (*vir*) proteins, which are important for targeting the plant cell and integrating into the genome. For plant transformation disarmed Ti-plasmids are used, which enable transfer function, but do not induce tumor formation due to the removal of oncogenes and opine synthases from the wild-type T-DNA (Bevan et al. 1983; Fraley et al. 1983; Herrera-Estrella et al. 1983).

The commonly used Agrobacteria strains are C58 with the disarmed Ti-plasmid pTiC58 (Wood et al. 2001) and the C58-derivatives GV3101::pMP90 and GV3101::pMP90RK (Koncz and Schell 1986). These strains confer resistance to rifampicin due to pTiC58. The strain GV3101::pMP90 carries an additional resistance to gentamycin.

T-DNA Binary Vector Systems

The finding that the T-DNA region and the *vir* genes of a Ti-plasmid can reside on different replicons led to the development of binary vector system (Hoekema et al. 1983; de Framond et al. 1983). These plasmids facilitated genetic engineering for many laboratories, because the recombination of foreign DNA with the Ti-plasmid is not required anymore and the cloning procedure became less difficult. In addition, binary vectors yield more DNA than the initial large T-DNA vectors, due to an increased copy number in *Escherichia coli* (Lee and Gelvin 2008).

The T-DNA binary vector system is composed of two vectors, a T-DNA binary vector and a second disarmed Ti-plasmid called *vir* helper plasmid. The binary vector harbors the GOI within the T-DNA region. In this region, which is delimited by left (LB) and right border (RB), the transfer of T-DNA into the plant genome is induced. The T-DNA vector also contains a marker for selection and maintenance in both *E. coli* and Agrobacteria, and a selectable marker for plants. The *vir* helper plasmid, such as pTiC58,

pMK90 or pMK90RK, is harbored in the Agrobacterium strain. It only carries the virulence effector proteins and a selection marker.

Over the past years binary vectors have become more sophisticated and suitable for genetic engineering. Table 1 summarizes many commonly used conventional or Gateway® compatible vector series.

The first T-DNA binary vectors were still large in size, thus plasmid size was progressively reduced and this led to minimal vectors, such as the pPZP or pGREEN plasmids. These plasmids have a more reduced *ori* than for example vectors of the pBIN series (Bevan 1984; Frisch et al. 1995). The integration of T-DNA into the plant genome is polar from RB to LB (Sheng and Citovsky 1996). Early binary T-DNA vectors, such as the pBIN19 (Bevan 1984; Frisch et al. 1995) harbor the resistance cassette close to the RB resulting in false positive transformants only containing the resistance marker, but not the GOI. The resistance cassette in pPZP, pGTPV and pGREEN series is located close to the LB (Table 1). This improvement reduces the number of false positives, because the insertion of the GOI precedes the selection marker (extensively reviewed in Hellens et al. 2000a).

In this review we focus on vector series, which often provide different promoter versions, selectable markers or fusion tags on the same vector backbone, so that it is possible to use vectors of the same series for multiple purposes (Table 1).

Principle of floral dip method

The transformation of Arabidopsis is an essential tool to study GOI function. This review describes Agrobacterium-mediated transformation of Arabidopsis using the floral dip method (Box). It can be performed within a short time without using special equipment and with high yield of transformants in every laboratory. Most Arabidopsis ecotypes, such as Col-0, Ws-0, Nd-0 and No-0 can be transformed with this method, whereas Ler-0 appears to be less efficient (Clough and Bent 1998). Optimal transformation efficiency is yielded when healthy plants are used having around 10 cm high bolts and flowers containing several unopened floral buds. With plants in the ideal status a transformation efficiency of 2-3% can be achieved (Martinez-Trujillo 2004).

To perform the floral dip method, Arabidopsis plants are grown on soil simultaneously to cloning and Agrobacteria transformation procedure. If the cloning procedure takes longer than expected, first bolts could be cut to keep plants in the right developmental stage. Secondary bolts will proliferate. Before dipping, an Agrobacteria over night culture is resuspended in 5% (w/v) sucrose solution to remove corresponding selective agents and other potentially harmful growth media components. The surfactant Silwet L-77 is added to the solution favoring plant transformation by reducing surface tension and promoting agrobacterial adhesion to the plant tissue. Silwet L-77 can be substituted by less-expensive surfactants, such as Tween-20, which is as efficient as Silwet L-77 (Das and Joshi 2011). Transformation of female gametes is achieved by dipping Arabidopsis plants into Agrobacteria solution (Desfeux et al. 2000; Bechthold et al. 2003). Dipped plants are covered with a plastic dome or a layer of saran wrap for one day and placed to low light conditions (50 $\mu\text{mol m}^{-2} \text{s}^{-1}$

Table 1: Overview of restriction-enzyme and Gateway® compatible binary T-DNA vector series

Vector	Application category	BSM	PSM	Ref
Vector series for restriction-enzyme cloning				
pGPTV series	Constitutive transgene expression; promoter studies (GUS)	Kan	HygB, Kan, Gluf, Ble, Mtx	1
pGreen/pGreenII series	Constitutive transgene expression; promoter studies (GUS, GFP, LUC,)	Kan	HygB, Kan, Gluf, Sul	2
pCAMBIA series	Constitutive transgene expression; promoter studies (GUS and GFP),	Kan, Clm	HygB, Kan, Gluf	3
pPZP series	Constitutive transgene expression	Spec, Clm	Kan, Gent	4
pORE series	Constitutive transgene expression; promoter studies and reporter gene assays (GUS, GFP)	Kan	Kan, Gluf	5
Gateway compatible vector series				
pMDC series	Constitutive/inducible expression; promoter studies (GUS and GFP), promoterless variants; various tags (6x His)	Kan, Spec*	HygB, Kan, Bar	6
pGWB series	Inducible expression; promoter studies (GUS, GFP, EYFP, ECFP, RFP), promoterless variants; various tags (6x His, 4x/10x Myc, FLAG, 3x HA, T7, TAP)	Kan, Spec*	Kan, HygB, Gluf	7, 8
GATEWAY destination vectors	Constitutive transgene expression; promoter studies (GUS, GFP); gene silencing (hairpin RNAi)	Spec*	HygB, Kan, Gluf	9
pHELLSGATE	Gene silencing (hairpin RNAi)	Spec	Kan	10, 11
pAGRIKOLA	Gene silencing (hairpin RNAi)	Kan	Kan, Gluf	12

* Gateway vector presented carries a chloramphenicol resistance, which can be used to maintain the Gateway cassette;

References (Ref) are: 1: (Becker 1990; Becker et al. 1992) 2: (Hellens et al. 2000b), 3: www.cambia.org, 4: (Hajdukiewicz et al. 1994), 5: (Coutu et al. 2007), 6: (Curtis and Grossniklaus 2003), 7: (Nakagawa et al. 2007), 8: (Nakamura et al. 2010), 9: (Karimi et al. 2002), 10: (Wesley et al. 2001), 11: (Helliwell and Waterhouse 2003), 12: (Hilson et al. 2004);

Abbreviations: BSM: Bacterial selection marker, PSM: Plant selection marker, Ble: Bleomycin, Clm: Chloramphenicol, Gent: Gentamycin, Gluf: Glufosinate ammonium (Basta), HygB: Hygromycin B, Kan: Kanamycin, Mtx: Methotrexate, Spec: Spectinomycin, Sul: Sulfonamides, CFP: Cyan fluorescent protein, EYFP: Enhanced yellow fluorescent protein, GFP: Green Fluorescent Protein, GUS: β -glucuronidase, LUC: Luciferase, RFP: Red fluorescent protein, TAP: Tandem affinity purification; Useful weblinks: <http://www.pgreen.ac.uk/>; <http://www.cambia.org>; <http://www.psb.ugent.be/gateway/>; antibiotics are dissolved in water, except HygB, which is dissolved in HEPES, ampicillin (dissolved in 50% ethanol) and chloramphenicol (dissolved in 100% ethanol).

light intensity), and moderate temperature (20°C). This retains humidity and favors both Agrobacteria and Arabidopsis growth to enhance transformation efficiency. After ripening, T₀ seeds are harvested for selection (Figure 1).

Screening for transgenic Arabidopsis plants

T₀ seeds are surface sterilized by chlorine gas or ethanol for selection (Clough and Bent 1998; Chang and Pikaard 2005). Several thousands of seeds are sufficient to identify positive transformants. Sterilized seeds are spread on half-strength MS medium (Murashige and Skoog 1962) including the according selective agent (Table 1 and 2). Depending on the selective agent, non-transformed plants are impaired in growth. In most cases sensitive seedlings are pale and arrested in development at the cotyledon stage. Milder selective agents retard growth. Surviving seedlings can be distinguished in early seedling establishment. There they show longer roots and true leaves emerge. Wild-type seedlings should always be included as negative control to monitor the appearance of non-transformed lines on the partic-

ular batch of selection media. At least 15 candidate seedlings are transferred to soil. Alternatively, the selection procedure can be accomplished without sterile culture as described in Davis et al. (2009).

The successful integration of the transgene into plant genomic DNA is verified by PCR analysis. Genomic DNA is isolated from a rosette leaf. A fast method for isolation of genomic DNA is presented in Berendzen et al. (2005). The preparation according to Edwards et al. (1991) is advisable for long-term storage of DNA. The choice of appropriate oligonucleotides for PCR amplification depends on the GOI. Vector specific primers binding to promoter and terminator are conceivable, but also a combination of T-DNA border specific and transgene specific primers. Genomic DNA from wild-type plants should be used as negative control, while vector DNA is the corresponding positive control.

Table 2: Genetic markers and selective agents for plant transformation

Gene, Enzyme, Source	PSM	Conc	Ref
<i>aac3</i> , Aminoglycoside-N-Acetyltransferase, <i>Serratia marcescens</i>	Gent	50 µg/mL	1
<i>aadA</i> , Amino-glycoside-3"-adenyltransferase, <i>Shigella sp.</i>	Spec	100 µg/mL	2
<i>bar</i> , Phosphinotricin acetyl transferase, <i>Streptomyces hygroskopicus</i>	Gluf	7.5 µg/mL	3
<i>dhfr</i> , Dihydrofolate reductase, <i>M. musculus</i>	Mtx	100 µg/mL	4
<i>hph</i> , Hygromycin phosphotransferase, <i>E. coli</i>	HygB	30 µg/mL	5
<i>nptII</i> , Neomycin Phosphotransferase II, <i>E. coli</i> Tn5	Kan	50 µg/mL	6, 7
<i>sulI</i> , Dihydropteroate synthase, <i>E. coli</i> pR46	Sul	7.5 µg/mL	8

References (Ref) are: 1: (Hayford et al. 1988) 2: (Svab and Maliga 1993), 3: (De Block et al. 1989), 4: (Kemper et al. 1992), 5: (Waldron et al. 1985) 6: (Bevan et al. 1983), 7: (Fraley et al. 1983), 8: (Guerineau et al. 1990). Selectable marker genes are extensively reviewed in: (Sundar and Sakthivel 2008).

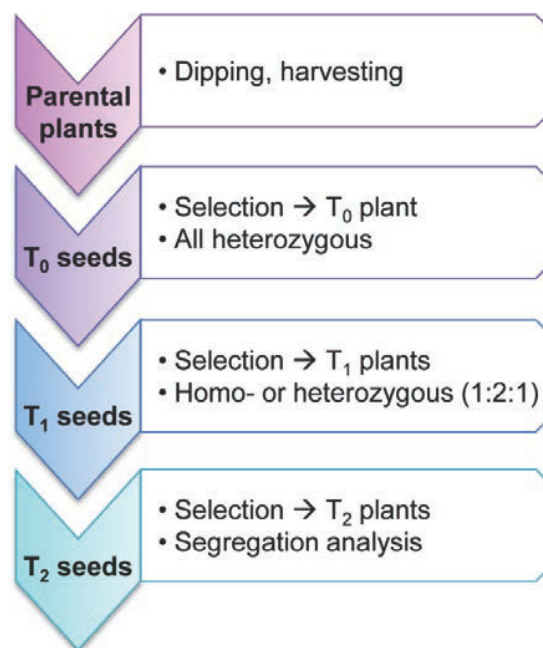
Abbreviations: Conc: Concentration of selective agent in the medium; PSM: Plant selection marker; Gent: Gentamycin, Gluf: Glufosinate ammonium (Basta), HygB: Hygromycin B, Kan: Kanamycin, Mtx: Methotrexate, Spec: Spectinomycin, Sul: Sulfonamides; antibiotics are dissolved in water, except HygB, which is dissolved in HEPES, ampicillin (dissolved in 50% ethanol) and chloramphenicol (dissolved in 100% ethanol).

Besides PCR screening using gDNA, protein or mRNA expression can be directly analyzed by immunoblot or RT-PCR, respectively. In case of an RNA interference (RNAi) approach, the down-regulation of the target transcript should be verified by qRT-PCR (Udvardi et al. 2008).

The progeny of confirmed T₀ plants is further analyzed (Figure 1). Seeds are again spread on half-strength MS medium with selective agent, and T₁ plants are verified via PCR. A T₁ plant with a single T-DNA insertion is considered homozygous when all descendants survive the marker screen. In the case of a heterozygous T₁ plant, the offspring will segregate 1:2:1. Consequently a quarter of the seedlings will show compromised growth during the screen (Figure 1). In the case of multiple insertions it is possible that all descendants of the T₁ generation survive the marker screen even though the T-DNA insertion is not homozygous for the GOI. Physiological experiments can be started with T₂ seeds, produced from homozygous T₁ seedlings.

Agrobacterium-mediated plant transformation may give rise to phenotypes independent of the GOI, such as embryo-lethality if the T-DNA disrupts essential genes (homozygous seeds will not germinate). T-DNA insertion is minimally biased (Alonso and Stepanova 2003), thus assumed to occur largely random (Ostergaard and Yanofsky, 2004). Analysis of more than several independent transgenic lines (multiple alleles) is required to preclude off-target effects.

Multiple T-DNA insertions can be detected by Southern blotting. The genomic DNA is restricted with a single endonuclease featuring a single restriction site in the T-DNA and using a T-DNA specific probe next to this site for hybridization. Multiple T-DNA insertions are expected to result in several bands (Southern 1975; Logemann et al. 2006). Multiple insertions can also be identified by T-DNA mapping (Liu et al. 1995) which additionally gives information about the place of insertion. The biochemical and physiological characterization of transgenic plants can begin as soon as the genetic analysis (Meinke et al. 1998) has been successfully finished.

**Figure 1: Selection of transgenic plants**

This figure displays the selection process from dipped plants to homozygous seeds, which can be used in physiological experiments.

Final remarks

The transformation of Arabidopsis is a multi-step process. The procedure from preparation to selection of homozygous lines is time-consuming, thus proper planning is necessary. Figure 2 sums up the key steps for Arabidopsis transformation. The successful transformation starts with the choice of an appropriate vector system (Gateway® or conventional), promoter and fusion tag. Attention has to be paid to the selective markers depending on the number of transgenes, which will be transformed into one plant line. The selection cassette might be present in a parental mu-

tant line. If it is intended to cross transgenic individuals, care should be taken to employ different selection markers.

Following the described scheme, transgenic Arabidopsis lines ready to be analyzed can be generated in six to eight months.

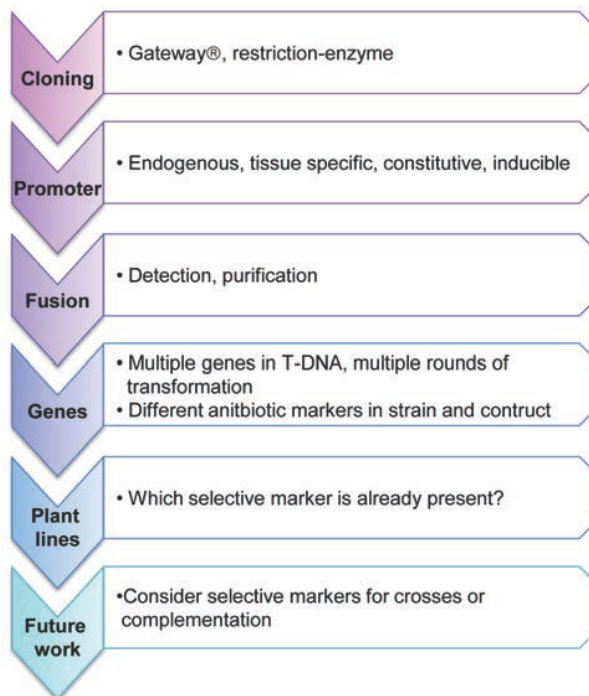


Figure 2: Key steps of Agrobacterium-mediated plant transformation procedure

In this scheme the main steps from cloning to future experiments with homozygous plants are explained.

References

Alonso JM, Stepanova AN (2003) T-DNA mutagenesis in Arabidopsis. *Methods Mol Biol.* 236:177-188.

Alvarez JP, Pekker I, Goldshmidt A, Blum E, Amsellem Z, Eshed Y. (2006) Endogenous and synthetic microRNAs stimulate simultaneous, efficient, and localized regulation of multiple targets in diverse species. *Plant Cell.* 18:1134-1151.

Bechtold N, Ellis J, Pelletier G. (1993) In planta Agrobacterium mediated gene transfer by infiltration of adult *Arabidopsis thaliana* plants. *C R Acad Sci Paris Life Sciences.* 316:1194-1199.

Bechtold N, Jolivet S, Voisin R, Pelletier G. (2003) The endosperm and the embryo of *Arabidopsis thaliana* are independently transformed through infiltration by *Agrobacterium tumefaciens*. *Transgenic Res.* 12:509-517

Becker D. (1990) Binary vectors which allow the exchange of plant selectable markers and reporter genes. *Nucleic Acids Res.* 18:203.

Becker D, Kemper E, Schell J, Masterson R. (1992) New plant binary vectors with selectable markers located proximal to the left T-DNA border. *Plant Mol Biol.* 20:1195-1197.

Bent AF. (2000) Arabidopsis in planta transformation. Uses, mechanisms, and prospects for transformation of other species. *Plant Physiol.* 124:1540-1547.

Berendzen K, Searle I, Ravenscroft D, Koncz C, Batschauer A, Coupland G, Somssich IE, Ulker B. (2005) A rapid and versatile combined DNA/RNA extraction protocol and its application to the analysis of a novel DNA marker set polymorphic between *Arabidopsis thaliana* ecotypes Col-0 and Landsberg erecta. *Plant Methods.* 1:4.

Bevan M. (1984) Binary Agrobacterium vectors for plant transformation. *Nucleic Acids Res.* 12:8711-8721.

Bevan M, Barnes WM, Chilton MD. (1983) Structure and transcription of the nopaline synthase gene region of T-DNA. *Nucleic Acids Res.* 11:369-385.

Chang S, Pikaard CS. (2005) Transcript profiling in Arabidopsis reveals complex responses to global inhibition of DNA methylation and histone deacetylation. *J Biol Chem.* 280:796-804.

Chilton MD, Drummond MH, Merio DJ, Sciaky D, Montoya AL, Gordon MP, Nester EW. (1977) Stable incorporation of plasmid DNA into higher plant cells: the molecular basis of crown gall tumorigenesis. *Cell.* 11:263-271.

Clough SJ, Bent AF. (1998) Floral dip: a simplified method for Agrobacterium-mediated transformation of *Arabidopsis thaliana*. *Plant J.* 16:735-743.

Clough SJ, Fengler KA, Yu IC, Lippok B, Smith RK Jr, Bent AF. (2000) The Arabidopsis dnd1 "defense, no death" gene encodes a mutated cyclic nucleotide-gated ion channel. *Proc Natl Acad Sci USA.* 97:9323-9328.

Coutu C, Brandle J, Brown D, Brown K, Miki B, Simmonds J, Hegedus DD. (2007) pORE: a modular binary vector series suited for both monocot and dicot plant transformation. *Transgenic Res.* 16:771-781.

Curtis MD, Grossniklaus U. (2003) A gateway cloning vector set for high-throughput functional analysis of genes in planta. *Plant Physiol.* 133:462-469.

Das P, Joshi NC. (2011) Minor modifications in obtainable Arabidopsis floral dip method enhances transformation efficiency and production of homozygous transgenic lines harboring a single copy of transgene. *ABB.* 2:59-67.

Davis AM, Hall A, Millar AJ, Darrah C, Davis SJ. (2009) Protocol: Streamlined sub-protocols for floral-dip transformation and selection of transformants in *Arabidopsis thaliana*. *Plant Methods.* 5:3.

De Block M, De Brouwer D, Tenning P. (1989) Transformation of *Brassica napus* and *Brassica oleracea* using *Agrobacterium tumefaciens* and the expression of the bar and neo genes in the transgenic plants. *Plant Physiol.* 91:694-701.

de Framond AJ, Barton KA, Chilton M-D. (1983) Mini-Ti: A new vector strategy for plant genetic engineering. *Nat Biotech.* 1:262-269.

Desfeux C, Clough SJ, Bent AF. (2000) Female reproductive tissues are the primary target of Agrobacterium-mediated transformation by the Arabidopsis floral-dip method. *Plant Physiol.* 123:895-904.

Edwards K, Johnstone C, Thompson C. (1991) A simple and rapid method for the preparation of plant genomic DNA for PCR analysis. *Nucleic Acids Res.* 19:1349.

Feldman KA, Marks DM. (1987) Agrobacterium mediated transformation of germinating seeds of *Arabidopsis thaliana*: A non-tissue culture approach. *Mol Gen Genet.* 208:1-9.

Fraley RT, Rogers SG, Horsch RB, Sanders PR, Flick JS, Adams SP, Bittner ML, Brand LA, Fink CL, Fry JS, Galluppi GR, Goldberg SB, Hoffmann NL, Woo SC. (1983) Expression of bacterial genes in plant cells. *Proc Natl Acad Sci USA.* 80:4803-4807.

Frisch DA, Harris-Haller LW, Yokubaitis NT, Thomas TL, Hardin SH, Hall TC. (1995) Complete sequence of the binary vector Bin 19. *Plant Mol Biol.* 27:405-409.

Guerineau F, Brooks L, Meadows J, Lucy A, Robinson C, Mullineaux P. (1990) Sulfonamide resistance gene for plant transformation. *Plant Mol Biol.* 15:127-136.

Hajdukiewicz P, Svab Z, Maliga P. (1994) The small, versatile pPZP family of Agrobacterium binary vectors for plant transformation. *Plant Mol Biol.* 25:989-994.

Hayford MB, Medford JI, Hoffman NL, Rogers SG, Klee HJ. (1988) Development of a plant transformation selection system based on expression of genes encoding gentamicin acetyltransferases. *Plant Physiol.* 86:1216-1222.

Hellens R, Mullineaux P, Klee H. (2000a) Technical focus: a guide to Agrobacterium binary Ti vectors. *Trends Plant Sci.* 5:446-451.

Hellens RP, Edwards EA, Leyland NR, Bean S, Mullineaux PM. (2000b) pGreen: a versatile and flexible binary Ti vector for Agrobacterium-mediated plant transformation. *Plant Mol Biol.* 42:819-832.

- Helliwell C, Waterhouse P. (2003) Constructs and methods for high-throughput gene silencing in plants. *Methods*. 30:289-295.
- Herrera-Estrella L, Block MD, Messens E, Hernalsteens JP, Montagu MV, Schell J. (1983) Chimeric genes as dominant selectable markers in plant cells. *EMBO J*. 2:987-995.
- Hilson P, Allemeersch J, Altmann T, Aubourg S, Avon A, Beynon J, Bhalerao RP, Bitton F, Caboche M, Cannoot B, Chardakov V, Cagnet-Holliger C, Colot V, Crowe M, Darimont C, Durinck S, Eickhoff H, de Longevialle AF, Farmer EE, Grant M, Kuiper MT, Lehrach H, Leon C, Leyva A, Lundeberg J, Lurin C, Moreau Y, Nietfeld W, Paz-Ares J, Reymond P, Rouze P, Sandberg G, Segura MD, Serizet C, Tabrett A, Taconnat L, Thareau V, Van Hummelen P, Vercruyssen S, Vuylsteke M, Weingartner M, Weisbeek PJ, Wirta V, Wittink FR, Zabeau M, Small I. (2004) Versatile gene-specific sequence tags for Arabidopsis functional genomics: transcript profiling and reverse genetics applications. *Genome Res*. 14:2176-2189.
- Hoekema A, Hirsch PR, Hooykaas PJJ, Schilperoort RA. (1983) A binary plant vector strategy based on separation of vir- and T-region of the *Agrobacterium tumefaciens* Ti-plasmid. *Nature*. 303:179-180.
- Hofgen R, Willmitzer L. (1988) Storage of competent cells for Agrobacterium transformation. *Nucleic Acids Res*. 16:9877.
- Jefferson RA, Kavanagh TA, Bevan MW. (1987) GUS fusions: beta-glucuronidase as a sensitive and versatile gene fusion marker in higher plants. *EMBO J*. 6:3901-3907.
- Karimi M, Inze D, Depicker A. (2002) GATEWAY vectors for Agrobacterium-mediated plant transformation. *Trends Plant Sci*. 7:193-195.
- Karimi M, Depicker A, Hilson P. (2007) Recombinational cloning with plant gateway vectors. *Plant Physiol*. 145:1144-1154.
- Kemper E, Greveling C, Schell J, Masterson R. (1992) Improved method for the transformation of *Arabidopsis thaliana* with chimeric dihydrofolate reductase constructs which confer methotrexate resistance. *Plant Cell Rep*. 11:118-121.
- Koncz C, Schell J. (1986) The promoter of the TL-DNA gene 5 controls the tissue-specific expression of chimeric genes carried by a novel type of Agrobacterium binary vector. *Mol Gen Genet*. 204:383-396.
- Lee LY, Gelvin SB. (2008) T-DNA binary vectors and systems. *Plant Physiol*. 146:325-332.
- Liu YG, Mitsukawa N, Oosumi T, Whittier RF. (1995) Efficient isolation and mapping of *Arabidopsis thaliana* T-DNA insert junctions by thermal asymmetric interlaced PCR. *Plant J*. 8:457-463.
- Lloyd AM, Barnason AR, Rogers SG, Byrne MC, Fraley RT, Horsch RB. (1986) Transformation of *Arabidopsis thaliana* with *Agrobacterium tumefaciens*. *Science*. 234:464-466.
- Logemann E, Birkenbihl RP, Ulker B, Somssich IE. (2006) An improved method for preparing Agrobacterium cells that simplifies the Arabidopsis transformation protocol. *Plant Methods*. 2:16.
- Martinez-Trujillo ML-B, Cabrera-Ponce V, Luis J, Herrera-Estrella L. (2004) Improving transformation efficiency of *Arabidopsis thaliana* by modifying the floral dip method. *Plant Mol Biol Rep*. 22:7.
- McCullen CA, Binns AN. (2006) *Agrobacterium tumefaciens* and plant cell interactions and activities required for interkingdom macromolecular transfer. *Annu Rev Cell Dev Biol*. 22:101-127.
- Meinke DW, Cherry JM, Dean C, Rounsley SD, Koornneef M. (1998) *Arabidopsis thaliana*: A model plant for genome analysis. *Science*. 282:662-682.
- Mersereau M, Pazour GJ, Das A. (1990) Efficient transformation of *Agrobacterium tumefaciens* by electroporation. *Gene*. 90:149-151.
- Murashige T, Skoog F. (1962) A revised medium for rapid growth and bio assays with tobacco tissue cultures. *Physiol Plant*. 15:14.
- Nakagawa T, Kurose T, Hino T, Tanaka K, Kawamukai M, Niwa Y, Toyooka K, Matsuoka K, Jinbo T, Kimura T. (2007) Development of series of gateway binary vectors, pGWBs, for realizing efficient construction of fusion genes for plant transformation. *J Biosci Bioeng*. 104:34-41.
- Nakamura S, Mano S, Tanaka Y, Ohnishi M, Nakamori C, Araki M, Niwa T, Nishimura M, Kaminaka H, Nakagawa T, Sato Y, Ishiguro S. (2010) Gateway binary vectors with the bialaphos resistance gene, bar, as a selection marker for plant transformation. *Biosci Biotechnol Biochem*. 74:1315-1319.
- Negrutiu I, Shillito RD, Potryskus I, Biasini G, Sala F. (1987) Hybrid genes in the analysis of transformation conditions. I. Setting up a simple method for direct gene transfer in plant protoplasts. *Plant Mol Biol*. 8:363-373.
- Ostergaard L, Yanofsky MF. (2004) Establishing gene function by mutagenesis in *Arabidopsis thaliana*. *Plant J*. 39:682-696.
- Sambrook JR, Russel DW. (2001) Molecular Cloning: A Laboratory Manual (Third Edition), CSHL Press.
- Schwab R, Ossowski S, Riester M, Warthmann N, Weigel D. (2006) Highly specific gene silencing by artificial microRNAs in Arabidopsis. *Plant Cell*. 18:1121-1133.
- Schwab R, Palatnik JF, Riester M, Schommer C, Schmid M, Weigel D. (2005) Specific effects of microRNAs on the plant transcriptome. *Dev Cell*. 8:517-527.
- Sheng J, Citovsky V. (1996) Agrobacterium-plant cell DNA transport: have virulence proteins, will travel. *Plant Cell*. 8:1699-1710.
- Small I. (2007) RNAi for revealing and engineering plant gene functions. *Curr Opin Biotechnol*. 18:148-153.
- Smith NA, Singh SP, Wang MB, Stoutjesdijk PA, Green AG, Waterhouse PM. (2000) Total silencing by intron-spliced hairpin RNAs. *Nature*. 407:319-320.
- Southern EM. (1975) Detection of specific sequences among DNA fragments separated by gel electrophoresis. *J Mol Biol*. 98:503-517.
- Sundar IK, Sakthivel N. (2008) Advances in selectable marker genes for plant transformation. *J Plant Physiol*. 165:1698-1716.
- Svab Z, Maliga P. (1993) High-frequency plastid transformation in tobacco by selection for a chimeric aadA gene. *Proc Natl Acad Sci USA*. 90:913-917.
- Udvardi MK, Czechowski T, Scheible WR. (2008) Eleven golden rules of quantitative RT-PCR. *Plant Cell*. 20:1736-1737.
- Vain P. (2007) Thirty years of plant transformation technology development. *Plant Biotech J*. 5:221-229.
- Valvekens D, Montagu MV, Van Lijsebettens M. (1988) *Agrobacterium tumefaciens* mediated transformation of *Arabidopsis thaliana* root explants by using kanamycin selection. *Proc Natl Acad Sci USA*. 85:5536-5540.
- Van Larebeke N, Engler G, Holsters M, Van den Elsacker S, Zaenen I, Schilperoort RA, Schell J. (1974) Large plasmid in *Agrobacterium tumefaciens* essential for crown gall-inducing ability. *Nature*. 252:169-170.
- Waldron C, Murphy EB, Roberts JL, Gustafson GD, Armour SL, Malcolm SK. (1985) Resistance to hygromycin B. *Plant Mol Biol*. 5:103-108.
- Wesley SV, Helliwell CA, Smith NA, Wang MB, Rouse DT, Liu Q, Gooding PS, Singh SP, Abbott D, Stoutjesdijk PA, Robinson SP, Gleave AP, Green AG, Waterhouse PM. (2001) Construct design for efficient, effective and high-throughput gene silencing in plants. *Plant J*. 27:581-590.
- Wood DW, Setubal JC, Kaul R, Monks DE, Kitajima JP, Okura VK, Zhou Y, Chen L, Wood GE, Almeida NF Jr, Woo L, Chen Y, Paulsen IT, Eisen JA, Karp PD, Bovee D Sr, Chapman P, Clendenning J, Deatherage G, Gillet W, Grant C, Kutayav T, Levy R, Li MJ, McClelland E, Palmieri A, Raymond C, Rouse G, Saenphimmachak C, Wu Z, Romero P, Gordon D, Zhang S, Yoo H, Tao Y, Biddle P, Jung M, Krespan W, Perry M, Gordon-Kamm B, Liao L, Kim S, Hendrick C, Zhao ZY, Dolan M, Chumley F, Tingey SV, Tomb JF, Gordon MP, Olson MV, Nester EW. (2001) The genome of the natural genetic engineer *Agrobacterium tumefaciens* C58. *Science*. 294:2317-2323.

BOX - Plant transformation method

Step 1 Cloning

Clone the GOI in an appropriate binary vector (Table 1). Consider features like promoter, fusion tag and selection cassette (Table 1 and 2). Isolate 1 μg of plasmid DNA of the final construct for transformation into *Agrobacteria* (Sambrook 2001).

Step 2 Plant growth

Sow *Arabidopsis* seeds on well-watered soil and stratify at 4°C in the dark for two days. Germinate seeds and grow the seedlings under long day conditions (16 h light/8 h darkness, 100 $\mu\text{mol m}^{-2} \text{s}^{-1}$ light intensity, 20°C/18°C) for three weeks. Transfer five plants to a fresh pot filled with watered soil. Grow the plants under long day conditions for three to four weeks until they begin to bolt. Prepare four pots with five plants per construct (Figure 3A).

Step 3 Competent *Agrobacteria*

Produce competent *Agrobacteria* by inoculating 200 mL LB medium with 2 mL of an *agrobacterium* over-night culture. Incubate main culture aerobically at 28°C for 6 h to grow the cells to OD_{600} 0.5-0.8. At this OD the transition to the log-phase begins. Centrifuge the culture at 4,500 g at 4°C for 10 min. Wash the pellet in 10 mL ice-cold TE-buffer. Resuspend the pellet in 20 mL LB medium. Aliquot 500 μL fractions in microcentrifuge tubes. Shock-freeze in liquid nitrogen and store at -80°C (Hofgen and Willmitzer 1988).

Step 4 *Agrobacteria* transformation using the freeze-thaw method

Transform the construct with the GOI into *Agrobacteria*.

Thaw one aliquot of competent cells per construct on ice. Add 1 μg plasmid DNA and keep the mixture on ice for 5 min. Freeze it in liquid nitrogen for 5 min. Heat-shock the mixture for 5 min at 37°C. Add 0.8 mL LB medium and incubate on a rocker at 28°C for 2-4 h. Centrifuge for 2 min at 3,000 g. Discard the supernatant, resuspend the pellet in 100 μL LB, and spread the *Agrobacteria* suspension on YEP-plates with appropriate antibiotics. Incubate the plates at 28°C for two days. Re-streak four single colonies on a new plate and incubate these plates at 28°C for one to two days (Hofgen and Willmitzer 1988). To verify the presence of the construct perform a colony PCR (Sambrook 2001). Consider that larger constructs (>20 kb) might require electro-transformation (Mersereau et al. 1990).

Step 5 Plant status optimal for transformation

Grow plants until bolts reach 10 cm height. The plants should have several unopened floral buds and a low number of siliques. When the plants get the first bolts, but the cloning is not yet finished, they can be removed. Cutting first bolts allows proliferation of secondary inflorescences from axillary buds.

Step 6 *Agrobacteria* culture for dipping

Inoculate a 5 mL liquid culture of *Agrobacteria* in LB medium supplied with antibiotics that select for both the *vir* helper plasmid and T-DNA binary vector two days prior to plant transformation. Incubate it aerobically at 28°C over night.

Inoculate 250 mL of YEP medium with 1 mL of the pre-culture and incubate under the same conditions for 16-24 h ($\text{OD}_{600} = 1.5 - 2$). Measure the OD_{600} of your *Agrobacteria* culture.

Sediment the cells at 5,500 g for 10 min at room temperature (note that the pellet is pink). Resuspend it in 5 % (w/v) sucrose solution to a final OD_{600} of 0.8. Add 0.02 % (v/v) Silwet L-77 or 0.07 % (v/v) Tween-20. Note that high concentrations of surfactant are toxic. For transformation of varying T-DNA binary vectors with different selection markers, mix equal volumes of the *Agrobacteria* strains resuspended in sucrose solution. Nest a tall 250 mL beaker in a 600 mL beaker to easily dip the plants overhead. This minimizes the contamination of *Agrobacterium* solution with soil. Transfer the *Agrobacteria* suspension to the 250 mL beaker.

Step 7 Preparation of plants

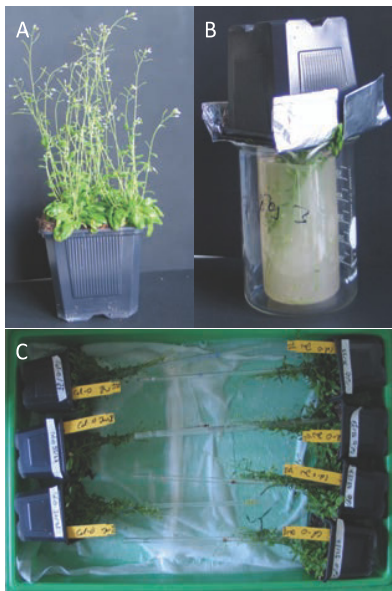
Remove already developed siliques from the plants to minimize the number of non-transformed seeds in your batch, which increases the ratio of transformed to untransformed seeds. This step might be time consuming.

Step 8 Dipping – Plant transformation

Prepare two stripes of aluminum foil to cover the rosette leaves and the soil, leaving a gap for the inflorescences (Figure 3B). This prevents loss of soil and contamination of leaves with Agrobacteria suspension. Dip the inflorescences into the Agrobacteria suspension by inverting the plants. Allow soaking for 1 min (Figure 3B). The same suspension can be used for ten or more pots and for different plants. To prevent damage of the flower buds, remove excess liquid by draining plants for a few seconds. Staking bolts facilitates harvesting of seeds.

Step 9 Plant handling after transformation

Place pots on their sides in a plastic tray lined with humid paper. Cover the trays with a dome or saran wrap maintaining humidity. Keep the plants in low light ($50 \mu\text{mol m}^{-2} \text{s}^{-1}$ light) for one day (Figure 3C). Put the plants upright and return them to normal growth conditions the next day. Grow the transformed plants for further 3-4 weeks until the first siliques become brown. Stop watering and let the siliques ripen.

**Figure 3: Floral dip procedure**

(A) Arabidopsis plants with 10 cm high bolts. Flowers containing several unopened floral buds should be used for optimal transformation efficiencies. (B) Arabidopsis plants, prepared for transformation, are dipped in Agrobacteria solution. (C) After dipping the plants are placed horizontally in a tray with humid paper and covered with transparent foil to maintain humidity.

Step 10 Collection of seeds

Harvest dried seeds with a mesh sieve and pool the T₀ seeds of plants transformed with the same construct.

Step 11 Seed surface sterilization

Seeds can be surface sterilized either by chlorine gas (A), or ethanol (B).

A) Chlorine gas method

Fill one spatula tip of seeds (around 20 μ L volume) in one microcentrifuge tube and place it opened into a desiccator jar under a fume hood. Sterilize four to six seed aliquots per seed pool. Store non-sterilized seeds of the original seed batch. Storage of sterilized seeds decreases germination efficiency.

Place a beaker containing 100 mL of sodium hypochlorite (13% of active chlorine) next to the seeds in the desiccator. Add 3 mL of concentrated hydrochloric acid to initiate chlorine gas formation. Immediately close the desiccator to prevent gas emission. Expose the seeds for 2 h, release the gas and close the tubes quickly to prevent contamination. Open the microcentrifuge tubes under a sterile laminar flow hood and let remaining chlorine gas evaporate for 30 min (Clough and Bent 1998).

B) Ethanol liquid method

Fill up to 50 μ L seeds in a microcentrifuge tube (three aliquots per seed batch) and add 500 μ L of 70% ethanol. Shake the seeds continuously for 5-10 min. Remove the liquid and let the seeds dry in the microcentrifuge tube under the laminar flow hood (~ 30 min-1 h). Sterile seeds can alternatively be poured on a sterile filter paper for drying (~ 15 min). Sterilization by this method does not allow longer-term seed storage (modified after Chang and Pikaard 2005).

Step 12 Selection of primary transformants

Spread the seeds of one seed pool on four to eight half-strength MS plates with the appropriate selection agents (Table 1 and 2). Stratify the seeds at 4°C in the dark for two days. Grow the seedlings for up to three weeks under long day conditions (16 h light/8 h darkness, 20°C). Transformed plants are easily distinguishable from non-transformed seedlings. They are greener, have longer roots, and produce true leaves. Non-resistant seeds germinate, but appear yellowish. In most cases growth is arrested at the cotyledon stage. Transfer resistant seedlings to new pots filled with watered soil. Grow plants under long day conditions and harvest T₁ seeds.

Step 13 gDNA isolation using sucrose buffer

To test if resistant plants carry the T-DNA, gDNA from leaves is isolated. Cut one leaf disc with a microcentrifuge tube cap and store it on ice until extraction. Add 200 μ L sucrose buffer and grind the tissue with a blue pipette tip at room temperature until the solution becomes greenish and the tissue appears macerated. Boil the sample at 100°C for 10 min. Centrifuge for 5 seconds. Place the samples on ice. Perform a 20 μ L PCR reaction with 1 μ L of the supernatant, containing the genomic DNA. Store the samples at 4°C over night or at -20°C for long-term storage (Berendzen et al. 2005)

Step 14 Segregation analysis

T₂ plants are verified by growth on selective medium and PCR. Segregation analysis will reveal whether the ancestor is a homo-, or heterozygous plant. The offspring of homozygous plants survives the marker screen to 100% and can be used for physiological experiments. Southern Blotting is only performed when no independent lines are available.

Equipment and reagents

Equipment

Pots, VQB 9 x 9 x 8 cm, TEKU, Germany
Aluminum foil, Carl Roth, Germany
Plastic tray and dome or plastic film
Sticks for plant staking
Mesh sieve, 450 μ m, Retsch, Germany
Scissors
Jeweler's forceps (Dumont type 5)
Microcentrifuge tubes, 1.5 mL, Sarstedt, Germany
Pipette tips, Sarstedt, Germany
Erlenmeyer flasks for Agrobacteria cultivation, VWR, Germany
Tall 250 mL beaker and a 600 mL beaker for dipping
Desiccator jar
BioPhotometer, Eppendorf, Germany
Centrifuge J2-21, Rotor JA-10, Beckman, USA
Centrifuge 5424, Eppendorf, Germany
Veriti 96-Well Thermal Cycler, Applied Biosystems, USA
Thermomixer comfort, Eppendorf, Germany
Incubator shakers, Innova 44, New Brunswick scientific, USA
Growth chamber, Model AR-66C and CU-36C, Percival scientific, USA
Fume hood
Sterile laminar flow hood

Reagents

Buffers and solutions:

TE-buffer:

10 mM Tris-HCl, pH 7.5; 0.1 mM EDTA

Sucrose solution:

5% (w/v) sucrose in water

Sucrose buffer for gDNA isolation:

50 mM Tris-HCl, pH 7.5; 300 mM sodium chloride; 300 mM sucrose

Media:

Luria-Bertani medium (LB):

1% (w/v) Tryptone; 0.5% (w/v) Yeast extract; 1% (w/v) Sodium chloride; 1.5% (w/v) Agar for plates

YEP medium:

1% (w/v) yeast extract; 1% (w/v) peptone; 0.5% (w/v) sodium chloride; 1.5% (w/v) Agar for plates

Half-strength MS medium:

0.44% (w/v) MS salts, including vitamins; 0.05% (w/v) MES, pH 5.7 (KOH); 0.8% (w/v) phytoagar for plates

Soil:

2/3 Top soil; 1/3 Vermiculite

Other chemicals:

Liquid nitrogen

Silwet L-77 or Tween-20

Sodium hypochlorite (13% of active chlorine)

Concentrated hydrochloric acid (HCl)

Sterile 70% ethanol and 100% ethanol

Selection agents

Authors contributions

Jan Wiese, Sarah Vigelius and Kirstin Bernhardt wrote the manuscript as co-authors with equal contribution. Nicole Linka and Andreas P.M. Weber assisted in drafting and submitting this manuscript.

VI.2 Manuscript 5

An engineered plant peroxisome and its application in biotechnology

Sarah K.-Kessel-Vigelius*, Jan Wiese*, Martin G. Schroers*, Thomas J. Wrobel*,
Florian Hahn and Nicole Linka[¶]

Department of Plant Biochemistry, Heinrich-Heine University Düsseldorf, 40225
Düsseldorf, Germany

* Co-first authors, equal contribution to the manuscript

[¶] Corresponding author



Contents lists available at SciVerse ScienceDirect

Plant Science

journal homepage: www.elsevier.com/locate/plantsci

Review

An engineered plant peroxisome and its application in biotechnology[☆]Sarah K. Kessel Vigelius¹, Jan Wiese¹, Martin G. Schroers¹, Thomas J. Wrobel¹, Florian Hahn, Nicole Linka*

Heinrich Heine University, Plant Biochemistry, Universitätsstrasse 1, Building 26.03.01, D-40225 Düsseldorf, Germany

ARTICLE INFO

Article history:

Received 20 March 2013

Received in revised form 8 June 2013

Accepted 10 June 2013

Available online 17 June 2013

Keywords:

Peroxisome

Biotechnology

Genetic engineering

Metabolism

Stress tolerance

ABSTRACT

Plant metabolic engineering is a promising tool for biotechnological applications. Major goals include enhancing plant fitness for an increased product yield and improving or introducing novel pathways to synthesize industrially relevant products. Plant peroxisomes are favorable targets for metabolic engineering, because they are involved in diverse functions, including primary and secondary metabolism, development, abiotic stress response, and pathogen defense. This review discusses targets for manipulating endogenous peroxisomal pathways, such as fatty acid β oxidation, or introducing novel pathways, such as the synthesis of biodegradable polymers. Furthermore, strategies to bypass peroxisomal pathways for improved energy efficiency and detoxification of environmental pollutants are discussed. In sum, we highlight the biotechnological potential of plant peroxisomes and indicate future perspectives to exploit peroxisomes as biofactories.

© 2013 The Authors. Published by Elsevier Ireland Ltd. All rights reserved.

Contents

1. Introduction	232
2. Improving seed oil yield and quality	233
3. Plant peroxisomes confer stress tolerance	233
3.1. Increasing the peroxisome population	233
3.2. Improving peroxisomal ROS scavenging systems	234
3.3. Improved pest and pathogen resistance	235
3.4. Peroxisomal small heat shock proteins for enhanced stress tolerance	235
4. Modulating auxin synthesis in peroxisomes	235
5. Implementation of artificial metabolic pathways to gain novel peroxisomal functions	235
5.1. Production of biodegradable polymers in plant peroxisomes	235
5.2. Peroxisomal bypass pathways to reduce photorespiration	236
5.3. Peroxisomal degradation pathways for pollutants	236
6. Concluding remarks	237
Acknowledgements	238
References	238

Abbreviations: H₂O₂, hydrogen peroxide; JA, jasmonic acid; PHA, polyhydroxyalkanoate; ROS, reactive oxygen species.

[☆] This is an open access article distributed under the terms of the Creative Commons Attribution NonCommercial No Derivative Works License, which permits non commercial use, distribution, and reproduction in any medium, provided the original author and source are credited.

* Corresponding author. Tel.: +49 0211 81 10412.

E-mail addresses: Sarah.Vigelius@hhu.de (S.K. Kessel Vigelius), Jan.Wiese@hhu.de (J. Wiese), Martin.Schroers@hhu.de (M.G. Schroers), Thomas.Jan.Wrobel@hhu.de (T.J. Wrobel), Florian.Hahn@hhu.de (F. Hahn), Nicole.Linka@hhu.de (N. Linka).

¹ Co-first authors.

1. Introduction

Plants have evolved the ability to produce a wide range of molecules. Many of these compounds are of biotechnological importance, as they serve as food, colorants, flavors, fragrances, traditional medicines, pharmaceuticals, cosmetics, and renewable fuels [1]. Their chemical synthesis is often difficult and expensive, thus genetic engineering is an alternative approach to optimize the production of desired metabolites in plants.

In plants, biochemical pathways are compartmentalized and individual steps of a particular pathway are distributed over

different compartments. In this context, peroxisomes, which are subcellular organelles 1 μm in diameter [2], represent as organelles at a metabolic crossroads [3,4], because they participate in one or more steps in many significant metabolic reactions, including primary carbon metabolism (e.g. beta oxidation of fatty acids and photorespiration), secondary metabolism (e.g. production of glucosinolates), development (e.g. synthesis of plant hormones), abiotic stress response, and pathogen defense [4].

Thus, peroxisomes are an attractive target for metabolic engineering, to increase yield and quality of plant products. Manipulation of peroxisomal scavenging systems for reactive oxygen species (ROS) might enhance plant fitness under environmental stress conditions [5]. Besides altering peroxisomal functions, novel pathways can be implemented in peroxisomes, enabling the synthesis of desired metabolites or degradation of toxic molecules. The following characteristics illustrate why peroxisomes are well suited for biotechnological purposes:

- (i) Peroxisomes are surrounded by a single lipid bilayer membrane [4]. Novel reactions can be compartmentalized within peroxisomes. A peroxisomal compartmentation is favorable because end products or intermediates can be toxic for the cell. As peroxisomes are equipped with efficient ROS detoxifying systems [6], ROS producing reactions can be introduced in peroxisomes without deleterious effects.
- (ii) Peroxisomes allow an efficient targeting of heterologous proteins, since protein targeting signals for the peroxisome are well established. Soluble, nuclear encoded proteins are targeted to peroxisomes by two different targeting signals, which direct soluble proteins to peroxisomes. Most proteins use the Type 1 Peroxisomal Targeting Signal (PTS1) to enter peroxisomes, which consists of three amino acids at the carboxyl terminus (SKL, or a conserved variant) [7,8]. The Type 2 Peroxisomal Targeting Signal (PTS2) is a conserved nonapeptide (9 amino acids), which is attached to the amino terminus of peroxisomal proteins [9]. Fusion of either signal peptide to a heterologous protein results in direct targeting to peroxisomes. Thus, the enzymatic content of peroxisomes can be easily modified. In contrast to plastids and mitochondria, the peroxisomal protein import machinery is able to import fully folded proteins and stable protein complexes in a receptor independent fashion [4]. The import of heterologous protein complexes into peroxisomes depends on a mechanism called piggybacking, where a protein without a peroxisomal targeting signal uses a PTS carrying protein as shuttle [10,11]. Therefore, coupling of a shuttle protein to other proteins might enable the targeting of even larger protein complexes to peroxisomes without modifying the import receptor machinery.
- (iii) Peroxisomes are highly dynamic organelles, which are able to adjust size and number [12]. They multiply by division and proliferation [4]. Latter is induced by various environmental, developmental and metabolic cues and is controlled by the PEROXIN11 protein family and several transcription factors [13,14]. A rapid increase in peroxisome number allows an accumulation of substances produced in peroxisomes [2].

In recent years, major progress has been made in genomics and proteomics, revealing the diversity of peroxisomal metabolism [4,15]. However, mechanisms to exploit plant peroxisomes for optimizing metabolism or modifying metabolic fluxes toward compounds of interest are not well studied. Here, we present recent pioneering approaches to produce plant peroxisome biofactories. Moreover, we indicate putative targets and possible strategies that in the future could be exploited to engineer peroxisomes for biotechnological purposes.

2. Improving seed oil yield and quality

One of the major goals of agricultural biotechnology is to increase the content and/or improve the value of oils in oilseed plants, including sunflower, soybean, palm, oilseed rape, and maize crops [16]. Oilseed crops are not only important for human nutrition [17], but can also be used for a variety of chemical applications.

Plants are able to produce a wide range of different fatty acids, whereas the number of fatty acids shared between plant species is relatively low. All conventional crops contain palmitic acid, stearic acid, oleic acid, linoleic acid, and linolenic acid. These are termed usual fatty acids. Fatty acids, which in their chemical structures differ from usual fatty acids, are referred to as unusual fatty acids. Unusual fatty acids, exhibiting hydroxylations or acetylations, are of major industrial interest, as they provide raw materials for the generation of biopolymers or fuels [18].

Vegetable oils, for example, serve as a sustainable replacement of petroleum based chemicals [16]. One appealing method to produce high value oils is the genetic engineering of plants accumulating ricinoleic acid, which serves as precursor for economically viable products, such as ink, lubricants, varnishes, emulsifiers, nylon, or biodiesel [18,19].

The bottleneck for increased oilseed content and the production of designer oils is the channeling of fatty acids into storage oil. Inefficient integration arises either by enhanced biosynthesis of native fatty acids or by the low affinity of acyltransferases to unusual fatty acids [20,21]. As a consequence, accumulated fatty acids are degraded via peroxisomal beta oxidation, which simultaneously operates during lipid synthesis (Fig. 1).

Inactivating peroxisomal beta oxidation enzymes by using specific promoters only active during seedling could minimize such futile cycling. Another strategy is to produce the desired oil in a specific plant tissue with low beta oxidation activity (e.g. leaves). Leaf specific oil production might be favorable if the accumulation of industrial valuable oil in seeds affected germination or seedling establishment [22].

3. Plant peroxisomes confer stress tolerance

Various abiotic and biotic stress conditions, such as salinity, heat, cold, drought, and pathogen infection induce oxidative stress in plants. This results in overproduction of ROS in chloroplasts, mitochondria, and peroxisomes, with highly oxidative metabolism [23,24]. Plants are unable to escape exposure to environmental stresses, thus they have developed a complex antioxidant defense system to control ROS levels and protect cells from oxidative injury [6]. Here, we present several strategies to improve stress tolerance in plants through modified peroxisomal metabolism circumventing oxidative stress and thereby increasing fitness [25].

3.1. Increasing the peroxisome population

Plant peroxisomes multiply under stress conditions. In plants the PEROXIN11 family, which consist of five isoforms (a-e), controls proliferation of peroxisomes. When overexpressed, the number of peroxisomes increases. Conversely, reducing the expression of PEX11 genes results in decreased peroxisome abundance [26]. The expression of PEX11b is controlled through a phytochrome A dependent pathway, involving the far red light photoreceptor phyA and the bZIP transcription factor HY5 homolog [13,27].

Additionally, peroxisomal proliferation is induced by environmental stimuli and various stresses, such as high light intensities, H_2O_2 , ozone, xenobiotics, cadmium, salt, pathogens, and senescence. However, little is known about the principal molecular mechanisms [28–33]. Stress induced peroxisome proliferation

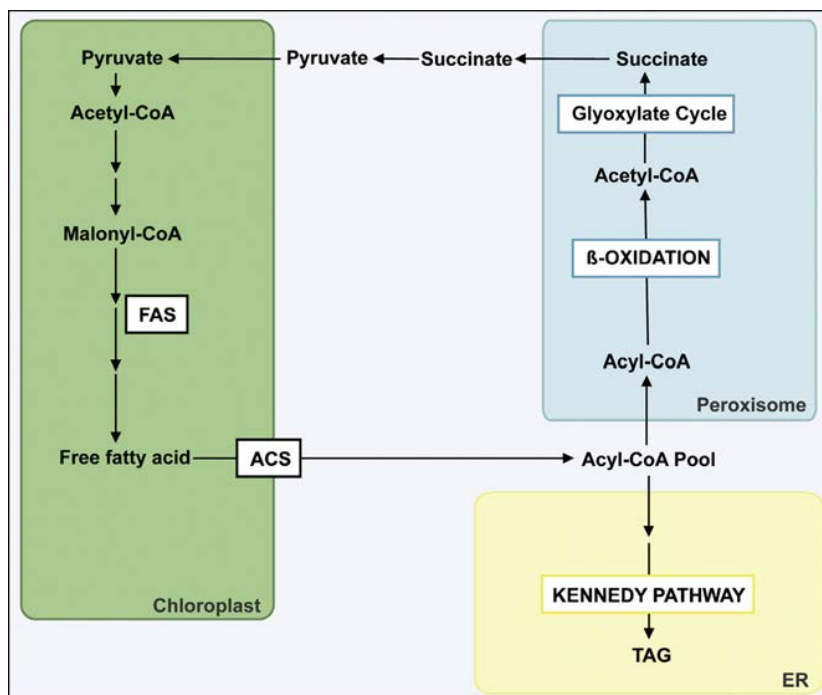


Fig. 1. Fatty acids synthesis and catabolism take place simultaneously in plant cells. In chloroplasts fatty acids (FAs) are generated from acyl CoA and pyruvate via the fatty acid synthesis complex and are then released into the cytosol. FAs are either catabolized via peroxisomal β oxidation or incorporated into triacylglycerols via the Kennedy pathway in the ER. CoA, coenzyme A; FAS, fatty acid synthesis complex; ACS, acyl CoA synthetase; ER, endoplasmic reticulum; TAG, triacylglycerol.

may reflect the ability to cope with oxidative damage. Consequently, controlling the peroxisomal population is a promising strategy to enhance stress tolerance in plants.

Introduction of a peroxisome proliferator activated receptor from *Xenopus laevis* in tobacco plants leads to increased peroxisome number in transgenic tobacco plants [34]. Expression of this regulatory complex increases peroxisome number in transgenic tobacco plants, as it was previously reported for animal tissues [35]. The activity of peroxisomal enzymes involved in ROS scavenging is increased, leading to potentially improved resistance to oxidative stress [36]. The induced peroxisome proliferation disrupts the plant's redox state, leading to modified salicylic acid levels and altered expression patterns of jasmonic acid and ethylene biosynthesis genes. These changes positively affect pathogen resistance [36].

In an independent approach, an enlarged peroxisome population was produced by up regulation of the *Arabidopsis* peroxisome biogenesis gene PEX11, the regulator of peroxisome proliferation [13]. However, increasing the peroxisome number did not result in elevated salt tolerance in *Arabidopsis* seedlings and older plants [37]. Future studies need to elucidate if manipulating peroxisome biogenesis can be a strategy to alter stress tolerance. However, understanding regulation and all possible side effects is crucial when increasing the peroxisomal population.

3.2. Improving peroxisomal ROS scavenging systems

Under non stress conditions ROS produced by peroxisomal metabolism are scavenged by the simultaneous action of the peroxisomal antioxidant systems catalase, ascorbate peroxidase and the ascorbate glutathione cycle [38]. However, under oxidative stress conditions peroxisomal ROS generation is enhanced and ROS scavenging is insufficient [38]. The ability to cope with an increased ROS production is correlated with upregulation of peroxisomal

antioxidant systems in natural stress tolerant plant species [39,40]. One goal for engineering plants with wide ranging stress resistance would be improving the peroxisomal ROS scavenging machinery (i.e. modulate the gene expression and enzymatic activity).

Catalase as a prominent H_2O_2 scavenger is an important target. It is highly abundant in plant peroxisomes but has a low substrate affinity [41]. Modulation of its catalytic activity might be a starting point to overcome this drawback, leading to more efficient ROS detoxification in plant peroxisomes. Because bacterial catalases offer higher H_2O_2 affinity, several studies have ectopically expressed the *Escherichia coli* catalase in plant species such as tobacco, tomato, and rice [42–44]. The resulting transgenic plants displayed an increased protection against oxidative stress. The same outcome was achieved by overexpression of the peroxisomal ascorbate peroxidase (APX), which acts in tandem with catalase to degrade H_2O_2 [45,46]. Alternatively, an enhanced ascorbate glutathione cycle in the peroxisomal matrix could reduce plant stress [38]. To accomplish this task various modifications are required simultaneously: (i) enlarging the peroxisomal glutathione and ascorbate pool by stimulating biosynthesis and uptake into peroxisomes, (ii) increasing the NADPH levels in peroxisomes by over expressing the peroxisomal NAD kinase for NADPH production [47], and (iii) constitutive peroxisomal targeting of glutathione reductase, which carries a weak peroxisomal targeting signal and is located in the cytosol and peroxisomes [48]. Previous studies have successfully induced the biosynthesis of glutathione and ascorbate, resulting in higher glutathione and ascorbate levels in the cytosol [49,50]. To increase peroxisomal import of glutathione and ascorbate, specific peroxisomal transport proteins remain to be identified. To date, modifying the redox state of peroxisomal ascorbate and glutathione pools is feasible [47,48]. Enhancing glutathione and ascorbate uptake remains to be achieved in future, since corresponding peroxisomal transporters have not been identified thus far.

3.3. Improved pest and pathogen resistance

Plants suffer from infections caused by fungi, bacteria, viruses and nematodes. Peroxisomes play a substantial role in disease resistance and are targets for genetic improvement to confer pathogen tolerance in plants [4].

The phytohormone jasmonic acid (JA) is a lipid derived signaling molecule that induces plant defense mechanisms [51]. Its production is triggered in response to tissue injury (wounding) caused by herbivore attack. The last steps of JA biosynthesis occur in peroxisomes [51]. The JA precursor 12-oxo-phytodienoic acid (OPDA) is imported into peroxisomes and is subsequently reduced to OPC8:0 (3-oxo-2-(2-[Z]-pentenyl)cyclopentan-1-octanoic acid). In three rounds of peroxisomal β -oxidation activated OPC8:0 is converted to JA [52]. Overexpression of the transcription factor WRKY30 in rice resulted in a constitutive expression of plastidic JA biosynthesis genes. This was associated with increased endogenous JA accumulation and enhanced tolerance against fungal pathogens [53]. As JA biosynthetic enzymes locate to companion cells and sieve elements of the vascular bundle [54], it might be beneficial to not only improve biosynthesis, but extend JA production to other tissues to prime plants against herbivore attack. This involves exploiting a natural peroxisomal function.

Plant peroxisomes contribute to extracellular defense mechanisms against fungi by preventing colonization. Upon fungal invasion peroxisomes migrate toward the site of invasion [55]. Under these conditions the myrosinase PEN2, which is bound to the peroxisomal membrane, hydrolyzes indolic glucosinolates to antifungal defense compounds protecting plants against fungal entry [56]. Furthermore, certain benzylglucosinolates play a role in pathogen defense and are found in developing seeds and germinating seedlings [57]. These active defense molecules are synthesized in the cytosol by transferring a benzoyl moiety from benzoyl CoA to a hydroxylated aliphatic glucosinolate, though the precursor benzoyl CoA is primarily produced from cinnamic acid via peroxisomal β -oxidation [58–60].

Engineering levels of these defense compounds might enhance plant immunity against pathogens. This can be achieved by targeting either biosynthetic or regulatory genes of glucosinolate biosynthesis [58,61]. Glucosinolates are naturally found in crucifers, including oilseed rape and *Arabidopsis*, but their production could be successfully implemented in non-cruciferous plants, such as tobacco [62]. However, cruciferous crop seeds with high glucosinolate content are unwanted as primary food source for animals or humans, because these metabolites have a bitter taste [63]. An agricultural challenge for the future is to eliminate glucosinolates from edible parts of crops, but retain their synthesis in source tissues for protection against pathogen attack. Specific expression and suppression of peroxisomal modules involved in benzylglucosinolate production might be a promising approach to solve this problem.

3.4. Peroxisomal small heat shock proteins for enhanced stress tolerance

Small heat shock proteins are induced in response to various stresses. They act as molecular chaperones preventing the aggregation of nascent and stress accumulated misfolded proteins [64,65]. Two peroxisome located small heat shock proteins called AtAc31.2 and AtHsp15.7 were identified in *Arabidopsis* [66]. AtAc31.2 is constitutively expressed, whereas AtHsp15.7 expression is strongly induced by heat and oxidative stress [66], suggesting that peroxisomal small heat shock proteins play a role in protecting proteins under both physiological and stress conditions [67]. The overexpression of small heat shock proteins might be a useful strategy to produce plants with enhanced tolerance against different stresses. Previous studies have demonstrated

that substantial tolerance to salt, drought and high light can be achieved by over-expressing cytosolic or plastidic heat shock proteins [67–69].

4. Modulating auxin synthesis in peroxisomes

Peroxisomes are involved in biogenesis of the auxin indole-3-acetic acid. Indole-3-butyric acid is metabolized to the active form indole-3-acetic acid by removing two side chain methylene units in a process similar to fatty acid β -oxidation [70,71]. It has been shown that indole-3-butyric acid derived auxin induces cell expansion in certain cell types, resulting in elongated root hairs and enlarged cotyledons [72]. Elongation of root hairs by stimulating auxin production is a promising approach to enlarge root surface area and thereby enhance water and nutrient uptake [73]. Whether this goal can be accomplished without major drawbacks on plant development remains to be shown.

5. Implementation of artificial metabolic pathways to gain novel peroxisomal functions

Besides optimizing peroxisomal metabolism, metabolic engineering can achieve novel peroxisomal functions. The goal is to introduce artificial pathways into plant peroxisomes for either producing novel substances or improving efficiency of peroxisomal pathways degrading toxic compounds.

5.1. Production of biodegradable polymers in plant peroxisomes

Plant peroxisomes are attractive factories for biodegradable polymers, such as polyhydroxyalkanoates (PHA). Renewable bioplastics are sustainable and have the potential to replace conventional mineral oil based plastics [74].

PHAs are a group of polyesters, which are naturally formed and deposited as inclusion bodies in many bacterial genera. They are not produced in eukaryotes [75]. PHAs can incorporate more than one hundred different hydroxyacids, mainly varying in functional groups of side chains and chain length [76]. Thus, physical properties of PHA range from glues to brittle plastics, depending on the composition [77]. The biosynthesis pathway of the most common type of PHAs, the homopolymer poly-3-hydroxybutyrate (PHB), was discovered first in *Ralstonia eutropha*, where it serves as a carbon sink [78,79]. Its synthesis pathway has been successfully introduced into different microorganisms, which naturally do not produce these polymers [80]. To increase substrate availability for PHA biosynthesis, overproduction of the starting substrate acetyl CoA was induced, which led to an improved PHA production in these organisms [81].

However, PHA production in microorganisms is not economical because of expensive bacterial feedstock, such as glucose [82]. To address economic inefficiency, plants producing high amounts of PHA were designed. Plants are well suited, as water, light, CO₂, and a few minerals suffice to produce high amounts of biomass. Moreover, plants are unable to degrade PHAs and thus can accumulate these polymers in high amounts. For successful PHA production in plants three prerequisites are needed: (i) the bacterial three gene pathway consisting of a 3-ketothiolase (*phaA*), an acetoacetyl CoA reductase (*phaB*) and a PHA synthase (*phaC*), (ii) a large acetyl CoA pool, and (iii) reducing power [83].

PHA production was first achieved in the cytosol of *Arabidopsis* and tobacco, because only two additional enzymes had to be introduced, *phaB* and *phaC*, as plants endogenously possess a cytosolic form of *phaA* as part of the mevalonate pathway (Fig. 2A). The production of PHA led to a strong reduction of plant growth, resulting from depletion of cytoplasmic acetyl CoA, inhibiting

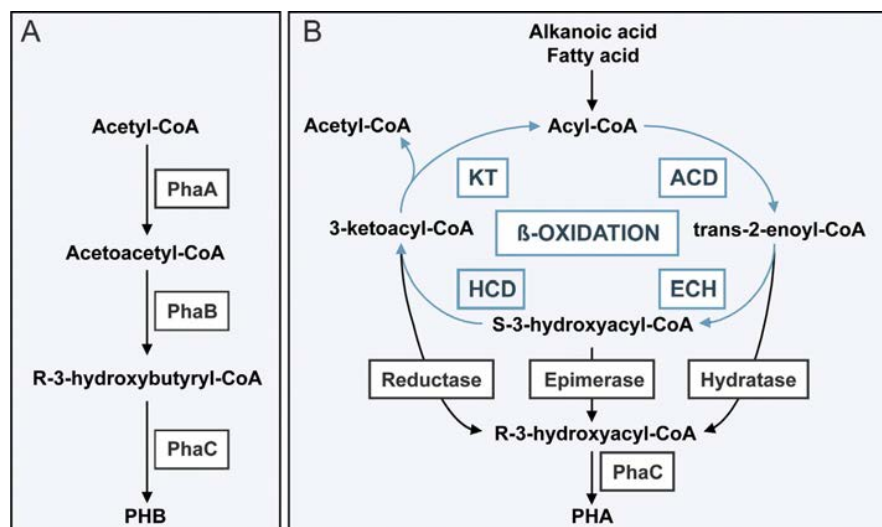


Fig. 2. (A) PHB synthesis in *Ralstonia eutropha*. Bacterial pathway of PHB production in *R. eutropha*. *phaA*, 3 ketothiolase; *phaB*, acetoacetyl CoA reductase; *phaC*, PHA synthase. (B) PHA synthesis in plants can be implemented into the beta oxidation cycle. Intermediates of the beta oxidation can be used for PHA synthesis. Either an epimerase, a hydratase, or a reductase is necessary to convert cycle intermediates into substrates for *phaC*. The beta oxidation core reactions are depicted in blue. KT, 3 ketothiolase; ACD, acyl CoA dehydrogenase; ECH, enoyl CoA hydratase I; HCD, S 3 hydroxyacyl CoA dehydrogenase.

isoprenoid and avonoid biosynthesis [75,84]. To achieve higher PHA levels, with less deleterious effects, production was targeted to chloroplasts of numerous plant species. PHA yield was predicted to increase, as plastids have a high flux of acetyl CoA, which is required for fatty acid biosynthesis. In transgenic plant lines accumulating high amounts of PHA in their chloroplasts, growth was reduced, plants were chlorotic, and sometimes fertility was impacted. The reasons for the strong phenotype have not been clearly determined [85–87].

To minimize plant growth defects, PHA synthesis was targeted to plant peroxisomes (Fig. 2B) exploiting peroxisomal carbon flux through beta oxidation for synthesis [88–91]. A peroxisomal targeting signal was fused to the bacterial *phaA*, *phaB*, and *phaC* genes. Peroxisomes of PHA producing plants are significantly enlarged. This reflects that these organelles have the capability to increase their size to accommodate large volumes of PHA granules [91]. Studies with the C4 grass sugarcane, a high biomass crop, showed that peroxisomal PHA biosynthesis significantly contributes to PHA production levels of commercial interest in crop plants, without interfering with plant growth [91].

5.2. Peroxisomal bypass pathways to reduce photorespiration

A central function of plant peroxisomes is their contribution to photorespiration (Fig. 3) [4]. This light dependent pathway is linked to photosynthesis by the dual function of plastidic RubisCO. Low carbon dioxide concentrations favor the oxygenase reaction of RubisCO leading to an accumulation of toxic 2-phosphoglycolate [92]. This compound is efficiently degraded via the photorespiratory C2 cycle, converting 2-phosphoglycolate to 3-phosphoglycerate, which re-enters the Calvin Benson cycle. CO₂ and ammonia (NH₃) are released. Substantial energy costs are required for re-assimilation (Fig. 3) [92]. The goal is to optimize plant metabolism and to increase biomass production by minimizing energy losses in photorespiration. As photorespiration is required in all photosynthetic organisms, it cannot be eliminated completely, but bypassed [93]. So far, three reactions have been tested in plants circumventing energy loss from photorespiration [94]. A reduction of the RubisCO oxygenase reaction was attempted by increasing CO₂ levels inside chloroplasts, utilizing

carbon derived from 2-phosphoglycolate (Fig. 3, blue pathway) [95]. Secondly, an alternative plastidic conversion route for 2-phosphoglycolate has been reported (Fig. 3, red pathway) [96]. Both approaches bypassing the mitochondrial CO₂ release led to an increase in biomass production under ambient CO₂ conditions [95,96].

To avoid mitochondrial NH₃ production a short circuit pathway of the photorespiratory nitrogen cycle was implemented into peroxisomes [97]. Glyoxylate carboxylase (GCL) and hydroxypyruvate isomerase (HYI) from *E. coli* were introduced into peroxisomes of transgenic tobacco leaves resulting in a peroxisomal conversion of glyoxylate to hydroxypyruvate (Fig. 3, green pathway). Unfortunately, this bypass did not show the benefits expected for biomass production [97]. Instead, leaves of transgenic tobacco displayed chlorotic lesions under ambient CO₂ levels. Detailed analyses revealed that the GCL/HYI pathway introduced was not fully operating, due to silencing of the bacterial hydroxypyruvate isomerase gene [97]. Thus, the functionality of this proposed pathway remains to be demonstrated. The use of RNA silencing tobacco mutants might overcome this obstacle [98]. It might enable further analyses studying peroxisomes as tools to bypass photorespiration [97].

5.3. Peroxisomal degradation pathways for pollutants

Genetically modified plants can help to reduce environmental pollution by degradation of long persisting chemical compounds in contaminated soil or ground water. The implementation of catabolic pathways from various bacterial and fungal organisms into plants allows detoxification of certain organic pollutants [99].

For example, tobacco plants have been developed which degrade the halogenated aliphatic compound 1,2-dichloroethane, a carcinogenic chemical of high stability. In these plants, two enzymes from *Xanthobacter autotrophicus* were expressed that catabolize 1,2-dichloroethane to glycolate in combination with endogenous enzymes [100]. High accumulation of the resulted end product glycolate is toxic for the plant cell and needs to be directly metabolized. In particular for the root tissue, it might be to ectopically introduce the photorespiratory enzyme glycolate oxidase in root cells for the conversion of glycolate to glyoxylate.

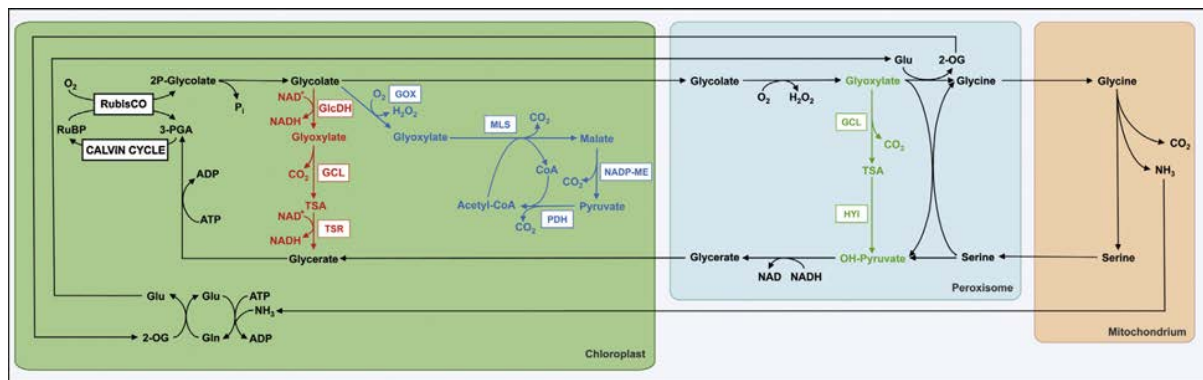


Fig. 3. The loss of ammonia during photorespiration can be bypassed. Ammonia and CO₂ are released in mitochondria during the conversion of glycine to serine. Ammonia can be re-assimilated in chloroplasts. The ammonia-consuming reactions can be bypassed by a photorespiratory short circuit in peroxisomes (shown in green) by introducing two bacterial enzymes GCL and HYI. The plastidic bypasses introduced by Maier et al. [95] and Kebeish et al. [96] are presented in blue and red, respectively. RuBP, ribulose 1,5 biphosphate; PGA, phosphoglycerate; Glu, glutamate; Gln, glutamine; 2 OG, 2 oxoglutarate; ATP, adenosine triphosphate; ADP, adenosine diphosphate; NAD(H), nicotinamide adenine dinucleotide; TSA, tartronic semialdehyde; GCL, glyoxylate carbolyase; HYI, hydroxypyruvate isomerase.

Sulfur dioxide is a major air pollutant emitted by industrial processes. SO₂ adversely affects growth and development of crop species, causing chlorosis, necrosis and long term yield reduction [101–103]. It enters plant tissues as gas, where it is transformed to sulfate. Excess amounts of sulfate are toxic to the plant cell. Peroxisomal catalase activity is sensitive to sulfate, resulting in high H₂O₂ levels upon sulfate stress [104]. The key enzyme to protect plants against sulfate toxicity is the peroxisomal sulfate oxidase, catalyzing the oxidation of sulfate to sulfate. To improve sulfate detoxification, the peroxisomal sulfate oxidase from maize was overexpressed in plants [105,106]. Transgenic lines exhibiting elevated sulfate oxidase levels confer enhanced tolerance to excess sulfate, which is indicated by lower H₂O₂ and higher catalase levels. Hence, the overexpression of sulfate oxidase may protect peroxisomal catalase from inhibition by sulfate [106].

6. Concluding remarks

Besides recent progress in the field of peroxisome engineering, the emerging potential of plant peroxisomes for green biotechnology is described in this review. Strategies are presented which either (i) manipulate peroxisomal pathways to alter oilseed quantity and quality, or (ii) improve tolerance toward abiotic and biotic stresses. Further, approaches are shown which involve (iii) implementing new pathways in peroxisomes, such as the production of biodegradable polymers, (iv) bypassing peroxisomal pathways for a better energy cost efficiency, and (v) detoxifying pollutants from contaminated soil, water and air.

However, several limitations have to be considered when modifying or introducing pathways to peroxisomes. If fluxes through endogenous peroxisomal pathways are changed, overall cellular metabolism and substrate homeostasis could be negatively influenced. For example, changes in peroxisomal contributions to auxin synthesis or photorespiration were reported to create substantial reductions in fitness [107,108]. In order to estimate the biotechnological potential of plant peroxisomes, it is necessary to understand how peroxisomal metabolism is regulated and coordinated.

When implementing novel pathways, the pH optimum inside peroxisomes needs to be considered, because newly introduced enzymes with a strict cofactor and pH dependency might be impaired. The pH of plant peroxisomes has not yet been determined. Reports for other eukaryotic organisms, including yeast and mammals, indicated contradictory results the peroxisomal matrix is either acidic or alkaline [109–112]. In addition, cofactors need to

be available in peroxisomes, when implementing certain enzymatic reactions. Peroxisomes are capable of importing fully folded proteins, which have already bound their cofactor in the cytosol [113]. For ATP, NAD and CoA transporters have been identified importing these cofactors into peroxisomes [114–116]. Further, the level of peroxide radicals could interfere with enzyme activities, since peroxisomes exhibit an oxidative metabolism producing ROS.

Successful engineering of plant peroxisomal metabolism requires insights into the complete protein inventory. To date, proteome analyses identified more than 100 peroxisomal proteins in plants. However, further enzymes are necessary to fulfill proposed or described metabolic functions [117]. In this context, a major obstacle is the missing comprehensive knowledge about metabolite transport proteins, mediating the flux of solutes across the peroxisomal membrane [118]. Although many peroxisomal transport steps are hypothesized in plants, the corresponding transporter genes have not yet been assigned. Besides the three cofactor carriers mentioned earlier, only the carrier importing fatty acids has been identified so far [114, 116, 118–120]. With regard to metabolite transport, biotechnological implementations have to be considered carefully, because the prospective substrates and products need to be shuttled in and out of peroxisomes.

As very little is known about endogenous export from peroxisomes, secretion of substances produced in peroxisomes might even be a favorable trait for biotechnological production, as it is known for algae [121]. Such a process protects the cell from potential toxic effects of compounds created in this organelle. On the other hand, secretion of products can be favorable to avoid expensive downstream processing after biotechnological production. In a process called peroxicretion, subsequent excretion of peroxisomal products from cells was achieved by fusing the soluble domain of a Golgi derived v-SNARE to a peroxisomal membrane protein used as an anchor. Fusion of peroxisomes with the plasma membrane was induced and products were released into the extracellular space [122]. This artificial secretion pathway, coupled to an inducible promoter controlling the time point of product release, might raise the utility of engineered production in plant peroxisomes for industrial biotechnology.

A long term goal of engineering plant peroxisomes is the construction of synthetic peroxisomes in plants or other eukaryotic organisms, such as yeast. First steps toward this goal have been taken recently, when in a human cell line two antioxidant enzymes, a Cu/Zn superoxide dismutase and a catalase isoform, were expressed in polymer vesicles, which have a membrane made

permeable by insertion of channel proteins. In this artificial peroxisome, some superoxide radicals and H₂O₂ detoxification was functional [123].

Acknowledgements

This work was supported by the DFG grant 1781/1-1, 1781/2-1 and GRK 1525. The authors thank Andreas P.M. Weber for helpful discussion and P.K. Lundqvist for reading the manuscript.

References

- [1] J.M. Hibberd, A.P.M. Weber, Plant metabolism and physiology, *Curr. Opin. Plant Biol.* 15 (2012) 225–227.
- [2] M. Hayashi, M. Nishimura, Entering a new era of research on plant peroxisomes, *Curr. Opin. Plant Biol.* 6 (2003) 577–582.
- [3] R. Erdmann, M. Veenhuis, W.H. Kunau, Peroxisomes: organelles at the crossroads, *Trends Cell Biol.* 7 (1997) 400–407.
- [4] J. Hu, et al., Plant peroxisomes: biogenesis and function, *Plant Cell* 24 (2012) 2279–2303.
- [5] J. Nielsen, Metabolic engineering: techniques for analysis of targets for genetic manipulations, *Biotechnol. Bioeng.* 58 (1998) 125–132.
- [6] J.M. Palma, et al., Antioxidative enzymes from chloroplasts, mitochondria, and peroxisomes during leaf senescence of nodulated pea plants, *J. Exp. Bot.* 57 (2006) 1747–1758.
- [7] S.J. Gould, G.A. Keller, N. Hosken, J. Wilkinson, S. Subramani, A conserved tripeptide sorts proteins to peroxisomes, *J. Cell Biol.* 108 (1989) 1657–1664.
- [8] C. Ma, S. Reumann, Improved prediction of peroxisomal PTS1 proteins from genome sequences based on experimental subcellular targeting analyses as exemplified for protein kinases from *Arabidopsis*, *J. Exp. Bot.* 59 (2008) 3767–3779.
- [9] B.W. Swinkels, S.J. Gould, A.G. Bodnar, R.A. Rachubinski, S. Subramani, A novel, cleavable peroxisomal targeting signal at the amino terminus of the rat 3-ketoacyl CoA thiolase, *EMBO J.* 10 (1991) 3255–3262.
- [10] M.S. Lee, R.T. Mullen, R.N. Trelease, Oilseed isocitrate lyases lacking their essential type 1 peroxisomal targeting signal are piggybacked to glyoxysomes, *Plant Cell* 9 (1997) 185–197.
- [11] T. Meyer, C. Holscher, C. Schwoppe, A. von Schaewen, Alternative targeting of *Arabidopsis* plastidic glucose 6-phosphate dehydrogenase G6PD1 involves cysteine-dependent interaction with G6PD4 in the cytosol, *Plant J.* 66 (2011) 745–758.
- [12] M. Schrader, N.A. Bonekamp, M. Islinger, Fission and proliferation of peroxisomes, *Biochim. Biophys. Acta* 1822 (2011) 1343–1357.
- [13] T. Orth, et al., The PEROXIN1 protein family controls peroxisome proliferation in *Arabidopsis*, *Plant Cell* 19 (2007) 333–350.
- [14] M. Yan, N. Rayapuram, S. Subramani, The control of peroxisome number and size during division and proliferation, *Curr. Opin. Cell Biol.* 17 (2005) 376–383.
- [15] M. Islinger, S. Grille, H.D. Fahimi, M. Schrader, The peroxisome: an update on mysteries, *Histochem. J.* 137 (2012) 547–574.
- [16] J.A. Napier, I.A. Graham, Tailoring plant lipid composition: designer oilseeds come of age, *Curr. Opin. Plant Biol.* 13 (2010) 330–337.
- [17] N. Ruiz Lopez, O. Sayanova, J.A. Napier, R.P. Haslam, Metabolic engineering of the omega-3 long chain polyunsaturated fatty acid biosynthetic pathway into transgenic plants, *J. Exp. Bot.* 63 (2012) 2397–2410.
- [18] J.A. Napier, The production of unusual fatty acids in transgenic plants, *Annu. Rev. Plant Biol.* 58 (2007) 295–319.
- [19] J. Jaworski, E.B. Cahoon, Industrial oils from transgenic plants, *Curr. Opin. Plant Biol.* 6 (2003) 178–184.
- [20] V. Eccleston, J. Ohlrogge, Expression of lauroyl acyl carrier protein thioesterase in *Brassica napus* seeds induces pathways for both fatty acid oxidation and biosynthesis and implies a set point for triacylglycerol accumulation, *Plant Cell* 10 (1998) 613–622.
- [21] L. Moire, E. Rezzonico, S. Goepfert, Y. Poirier, Impact of unusual fatty acid synthesis on futile cycling through beta-oxidation and on gene expression in transgenic plants, *Plant Physiol.* 134 (2004) 432–442.
- [22] S.P. Slocombe, et al., Oil accumulation in leaves directed by modification of fatty acid breakdown and lipid synthesis pathways, *Plant Biotechnol. J.* 7 (2009) 694–703.
- [23] B. Halliwell, Reactive species and antioxidants. Redox biology is a fundamental theme of aerobic life, *Plant Physiol.* 141 (2006) 312–322.
- [24] R. Mittler, Oxidative stress, antioxidants and stress tolerance, *Trends Plant Sci.* 7 (2002) 405–410.
- [25] W. Wang, B. Vinocur, A. Altman, Plant responses to drought, salinity and extreme temperatures: towards genetic engineering for stress tolerance, *Planta* 218 (2003) 1–14.
- [26] N. Kaur, J. Hu, Dynamics of peroxisome abundance: a tale of division and proliferation, *Curr. Opin. Plant Biol.* 78 (2009) 781–788.
- [27] M. Desai, J. Hu, Light induces peroxisome proliferation in *Arabidopsis* seedlings through the photoreceptor phytochrome A, the transcription factor HY5 HOMOLOG, and the peroxisomal protein PEROXIN1b, *Plant Physiol.* 146 (2008) 1117–1127.
- [28] M.C. Castillo, L.M. Sandalio, L.A. del Rio, J. Leon, Peroxisome proliferation, wound activated responses and expression of peroxisome associated genes are cross-regulated but uncoupled in *Arabidopsis thaliana*, *Plant Cell Environ.* 31 (2008) 492–505.
- [29] E. Lopez Huertas, W.L. Charlton, B. Johnson, I.A. Graham, A. Baker, Stress induces peroxisome biogenesis genes, *EMBO J.* 19 (2000) 6770–6777.
- [30] D.J. Morre, et al., Peroxisome proliferation in Norway spruce induced by ozone, *Protoplasma* 155 (1990) 58–65.
- [31] J.M. Palma, M. Garrido, M.I. Rodriguez Garcia, L.A. del Rio, Peroxisome proliferation and oxidative stress mediated by activated oxygen species in plant peroxisomes, *Arch. Biochem. Biophys.* 287 (1991) 68–74.
- [32] G.M. Pastori, L.A. del Rio, An activated oxygen-mediated role for peroxisomes in the mechanism of senescence of *Pisum sativum* leaves, *Planta* 193 (1994) 385–391.
- [33] M.C. Romero Puertas, et al., Cadmium toxicity and oxidative metabolism of pea leaf peroxisomes, *Free Radic. Res.* 31 (Suppl) (1999) S25–S31.
- [34] A.G. Nila, et al., Expression of a peroxisome proliferator-activated receptor gene (xPPARalpha) from *Xenopus laevis* in tobacco (*Nicotiana tabacum*) plants, *Planta* 224 (2006) 569–581.
- [35] I. Isemann, S. Green, Activation of a member of the steroid hormone receptor superfamily by peroxisome proliferators, *Nature* 347 (1990) 645–650.
- [36] J.H. Valenzuela Soto, et al., Transformed tobacco (*Nicotiana tabacum*) plants overexpressing a peroxisome proliferator-activated receptor gene from *Xenopus laevis* (xPPARα) show increased susceptibility to infection by virulent *Pseudomonas syringae* pathogens, *Planta* 233 (2011) 507–521.
- [37] S. Mitsuya, et al., Salt stress causes peroxisome proliferation, but inducing peroxisome proliferation does not improve NaCl tolerance in *Arabidopsis thaliana*, *PLoS One* 5 (2010) e9408.
- [38] L.A. del Rio, et al., Reactive oxygen species, antioxidant systems and nitric oxide in peroxisomes, *J. Exp. Bot.* 53 (2002) 1255–1272.
- [39] V. Mittova, M. Guy, M. Tal, M. Volokita, Salinity up-regulates the antioxidative system in root mitochondria and peroxisomes of the wild salt-tolerant tomato species *Lycopersicon pennellii*, *J. Exp. Bot.* 55 (2004) 1105–1113.
- [40] V. Mittova, M. Tal, M. Volokita, M. Guy, Up-regulation of the leaf mitochondrial and peroxisomal antioxidative systems in response to salt-induced oxidative stress in the wild salt-tolerant tomato species *Lycopersicon pennellii*, *Plant Cell Environ.* 26 (2003) 845–856.
- [41] A. Mhamdi, G. Noctor, A. Baker, Plant catalases: peroxisomal redox guardians, *Arch. Biochem. Biophys.* 61 (2012) 4197–4220.
- [42] E.A. Mohamed, et al., Overexpression of bacterial catalase in tomato leaf chloroplasts enhances photo-oxidative stress tolerance, *Plant Cell Environ.* 26 (2003) 2037–2046.
- [43] T. Moriwaki, et al., Overexpression of the *Escherichia coli* catalase gene, katE, enhances tolerance to salinity stress in the transgenic indica rice cultivar, BR5, *Plant Biotechnol. Rep.* 2 (2008) 41–46.
- [44] T. Shikanai, et al., Inhibition of ascorbate peroxidase under oxidative stress in tobacco having bacterial catalase in chloroplasts, *FEBS Lett.* 428 (1998) 47–51.
- [45] Y. J. Li, R. L. Hai, X. H. Du, X. N. Jiang, H. Lu, Overexpression of a Populus peroxisomal ascorbate peroxidase (PpAPX) gene in tobacco plants enhances stress tolerance, *Plant Breeding* 128 (2009) 404–410.
- [46] J. Wang, H. Zhang, R.D. Allen, Overexpression of an *Arabidopsis* peroxisomal ascorbate peroxidase gene in tobacco increases protection against oxidative stress, *Plant Cell Physiol.* 40 (1999) 725–732.
- [47] J.C. Waller, P.K. Dhanoa, U. Schumann, R.T. Mullen, W.A. Snedden, Subcellular and tissue localization of NAD kinases from *Arabidopsis*: compartmentalization of *de novo* NADP biosynthesis, *Planta* 231 (2010) 305–317.
- [48] A.R. Kataya, S. Reumann, *Arabidopsis* glutathione reductase 1 is dually targeted to peroxisomes and the cytosol, *Plant Signal. Behav.* 5 (2010).
- [49] Z. Chen, T.E. Young, J. Ling, S.C. Chang, D.R. Gallie, Increasing vitamin C content of plants through enhanced ascorbate recycling, *Proc. Natl. Acad. Sci. USA* 100 (2003) 3525–3530.
- [50] C.H. Foyer, et al., Overexpression of glutathione reductase but not glutathione synthase leads to increases in antioxidant capacity and resistance to photoinhibition in poplar trees, *Plant Physiol.* 109 (1995) 1047–1057.
- [51] I.F. Acosta, E.E. Farmer, Jasmonates, *The Arabidopsis Book*, vol. 8, 2010, pp. e0129.
- [52] C. Wasternack, E. Kombrink, Jasmonates: structural requirements for lipid-derived signals active in plant stress responses and development, *ACS Chem. Biol.* 5 (2010) 63–77.
- [53] X. Peng, et al., Constitutive expression of rice WRKY30 gene increases the endogenous jasmonic acid accumulation, PR gene expression and resistance to fungal pathogens in rice, *Planta* 236 (2012) 1485–1498.
- [54] B. Hause, G. Hause, C. Kutter, O. Miersch, C. Wasternack, Enzymes of jasmonate biosynthesis occur in tomato sieve elements, *Plant Cell Physiol.* 44 (2003) 643–648.
- [55] V. Lipka, et al., Pre- and postinvasion defenses both contribute to nonhost resistance in *Arabidopsis*, *Science* 310 (2005) 1180–1183.
- [56] P. Bednarek, et al., A glucosinolate metabolism pathway in living plant cells mediates broad spectrum antifungal defense, *Science* 323 (2009) 101–106.
- [57] G. Graser, N.J. Oldham, P.D. Brown, U. Temp, J. Gershenzon, The biosynthesis of benzoic acid glucosinolate esters in *Arabidopsis thaliana*, *Phytochemistry* 57 (2001) 23–32.
- [58] V. Baskar, M.A. Gururani, J.W. Yu, S.W. Park, Engineering glucosinolates in plants: current knowledge and potential uses, *Appl. Biochem. Biotechnol.* 168 (2012) 1694–1717.

- [59] S. Lee, et al., Benzoylation and sinapoylation of glucosinolate R groups in *Arabidopsis*, *Plant J.* 72 (2012) 411–422.
- [60] A.V. Qualley, J.R. Widhalm, F. Adebessin, C.M. Kish, N. Dudareva, Completion of the core β oxidative pathway of benzoic acid biosynthesis in plants, *Proc. Natl. Acad. Sci. U.S.A.* 109 (2012) 16383–16388.
- [61] F. Geu Flores, C.E. Olsen, B.A. Halkier, Towards engineering glucosinolates into non cruciferous plants, *Planta* 229 (2009) 261–270.
- [62] M.E. M Idrup, et al., Engineering of benzylglucosinolate in tobacco provides proof of concept for dead end trap crops genetically modified to attract *Plutella xylostella* (diamondback moth), *Plant Biotechnol. J.* 10 (2012) 435–442.
- [63] N. Nesi, R. Delourme, M. Brignon, C. Falentin, M. Renard, Genetic molecular approaches to improve nutritional value of *Brassica napus* L. seed, *C. R. Biol.* 331 (2008) 763–771.
- [64] W. Wang, B. Vinocur, O. Shoseyov, A. Altman, Role of plant heat shock proteins and molecular chaperones in the abiotic stress response, *Trends Plant Sci.* 9 (2004) 244–252.
- [65] J.C. Young, J.M. Barral, F. Ulrich Hartl, More than folding: localized functions of cytosolic chaperones, *Trends Biochem. Sci.* 28 (2003) 541–547.
- [66] C. Ma, M. Haslbeck, L. Babujee, O. Jahn, S. Reumann, Identification and characterization of a stress-inducible and a constitutive small heat shock protein targeted to the matrix of plant peroxisomes, *Plant Physiol.* 141 (2006) 47–60.
- [67] H. Chauhan, N. Khurana, A. Nijhavan, J.P. Khurana, P. Khurana, The wheat chloroplastic small heat shock protein (sHSP26) is involved in seed maturation and germination and imparts tolerance to heat stress, *Plant Cell Environ.* 35 (2012) 1912–1931.
- [68] Y. Sato, S. Yokoya, Enhanced tolerance to drought stress in transgenic rice plants overexpressing a small heat shock protein, sHSP17.7, *Plant Cell Rep.* 27 (2008) 329–334.
- [69] J. Zou, C. Liu, A. Liu, D. Zou, X. Chen, Overexpression of OsHsp17.0 and OsHsp23.7 enhances drought and salt tolerance in rice, *J. Plant Physiol.* 169 (2012) 628–635.
- [70] L.C. Strader, A.H. Culler, J.D. Cohen, B. Bartel, Conversion of endogenous indole 3 butyric acid to indole 3 acetic acid drives cell expansion in *Arabidopsis* seedlings, *Plant Physiol.* 153 (2010) 1577–1586.
- [71] B.K. Zolman, N. Martinez, A. Millius, A.R. Adham, B. Bartel, Identification and characterization of *Arabidopsis* indole 3 butyric acid response mutants defective in novel peroxisomal enzymes, *Genetics* 180 (2008) 237–251.
- [72] L.C. Strader, B. Bartel, The *Arabidopsis* PLEIOTROPIC DRUG RESISTANCE8/ABCG36 ATP binding cassette transporter modulates sensitivity to the auxin precursor indole 3 butyric acid, *Plant Cell* 21 (2009) 1992–2007.
- [73] A.P. Wasson, et al., Traits and selection strategies to improve root systems and water uptake in water limited wheat crops, *J. Exp. Bot.* 63 (2012) 3485–3498.
- [74] K. Sudesh, H. Abe, Y. Doi, Synthesis, structure and properties of polyhydroxyalkanoates: polyhydroxyesters, *Prog. Polym. Sci.* 25 (2000) 1503–1555.
- [75] Y. Poirier, D.E. Dennis, C. Klomparens, C. Somerville, Polyhydroxybutyrate, a biodegradable thermoplastic, produced in transgenic plants, *Science* 256 (1992) 520–523.
- [76] A. Steinbüchel, et al., Considerations on the structure and biochemistry of bacterial polyhydroxyalkanoic acid inclusions, *Can. J. Microbiol.* 41 (1995) 94–105.
- [77] Q. Ren, N. Sierro, M. Kellerhals, B. Kessler, B. Witholt, Properties of engineered poly 3 hydroxyalkanoates produced in recombinant *Escherichia coli* strains, *Appl. Environ. Microbiol.* 66 (2000) 1311–1320.
- [78] Y. Poirier, Polyhydroxyalkanoate synthesis in plants as a tool for biotechnology and basic studies of lipid metabolism, *Prog. Lipid Res.* 41 (2002) 131–155.
- [79] A. Steinbüchel, S. Hein, in: W. Babel, A. Steinbüchel (Eds.), *Biopolyesters*, vol. 71, Springer, Berlin, Heidelberg, 2001, pp. 81–123.
- [80] Y. Poirier, N. Erard, J. MacDonald Comber Petetot, Synthesis of polyhydroxyalkanoate in the peroxisome of *Pichia pastoris*, *FEMS Microbiol. Lett.* 207 (2002) 97–102.
- [81] K. Kocharin, Y. Chen, V. Siewers, J. Nielsen, Engineering of acetyl CoA metabolism for the improved production of polyhydroxybutyrate in *Saccharomyces cerevisiae*, *AMB Express* 2 (2012) 52.
- [82] Y. Poirier, Polyhydroxyalkanoate synthesis in plants as a tool for biotechnology and basic studies of lipid metabolism, *Prog. Lipid Res.* 41 (2002) 131–155.
- [83] K. Tilbrook, L. Gebbie, P.M. Schenk, Y. Poirier, S.M. Brumbley, Peroxisomal polyhydroxyalkanoate biosynthesis is a promising strategy for bioplastic production in high biomass crops, *Plant Biotechnol. J.* 9 (2011) 958–969.
- [84] H. Nakashita, et al., Production of biodegradable polyester by a transgenic tobacco, *Biosci. Biotechnol. Biochem.* 63 (1999) 870–874.
- [85] K. Bohmert, et al., Transgenic *Arabidopsis* plants can accumulate polyhydroxybutyrate up to 4% of their fresh weight, *Planta* 211 (2000) 841–845.
- [86] L.A. Petrasovits, et al., Enhanced polyhydroxybutyrate production in transgenic sugarcane, *Plant Biotechnol. J.* 10 (2012) 569–578.
- [87] Y. Poirier, C. Nawrath, C. Somerville, Production of polyhydroxyalkanoates, a family of biodegradable plastics and elastomers, in bacteria and plants, *Biotechnology* 13 (1995) 142–150.
- [88] Y. Arai, et al., Synthesis of a novel class of polyhydroxyalkanoates in *Arabidopsis* peroxisomes, and their use in monitoring short chain length intermediates of beta oxidation, *Plant Cell Physiol.* 43 (2002) 555–562.
- [89] J.J. Hahn, A.C. Eschenlauer, U.B. Sleytr, D.A. Somers, F. Srien, Peroxisomes as sites for synthesis of polyhydroxyalkanoates in transgenic plants, *Biotechnol. Prog.* 15 (1999) 1053–1057.
- [90] V. Mittendorf, et al., Polyhydroxyalkanoate synthesis in transgenic plants as a new tool to study carbon flow through beta oxidation, *Plant J.* 20 (1999) 45–55.
- [91] V. Mittendorf, et al., Synthesis of medium chain length polyhydroxyalkanoates in *Arabidopsis thaliana* using intermediates of peroxisomal fatty acid beta oxidation, *Proc. Natl. Acad. Sci. USA* 95 (1998) 13397–13402.
- [92] S. Reumann, A.P. Weber, Plant peroxisomes respire in the light: some gaps of the photorespiratory C2 cycle have become filled others remain, *Biochim. Biophys. Acta* 1763 (2006) 1496–1510.
- [93] V.G. Maurino, C. Peterhansel, Photorespiration: current status and approaches for metabolic engineering, *Curr. Opin. Plant Biol.* 2010 (2010) 23.
- [94] C. Peterhansel, C. Blume, S. Offermann, Photorespiratory bypasses: how can they work? *J. Exp. Bot.* 64 (2013) 709–715.
- [95] A. Maier, et al., Transgenic introduction of a glycolate oxidative cycle into *A. thaliana* chloroplasts leads to growth improvement, *Front. Plant Sci.* 3 (2012) 38.
- [96] R. Kebeish, et al., Chloroplastic photorespiratory bypass increases photosynthesis and biomass production in *Arabidopsis thaliana*, *Nat. Biotechnol.* 25 (2007) 593–599.
- [97] J.d.F.C. Carvalho, et al., An engineered pathway for glyoxylate metabolism in tobacco plants aimed to avoid the release of ammonia in photorespiration, *BMC Biotechnol.* 11 (2011) 111.
- [98] O. Voignet, S. Rivas, P. Mestre, D. Baulcombe, An enhanced transient expression system in plants based on suppression of gene silencing by the p19 protein of tomato bushy stunt virus, *Plant J.* 33 (2003) 949–956.
- [99] B. Van Aken, Transgenic plants for phytoremediation: helping nature to clean up environmental pollution, *Trends Biotechnol.* 26 (2008) 225–227.
- [100] G.L. Mena Benitez, et al., Engineering a catabolic pathway in plants for the degradation of 1,2 dichloroethane, *Plant Physiol.* 147 (2008) 1192–1198.
- [101] H.A. Menser, H. He, Ozone and sulfur dioxide synergism injury to tobacco plants, *Science* 153 (1966) 424–425.
- [102] M. Noji, et al., Cysteine synthase overexpression in tobacco confers tolerance to sulfur containing environmental pollutants, *Plant Physiol.* 126 (2001) 973–980.
- [103] T. van der Kooij, L.J. DeKok, S. Haneklaus, E. Schnug, Uptake and metabolism of sulphur dioxide by *Arabidopsis thaliana*, *New Phytol.* 135 (1997) 101–107.
- [104] S. Veljovic Jovanovic, L. Milovanovic, T. Oniki, U. Takahama, Inhibition of catalase by sulfate and oxidation of sulfate by H₂O₂ cooperating with ascorbic acid, *Free Radic. Res.* 31 (Suppl) (1999) S51–S57.
- [105] G. Brychikova, et al., Sulfate oxidase protects plants against sulfur dioxide toxicity, *Plant J.* 50 (2007) 696–709.
- [106] Z. Xia, et al., Overexpression of a maize sulfate oxidase gene in tobacco enhances tolerance to sulfate stress via sulfate oxidation and CAT mediated H₂O₂ scavenging, *PLoS ONE* 7 (2012) e37383.
- [107] D. Igarashi, et al., Identification of photorespiratory glutamate:glyoxylate aminotransferase (GGAT) gene in *Arabidopsis*, *Plant J.* 33 (2003) 975–987.
- [108] B.K. Zolman, A. Yoder, B. Bartel, Genetic analysis of indole 3 butyric acid responses in *Arabidopsis thaliana* reveals four mutant classes, *Genetics* 156 (2000) 1323–1337.
- [109] T.B. Dansen, K.W. Wirtz, R.J. Wanders, E.H. Pap, Peroxisomes in human fibroblasts have a basic pH, *Nat. Cell Biol.* 2 (2000) 51–53.
- [110] A. Jankowski, et al., In situ measurements of the pH of mammalian peroxisomes using the fluorescent protein pHluorin, *J. Biol. Chem.* 276 (2001) 48748–48753.
- [111] F.M. Lasorsa, et al., The yeast peroxisomal adenine nucleotide transporter: characterization of two transport modes and involvement in delta pH formation across peroxisomal membranes, *Biochem J.* 381 (2004) 581–585.
- [112] C.W. van Roermund, et al., The peroxisomal lumen in *Saccharomyces cerevisiae* is alkaline, *J. Cell Sci.* 117 (2004) 4231–4237.
- [113] T. Lanyon Hogg, S.L. Warriner, A. Baker, Getting a camel through the eye of a needle: the import of folded proteins by peroxisomes, *Biol. Cell* 102 (2010) 245–263.
- [114] Y. Arai, M. Hayashi, M. Nishimura, Proteomic identification and characterization of a novel peroxisomal adenine nucleotide transporter supplying ATP for fatty acid beta oxidation in soybean and *Arabidopsis*, *Plant Cell* 20 (2008) 3227–3240.
- [115] K. Bernhardt, S. Wilkinson, A.P.M. Weber, N. Linka, A peroxisomal carrier delivers NAD(+) and contributes to optimal fatty acid degradation during storage oil mobilization, *Plant J.* 69 (2012) 1–13.
- [116] N. Linka, et al., Peroxisomal ATP import is essential for seedling development in *Arabidopsis thaliana*, *Plant Cell* 20 (2008) 3241–3257.
- [117] S. Reumann, Toward a definition of the complete proteome of plant peroxisomes: Where experimental proteomics must be complemented by bioinformatics, *Proteomics* 11 (2011) 1764–1779.
- [118] N. Linka, C. Esser, Transport proteins regulate the flux of metabolites and cofactors across the membrane of plant peroxisomes, *Front. Plant Sci.* 3 (2012) 3.
- [119] S. Footitt, et al., Control of germination and lipid mobilization by COMATOSE, the *Arabidopsis* homologue of human ALDP, *EMBO J.* 21 (2002) 2912–2922.

- [120] M. Hayashi, et al., Ped3p is a peroxisomal ATP binding cassette transporter that might supply substrates for fatty acid beta oxidation, *Plant Cell Physiol.* 43 (2002) 1–11.
- [121] R. Radakovits, R.E. Jinkerson, A. Darzins, M.C. Posewitz, Genetic engineering of algae for enhanced biofuel production, *Eukaryot. Cell* 9 (2010) 486–501.
- [122] C.M. Sagt, et al., Peroxcretion: a novel secretion pathway in the eukaryotic cell, *BMC Biotechnol.* 9 (2009) 48.
- [123] P. Tanner, V. Balasubramanian, C.G. Palivan, Aiding nature's organelles: artificial peroxisomes play their role, *Nano Lett.* (2013), <http://dx.doi.org/10.1021/nl401215n>.

Authors contributions

Jan Wiese, Sarah Vigelius, Martin G. Schroers and Thomas J. Wrobel wrote the manuscript as co-authors with equal contribution. Nicole Linka assisted in drafting and submitting this manuscript. Florian Hahn assisted with figure layouts.

VII. Acknowledgements

PD Dr. Nicole Linka möchte ich von Herzen für die großartige Betreuung danken. Du hast keine Zeit und Mühe gescheut mich zu unterstützen, vor allem auch in der Zeit an der Michigan State war immer Verlass auf Dich.

Prof. Dr. Andreas Weber danke ich für die Bereitschaft mich in das iGRAD plant Programm und die Arbeitsgruppe aufzunehmen. Sie haben mich stets unterstützt und meine Projekte weiter voran gebracht.

Prof. Dr. Georg Groth möchte ich für die Unterstützung dieser Arbeit mit hilfreichen Diskussionen im Rahmen der Komitee-Treffen danken.

Prof. Dr. Jianping Hu danke ich für die herzliche Aufnahme in das Hu-Lab und die Unterstützung während meines Aufenthaltes an der MSU danken.

Prof. Dr. John Ohlrogge und **Prof, Dr. Robert Last** danke ich für die Unterstützung und hilfreiche Gespräche.

Dr. Sigrun Wegener-Feldbrügge gilt Dank für die Unterstützung als Koordinatorin des iGRAD-Plant. Du hast mir durch die gute Organisation des Programms das Doktorandenleben sehr erleichtert.

Dem **Weberlab** möchte ich für eine super Zeit danken.

Martin Schroers, Dr. Sarah Keßel-Vigelius, Canan Külahoglu, Daria Chrobok, Christian Bordych, Samantha Kurz, Alisandra Denton, Dr. Kristin Bernhardt, Dominik Brillhaus, Manuel Sommer, Dr. Thea Pick, Thomas Wrobel, Florian Hahn, Dr. Christian Rosar, Dr. Frederique Breuers, Dr. Fabio Facchinelli, Nadine Hocken, Simon Schliesky und **Lisa Leson** für die tolle Zeit! Ihr wart tolle Kollegen. Danke für eure Hilfsbereitschaft, Unterstützung und Freundschaft.

Martin Schroers und **Canan Külahoglu** danke ich für das Korrekturlesen einiger Kapitel der Arbeit.

Danke an alle, die mich an der MSU unterstützt haben; im Besonderen **Ronghui Pan** und **Dr. Henrik Tjellström**. Ebenso **Cheng Peng**, **Jiying Li**, **Navneet Kaur**, **Dr. Gaëlle Cassin**, **Ye Xu**, **Tiffany Liu**, **Linda Savage** und **Dr. Jeffrey Cruz**.

Ich danke allen, die an den Manuskripten beteiligt waren und jenen, die ich an dieser Stelle vergessen habe.

Meinen Eltern, meiner Familie und **meinen Freunden** danke ich für viel Unterstützung.

Der **DFG** und **iGRAD-plant** danke ich für das Stipendium.